A STUDY OF THE MISCIBILITY OF

ACRYLIC-BASED POLYMER BLENDS

by

NIGEL McCONNELL HODGKINSON

A Doctoral Thesis

Submitted in partial fulfilment of the requirements

for the award of Doctor of Philosophy of the

Loughborough University of Technology.

JUNE 1991

Supervisor: Professor J.V. Dawkins

Department of Chemistry

i

Dedicated to the memory of my Father

Arthur McConnell Hodgkinson

4/3/14 - 9/7/89

2·4

ACKNOWLEDGMENTS

ORIGINALITY

iv

All the work presented in this thesis has been carried out by the author except where acknowledged and has not previously been presented for a degree at this University or any other institution.

ABSTRACT

The work carried out in this study, constitutes an investigation of the miscibility behaviour of a number of acrylic-based polymers with the high performance, fluoropolymer surface coating material Lumiflon LF200. The aim was to find ways of improving the miscibility of LF200 with lower cost acrylic type surface coating materials. In order to more fully understand the mixing behaviour of LF200, blends were prepared with acrylic copolymers and a number of other polymeric materials. LF200 was found to be immiscible with a copolymer based on styrene (ST) and methacrylic acid (MAA), irrespective of the ST:MAA ratio. Miscible blends of LF200 were however, prepared with n-butyl acrylate (PBA) and polyethylene glycol (PEG) homopolymers, among others. Based on these findings, ternary blends were produced consisting of the fluoropolymer and acrylic surface coating polymers, along with low molecular weight PBA or polypropylene glycol (PPG). Both low molecular weight materials appeared to act as compatibilising agents and single Tg transitions were observed for many of the ternary blends using dynamic mechanical thermal analysis (DMTA).

Fourier transform infrared spectroscopy (FTIR) was employed to detect any specific interactions present between the blend components. Hydrogen bonding interactions were observed between the carbonyl group of methacrylic acid containing polymers and the ether oxygen of polypropylene glycol, in blends containing these constituents. LF200 did not appear to be involved in hydrogen bonding in any of the blends studied.

The use of scanning electron microscopy (SEM) to study the phase behaviour of binary and ternary blends was investigated with only limited success, due to problems associated with specimen preparation. The technique did however, confirm the single phase

nature of a small number of blends shown to have single glass transitions.

1.0 Introduction

1.1 Polymer Blends

A polymer blend is simply a mixture of two or more polymers not chemically bonded together. There has been considerable interest in this area of polymer science and technology in recent years,[1-5] because of the inherent advantages in producing polymer mixtures. Polymer blends can offer either superior or intermediate physical and mechanical properties relative to the blend components and can offer significant commercial benefits. Polymer mixtures are usually less expensive to develop than new polymers or copolymers and the blending process can be done economically on a large industrial scale at various stages of the manufacture. Cost savings can also be achieved if an expensive polymer is mixed with a cheaper one, perhaps coupled with a compromise in the properties of the blend compared to it's components. There are now a large number of well established commercial blends available. One example is the blend of poly(methyl methacrylate) (PMMA) and poly(vinylidene fluoride) (PVF_2),[6] which has a better chemical and U.V. resistance than PMMA, whilst having a better optical clarity than PVF_2. Another example is the blend of poly(carbonate) and poly(ethylene terephthalate),[7] which has a better chemical resistance and processability than poly(carbonate), at a lower cost.

1.2 Polymer Blend Miscibility

The mixing of polymeric materials is not as straightforward or predictable as the mixing of low molecular weight liquids. The vast majority of polymer pairs when blended do not mix but form separate phases or domains within the mixture. Such blends are termed immiscible. It is important to understand what is meant by miscibility. The most widely used definition of a miscible polymer

blend is one which exhibits a single glass transition. Miscibility therefore implies, by this definition, a level of homogeneity within the mixture, such that any separate domains present are smaller than the segmental size responsible for the glass transition. In other words, miscibility in this sense, does not imply ideal molecular mixing, but suggests a level of mixing adequate to yield the macroscopic properties expected of a single phase material. It is clear therefore, that a technique used for studying miscibility on the basis of the glass transition, may lead to the conclusion of a single phase, whilst a more sensitive technique may be capable of differentiating between smaller separate domains, leading to a conclusion of immiscibility. It has been suggested that the segmental size associated with the glass transition is of the order of 15nm.[8]

In practice, many polymer blends are neither completely miscible or completely immiscible, but exhibit a degree of partial miscibility. In this situation, two glass transitions may occur at temperatures intermediate between those at which the transitions would occur in an immiscible blend of the two polymers. This suggests, in effect, that there is a limited solubility of the two polymers in each other, but not to a sufficient extent to yield a single glass transition. A partially miscible system may however, show a single very broad glass transition, which might span over the range between the transitions of the blend components.

Clearly, when studying the miscibility of a blend using the single glass transition criterion, problems will arise if the two polymers have transitions at similar temperatures. In this situation it is very difficult to determine whether one or two transitions are present, making conclusions about miscibility almost impossible. In such cases it is necessary to employ another technique, such as

microscopy, in order to clarify the phase behaviour of the blend. One simple way of confirming miscibility is optical clarity. It has been suggested that domains having a size of less than 100nm or thereabouts,[9] will not have the effect of scattering light, and such blends will therefore, appear transparent. Likewise immiscible or partially miscible blends having domains larger that this will appear translucent or opaque, except in the case where the refractive indices of the blend components are very similar. This will lead to a transparent appearance, and the erroneous conclusion of miscibility. Caution must therefore, be applied when using optical clarity as a test for miscibility.

In order to more fully understand the phenomena associated with the mixing of polymers, a number of thermodynamic theories have been developed, which attempt to explain and often, predict, the miscibility of a given blend system. Such theories are discussed in more detail in section 2.1, but the basic criterion for the miscibility of two polymers is that the Gibbs free energy of mixing $\triangle G_m$ is negative, as determined by the following equation

$$\triangle G_m = \triangle H_m - T \triangle S_m \qquad (1.1)$$

Since the entropy change ($\triangle S_m$) on mixing two polymers is small or negligible, miscibility is usually only achieved if the enthalpy of mixing ($\triangle H_m$) is negative. This is often the case if specific intermolecular interactions, such as hydrogen bonding, are present between the blend components. Choosing polymers which have functional groups likely to be susceptible to such interactions, is one way of promoting blend miscibility.

1.3. Miscibility Enhancement

A large number of binary polymer blends are miscible in some, if not all, proportions. However, the vast majority of blend pairs are immiscible and whilst this does not necessarily forego their commercial utility, it is often desirable to improve the miscibility of such blends. There are a number of approaches when it comes to achieving or improving the miscibility of polymer mixtures. Recently, much work has concentrated on the careful selection of blend components, such that specific interactions between them are favoured. The polymers are chosen so that the functional groups on each are likely to participate in intermolecular interaction, usually hydrogen bonding. It has been found in many cases that the presence of such interactions is an important factor in producing miscibility. An example of such a system, is the miscible blend of poly(ϵ - caprolactone) (PCL) and the poly(hydroxy ether of bisphenol A).[10] Fourier transform infrared spectroscopy[23,24] confirms the presence of a hydrogen bonding interaction between the carbonyl group of the PCL and the hydroxyl group of the phenoxy polymer.

Hydrogen bonding is not the only type of interaction that can lead to blend miscibility. It has been found that ion-dipole interactions can improve the miscibility in a number of binary blend systems.[11-13] Polystyrene for example, is not miscible with poly(ethylene oxide) or poly(propylene oxide), whilst an ionomeric styrene copolymer has a very high miscibility with these materials[11].

Another approach to improving the miscibility of two polymers is to employ a so-called compatibilising agent. A recent review by Xanthos[14] discussed the use of such interfacial agents for enhancing the miscibility of immiscible blends. The most widely used type of compatibiliser discussed by Xanthos are block copolymers $(A-B)_n$,[15-16] usually made up of units of the two immiscible polymers in question,

A and B. It is not difficult to understand the principle behind this approach, since it is likely that polymers A and B will mix with the blocks in the copolymer having the same units.

Another way in which it is possible to improve the mixing behaviour of two polymers is to form an interpenetrating polymer network (IPN).[17] This is done by crosslinking polymer 1, which is then swelled by incorporating into the network the monomer of polymer 2. The monomer is then polymerised and crosslinked is situ to form a second network, which is interwoven with the first. This procedure does not necessarily yield a single phase material and indeed two phases may be present, however, the extent of phase separation is limited due to the irreversible interpenetration of the two polymers.

The phase separation of two immiscible polymers can also be discouraged by promoting grafting reactions between the chains; usually achieved by the incorporation of a suitable reactive small molecule into the system,[14] which causes linkages to be formed at melt temperatures. The resulting material is no longer technically a mixture, since chemical bonds have been formed between the polymers.

Recently, a number of ternary polymer blends have been prepared and studied,[18-20,51] but often the third component is a block copolymer of the other two, although this is not always true. A comprehensive and up to date listing of miscible binary and ternary blends has been compiled by Krause.[21,22]

1.4   Summary of Work Carried Out in This Study

Before describing the work undertaken, it is first appropriate to discuss a little of the background to the work and to explain the reason for the approach that was taken. Lumiflon is a novel fluoroploymer designed for long life, high performance surface coatings (see section 3.1.3). The polymer comprises four monomer

units, three of them containing hydroxyl and/or ether functional groups. Because of the material's high performance characteristics, Lumiflon is therefore, relatively expensive. Clearly, there is a potential for blending Lumiflon with other polymers in order to produce a material of intermediate performance, but of lower cost. Acrylic polymers are widely used in the surface coatings industry, but although less expensive, they cannot match the high performance of Lumiflon. The aim of this work, therefore, was to blend Lumiflon with various acrylic-based polymers in order to produce a miscible system. The functional groups on the fluoroploymer and groups on the acrylic polymers have, in theory, the potential for specific interactions, and it was hoped that the miscibility of such systems might be enhanced by promoting these interactions.

A copolymer of styrene and methacrylic acid was chosen to be a model for the two acrylic based surface coating systems studied (each having methacrylic acid, 2-hydroxyethyl acrylate and n-butyl acrylate components in the proportions indicated in section 3.1.3). It was hoped that it might be possible to obtain specific interactions between the methacrylic acid portion of the copolymer and the hydroxy or ether groups of LF200. These could then be observed by Fourier transform infrared spectroscopy (FTIR).[23,24] The copolymer also had the advantage that its glass transition was well separated from that of LF200, therefore facilitating the study of miscibility by dynamic mechanical thermal analysis (DMTA).[25] It soon became clear however, that LF200 was completely immiscible with the copolymer and so it was decided to investigate the miscibility with a range of homopolymers and copolymers, in order to discover the type of polymer with which LF200 may be miscible. These experiments identified a number of interesting blends in which miscibility was produced. Several polymers were chosen based on these results, as potential

- 6 -

compatibilising agents. Binary blends of LF200 with the acrylic surface coating polymers were studied in some detail, along with the corresponding three component blends incorporating the potential compatibilisers. Miscibility was studied mainly by DMTA and the existence or otherwise of hydrogen bonding interactions was monitored by FTIR spectroscopy.

2.0 Thermodynamic Theories of Polymer-Polymer Mixtures

2.1 Introduction

The purpose of thermodynamic theories as applied to polymer-polymer systems is to explain the nature and extent of mixing and any phase separation behaviour that is observed. Another desirable feature of such a theory would be the ability to predict the miscibility of a given polymer pair, from a knowledge of readily obtainable physical parameters relating to each of the components.

From basic thermodynamics, we have the criterion that any system in stable equilibrium will have a minimum value of the free energy of mixing ($\triangle G_m$), and this also applies to polymer-polymer blends. The equilibrium state of mixing of a polymer blend at constant pressure and temperature T, is determined by the value of $\triangle G_m$, which is made up of the following components:-

$$\triangle G_m = \triangle H_m - T \triangle S_m \qquad (2.1)$$

$\triangle H_m$ =enthalpy of mixing

$\triangle S_m$ =entropy of mixing.

A plot of $\triangle G_m$ against blend composition (ϕ_2, volume fraction of component 2) as in figure 2.1, shows three possible types of mixing behaviour for a binary system. The three curves represent the miscible (A), partially miscible (B) and completely immiscible (C) situations.

The necessary conditions for a binary system to be miscible at a particular composition are:-

$$\triangle G_m < 0 \qquad (2.2)$$

and

$$\left(\frac{\delta^2 \triangle G_m}{\delta \phi_2^2} \right)_{TP} > 0 \qquad (2.3)$$

Clearly, to determine the nature of the miscibility of a given binary system, information quantifying $\triangle H_m$ and $\triangle S_m$ are required in

Figure 2.1

ΔG_m vs. Composition Curves Illustrating
3 Types of Mixing Behaviour
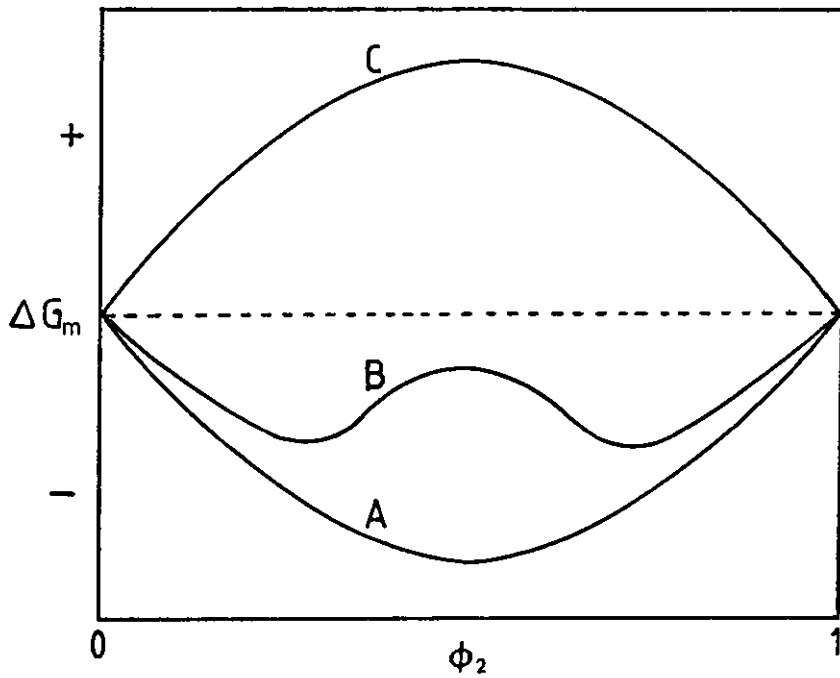
Figure 2.2

Phase Separation Behaviour in a Binary System
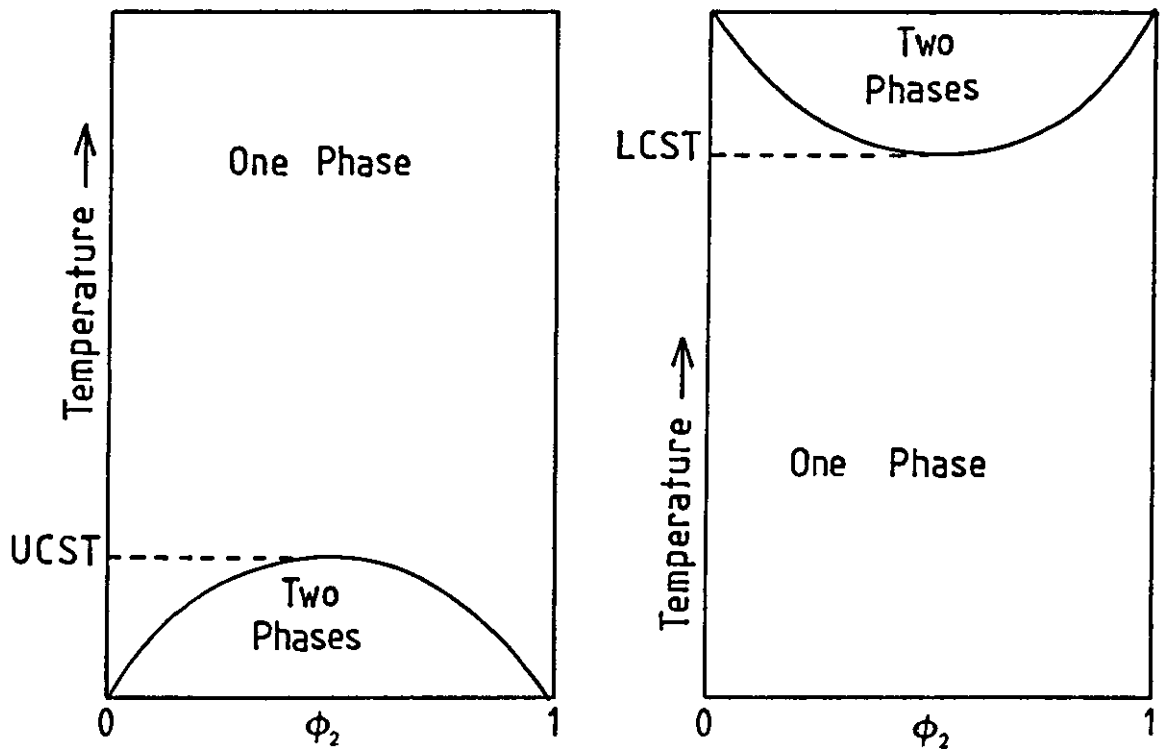
order to know the sign and magnitude of ΔG_m at a given composition. The various thermodynamic theories, therefore, attempt to relate ΔH_m and ΔS_m to physical parameters of the two components of the blend which can be easily obtained, experimentally or otherwise.

The most widely known theories will be discussed, mentioning the basis of the treatments, any assumptions made and shortcomings apparent. Some more recent theoretical treatments will be mentioned, especially those attempting to account for specific interactions, a consideration largely ignored in the earlier fundamental theories. No attempt will be made to reproduce the detailed derivation of thermodynamic equations, since many are complex and lengthy and are covered adequately elsewhere. Firstly however, it is appropriate to discuss the phase equilibria and separation of polymer blends, since many of the theoretical treatments attempt to explain such behaviour, their ability to do so, an indication of the suitability of the approach.

2.2   Phase Equilibria in Binary Polymer Blends

It is rare that enough information is available from either experiment or theory to be able to predict the miscibility of a given system. It is more common to first observe the phase behaviour and then to explain it using a combination of theoretical and experimental knowledge.

The phase diagrams for a typical binary polymer mixture are shown in figure 2.2, illustrating upper and lower critical solution temperature behaviour (UCST and LCST). It is assumed that the polymers are in their liquid state and the presence of the glass transition is neglected. It has been well established that lower critical solution temperature (LCST) behaviour is the predominant mode of phase separation in polymer-polymer mixtures and has been

observed for many blend systems.[26,27,28,12,72] It can be seen from figure 2.1 that the shape of the free energy of mixing ΔG_m - composition (ϕ_2) curve can indicate the state of miscibility of a binary system. Since the entropy change (ΔS_m) on mixing two polymers is very small (unlike small molecules), from equation 2.1 it can be seen that a small positive ΔH_m can lead to a positive ΔG_m, and hence, phase separation. At constant temperature and pressure, for a binary mixture to be homogeneous at all compositions, the equilibrium condition of minimum free energy requires a free energy-composition curve that is curved upwards over the whole composition range from it's minimum point. Figure 2.3 shows free energy-composition curves for a completely miscible system (a) and a partially miscible system (b), which is characterised by a curve having a portion showing negative curvature. In this two phase system, a double tangent can be drawn which touches the curve at two points, representing the compositions of two coexisting phases ϕ_2' and ϕ_2''. The double tangent intercepts the free energy axes at points representing the chemical potential of the two components. The chemical potential or partial molar free energy of a species i in solution (μ_i) relative to it's chemical potential in the pure state $(\mu_i^\bullet)$ is defined as the first derivative of ΔG_m with respect to the concentration (m_i) of i

$$\mu_i - \mu_i^\bullet = \Delta \mu_i = \left(\frac{\delta \Delta G_m}{\delta m_i} \right)_{T,P,m} \qquad (2.4)$$

The two inflexion points on this curve separate the positively and negatively curved parts of ΔG_m. Any system within this region is unstable and will phase separate, because the slightest change in concentration will lead to a decrease in the free energy of the system and cause further separation, until the stable situation of minimum free energy for the two phase system has been reached (i.e., a point on the double tangent). This process is known as spinodal

Figure 2.3
ΔG—Composition Curves

(a)

Completely Miscible System

(b)

Partially Miscible System

(c)

Temperature Dependence of ΔG_m

$T_1 < T_{cR} < T_2 < T_3$
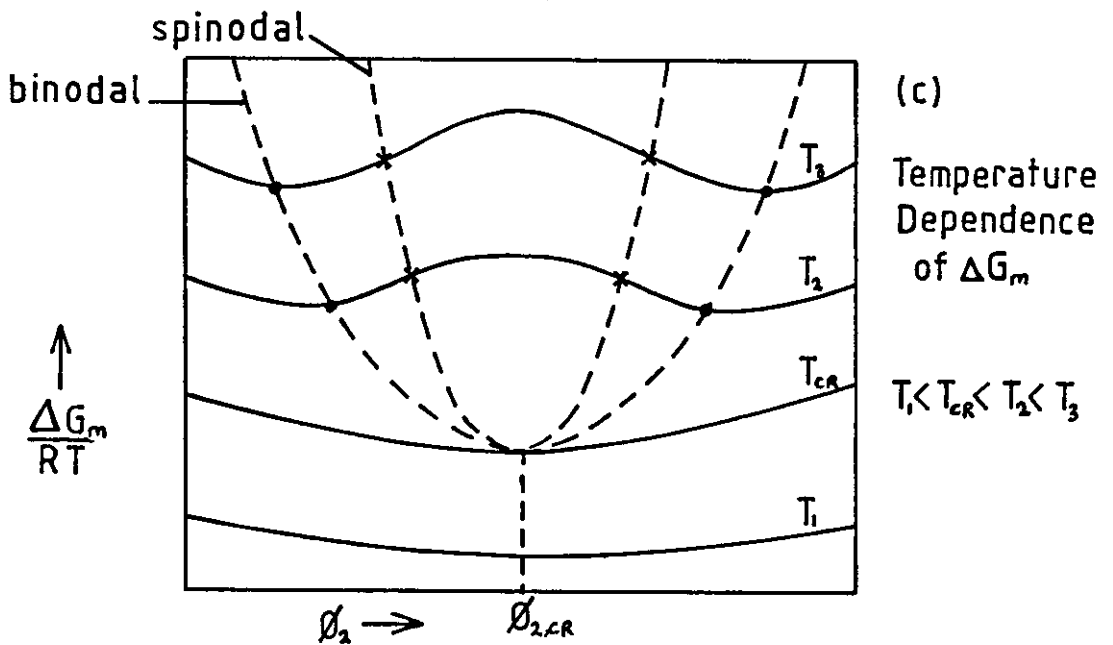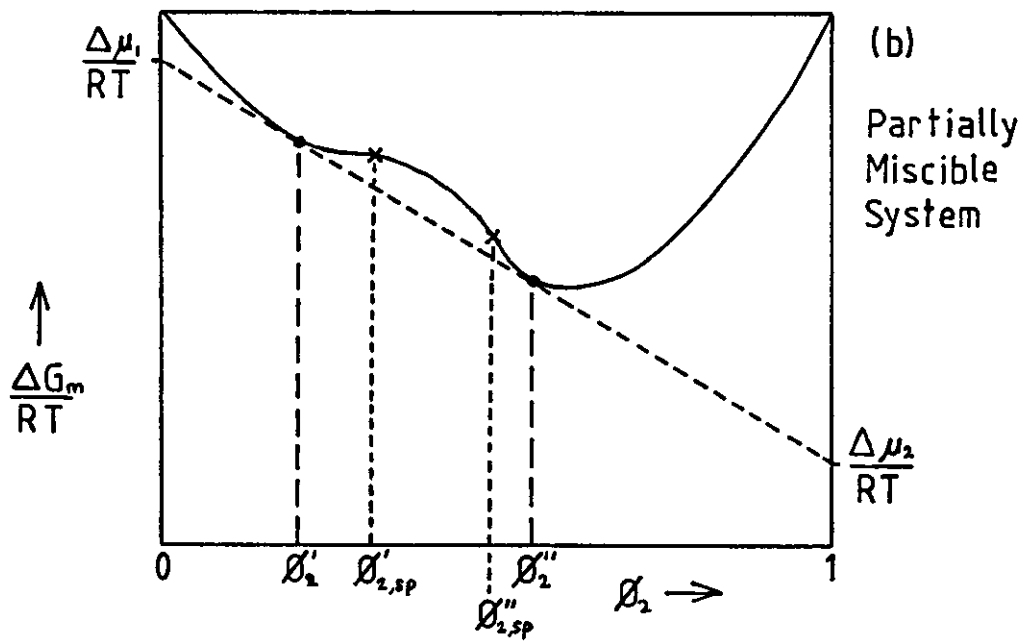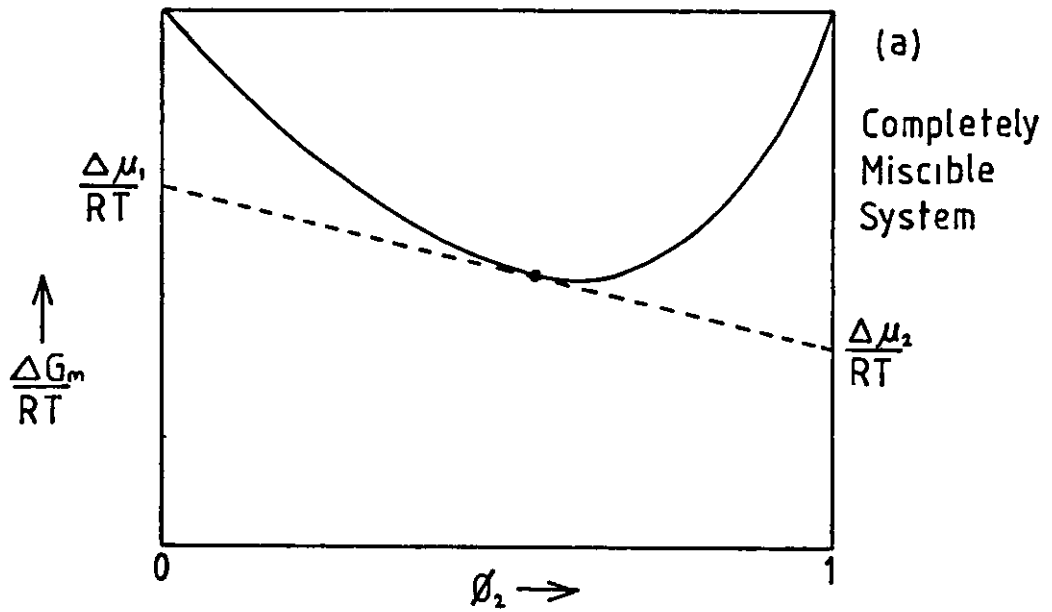
phase separation.[52]

At the inflexion points:-

$$\left(\frac{\delta^2 \Delta G_m}{\delta \phi_2^2}\right)_{P,T} = 0 \qquad (2.5)$$

ΔG_m = free energy of mixing per unit volume.

The range of concentrations between the point of inflexion and tangent point are called metastable, since the system can resist small concentration fluctuations on account of the positive curvature.

Increasing the temperature in a two phase system, serves to bring together the two sets of tangent and inflexion points until they form the critical point (see figure 2.3(c)), at which:-

$$\left(\frac{\delta^3 \Delta G_m}{\delta \phi_3^3}\right)_{T,P} = 0 \qquad (2.6)$$

Plotting the concentration of tangent and inflexion points as a function of temperature yields the phase diagram showing the coexistence curve (binodal) and locus of inflection points (spinodal) (figure 2.4). These two curves have a common horizontal tangent at the critical point, parallel to the lines which connect the compositions of the coexisting phases.

It is likely that figure 2.4 represents only the simplest case and many polymer systems will be characterised by curves having more complicated shapes. It should also be noted that the critical point may be effected by polydispersity, chain length, temperature and composition.

Figure 2.4

Binary phase diagram for a liquid mixture
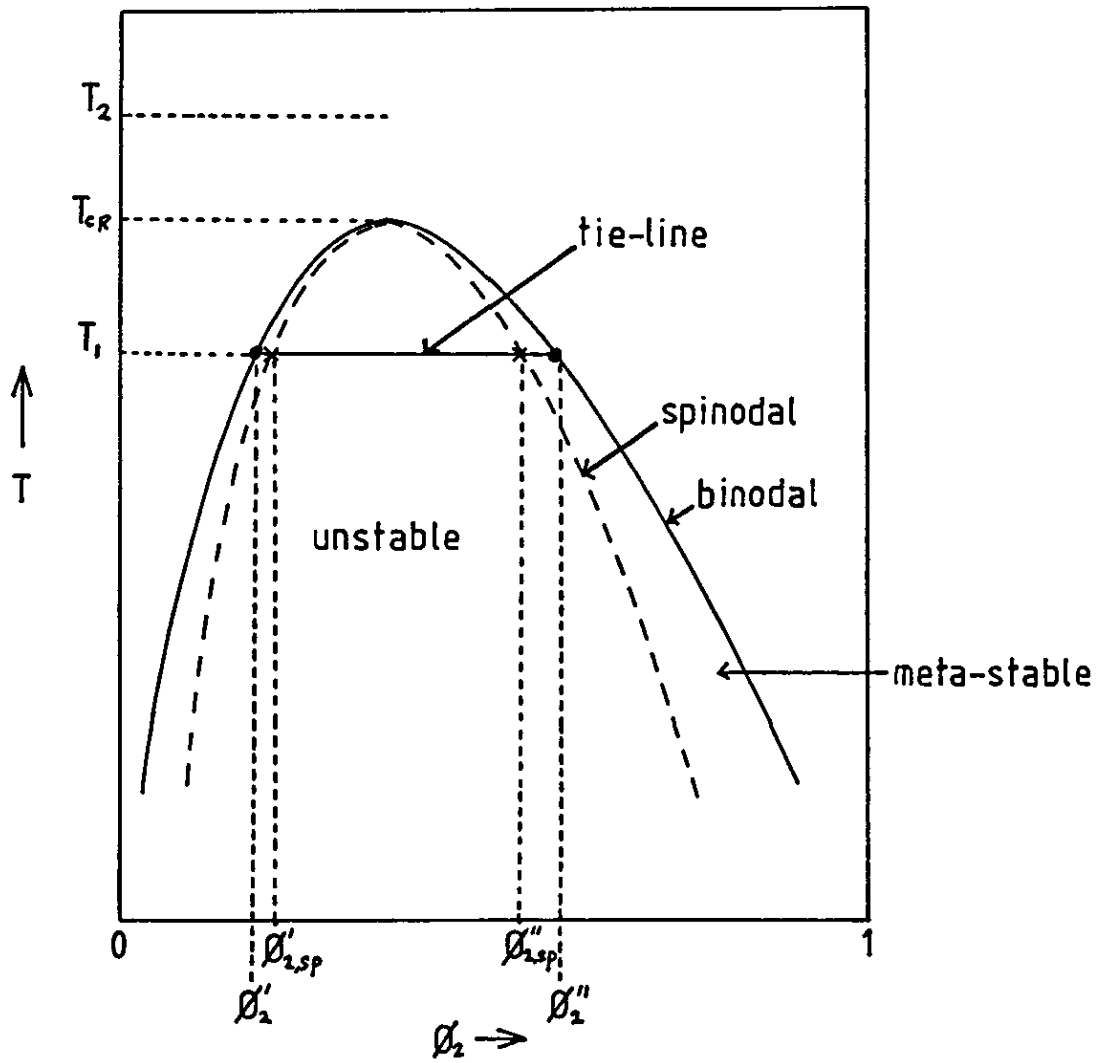
2.3 The Flory-Huggins Lattice Theory of Polymer-Polymer Thermodynamics

The theory developed to describe the thermodynamics of polymer mixture is an extension of the theory relating to polymer-solvent systems, proposed simultaneously by Flory[29] and Huggins.[30] Each suggested a lattice model in order to derive expressions for the enthalpy and entropy of mixing, enabling the evaluation of the free energy of mixing from equation 2.1.

When a polymer chain is placed in an imaginary two-dimensional lattice, each polymer segment occupies a site in the lattice in an overall random way, as permitted by chain restrictions. A second polymer can then be placed randomly in the remaining lattice sites. Two important assumptions should be noted at this point. Firstly, it is assumed that the same lattice may be used to describe the configurations of both components, and secondly, that the geometry of the two species is identical. In other words, the size of the polymer segments of each polymer and their allowable conformations are assumed to be equal. It should also be noted that the model makes no allowances for specific inter-molecular interactions. The derivations of expressions for the entropy and enthalpy of mixing will now be discussed.

2.3.1 Entropy of Mixing

The blend is considered to consist of two polymers 1 and 2, each one having a chain made up of a number of segments X_1 and X_2, respectively. Since the segment sizes for each polymer are considered to be equal, they can be defined as a ratio of the molar volumes of the two polymers. An expression is then derived to calculate the number of ways in which the polymer chains can be arranged in a lattice, consisting of a given number of sites or

- 12 -

cells, the volume of each cell being equal to that of a polymer segment. It is assumed that each segment in a chain is placed randomly in the lattice, adjacent segments of the chain going into adjacent cells, allowing for cells that have already been occupied.

If the combination entropy of mixing polymers 1 and 2 is defined as

$$\Delta S_m = \left[S_c - \left(S_1 + S_2 \right) \right] \qquad (2.7)$$

and the volume fraction of polymers 1 and 2 are defined as

$$\phi_1 = n_1 x_1 / n_o \\ \text{and} \quad \phi_2 = n_2 x_1 / n_o \qquad (2.8)$$

Where n_1 is the number of ways in which identical polymer segments can be arranged in a lattice of n_o cells, then the combinatorial entropy of mixing $\Delta S_m(c)$ can be written

$$- \Delta S_m(c) / k = \left(m_1 \ln \phi_1 + m_2 \ln \phi_2 \right) \qquad (2.9)$$

Where k is the Boltzmann constant and m_i is the number of moles of species i. This expression is similar to that applied to polymer-solvent systems, derived by Flory.

2.3.2 Enthalpy of Mixing

The enthalpy of mixing (ΔH_m) is derived by considering the energy change $(\Delta \epsilon_{12})$ involved in replacing like segments, in adjacent sites to a reference segment, by unlike segments.

$$\Delta \epsilon_{12} = \epsilon_{12} - \left(\epsilon_{11} + \epsilon_{22} \right) / 2 \qquad (2.10)$$

- 13 -

Where ϵ_{ij} is the interaction energy of segments 1 and 2.

The enthalpy of mixing ΔH_m is the difference between the total enthalpy of the mixture and the combined enthalpy of the two unmixed components.

Equation (2.10) can also be written

$$\Delta H_m = \Delta \epsilon_{12} \, p_{12} \qquad (2.11)$$

Where p_{12} is the average number of contacts between unlike segments at a particular composition, and is given by

$$p_{12} = Z x_1 n_1 \phi_2 \qquad (2.12)$$

Z is the lattice coordination number and is the number of cells immediately adjacent to a given cell. $Z x_1 n_1$, therefore, represents the total number of contacts of segments of polymer 1.

hence, $\qquad \Delta H_m = Z n_1 x_1 \phi_2 \Delta \epsilon_{12} \qquad (2.13)$

but $\qquad n_1 = N_A m_1$

Where n_1 is the number of chains having x_i segments

N_A is Avogadro's number

m_1 is the number of moles of polymer 1.

So equation (2.13) can be written

$$\Delta H_m = Z N_A m_1 x_1 \phi_2 \Delta \epsilon_{12} \qquad (2.14)$$

Equation (2.14) is one form of the Van Laar equation for the heat of mixing in any two component system. It is usually written in the form of the interaction parameter χ , defined as the interaction energy between two unlike segments, divided by kT.

So $\quad \Delta H_m = N_A k T \chi \, x_1 \phi_2 \qquad (2.15)$

Or $\quad \Delta H_m = R T \chi \, x_1 \phi_2 \qquad (2.16)$

Where $\quad \chi = Z \Delta \epsilon_{12} / kT \qquad (2.17)$

2.3.3 Free Energy of Mixing

The Gibbs free energy of mixing ΔG_m is then given by

$$\Delta G_m = \Delta H_m - T \Delta S_m \qquad (2.1)$$

substituting equation (2.9) and (2.15) gives

$$\Delta G_m = R T \left(\chi m_1 x_1 \phi_2 + m_1 \ln \phi_1 + m_2 \ln \phi_2 \right) \qquad (2.18)$$

For polydisperse polymers this can be generalised to

$$\Delta G_m = R T \left[\sum_i \phi_{1,j} \, \bar{x}_{1,j}^{-1} \ln \phi_{1,j} + \sum_j \phi_{2,j} \, \bar{x}_2^{-1} \ln \phi_{2,j} + \sum_i \phi_{1,i} \sum_j \phi_{2,j} \chi \right] \qquad (2.19)$$

These expressions can also be written in terms of chemical potential (partial molar free energy).

2.3.4 Assumptions and Simplifications in the Lattice Theory

As mentioned earlier, one major assumption is that the same lattice is applicable for describing the configurations of both components, and this cannot be justified if the two polymer chains have different spatial requirements. This may well lead to a difference between the observed behaviour and that predicted by the theory.

It is widely believed that the entropy contribution to the free energy of mixing, is in reality made up of both a combinatorial entropy term $(\Delta S_m(c))$ and an excess entropy term $(\Delta S_m(e))$. Thus, equation (2.1) becomes

$$\Delta G_m = \Delta H_m - T \left(\Delta S_m(c) + \Delta S_m(e) \right) \qquad (2.20)$$

The Flory-Huggins lattice theory takes into account only the

combinatorial entropy. However, if specific interactions occur between chain segments, then there will be a deviation from random mixing and this may result in a volume change on mixing. Attractive interactions between chains might be expected to lead to a reduction in volume compared to that predicted. The combinatorial entropy term alone takes no account of such volume changes, but so-called equation of state theories attempt to allow for this. The lattice theory is also not applicable to dilute solutions of one polymer in another, as this tends to lead to small clusters of the minor component separated by large regions of the major component. This defies the condition that segments of the two polymers should be distributed randomly.

As mentioned earlier, the success of a given theoretical treatment to describe polymer-polymer mixtures, can be judged to some extent by it's ability to explain phase separation behaviour, in particular lower critical solution behaviour, since this has been observed for many miscible blend systems. The Flory-Huggins theory is unable to predict LCST behaviour, but to understand why, it is necessary to consider the spinodal and critical conditions as applied to the interaction parameter χ. If equation (2.18) is differentiated with respect to m, we get

$$\frac{\Delta \mu_1}{RT} = \ln \phi_1 + \left(1 + x_1 / x_2\right) \phi_2 + \chi_1 x_1 \phi_2^2 \qquad (2.21)$$

Where μ_1 , is the chemical potential of polymer 1.

If the spinodal condition

$$\left(\frac{\delta^2 \Delta G_m}{\delta \phi_2^2}\right)_{P,T} = 0 = \left(\frac{\delta \Delta \mu_2}{\delta \phi_2}\right)_{P,T} = \left(\frac{\delta \Delta \mu_1}{\delta \phi_1}\right)_{P,T} \qquad (2.22)$$

is applied to equations (2.21) the following expression is obtained

$$\chi_{sp} = \frac{1}{2}\left[\left(1/x_1(\phi_1)_{sp}\right) + \left(1/x_1(\phi_2)_{sp}\right)\right] \qquad (2.23)$$

Likewise, if the critical condition,

$$\left(\frac{\delta^3 \Delta G_m}{\delta \phi_2^3}\right)_{PT} = 0 \qquad (2.24)$$

is applied to equation (2.21), an expression for χ_{cr} can be obtained

$$\chi_{cr} = \left(1 - x_1/x_2\right)\Big/ 2x_1\left(1 - 2(\phi_2)_{cr}\right) \qquad (2.25)$$

Where $\qquad (\phi_2)_{cr} = \left(x_1\right)^{1/2}\Big/ \left(x_1^{1/2} + x_2^{1/2}\right) \qquad (2.26)$

Hence $\qquad \chi_{cr} = \frac{1}{2}\left[\left(1/x_1\right)^{1/2} + \left(1/x_2^{1/2}\right)\right] \qquad (2.27)$

x_i is the number of segments in a chain of polymer i.

From equations (2.23) and (2.27) it is clear that χ can never be negative despite approaching zero at high chain lengths. This means that the free energy of mixing ΔG_m(see equation (2.18)) cannot be negative, and hence, the theory cannot predict LCST behaviour. One reason for this inability to describe experimental observations, could be due to the definition of the interaction parameter as depending on temperature alone. However, it has been shown from recent small angle neutron scattering experiments that χ is a complicated function of temperature, density, concentration, intermolecular structure and flexibility.[31,32,33,34] Tompa[35] suggested an expression for χ of the form $\chi = \chi_1 + \chi_2\phi_2 + \chi_3\phi_2^2$ in which the temperature dependence of χ can be restricted to the

first term. Koningsveld[36] proposed a similar expression using an interaction parameter term, g which could be written as a function of temperature. The g parameter could in some cases be measured in terms of physical quantities, but no acceptable molecular interpretation for g was proposed. Schweizer and Curro[31] have derived a general formula for the χ parameter measured in small angle neutron scattering (SANS) experiments. The use of SANS and inverse gas chromatography (IGC) to determine the χ parameter will be discussed later (sections 2.6.2 and 2.6.3).

The inability of the lattice theory to predict LCST behaviour, led to the development of equation of state theories to explain or predict the miscibility of polymers.

2.4   Equation of State Theories

Molecular theories which take into account the compressible nature of the pure components as well as that of the mixture and which relate the pressure, volume and temperature of a system at equilibrium, are known as equation of state theories. Early theories were first developed from Van der Waals theory in order to describe mixtures of small molecules. The two most widely known theories applicable to polymer mixtures are those proposed by Flory et al,[37,38,39] and the lattice fluid theory of Sanchez and Lacombe.[40,41,42,43] The most widely applied theory of the two is that of Flory, the outline of which is discussed below.

The Flory treatment involves considering the ways in which segments of volume V^* can fill a lattice having cells of volume V. V^* is the volume taken up by the "hard-core" of a segment and this is less than the actual molecular volume of the segment V. The difference $V-V^*$ is the free volume of the system and accounts for the expanded configurations of the chain segments. One of the most

- 18 -

important assumptions of the theory, originally proposed by Prigogine,[44] is that a molecule in a liquid has both external and internal degrees of freedom. The external degrees of freedom in a polymer chain depend on intermolecular forces and are related to translational motions. The external degrees of freedom are usually expressed as $3c$ per chain segment. Where c is a number less than one. The internal degrees of freedom depend on intramolecular forces and relate to vibrations and rotations. The partition function (Z) is given by

$$Z = Z_{int} \cdot Z_{ext} \qquad (2.28)$$

Z_{int} makes no contributes to the equation of state, since it is assumed to be independent of density and is not influenced by neighbouring segments. The external partition function which is determined effectively by the translational degrees of freedom, can be calculated using the classical integral for a translational partition function and results in

$$Z_{ext} = Q \left(2\pi m kT / h^2 \right)^{3n_i x_i c_i / 2} \qquad (2.29)$$

Where n_i is the number of chains having x_i segments of mass m,

$\qquad$ h is Planck's constant

$\qquad$ and Q is the configuration integral and is given by

$$Q = Q(comb) \left[4\pi \gamma / 3 \left(v_i^{1/3} - v_i^{*1/3} \right)^{3n_i x_i c_i} \cdot exp \left(-E_{0,i} / kT \right) \right] \qquad (2.30)$$

Where γ is a geometric factor. E_0 is the lattice energy and is inversely proportional to the cell volume to the power a (where a is number between 1 and 1.5).

$\qquad$ The pressure P, of the system can be defined as

$$P = \frac{kT}{n_i r_i} \left(\frac{\delta \ln Z_i}{\delta v_i} \right)_{T, n_i} \qquad (2.31)$$

where r_i is the segment ratio defined as v_i / v^*

The equation of state for an unmixed polymer component can be found by differentiating equation (2.29):

$$\frac{\tilde{P}_i \tilde{v}_i}{\tilde{T}_i} = \frac{\tilde{v}_i^{1/3}}{\tilde{v}_i^{1/3} - 1} - \frac{1}{\tilde{T} \tilde{v}_i^a} \qquad (2.32)$$

where the reduced temperature, volume and pressure are defined as

$$\left. \begin{array}{l} \tilde{P} = P/P^* \\ \tilde{T} = T/T^* \\ \tilde{v} = v_i/v^* \end{array} \right\} \qquad (2.33)$$

The characteristic parameters in the equations of state can be obtained by measuring the thermal expansion coefficient (α) and the thermal pressure coefficient (γ)

$$\alpha = \frac{1}{v} \left(\frac{\delta v}{\delta T} \right)_{P, n_i} \qquad (2.34)$$

$$\gamma = \left(\frac{\delta P}{\delta T} \right)_{v, n_i} \qquad (2.35)$$

By extrapolating these quantities to zero pressure, the reduced parameters become

$$P_i^* = \tilde{v}_i \gamma_i T \qquad (2.36)$$

$$\tilde{T}_i = \left[\left(\tilde{v}_i^{1/3} - 1 \right) / \tilde{v}_i^{(1/3 + a)} \right] \qquad (2.37)$$

- 20 -

$$\tilde{v}_i = \left[\left(\alpha_i T / 3a\alpha_i + 3 \right) + 1 \right]^3 \qquad (2.38)$$

By using a number of mixing rules, as discussed by Olabisi et al,[2] these relationships can be related to binary polymer systems and equations for the characteristic temperature and pressure of a multicomponent mixture can be obtained :

$$P^* = \sum_{i=1}^{n} \psi_i P_i^* - \sum_{j=2}^{n} \sum^{j-1} \psi_i \theta_j X_{ij} \qquad (2.39)$$

$$\frac{1}{T^*} = \frac{k}{P^* v^*} \left[\sum_{i=1}^{n} c_i \psi_i - \sum_{j=2}^{n} \sum_{i=1}^{j-1} c_{ij} \psi_{ij} \right] \qquad (2.40)$$

The term in brackets in equation (2.40) gives the total number of external degrees of freedom per segment. c_{ij} is a correction factor to account for deviations from additivity. ψ_i is the segment fraction, equivalent to the volume fraction based on the "hard-core" volume of v^*. X_{ij} arises from the difference in interaction energies for unlike segments. θ represents the total surface area of segments occupied by type j molecules.

The chemical potential for each component in a system is given by

$$\Delta \mu_k = \left(\frac{\delta \Delta F_m}{\delta n_k} \right)_{T,V,n_j \atop j \neq k} + \left(\frac{\delta \Delta F_m}{\delta \tilde{v}} \right)_{T,n_k n_j} \cdot \left(\frac{\delta \tilde{v}}{\delta n_k} \right)_{T,V,n_j} \qquad (2.41)$$

Where $\quad \Delta F_m = -kT \ln \left(Z / \prod_{i=1}^{n} Z_i \right) \qquad (2.42)$

The second term was found by McMaster[45] to be necessary in order for accurate predictions of the effect of pressure, even though it only makes a small contribution at low pressures. If a full expression for $\triangle F_m$ is incorporated into the above equation (2.41), followed by differentiation, the chemical potential μ of a component (k) in the mixture can be found from the very lengthy equations which result.

2.4.1. Applicability of the Flory Equation of State Theory

McMaster[45] carried out a detailed examination of the Flory theory for polymer blends by simulating a series of binodal and spinodal curves for hypothetical polymer mixtures. The effect of varying interaction parameters X_{12} is discussed as follows (see figure 2.5), along with other factors influencing miscibility.

(1) Negative or very small positive values of the interaction parameter X_{12} favour miscibility. Small positive values lead to phase diagrams similar to figure (2.5)(iii); larger positive values have phase diagrams represented by (ii). Negative values of X_{12} show behaviour as shown in (i).

(2) Miscibility is favoured by either one or both components having low molecular weight.

(3) Miscibility is favoured if the two components have similar thermal expansion coefficients, the implication being that similar characteristic temperatures T^* are required for miscibility.

(4) If $\alpha_1 < \alpha_2$ or if $T_1^* > T_2^*$, then miscibility is favoured if $\gamma_1 > \gamma_2$ or $P_1^* > P_2^*$

Figure 2.5 The Effect of Varying the χ Parameter on the Binary Phase Diagram

(i) negative χ_{12}

2-Phase

LCST

T

Homogeneous

0 ϕ_2 1

(ii) χ_{12} large and positive

2-Phase

2-Phase

T

0 ϕ_2 1

(iii) χ_{12} small and positive

2-Phase

LCST

T

Homogeneous

UCST

2-Phase

0 ϕ_2 1
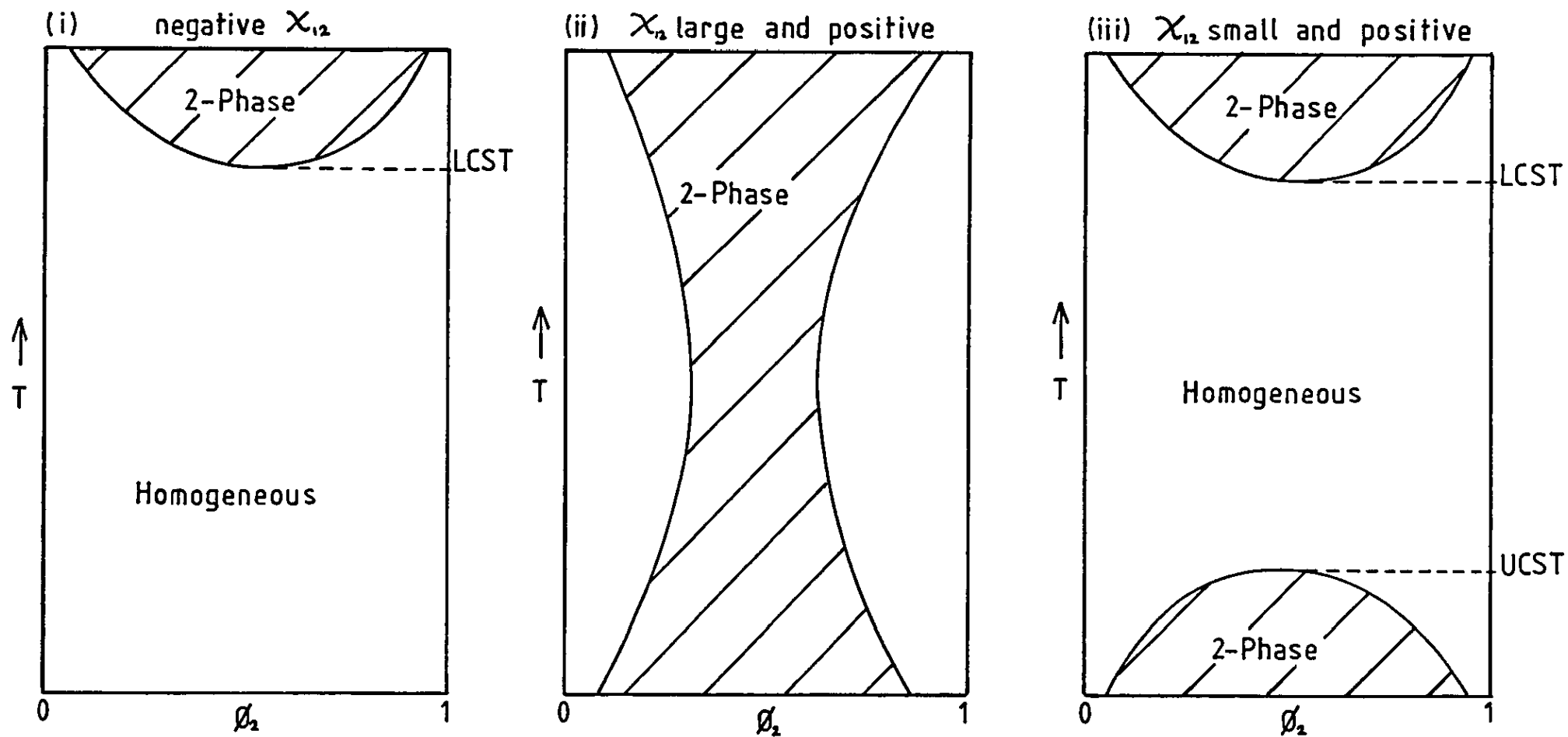
X_{12} is usually negative when specific interactions are present and this is a driving force for miscibility. However, miscible blends have been observed in which no specific interactions are involved. A number of such systems involve random copolymers, where the relationship between intermolecular and intramolecular forces are more important.[26,47,53,73]

2.5 Thermodynamic Theories of the Miscibility of Blends Involving Random Copolymers

A mean field theory based on the simple Flory-Huggins lattice theory, has been used to describe the miscibility behaviour of binary systems containing at least one copoloymer.[46,47,53] Like the basic lattice theory, the treatment does not allow for the presence of specific interactions.

Consider a copolymer/homopolymer system involving copolymer A, having units 1 and 2, and homopolymer B having a structural unit 3.

The volume fractions of the various components are

ϕ_A , ϕ_B - the volume fractions of A and B, $\phi_A + \phi_B = 1$

ϕ_1' , ϕ_2' - the volume fractions of comonomer units in copolymer A.

$\phi_1 , \phi_2 \& \phi_3$ - the overall volume fractions of monomer units 1,2 and 3 where $\phi_1 + \phi_2 + \phi_3 = 1$

and
$$\phi_1 = \phi_1' \phi_A$$
$$\phi_2 = \phi_2' \phi_A$$
$$\phi_3 = \phi_B$$

The Flory-huggins relationship for the free energy of mixing can then be written:

$$\frac{\Delta G_m}{RT} = \left(\phi_A/x_A\right) \ln \phi_A + \left(\phi_B/x_B\right) \ln \phi_B +$$

$$\phi_A \phi_B \left[\phi_1' X_{13} \ \phi_2' X_{23} \ \phi_1' \phi_2' X_{12} \right] \qquad (2.43)$$

given that the effective interaction parameter for mixing A and B is represented by

$$X_{eff} = \phi_1' X_{13} + \phi_2' X_{23} + \phi_1' \phi_2' X_{12} \qquad (2.44)$$

Equation (2.43) is then identical to equation (2.18), the Flory lattice theory equation derived earlier.

X_{13} and X_{23} are interaction parameters relating the interactions between units 1 and 2 of the copolymer and unit 3 of the homopolymer. X_{12} is the interaction parameter describing interactions between the two comonomer units or segments in the copolymer.

The necessary condition for mixing is that the free energy of mixing should be negative. The first two terms in equation (2.43), due to the combinatorial entropy, are always negative and so for miscibility, should be sufficiently small and positive in order for ΔG_m to be negative. Figure (2.6) illustrates the ways in which the effective interaction parameter may vary with copolymer composition. The dashed lines show the additive case resulting when $X_{12} = 0$. The implication of each possibility is discussed below.

(a) shows the effect of having a negative or positive X_{12}, resulting in an upward or downward curve of X_{eff} respectively. The X_{ij} parameters indicate the attraction (negative X_{ij}) or repulsion (positive X_{ij}) between the components i and j within the system.

(b) In this case, X_{12}, X_{13} and X_{23} are all positive, that is, the monomer units 1 and 2 of the copolymer (A) repel each other, as well as each repelling the unit 3 of the homopolymer (b). Miscibility is

- 24 -

Figure 2.6
Variation of the Effective Interaction Parameter with Copolymer Composition in a Binary Homopolymer-Copolymer Mixture
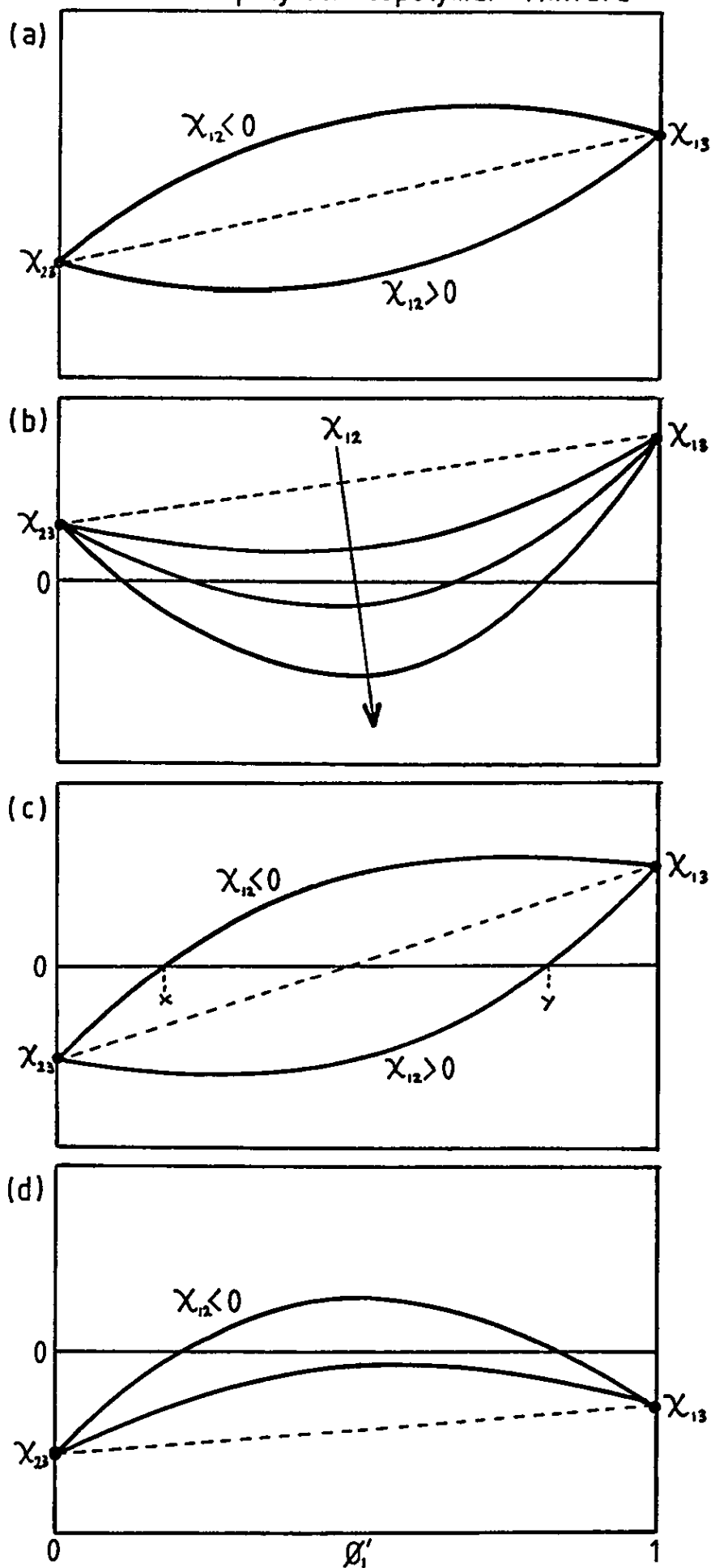
possible for certain compositions, however, if χ_{12} is sufficiently large as to cause χ_{eff} to become negative. In other words, miscibility is favoured when there are strong repulsions between the two units 1 and 2 of the copolymer, provided 1 and 2 attract or only slightly repel the unit 3 of the homopolymer.

(c) Since χ_{23} is negative, copolymers containing a high enough proportion of unit 2 will be miscible when χ_{12} is either negative or positive. Clearly, if units 1 and 2 attract one another, miscibility will result at compositions richer in unit 2 (x), than if 1 and 2 repelled each other (y).

(d) If χ_{12}, χ_{23} and χ_{13} are all negative, miscibility occurs at all compositions, providing the attraction between the copolymer units 1 and 2 is not too great (i.e. χ_{12} highly negative). If this is the case, then at some compositions the effective interaction parameter will become positive leading to phase separation.

Systems showing type (b) behaviour have been observed, examples being styrene-acrylonitrile copolymer with poly(methyl methacrylate), poly(ethyl methacrylate) and poly(n-propyl methacrylate).[26] The methacrylate homopolymers are each immiscible with poly(styrene) and poly(acrylonitrile) respectively, but the blends involving the copolymer exhibit so-called miscibility windows over a range of copolymer compositions.

For a system having $\chi_{eff} < 0$, the relationship between LCST behaviour and the interactions parameter, can be explained in terms of the decreasing effectiveness of intermolecular attractions as the temperature is increased, associated with an increase in free volume. Phase separation occurs at the point when the effective interaction parameter of the system becomes zero. The phase relations and

miscibility in polymer blends containing copolymers was recently discussed by Roe and Rigby,[48] covering both binary and ternary systems.

Recently, the miscibility behaviour of random copolymer blends has been discussed based on Flory's equation of state theory.[133] Miscibility was explained by the change of sign of the intermolecular interaction parameter X, expressed in terms of the intersegmental interaction parameters. The way in which the temperature dependence of X changes with copolymer composition was also discussed.

2.6 Methods of Determining the Interaction Parameter

2.6.1 Solubility Parameter Theory

The Flory-Huggins lattice theory and the equation of state theories, both attempt to explain or model, experimentally observed miscibility behaviour, but they cannot easily predict such behaviour given only information about the physical properties of the pure unmixed components. Since the interaction parameter X, is clearly an important factor determining the miscibility of a given system, it would be useful to be able to estimate its value experimentally. One of the ways in which this can be achieved is by utilising solubility parameters. Hilderbrand[49] proposed that the solubility of a solute in a solvent was related to the energy of vaporisation per unit volume, or "internal pressure" $(\Delta E/V)$. This quantity is also termed the cohesive energy density (CED), the square root of which is defined as the solubility parameter.

$$\left(\frac{\Delta E^v}{V}\right)^{1/2} = \delta = (CED)^{1/2} \qquad (2.45)$$

δ is proportional to the cohesion of the solution, equivalent to the strength of attraction between the molecules in the solution. Obviously, the energy of vaporisation cannot be found for polymer-

polymer mixtures. The cohesive energy density (hence δ) can, however, be determined in a number of ways. Olabisi and Simha[50] calculated δ by considering the internal pressure

$$\delta^2 = P_i \left(\frac{\delta U}{\delta V}\right)_T \cong \frac{T\alpha}{\beta} \qquad (2.46)$$

Where α is the thermal expansion coefficient ($^{\circ}C^{-1}$), and β is the compressibility (m^3/J). A semi-empirical equation of state of polymer melts was used to develop a generalised relation for P_i which could be used to calculate δ from the above equations.

The solubility parameter can also be calculated directly from heats of solution, by chromatography or solution behaviour. Methods which allow estimation of δ from group contribution methods have also been compiled by Van Krevelen. This method is based only on the chemical structure of the polymer repeat units and the related molar volumes.

Hildebrand derived an equation allowing the calculation of the enthalpy of mixing ΔH_m from solubility parameters.

$$\frac{\Delta H_m}{V} = \phi_1 \phi_2 (\delta_1 - \delta_2)^2 \qquad (2.47)$$

Where V is the total volume of the mixture. If the expression for ΔH_m from the Flory-Huggins lattice theory (equation 2.14) is substituted into the above relationship, the resulting expression is

$$\frac{RT\chi}{V} = (\delta_1 - \delta_2)^2 = B \qquad (2.48)$$

The term $RT\chi/V$ is generally defined as B, the binary interaction energy density.

It is clear from equation (2.47) that the enthalpy of mixing is always positive when calculated from solubility parameters, hence,

predicting immiscibility. The Hildebrand relationship does not take into account specific interactions and in many miscible blends, such interactions are the principle reason for miscibility. It is necessary, therefore, to modify the expression for cohesive energy density and solubility parameters to account for this. One simple modification for the cohesive energy of a system is as follows

$$E_{COH} = E_d + E_p + E_h \qquad (2.49)$$

where the subscripts d, p and h stand for dispersive, polar and hydrogen-bonding contributions respectively. The enthalpy of mixing is then given by

$$\frac{\Delta H_m}{V} = \phi_1 \phi_2 \left[\left(\delta_{d_1} - \delta_{d_2} \right)^2 + \left(\delta_{p_1} - \delta_{p_2} \right)^2 + \left(\delta_{h_1} - \delta_{h_2} \right)^2 \right] \qquad (2.50)$$

This still does not allow for negative values for ΔH_m. Paul and Barlow[47] have developed a binary interaction model for predicting the miscibility of blends involving copolymers, based on the solubility parameter approach. The assumption that the cohesive energy density (c_{ij}) between unlike pairs i and j can be given by

$$c_{ij} = \sqrt{c_{ii} \cdot c_{jj}} \qquad (2.51)$$

was modified by the incorporation of a parameter k which then allows a negative value of B and hence ΔH_m

$$c_{ij} = \left(1 - k_{ij} \right) \sqrt{c_{ii} c_{jj}} \qquad (2.52)$$

The binary interactions energy density B_{ij} can be found as follows

$$B_{ij} = c_{ii} - 2c_{ij} + c_{jj} \qquad (2.53)$$

Incorporation of (2.52) into (2.53) leads to the expression

$$B_{ij} = \left(\delta_i - \delta_j\right)^2 + 2k_{ij}\delta_i\delta_j \qquad (2.54)$$

It was shown that B_{ij} can be negative for certain values of the parameter k_{ij}.

2.6.2 Inverse Gas Chromatography (IGC)

Inverse gas chromatography (IGC) is so called because the stationary phase is the phase of interest, in contrast to conventional gas chromatography. The polymer or polymer mixture to be studied is coated onto an inert support material.[55] This is usually done by dissolving the polymer in as suitable solvent, mixing with the support, followed by removal of the solvent by evaporation. It is then possible to measure and evaluate the thermodynamic interaction of polymers (above their glass transition) with low molecular weight probes.

Despande et al[56] were the first to suggest the use of IGC for studying polymer mixtures. Based on Flory-Huggins expression for the enthalpy change on mixing (ΔH_m), a method was proposed which led to the evaluation of the polymer-polymer interaction parameter, χ. The method has been used to study several oligomeric binary polymer blends.[57] Olabisi[58] was one of the first to study high polymers by this technique. Systems such as poly(vinyl chloride) with several acrylates and methacrylates,[59] and also with chlorinated polyethylene have also been studied.[60]

A brief discussion of the theory enabling the evaluation of χ is now appropriate.[61] The elution behaviour of a volatile substance

(probe) on a gas chromatographic column is usually described by its specific retention volume, V_g such that

$$V_g = \left(V_r - V_0\right)/w = V_n/w$$

(2.55)

Where V_r is the probe elution volume, V_0 is the column void volume and V_n is the net retention volume ($V_r - V_0$). w is the mass of the polymer on the column. A superscript of 1 denotes the probe, whilst subscripts 2 and 3 denote the two polymers within the blend. If the Flory-Huggins theory is now combined with expressions relating chromatographic calculations, a relationship for the residual binary interaction parameter χ_{12} can be written

$$\chi_{12} = \ln\left(RTV_2/V_g V_1 P_1^\circ\right) - 1 + V_1/M_2 V_2 - \left(B_{11} - V_1\right)P_1^\circ/RT$$

(2.56)

V_1 and P_1° are the probe molar volume in the liquid phase and the saturated vapour pressure respectively. B_{11} is the second virial coefficient of the probe in the gas phase and V_2 is the specific volume of the polymer at the experimental temperature. R is the universal gas constant. For most cases involving high molecular weight polymers the third term in the equation can be omitted. Equation (2.56) applies to a single polymer system and therefore, must be modified to allow for the second polymer.

If χ_{23} is the binary interaction parameter for the two polymers in the system, the related parameter χ'_{23} can be defined as

$$\chi'_{23} = \left(V_1/V_2\right)\chi_{23}$$

(2.57)

χ'_{23} is a less cumbersome term since it no longer contains the large molar volume term. The χ'_{23} parameter can then be evaluated from the following expression

$$\chi'_{23} \quad (1/\phi_2\phi_3) \left[\ln \left(\frac{V_{g,\,blend}}{w_2V_2 + w_3V_3} \right) - \phi_2 \ln \left(\frac{V_{g,2}}{V_2} \right) - \phi_3 \ln \left(\frac{V_{g,3}}{V_3} \right) \right] \quad (2.58)$$

The second subscript after V_g indicates the nature of the column and w_i is the weight fraction of the two components in the blend.

In recent review, Mandal et al[62] conclude that determining polymer-polymer miscibility from the sign of χ'_{23} as determined by IGC, is possible for systems associated with strong specific interactions, but that such values are not reliable. It is suggested that if several binary blends are studied in which one component is one of a homologous series (for example PVC with methacrylates), much information can be obtained about the relative miscibility from an examination of the χ'_{23} values. It is also suggested that the method is insufficiently accurate to allow determination of miscibility in systems where χ'_{23} is near to zero. Mandal et al[62] also conclude that the accuracy of the method may be expected to improve in the future, as a result of sustained research and thus its usefulness will correspondingly increase.

2.6.3 Small Angle Neutron Scattering

Small angle neutron scattering (SANS)[32,63,64] is a technique which has been applied recently to the investigation of polymer blends and in particular, to the determination of the interaction parameter χ. SANS involves the bombardment of a sample with a beam of neutrons and this necessitates a nuclear reactor as source. One of the blend components is isotopically labelled with deuterium, because of the large difference in scattering lengths of protons and deuterium. This allows the scattering due to varying concentrations of the deuterated polymer phase to be observed, at temperatures in

excess of the glass transition temperatures of the polymers involved. The scattering from binary mixtures can be split up into terms arising from intermolecular and intramolecular correlations. The intermolecular component of the interaction parameter χ can then be evaluated from scattering by systematically analysing either the scattering intensity extrapolated to zero, or the apparent radius of gyration.

The derivation of equations enabling the evaluation of χ have been discussed by Higgins et al,[33] as applied to the temperature and concentration dependencies of the interaction parameter in oligomeric polymer blends and also to molecular conformation. The technique has been used to study interactions in mixtures of poly(ethylene oxide) and poly(methyl methacrylate),[65] leading to the observation of a small negative value for χ_{AB} for the mixture.

Curro and Schweizer[66] have recently formulated and implemented a microscopic, statistical mechanical theory of the structure and thermodynamics of polymer blends, which they anticipate will provide a molecular basis for the understanding of a wide range of interesting phenomena including neutron scattering. Density, concentration fluctuations and intramolecular structural details are included in the treatment, which allows a unified approach to small and large wavelength phenomena. A general formula for the interaction parameter is presented as a function of concentration, packing fraction, molecular weight and structural symmetry.

2.6.4 Group Contribution Methods for Predicting Polymer-Polymer
Miscibility

A group contribution method for predicting polymer-polymer miscibility, is one which is able to estimate the heat of mixing of two polymers in a binary system, by considering the heats of mixing

of low molecular weight liquids having similar structures to the polymer repeat units involved. Providing the low molecular weight liquids are chosen carefully, such that they closely approximate to the multigroup structure of the blend components, it should in theory be possible to predict the heat of mixing of the two polymers from the heats of mixing of their analogues.

Lai et al[67,68] have compared the ability of two group contribution methods, to fit and predict the heats of mixing of a variety of ester alkanes and chlorinated hydrocarbons, as well as using one of the methods to predict the heats of mixing of various polyester containing blends. The two models considered were the universal quasi-chemical (UNIQUAC)[69] method and a modified Guggenheim quasi-chemical(MGQ)[70,71] method. Lai et al concluded the MGQ method was more applicable to predicting the heats of mixing in systems involving at least one polar component. Since miscible systems often necessitate interactions between polar groups, it was suggested that the MGQ method should prove superior to the UNIQUAC method in general. Preliminary results suggested that it is possible to predict the heats of mixing, and hence, the nature of miscibility for a chosen system, provided accurate values are available for the heats of mixing of the low molecular weight analogues.

The MGQ method was applied to blends of aliphatic polyesters with bisphenol A polycarbonate, the poly(hydroxy ether) of bisphenol A and with tetramethylbisphenol A polycarbonate. Other systems studied include bisphenol A polycarbonate with poly(methyl methacrylate).[68] It was concluded that the method could, with varying degrees of success, predict the limits of miscibility of the systems studied and adequately predict the magnitude of interaction parameters for some of the blends. Problems were encountered as the complexity of the blend components increased, this related to the

failure to model accurately the monomer repeat units by low molecular weight analogues. Other shortcomings of this approach are that the influences of polymer tacticity and branching are not considered. Another factor overlooked is the restricted access of the groups attached to polymer chains, compared to the small molecule analogues. Such analogues must also be carefully chosen, so that the molecular surroundings of the analogues are comparable to the molecular surroundings of the groups on the polymer chains. Consider, for example the varying acidity of -OH groups, depending on the groups to which they are attached. Despite the shortcomings mentioned above, the method could be useful for predicting polymer-polymer miscibility in some cases, providing appropriate analogues are chosen, having accurately known heats of mixing, and providing the monomer units of the components are not too complex.

2.7 Thermodynamic Theory of Hydrogen Bonding in Polymer Blends

The simple Flory Huggins theory for the thermodynamics of the mixing of polymers, predicts negligibly small combinatorial entropy and positive enthalpy terms, for a system in which Van der Waals - type interactions are present. To obtain miscible homopolymer blends it is usually necessary to have some sort of attractive force between unlike segments. Hydrogen bonding interactions lead to true association of polymer segments, and above the Tg there is a dynamic equilibrium distribution of hydrogen bonded species. For example, in ethylene-methacrylic acid copolymers containing only 5% acid units, virtually all of the carboxyl groups are present as hydrogen bonded pairs.[74] This could not be predicted on the basis of random mixing.

Another problem in treating hydrogen bonded systems is that the forces between interacting functional groups are a complex function of electrostatic, dispersive and repulsive terms, and the description

- 34 -

of a potential function requires a knowledge of the charge distribution and specific arrangement of molecules. A further limitation of lattice theories, is that they assume that the internal degrees of freedom of each molecule or segment are not seriously disturbed by the proximity of other molecules in the mixture. When polymer segments are associated by hydrogen bonding, the rotational and vibrational degrees of freedom become seriously modified. This can be observed in the infrared spectrum. Painter et al[74,75] have developed an association model for a binary polymer blend in which one polymer self-associates, whilst the second does not, but is capable of hydrogen bonding with the first. The theory is based on that proposed by Kretschmer and Wiebe, which treats the associated complexes as distinguishable and independent molecular species. The hydrogen bonding interaction is considered separately from the forces involved in mixing and the number and distribution of species present is defined by means of particular types of hydrogen bonds. Painter et al made the following three assumptions, upon which their theory depended.

(a) The hydrogen bonded species that can form are unaffected by the covalent linkage of interacting units into polymer chains.

(b) The equilibrium constants are independent of the length of the hydrogen bonded chains.

(c) the equilibrium constants can be defined in terms of a chemical repeat unit and can thus be experimentally determined by spectroscopic measurements.

It is argued that (b) may not be accurate and that two equilibrium constants are required, one to describe dimer formation and a second for the formation of associations involving longer chains. In the main treatment only one equilibrium constant is used, but a two-equilibrium constant model is also discussed.

- 35 -

An expression for the free energy of mixing was derived, which was made up of parameters which can be determined experimentally by infrared spectroscopy. In order to investigate the model's ability to describe the phase behaviour of binary polymer systems, an expression for the spinodal was derived from the equation for the free energy of mixing. A wide variety of phase behaviour was predicted due to the temperature dependence of the hydrogen bonding and physical interactions in the simulated mixtures.

The ability of the theory to accurately predict miscibility and phase behaviour has been tested by calculating free energy changes, and by comparing the phase diagrams calculated theoretically to those obtained experimentally, for a number of blends of poly(4-vinyl phenol) with various polyacrylates, polyacetates and polylactones.[77] The fractions of hydrogen bonded acrylate carbonyls in the blends were determined using FTIR spectroscopy, and a very good agreement was found to the fractions predicted by the theory based on equilibrium constants. Spinodals were calculated for all the polymer pairs studied and there was a broad general agreement with experimentally observed phase behaviour, as determined by thermal analysis.

The association model of Painter and co-workers does appear to be potentially quite valuable for predicting the miscibility and phase behaviour of polymer blends in which hydrogen bonding is a factor. However, many more blend systems must be studied in order to confirm the general applicability of this particular theoretical treatment.
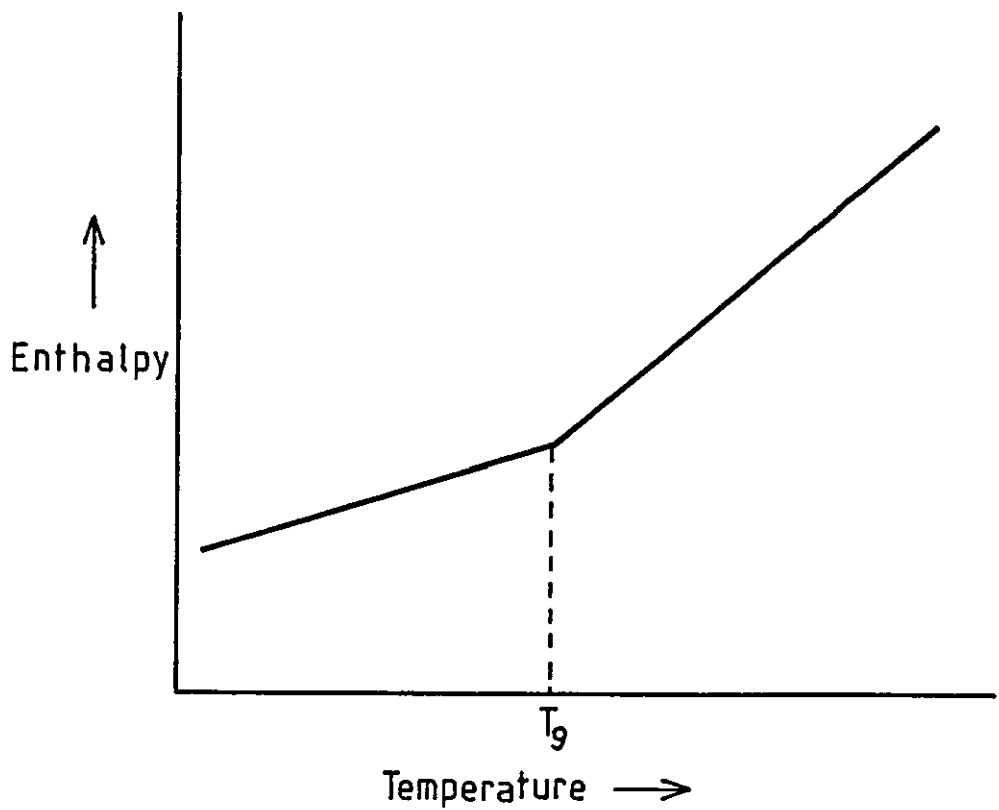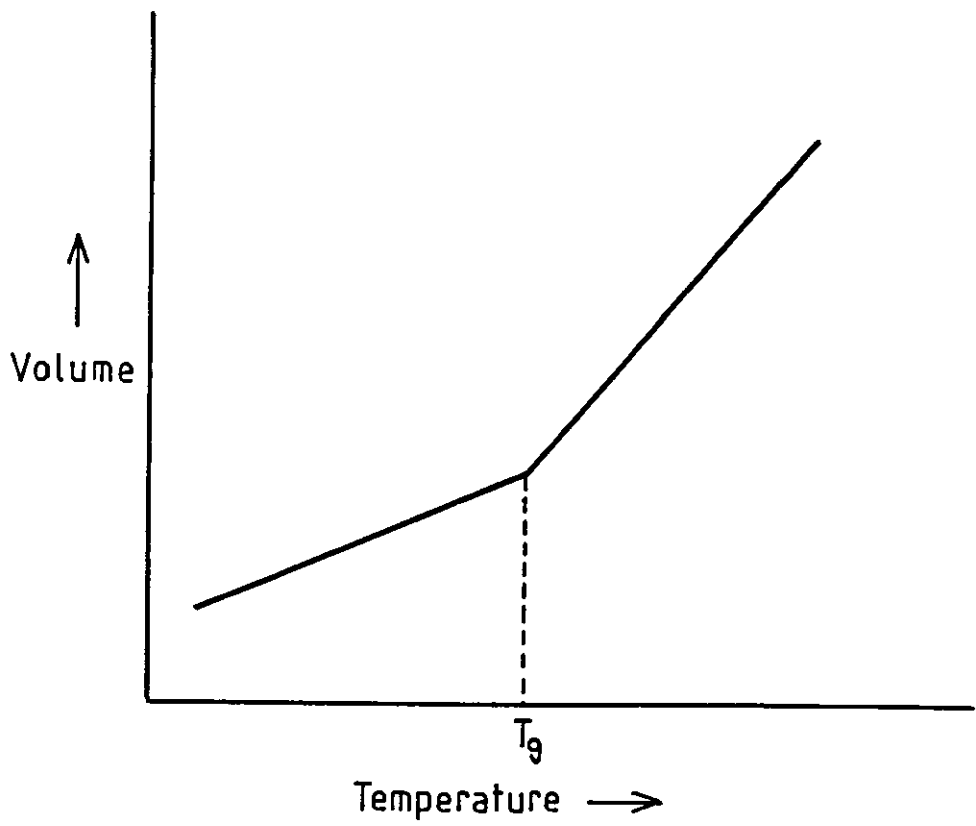
2.8 The Glass Transition

When a high molecular weight amorphous polymer in its liquid or rubbery phase is cooled, at some temperature, called the glass transition temperature (Tg), the physical and mechanical behaviour of the polymer will be transformed to that of a rigid glassy material. At this temperature there is a marked change in the temperature dependence of volume (V) and enthalpy(H), as shown in figure (2.7). There is also a discontinuity in the temperature dependence of heat capacity ($C_p = dH/dT$) and expansion coefficient (dV/dT) at the Tg. The position of the Tg depends on the rate of cooling, with different cooling rates leading to different observed Tg transitions, each reflecting a difference in the nature of the glassy phase formed.

There has been some debate as to whether or not the glass transition is a true thermodynamic phenomenon. Tg does correspond to a second order transition, but it is likely that the kinetics of the process are also important. On heating, the Tg is usually interpreted as the point at which there is sufficient thermal energy to initiate the onset of molecular motion and conformational changes, due to rotation about the bonds along the main backbone of the polymer chain. Below the Tg (α-transition) such movement is severely limited, although for many polymers β-transitions (secondary relaxations) have been observed, which are believed to be due to movements in side chains or groups. Such secondary relaxations are on a much smaller scale than the Tg process, and so will be neglected in the following discussion.

The two main theoretical explanations for Tg behaviour are the thermodynamic and kinetic treatments. Neither theory is able to fully explain the phenomenon, and it is likely that a combination of

Figure 2.7
Volume and Enthalpy vs Temperature
Showing Discontinuity at T_g

the two would be required for a more complete explanation of the process.

2.8.1 Kinetic Theory

The most widely used theory for quantifying the behaviour observed in the region of the glass transition is the kinetic theory of Flory and Fox.[79],[80] They proposed that a material may be considered to have a volume made up of two contributions, that which is occupied by molecules and that which consist of vacancies or holes, making up the free volume. Conformational changes are, therefore, movements of chain segments into free volume. The greater the free volume, the greater the extent of molecular motion possible. The glass transition temperature is the point below which there is insufficient free volume for significant molecular motion to be possible, and so below this temperature the conformational structures of the chains are "frozen" in.

Below Tg, the only temperature - induced volume changes are due to molecular expansion or contraction, as the free volume is considered to be constant. The total volume at Tg (V_g) is given by

$$V_g = V_0 + V_f \left(\frac{dV}{dT}\right)_g T_g \qquad (2.59)$$

Where V_o is the molecular volume of the material at absolute zero, V_f represents the free volume within the glassy region and $(dV/dT)_g$ is the expansivity of the molecular or occupied volume in the glass. At a temperature T, above the Tg, the total volume, V_R is given by

$$V_R = V_g + \left(dV/dT\right)_R \left(T - T_g\right) \qquad (2.60)$$

$(dV/dT)_R$ represents the expansivity of the total volume above Tg, consisting of both molecular and free volume expansions.

$$\left(\frac{dV_f}{dT}\right) = \left(\frac{dV}{dT}\right)_R - \left(\frac{dV}{dT}\right)_g \qquad (2.61)$$

If α_R and α_g are the thermal expansion coefficients immediately above and below Tg respectively,

$$\alpha_R = \frac{1}{V_g}\left(\frac{dV}{dT}\right)_R \qquad\qquad \alpha_g = \frac{1}{V_g}\left(\frac{dV}{dT}\right)_g \qquad (2.62)$$

The expansion in free volume in the region of Tg is then given by $\qquad \alpha_R - \alpha_g = \Delta\alpha \qquad\qquad (2.63)$

Doolittle[81,82] derived an expression relating viscosity and volume, incorporating the concept of free volume which proved useful when considering small molecule liquids

$$\ln\eta = \ln A + B\left[(V-V_f)/V_f\right] \qquad (2.64)$$

Where A and B are constants and η is the viscosity of the liquid. V and V_f are the total volume and free volume respectively.

If the fractional free volume f, is defined as V_f/V the Doolittle expression becomes

$$\ln\eta = \ln A + B\left(\frac{1}{f} - 1\right) \qquad (2.65)$$

If Tg is used as a reference point, the viscosity of a liquid at a temperature above Tg, T can be found from

$$\ln\left(\frac{\eta}{\eta_g}\right) = B\left(\frac{1}{f} - \frac{1}{f_g}\right) \qquad (2.66)$$

Where f_g and η_g are the fractional free volume and viscosity at Tg. Assuming the value of f increases linearly above Tg, it can be written as follows

$$f = f_g + \Delta\alpha\left(T - T_g\right) \qquad (2.67)$$

Substituting in the previous equation gives

- 39 -

$$\ln\left(\frac{\eta}{\eta_g}\right) = \frac{B}{f_g}\left(\frac{T - T_g}{f_g/\Delta\alpha + (T - T_g)}\right) \qquad (2.68)$$

This equation is of the same form as the Williams, Landel, Ferry (WLF) equation[83]

$$\log_{10}\left(\frac{\eta}{\eta_g}\right) = \frac{-C_1(T - T_g)}{C_2 + (T - T_g)} = \log_{10}a_T \qquad (2.69)$$

Where C_1 and C_2 are constants for many glass forming liquids, ($C_1 = 17.44$ and $C_2 = 51.6$) and a_T is the ratio of relaxation time at T to the relaxation time at Tg.

2.8.2 Thermodynamic Theories

As already mentioned, on cooling the melt of an amorphous polymer, at some point it will undergo the transition to a glassy state. The nature of the glass and the extent of the disorder (hence, free volume) frozen in will depend on the rate at which the transition is approached, as will the temperature at which the transition occurs. Thermodynamic theories propose that there is a true thermodynamic glass transition, at some temperature below the experimentally observed (ie rate determined) Tg, which could be attained if the melt were cooled at an infinitely slow rate.

The concept of a thermodynamic transition is useful, because it resolves a paradox discovered by Kauzmann,[84] which is that if the equilibrium properties (volume and entropy) of a liquid are extrapolated through the glass transition, they appear to become smaller than the values obtained for the crystalline state below a certain temperature. If thermodynamics are neglected, however, kinetics and experimental observations show that the specific volume of a polymer able to crystallise will decrease significantly at a temperature below Tg, compared to an amorphous polymer, on passing

through it's glass transition. See figure (2.8).

The most well known thermodynamic theory of the glass transition is that developed by Gibbs and Dimarzio.[85] This attempts to explain the glass transition from a more molecular point of view, with allowances made for the chain stiffness and variation of volume with temperature. Using a lattice model similar to that used by Flory and Huggins, each segment of the polymer chain is allowed several different orientations, having different orientation (or flex) energies. In the lattice there are a number of vacant sites or holes into which segments of the chain can move. As the temperature is decreased, the system tends towards lower free energy, that is having a smaller number of holes and a larger percentage of bonds existing in the low flex-energy orientation (ie stiffer chain). As a result of this the entropy decreases until, at a temperature T_2, the number of allowed states available to the system is reduced to one or a very small number. In this state no conformation changes are possible, and below this temperature T_2, the entropy of the system remains constant, that is zero conformational entropy. Thus, T_2 is the equilibrium glass transition temperature, to which the experimentally observed glass transition converges in the case of an infinitely slow time scale.

Adams and Gibbs[86] extended the Gibbs Dimarzio approach to allow for non-equilibrium conditions. The theory attempts to explain the temperature dependence of relaxation behaviour in terms of the variation of the size of a 'co-operatively rearranging region' (CRR). The CRR is defined as the smallest unit that can undergo a transition to a new conformation without simultaneous conformation change, on or outside it's boundary. An equation was derived which is of the same form as the WLF equation:

$$-\log_{10} a_T = \frac{a_1 (T - T_s)}{a_2 + (T - T_s)} \qquad (2.70)$$

- 41 -

Figure 2.8

Volume – Temperature Relationship for a Typical Polymer
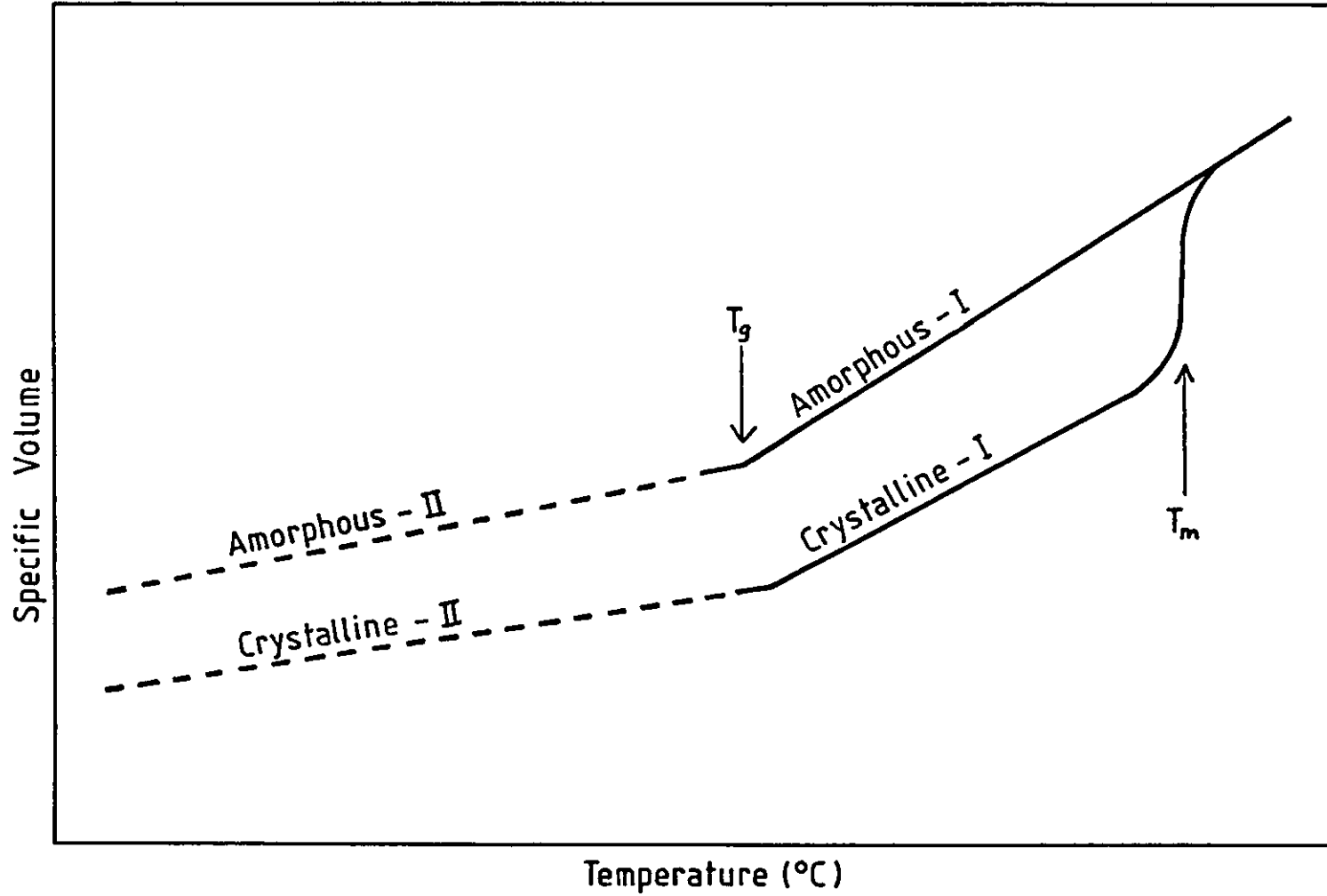
Where Ts is a reference temperature, and

$$a_1 = \frac{2.303 \, c}{\Delta c_p T_s \ln\left(T_s/T_2\right)} \qquad (2.71)$$

and

$$a_2 = \frac{T_s \ln\left(T_s/T_2\right)}{\ln\left(T_s/T_2\right) + \left[1 + T_s/T - T_s\right] \ln\left(T/T_s\right)} \qquad (2.72)$$

a_2, is in fact temperature dependent, but to an extent which only slightly affects the calculations. If T_s is appropriately chosen, a_1 and a_2 correspond closely to the constants in the WLF equation. The Adams-Gibbs theory uses thermodynamic properties of the equilibrium melt in order to explain the kinetic properties of a glass-forming liquid.

Cohen and Grest[87] have recently attempted to interpret more explicitly the concept of free volume, by devising a molecular theory in which solid-like and liquid-like cells surrounding each molecule are distinguished. The theory investigates how the fraction (p) of liquid-like cells varies with temperature. At a temperature Tp, there is a discontinuity in the change of the fraction p and below this temperature, p remains below a critical fraction P_c required for liquid-like flow. The temperature Tp is then identified as the glass transition temperature. The theory proposes that the glass transition is an equilibrium phenomenon, but unlike the Gibbs-Dimarzio theory, predicts the transition at Tp to be, most probably, 1st order. The Gibbs-Dimarzio theory predicted the transition T_2 to be a second order transition.

Chow[88] has developed a new approach to analyse the role of chain conformation in equilibrium thermodynamics and kinetics of the glass transition phenomenon. Chow treats the "equilibrium" glass transition temperature (Tr) as a thermodynamic anomaly not a second-

order transition, by using Flory's lattice statistics of chain molecules. T_r occurs when the most stable hole conformation is reached under the cooperative constraint of linear chains. It was found that T_r was determined mainly by the stiffness of the polymeric chains and that the ratio of the hole (intermolecular) and flex (intramolecular) energies varies only between 2 and 2.3, supporting the idea that the conformation theory is experimentally equivalent to the hole theory.

Recently,[104] a new relationship, which correlates the glass transition temperature with other molecular parameters, was developed by using Flory's lattice statistics of polymer chains and taking the dynamic segment as the basic statistical unit. The dependence of Tg on the chain stiffness factor, dynamic stiffness factor and polymer molecular weight are discussed in detail based on the theory. It was shown that Tg is governed by the chain stiffness factor at Tg. Good agreement was found between theoretical predictions and experimental data for many linear polymers.

2.8.3 Factors Which Affect the Glass Transition Temperature

The observed theories explain, at least in part, the observed dependence of the Tg on the nature and properties of the polymer in question. The main factors which affect the Tg are discussed below (all Tg values quoted, taken from Polymer Handbook).[89]

(a) Chemical Structure

There are several structural factors which influence the Tg of a polymer, one of the most important being the flexibility of the backbone chain. Clearly, a polymer having a structure which allows easy rotation around main chain bonds will have a lower Tg than one where such rotations, and hence conformational changes are hindered.

This can be illustrated by the following examples. Polyisoprene - $(-CH_2-CH=C(CH_3)CH-)$ has a Tg of $-73°C$ compared to bisphenol A polycarbonate having a Tg of $150°C$ with a structural formula
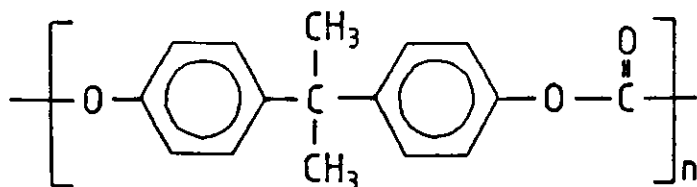
In general, polymers having p-phenylene type groups along the backbone chain tend to be very inflexible and therefore have high glass transition temperatures.

Side groups also influence the position of the glass transition. For example, poly(methyl acrylate) has a Tg of $10°C$, whereas poly(methyl methacrylate) has a Tg of $105°C$. The methyl group tends to hinder rotation about the main chain leading to a stiffer material and higher Tg. However, in some cases side groups can have the reverse effect. Consider the following series of poly(acrylates) and their respective glass transition temperatures. Poly(methyl acrylate) (Tg $10°C$), poly(ethyl acrylate) (Tg $-24°C$), poly(propyl acrylate) (Tg $-37°C$) and poly(n-butyl acrylate) (Tg $-54°C$). As the size of the side groups is increased the Tg decreases. This is due to an increase in free volume caused by poorer chain packing as the size of the side group increases. The greater the free volume, the lower the Tg.

The symmetry of the repeating unit in a polymer chain can also affect the Tg. One example of this sort of effect is the variation in Tg between poly(propylene) (Tg $-8°C$) and poly(iso-butylene) (Tg $-50°C$).[90] The decrease in Tg caused by the second methyl group can be explained in terms of the energy barriers to rotation between the various conformational isomers. In poly(iso-butylene) the energy

barriers between each conformational isomer are approximately equal, because of the symmetry of the carbon atom to which they are attached. This means there is no preferred isomer. This is not true for poly(propylene), where one of the three possible gauche states is of a higher energy than the other two, therefore, rotation to this conformational isomer is not favourable. This causes a decrease in the tendency to free rotation and this in turn leads to a higher Tg for poly(propylene) than for poly(iso-butylene).

The polarity of substituents also appears to have an effect on the Tg. Polymers having polar groups attached to the chain tend to have higher values of Tg than analogous polymers having no polar groups. Consider poly(acrylonitrile) with a Tg of 105°C and poly(propylene) with a Tg of -19°C. This could be explained in terms of hindered rotations caused by intermolecular interactions. Alternatively, the presence of intermolecular interactions can be expected to lead to a reduction in free volume, since the polymer chains would be brought closer together. This means that the fractional free volume required for the glass transition would be achieved at a higher temperature.

(b)   Crosslinking

Crosslinking has been observed to increase the Tg of a polymer to an extent depending on the degree of network formation. Crosslinking leads to a reduction in free volume and therefore, the fractional free volume necessary for the glass transition to occur is displaced to a higher temperature. Clearly a crosslinked network has fewer conformational possibilities and so a lower entropy than an uncrosslinked polymer.

(c)   Molecular Weight

For high molecular weight polymers, the Tg is effectively

independent of molecular weight. However, the Tg of shorter chain polymers decreases with chain length. This effect can be explained in terms of chain ends and the free volume associated with them. Chain ends, in effect, disrupt the packing of molecules and the greater the number of chain ends, the greater the free volume. Lower molecular weight polymers have a higher proportion of chain ends and hence, free volume. So by decreasing the chain length, the Tg is also decreased. An expression which relates the effect of molecular weight on the glass transition temperature is as follows

$$T_g = T_{g\infty} - \frac{K}{M} \qquad \text{where} \qquad K = \frac{2\rho L \phi}{\alpha} \qquad (2.73)$$

Where $T_{g\infty}$ is the glass transition temperature at infinite molecular weight M, of a polymer having a density ρ and expansion coefficient α. L is Avogadro's number and ϕ is the free volume occupied by a chain end.

(d) Effect of Diluents

Adding low molecular weight species to a polymer causes plasticisation. This is commonly utilised in polymer applications, an example being the conversion of poly(vinyl chloride) from a rigid to a much more flexible material, by the incorporation of low molecular weight additives or plasticisers.

Again, the decrease in the Tg observed on addition of diluents can be explained in terms of an increase in free volume. Smaller molecules have a greater free volume and their addition to a polymer increases the overall free volume.

(e) Copolymerisation and Blending

A special case of diluent addition is the incorporation of

- 46 -

another monomer unit or polymer. The effect this has on the Tg depends on the miscibility of the two polymers. A miscible polymer blend will exhibit a single Tg, at some point in between the Tg values of the two unmixed components, the exact position depending on the blend composition. An immiscible blend exhibits two glass transitions which correspond closely to the Tg values of the two components. A partially miscible blend will usually show two glass transitions at positions determined by the nature of the phases present in the mixture.

Several equations have been proposed to describe the composition dependence of miscible polymer blends, having been first developed for predicting the Tg values of random copolymers. Such equations attempt to relate the Tg of a copolymer to the Tg values of the homopolymers derived from the co-monomer units. Wood[91] has shown that this relationship can be generalised as follows

$$T_g = A_A T_{g_A} C_A + A_B T_{g_A} C_B \qquad (2.74)$$

Where the copolymer glass transition temperature (Tg) is related to the homopolymer glass transition temperatures (T_{g_A}, T_{g_B}), the concentration of monomer repeat units (C_A, C_B) and a constant (A_A, A_B) describing some physical property of the homopolymer.

An expression of this form was derived by Gordon and Taylor,[92] who assumed that in a copolymer, the partial specific volumes of the component repeat units are constant and equivalent to the specific volumes of the two homopolymers. An expression for the copolymer Tg was found by equating the specific volumes in the glassy and rubbery states

$$T_g = T_{g_A} + \frac{\left(K T_{g_B} - T_{g_A}\right) w_B}{1 + (1 - K) w_B} \qquad (2.75)$$

Where $K = \dfrac{A_A}{B_B} = \left[(\alpha_B/\rho_B)_r - (\alpha_B/\rho_B)_g\right] \Big/ \left[(\alpha_A/\rho_A)_r - (\alpha_A/\rho_A)_g\right]$ (2.76)

It was assumed also that the thermal expansion coefficients in the rubbery and glassy states are the same in the copolymer as in the homopolymers. The term α_i/ρ_i is the specific thermal expansivity of component i and W_B is the weight fraction of repeat unit B in the copolymer.

The Fox equation[93] is a special case of the Gordon-Taylor equation, where K is equal to the ratio of the equivalent homopolymer glass transition temperatures (T_{g_A}/T_{g_B})

$$\frac{1}{T_g} = \frac{W_A}{T_{g_A}} + \frac{W_B}{T_{g_B}} \qquad (2.77)$$

Another relationship resembling the Gordon-Taylor equation is the Kelly-Bueche[94] equation

$$T_g = \frac{\Delta\alpha_A\phi_A T_{g_A} + \Delta\alpha_B\phi_B T_{g_B}}{\Delta\alpha_A\phi_A + \Delta\alpha_B\phi_B} \qquad (2.78)$$

Here, the composition dependence of Tg is described for polymer-diluent systems with the concentrations being expressed in volume fractions.

Gibbs and Dimarzio[95] devised a thermodynamic interpretation of the Tg in random copolymers, using the basis that the conformational entropy for the two homopolymers at T_2 is zero.

$$W_A\left(\frac{X_A}{M_A}\right)\left(T_2 - T_{2A}\right) + W_B\left(\frac{X_B}{M_B}\right)\left(T_2 - T_{2B}\right) = 0 \qquad (2.79)$$

Where X_i is the number of flexible bonds of repeat unit i, having molecular weight M_i. W_i is the weight fraction of a repeat unit i.

The glass transition was assumed to be independent of molecular weight, being a function of ϵ/kT, where ϵ is the stiffness energy

of rotatable bonds and k is the Boltzmann constant. Although the equation applies to the second order transition, it can also be applied to the composition dependence of the glass transition without incurring significant errors.

One feature of several of the treatments so far mentioned, is that no allowance is made for the effect of A-B sequences in the copolymer, or the stiffness of A-A or B-B bonds. This is one reason why such relationships often predict a copolymer Tg which is at variance with the experimentally observed Tg. Johnston[96] devised an approach which accounts for the sequence distribution of the copolymer. AA and BB sequences were assumed to have the same Tg as the respective homopolymers, whereas AB sequences were assigned their own Tg value. The probabilities of like (P_{AA}) and unlike (P_{AB}) sequences can be found using equations to determine sequence length distributions. The resulting equation is

$$\frac{1}{T_g} = \frac{w_A P_{AA}}{T_{gAA}} + \frac{w_A P_{AB} + w_B P_{BA}}{T_{gAB}} + \frac{w_B P_{BB}}{T_{gBB}} \quad (2.80)$$

Johnston described a number of methods to determine T_{gAB}, all of which use experimentally determined Tg values of a series of copolymers.

A classical thermodynamic treatment of the effect of composition on glass transition temperatures, applying specifically to miscible polymer blends has been discussed by Couchman and Karasz.[97] It was assumed that the excess entropy change (ΔS_m) and volume change (ΔV_m) on mixing were continuous at the Tg. The validity of this assumption depends on the extent and nature of specific interactions present in a particular system. Two equations were derived, one arising from the entropy continuity condition and

the other one from the volume continuity criteria at Tg. The entropy derived equation is

$$\ln T_g = \frac{w_A \Delta c_{PA} \ln T_{g_A} + w_B \Delta c_{PB} \ln T_{g_B}}{w_A \Delta c_{PA} + w_B \Delta c_{PB}} \qquad (2.81)$$

It was further assumed that the heat capacity difference (Δc_{p_i}) between the glassy and rubbery states in the pure components, defined per unit mass, are temperature independent. Experimental analysis of the effectiveness of the equation of Couchman and Karasz indicates that the entropy derived expression is the more generally applicable of the two.[98]

Goldstein,[99] however disputes the fact that the Couchmann-Karasz equations can be justified from a purely thermodynamic standpoint. The basis for this argument is that the definition of the entropy of mixing when either or both polymers are in their glassy states is inappropriate. Goldstein also concluded that an alternative definition of ΔS_{mix} having a sounder physical basis does not lead to a prediction of the blend Tg. Nevertheless, the Couchman-Karasz equation does give a better correlation of experimental observations than any other similar equations. This points to the fact that entropy, rather than volume is the main factor controlling the onset of the glass transition.

More recently, attempts have been made to take account of polymer-polymer interactions and the effect these have on the composition dependence of the glass transition in miscible blends. Brekner, Schneider and Cantow[100,133,134] have developed a new concept based on the idea that surface barriers are responsible for both conformation and free volume distribution. An extended Gordon-Taylor relationship results, if both the effect of molecular surroundings on the contact contribution to the glass transition of the blend and the

- 50 -

effect of contact probabilities of the blend components are considered. The Gordon-Taylor constant, k is now related to the ratio of the different expansion coefficients of the free volume. Two parameters k_A and k_B are introduced, which are related to the intensity of polymer-polymer interactions and to the effect of immediate molecular surroundings on the interactions. Analysis of experimental data suggests the k_A and k_B are both polymer specific and molecular weight dependent. The relationship can be expressed as follows

$$\left(T_g - T_{g_A}\right)\Big/\left(T_{g_B} - T_{g_A}\right) = \left(1 + k_A\right)\phi_B - \left(k_A + k_B\right)\phi_B^2 + k_B \phi_B^3 \quad (2.82)$$

ϕ_B is the volume fraction of the stiffer component having T_{g_B}, where $k_A = k_A^* \big/ \left(T_{g_B} - T_{g_A}\right)$ and $k_B = k_B^* \big/ T_{g_B} - T_{g_B}$. k_A^* is related to the interaction energy differences between hetero- and homo-contacts and k_B^* considers the effects on the binary contacts of the molecular surroundings.

Aubin and Prud'homme[101] have recently noticed that for many systems a cusp or discontinuity is observed in the experimental Tg-composition curve. This cusp cannot appear when the Tgs of the two homopolymers involved are separated by less than about 50 degrees. It was shown that this behaviour can be explained within the framework of the free volume theory with equations derived by Kovacs.[102] A modification of the Kovacs theory to account for specific interactions has also been proposed.[103]

2.9   Dynamic Mechanical Properties of Polymers

Material under the influence of an applied strain are categorised depending on the nature of their response. Perfectly elastic materials obey Hook's Law, the applied strain being

proportional to the stress. Perfectly viscous liquids obey Newton's Law of viscosity, the applied stress being directly proportional to the stain rate. Polymeric materials are neither completely elastic nor viscous, but can exhibit both types of behaviour and are so termed viscoelastic. On application of a static load a polymer material experiences an instantaneous elastic response, follow by a time-dependent viscoelastic response. This can be observed as an initial elongation followed by a time-dependent elongation, during which the material is undergoing stress relaxation.

One of the most important techniques for studying the mechanical behaviour of polymers is dynamic mechanical analysis, which usually entails the application of a sinusoidal load leading to a sinusoidal deformation (see figure 2.9). The resulting strain is neither in phase with the stress (as in perfectly elastic materials) nor 90° out of phase (as in perfectly viscous liquids), instead there is a phase lag δ (Phase angle).

Dynamic mechanical analysis is usually carried out in association with a heating program as in dynamic mechanical thermal analysis (DMTA). It is possible to carry out the experiment at constant frequency whilst varying the temperature or vice versa. The stress (σ) resulting from the applied strain (γ) is measured and the time dependency of stress and strain can be written

$$\gamma = \gamma_0 \sin(\omega)t \qquad (2.83)$$

$$\sigma = \sigma_0 \sin(\omega t + \delta) \qquad (2.84)$$

ω is the cyclic frequency, γ_0 & σ_0 are the strain and stress amplitudes respectively.

Equation 2.84 can be expanded to
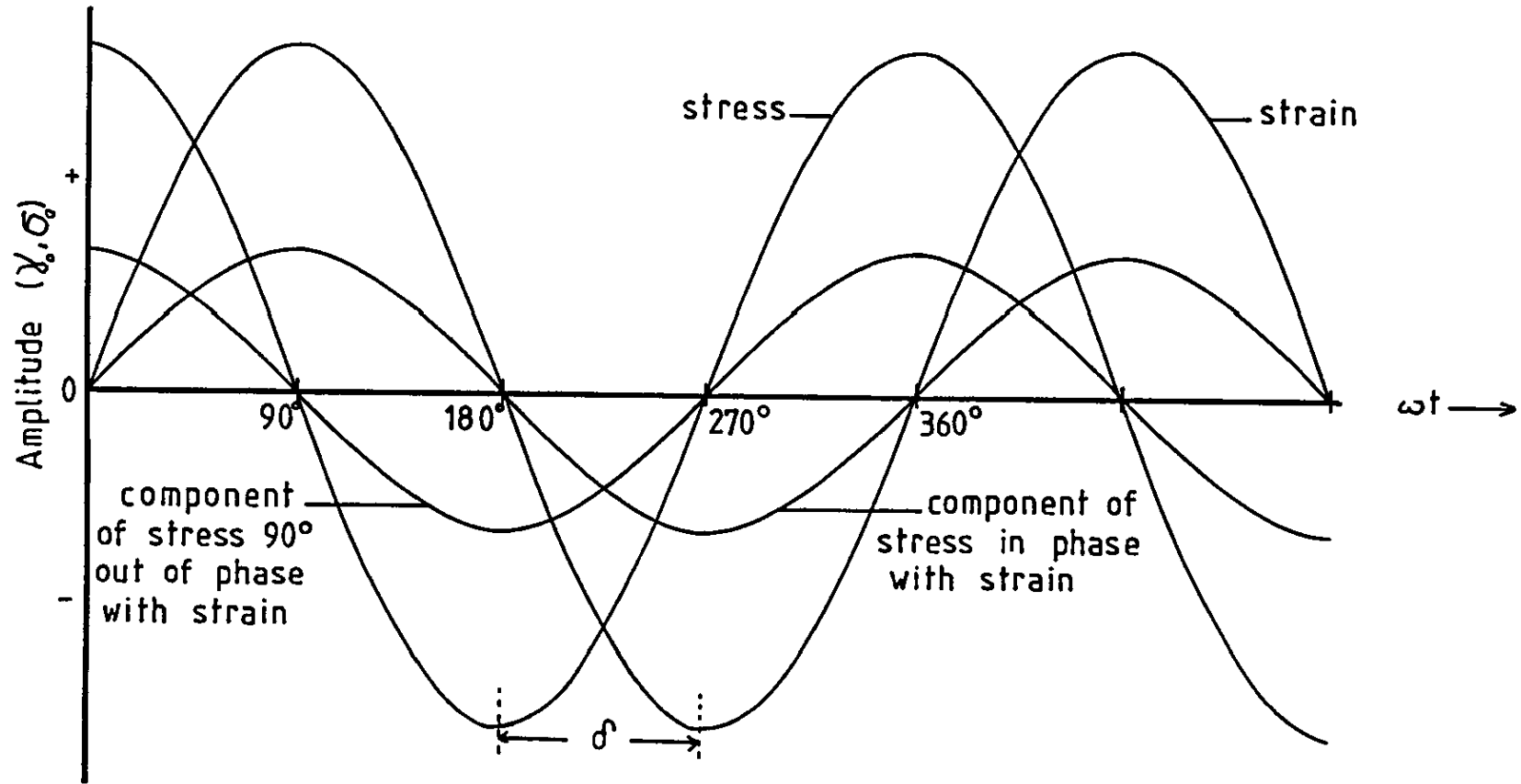
$$\sigma = \sigma_0 \sin\omega t \cos\delta + \sigma_0 \cos\omega t \sin\delta \qquad (2.85)$$

So, it can be seen that stress is made up of two components,

- 52 -

Figure 2.9

The Relationship Between Stress and Strain in Dynamic Mechanical Analysis.

one which is in phase with the strain (of magnitude $\sigma_0 \cos \delta$) and one which is out of phase with the strain (magnitude $\sigma_0 \sin \delta$).

The stress-strain relationship, therefore, is as follows

$$\sigma = \gamma_0 E' \sin \omega t + \gamma_0 E'' \cos \omega t \qquad (2.86)$$

Where the storage modulus E' is equal to $(\sigma_0/\gamma_0)\cos\delta$, that is, the component of stress in-phase with the strain divided by the strain amplitude, and the loss modulus E'' is equal to $(\sigma_0/\gamma_0)\sin\delta$, the component of stress out of phase with strain divided by the strain amplitude.

Dividing the loss modulus by the storage modulus leads to the loss tangent

$$\frac{E''}{E'} = \frac{(\sigma_0/\gamma_0)\sin\delta}{(\sigma_0/\gamma_0)\cos\delta} = \tan\delta \qquad (2.87)$$

This effectively means that $\tan\delta$ is the ratio of the energy stored to the energy lost per cycle, that is, the hysteresis.

A complex modulus E^* can be derived such that

$$E^* = \sqrt{(E')^2 + (E'')^2} \qquad (2.88)$$

This can be represented by an Argand diagram as in figure 2.10.

Figure 2.11 shows the variation of E' and $\tan\delta$ against frequency and temperature for a typical homopolymer in the region of it's glass transition. At high frequencies and low temperatures the storage modulus E_g' is characteristic of a glassy material. On decreasing the frequency or increasing the temperature, the storage modulus becomes characteristic of a rubbery material E_R', the loss

Figure 2.10

Argand Diagram Relating E', E" and δ

$$E^* = \sqrt{(E')^2 + (E'')^2}$$

= complex modulus

loss modulus E''

δ

E'

storage modulus

Figure 2.11

log E'

storage modulus

E'_g

E'_R

tan δ

tan δ

Temperature

log E'
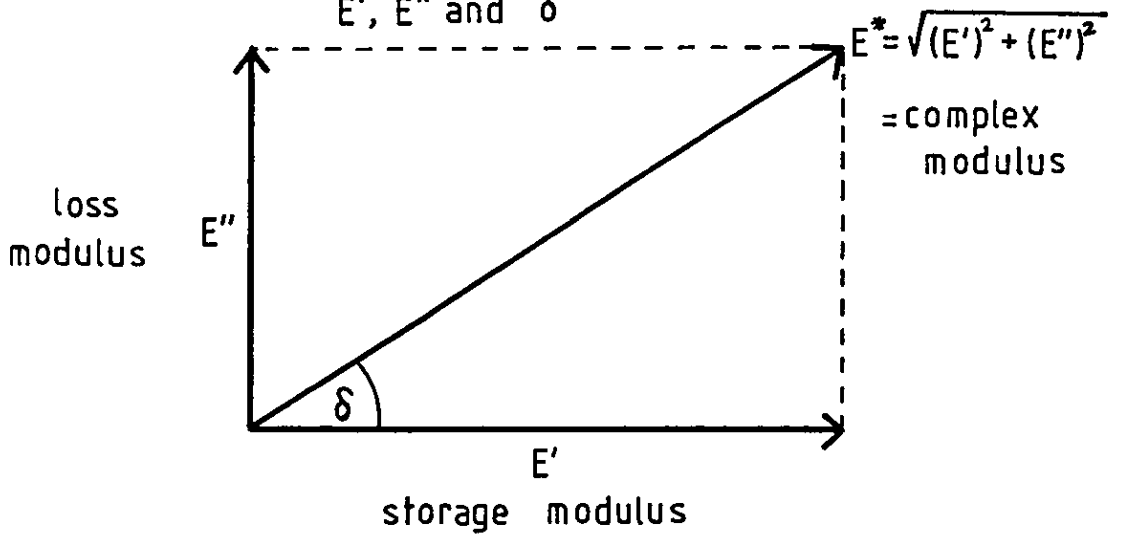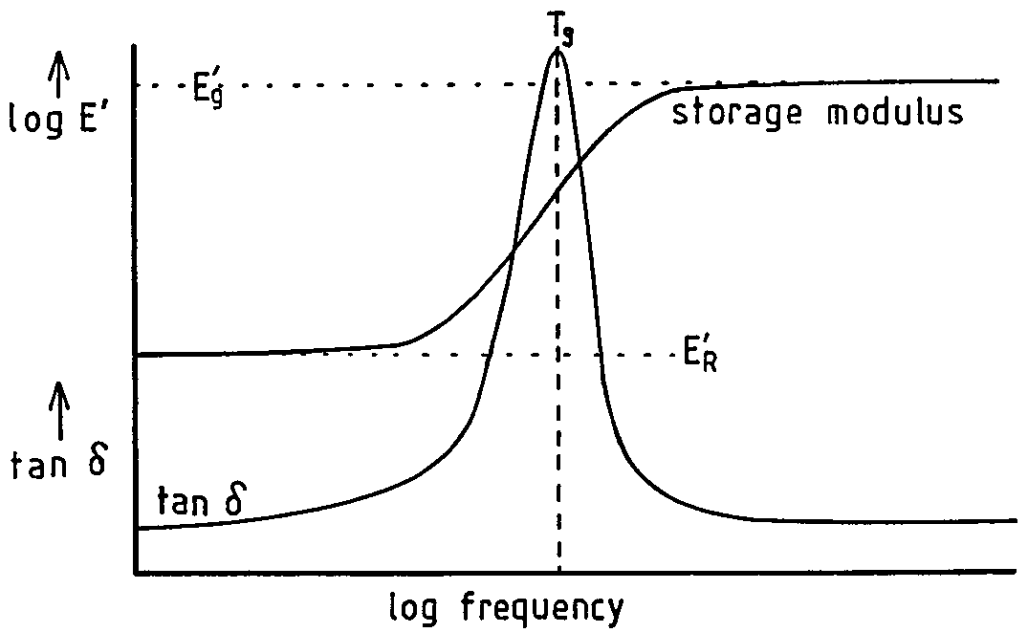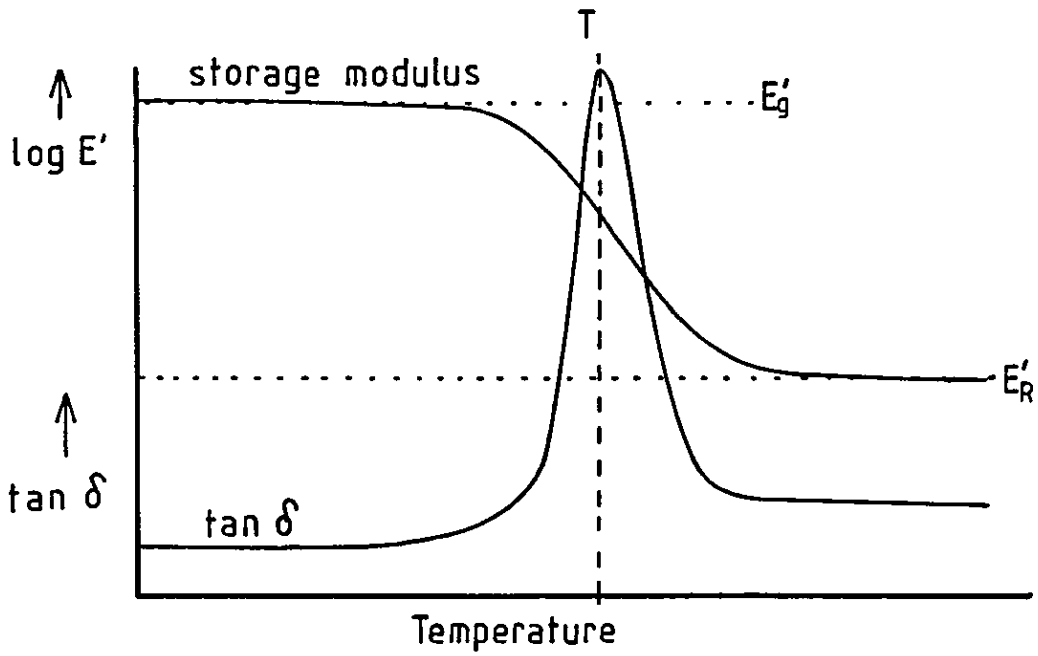
E'_g

T_g

storage modulus

E'_R

tan δ

tan δ

log frequency

modulus in both cases having passed through it's peak. The peak in tan δ corresponds to the maximum in the hysteresis or damping and is interpreted as the glass transition temperature of the polymer.

2.9.1 Factors Affecting the Dynamic Mechanical Behaviour

The glass transition is the phenomenon most often studied by this technique and the factors which affect the glass transition will correspondingly affect the dynamic mechanical properties observed. These factors have been discussed in section 2.8.3, however, the important points are summarised below.

At high molecular weights, the Tg is more or less independent of molecular weight, but at lower chain lengths, decreasing the molecular weight will cause the observed Tg to decrease. In dynamical mechanical terms, the tan δ peak and fall in loss modulus will be shifted to lower temperature at a given frequency.

Crosslinking tends to cause an increase in Tg, manifested in a shift to high temperature of the tan δ maximum and loss modulus curve. However, with very highly crosslinked networks, the storage modulus tends to be virtually temperature independent and no tan δ peak is observed. In the region of rubber-like behaviour, at temperatures above Tg, the polymer may experience viscous flow and this results in a gradual decrease in E', due to a greater number of chain entanglements.

Random or statistical copolymers are generally characterised by a single Tg and hence, a single tanδ peak at a temperature determined by the composition. A broadening of the peak may be observed if there are long sequences of a given comonomer unit, especially if these units experience poor mixing with the other comonomer segments.

Plasticisation, that is the incorporation of low molecular weight species into a polymer, has the effect of reducing the Tg,

- 54 -

resulting in a shift to lower temperature of the $\tan\delta$ peak. If there is poor mixing between the added low molecular weight compound and the polymer, a broadening of the loss tangent peak may result.

The miscibility of two or more component polymers within a blend can have a marked effect on the appearance of both the loss modulus and loss tangent curves. Figure 2.12 shows the loss modulus and $\tan\delta$ curves characteristic of miscible, particularly miscible and immiscible binary mixtures. Completely miscible blends are characterised by a single $\tan\delta$ peak, at some point between the positions expected for the Tg values of the unmixed components, due to a single glass transition for the single mixed phase present. The breadth of the $\tan\delta$ peak should, for completely miscible blends, be no wider than the $\tan\delta$ peaks of the blend components. A broadening of the peak may result if there is incomplete miscibility.

Totally immiscible blends are indicated by the observations of two $\tan\delta$ peaks at the temperatures close to the peaks for the unmixed components. A shift of the peaks towards each other relative to the two components, suggests some degree of partial mixing.

A broad loss peak covering the temperature range between the peak positions of the blend components is a special case of partial miscibility, termed microheterogeneity. This in effect is due to the presence of a large number of phases of varying compositions, the loss tangent breadth reflecting the composition distribution.

Dynamic mechanical thermal analysis is very sensitive to the glass transition, much more so than techniques such as differential scanning calorimetry (DSC).[106] Another advantage over DSC is that it is easier in DMTA to distinguish between Tgs which are close together (eg. < 30°C) in an immiscible or partially miscible system. Information can be obtained even from the analysis of two-phase blends having Tgs separated by only 15 or so degrees, from the shape

Figure 2.12

Tan δ and Log Modulus Curves Illustrating Different Types of Mixing Behaviour.

A

B

A+B
immiscible

A+B
partially-
miscible

A+B
microheterogeneous

A+B
miscible

tan δ / log modulus ⟶

Temperature ⟶

of the overlapped $\tan\delta$ peaks. A shoulder on the peak may be observed, corresponding approximately to the position of the Tg of one of the phases. The loss modulus (logE') curve may also yield useful information, since the fall in the curve corresponds to the glass transition and to the $\tan\delta$ peak. The two curves can be especially useful when used in conjunction with one another.

DMTA can detect separated phases in a mixture of the order of 15 nm^{-1}, phases smaller than this therefore, will not yield a characteristic $\tan\delta$ peak, leading to the conclusion, wrongly, of complete miscibility. However, it is likely that a large number of apparently miscible blends do in fact contain separated phases, too small to be identified by the particular analytical technique used for probing the miscibility.

2.10 Radical Polymerisation

There are three main reactions involved in the mechanism of radical chain polymerisation[107]

Initiation $\qquad I \xrightarrow{\ k_d\ } 2R_c^\bullet$

$\qquad\qquad\qquad R_c^\bullet + M \xrightarrow{\ k_i\ } R_x^\bullet$

Propagation $\qquad R_x^\bullet + M \xrightarrow{\ k_p\ } R_{x+1}^\bullet$

Termination $\qquad 2R_x^\bullet \xrightarrow{\ k_{tc}\ } P_{2x}$

$\qquad\qquad\qquad\quad \xrightarrow{\ k_{td}\ } P_x + P_x$

Where I is the initiation species, $R_c^\bullet$, $R^\bullet$ and $R_x^\bullet$ are the radicals, M is monomer and P denotes the polymer. The rate constants of each reaction are indicated above the arrows. In the first reaction, the subscript d on the rate constant denotes decomposition of initiator. In the termination reactions the two rate constants

- 56 -

relate to the way in which the chain reaction terminates. k_{tc} is the rate constant for termination by combination of two polymer chain radicals and k_{td} is the rate constant for the case where two polymer molecules are formed in the termination reaction.

It is assumed that radical reactivity is independent of radical size and that long chain radicals are formed due to many monomer additions to each primary radical R_c. It is also assumed that the consumption of monomer in initiation reactions is negligible compared to that consumed in propagation reactions.

The rate of polymerisation R_p can then be written

$$R_p = -\frac{d[M]}{dt} = k_p[R_x^\cdot][M] \qquad (2.89)$$

If one assumes a stationary state concentration of radicals during the polymerisation and also of primary radicals, the rate of polymerisation becomes

$$R_p = \frac{k_p}{\sqrt{k_t}}[M]\left(fk_d[I]\right)^{1/2} \qquad (2.90)$$

Where f is the initiator efficiency, that is, the fraction of primary radicals which initiate polymer chains.

A further reaction may occur during the polymerisation and is known as a chain transfer reaction. Most termination reactions involve the combination of two polymer chain radicals to form a longer chain. A chain transfer reaction is one in which polymer formation is achieved by the polymer chain radical reacting with another species in the polymerisation mixture, such as a solvent, initiator or monomer molecule. This results in a shorter chain length and hence, lower number average molecular weight ($\bar{M}n$).
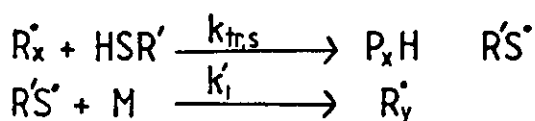
This type of reaction can be utilised in order to control the

molecular weight of a polymer by incorporation of a chain transfer agent, that is, a molecule which to a greater or lesser extent promotes chain transfer reactions. Neglecting chain transfer reactions to any other species, the effect of the concentration of added chain transfer agent [S] can be seen by considering the Mayo equation

$$\frac{1}{\bar{X}_n} = \left(\frac{1}{\bar{X}_n}\right)_o + c_s \frac{[S]}{[M]} \qquad (2.91)$$
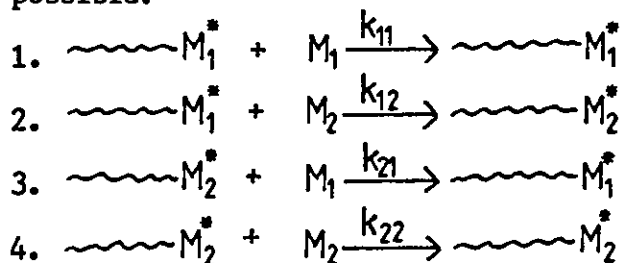
for the reaction

$$R_x^\bullet + HSR' \xrightarrow{\ k_{tr,s}\ } P_x H \quad R'S^\bullet$$
$$R'S^\bullet + M \xrightarrow{\ k_i'\ } R_y^\bullet$$

where $c_s = k_{tr,s}/k_p$

$\bar{X}_n$ is the number average degree of polymerisation and is the average number of structural units per polymer molecule.

2.10.1 Radical Copolymerisation and Copolymer Composition

The composition of a statistical copolymer usually differs from the composition of the monomer feed. This is due to the difference in the reactivities of the monomers and radicals involved. The reactivity of a given monomer depends on the second monomer and the copolymerisation conditions.

For monomers M_1 and M_2, there are the related propagating species $M_1^\bullet$ and $M_2^\bullet$ and so a total of 4 propagating reactions are possible:

1. $\sim\sim\sim M_1^\bullet + M_1 \xrightarrow{\ k_{11}\ } \sim\sim\sim M_1^\bullet$

2. $\sim\sim\sim M_1^\bullet + M_2 \xrightarrow{\ k_{12}\ } \sim\sim\sim M_2^\bullet$

3. $\sim\sim\sim M_2^\bullet + M_1 \xrightarrow{\ k_{21}\ } \sim\sim\sim M_1^\bullet$

4. $\sim\sim\sim M_2^\bullet + M_2 \xrightarrow{\ k_{22}\ } \sim\sim\sim M_2^\bullet$

k_{xy} is the rate constant for a growing chain with monomer x

being the propagating centre, adding monomer y.

It is assumed that the reactivity of the propagating centre does not depend on the chain composition, but depends only on the monomer unit at the end of the chain. It is also assumed that only long chain lengths are involved and therefore, that the consumption of monomers M_1 and M_2 in initiation and transfer reactions is negligible compared with the 4 propagating reactions.

The rates of consumption of monomers M_1 and M_2 are as follows:

$$- \frac{d[M_1]}{dt} = k_{11}[M_1^*][M_1] + k_{21}[M_2^*][M_1] \qquad (2.92)$$

$$- \frac{d[M_2]}{dt} = k_{12}[M_1^*][M_2] + k_2[M_2^*][M] \qquad (2.93)$$

dividing (2.93) by (2.94) gives

$$- \frac{d[M_1]}{d[M_2]} = \frac{k_{11}[M_1^*][M_1] + k_{21}[M_2^*][M_1]}{k_{12}[M_1^*][M_2] + k_{22}[M_2^*][M_2]} \qquad (2.94)$$

Where $\frac{d[M_1]}{d[M_2]}$ is the ratio of the rates of entry of monomers 1 and 2 into copolymer chains.

Assuming a stationary state concentration of $[M_1^*]$ and $[M_2^*]$, that is, the rates of conversion of $\sim\sim M_1^* \rightarrow \sim\sim M_2^*$ and $\sim\sim M_2^* \rightarrow \sim\sim M_1^*$ are equal, then

$$k_{12}[M_1^*][M_2] = k_{21}[M_2^*][M_1] \qquad (2.95)$$

Then rearranging for $[M_1^*]$ and substituting into 2.95 gives the copolymer composition equation:

$$\frac{d[M_1]}{d[M_2]} = \frac{[M_1](r_1[M_1] + [M_2])}{[M_2]([M_1] + r_2[M_2])} \qquad (2.96)$$

- 59 -

Where r_1 and r_2 are the monomer reactivity ratios of the propagation species, defined as:

$$r_1 = \frac{k_{11}}{k_{12}} \quad \& \quad r_2 = \frac{k_{21}}{k_{22}} \qquad (2.97)$$

$\dfrac{d[M_1]}{d[M_2]}$ is the mole ratio of monomer units in the copolymer.

The equation can also be written

$$f = \frac{(r_1 F + 1)}{(1 + r_2/F)} \qquad (2.98)$$

Where $\quad f = \dfrac{d[M_1]}{d[M_2]} \quad \& \quad F = \dfrac{[M_1]}{[M_2]}$

Given a knowledge of F and f over a range of compositions, monomer reactivity ratios can be determined graphically using the Finemann-Ross[108] method, by rearranging equation 6 as follows:

$$F = \frac{(f-1)}{f} = r_1 \frac{F^2}{f} - r_2 \qquad (2.99)$$

A plot of the left-hand side against F^2/f should yield a straight line of slope r_1 and y - intercept r_2.

It should be noted, however, that the copolymer composition equation is only valid at low conversion (<10% approximately), since the proportion of the less reactive monomer in the feed increases as the reaction proceeds.

An improved method of determining reactivity ratios has been developed by Kelen and Tudos,[109,110] using a procedure which gives a more even distribution of data points. Deviations from the copolymer composition equation are highlighted and can show up as a curvature in the plotted data. Such deviations may be due to too high a

conversion, or to the fact that the four propagating reactions used to derive the equation may not accurately describe the mechanism for chain growth.

From the following equation

$$\epsilon = \frac{F^2/f}{\alpha + F^2/f} \qquad \& \qquad \eta = \frac{F(f-1)/f}{\alpha + F^2/f} \qquad (2.100)$$

The reactivity ratios may be found by plotting η against ϵ. α is the square root of the product of the maximum values of (F^2/f). r_1 is given by the value of η at $\epsilon = 1$ and r_2 is given by multiplying the intercept on the η axis by $-\alpha$.

2.10.2 Significance of the Reactivity Ratios

The reactivity ratios r_1 and r_2 are the ratios of the rate constant for a given radical adding its own monomer, to that for it adding the other monomer. A reactivity ratio , $r_1 < 1.0$ means that M_1^* prefers to add M_2.

The values of the two reactivity ratios determine the type of copolymer formed, there being two main types, ideal and alternating. A copolymer is said to be ideal if the two radicals are equally reactive to the two monomers present. This is the case when k_{11}/k_{12} $= K_{21}/K_{22}$ or $r_1 = 1/r_2$. The two types of units are arranged randomly along the chain, the relative amounts being determined by the monomer feed ratio and the reactivities of the two monomers.

An alternating polymer chain will be formed if each radical prefers to react with the other monomer. This corresponds to $r_1 = r_2 = 0$. This situation is an extreme case. It is often observed that r_1 and r_2 are both less than zero. This does not give complete alternation, but a tendency towards alternation nevertheless.

Another possibility is if r_1 and r_2 are both greater than

unity. Here, the radicals both prefer to react with their own monomers and the tendency is towards blocks of each unit within the chain.

2.11 Infrared Spectroscopy

Infrared spectroscopy is a well established analytical technique employed particularly in the identification and study of organic molecules and is concerned with the detection of transitions between vibrational energy levels in molecules, resulting from vibrations of interatomic bonds. The frequencies of such vibrations are characteristic of specific functional groups and are affected by the molecular environment, chain conformation (in polymers), morphology and intermolecular interactions.

At room temperature most molecules exist in their ground vibrational energy state. When molecular vibrations cause a change in the bond dipole-moment, resulting from a change in the electron distribution in the bond, it is possible to stimulate transitions between energy levels by interaction with electro-magnetic radiation of the appropriate frequency. Molecular vibrations are enhanced when the electric sector of the incident radiation is in phase with the vibration dipole. When this happens energy is transferred from the incident radiation to the molecule and it is this absorption of energy which is the basis of IR spectroscopy. In practice, spectral transitions are detected by scanning through the frequency range (typically 4000-400 cm^{-1}), whilst monitoring the intensity of the transmitted light. Alternatively, in Fourier transform infrared spectroscopy (FTIR)[23] the entire frequency range is effectively scanned instantaneously using a broad band radiation source. The basic principle of FTIR is discussed in section 3.4.4.

- 62 -

One of the main advantages of FTIR spectroscopy is the speed with which spectra can be obtained (in a few seconds, compared to at least 3 minutes with conventional IR instruments). This allows scans to be repeated a large number of times in only a few minutes. An averaging procedure then eliminates much of the background "noise", greatly improving the signal to noise ratio. This, combined with the advantage of wavenumber resolutions in the order of $2cm^{-1}$ or better, enables FTIR to be used to study physical interactions between the components of a mixture. Interactions between the functional groups of two components in a polymer blend, are often an important factor which promotes miscibility, and such interactions can often be observed as a shift in the wavenumber of the bands relating to the groups involved in the interaction. Sometimes shifts may only be a few wavenumbers (cm^{-1}), but shifts of around $30cm^{-1}$ have been observed, an example being the carbonyl shift observed in blends of a methacrylic acid copolymer and a polyether.[111,112] The acid has a tendency to dimerise (via hydrogen bonding) in the unmixed copolymer and shows a carbonyl absorption band at around $1700cm^{-1}$. The acid carbonyl when not interacting in this way has a band at $1760cm^{-1}$, which is rarely observed. However, in a mixture of the acid copolymer with a polyether, hydrogen bonding occurs between the acid carbonyl and the ether oxygen which causes the band to shift to around $1728cm^{-1}$. Fourier transform infrared spectroscopy is easily able to differentiate between each of these bands.

Other applications of this very versatile technique include its use in the study of surfaces and powders directly using a variety of special attachments. Infrared microscopy is a technique which enables spectra to be obtained from very small areas of a specimen and can be used in either transmission or reflection mode.

Coleman and Painter have reviewed the use of FTIR spectroscopy

to probe the structure of multicomponent polymer blends and have studied a number of different polymer blend systems.[113]

3.0   Experimental Details

3.1   Preparation of Homopolymers and Copolymers

3.1.1 Purification of Monomers

All monomers except 2-hydroxyethyl methacrylate were purified by vacuum distillation and were thereafter, stored in stoppered flasks over anhydrous magnesium sulphate in a refrigerator.   2-hydroxyethyl methacrylate was not purified in this way, since it tended to crosslink during the distillation.   It was therefore, used as supplied, except it was also dried over anhydrous magnesium sulphate.   The distillation procedure was carried out on a vacuum line, and involved first degassing the monomer.   This was achieved by freezing the monomer using liquid nitrogen before evacuating the flask.   The flask was then sealed and the monomer melted, releasing dissolved gas into the vacuum above the liquid.   This process was repeated usually three times, or until all the dissolved gas had been removed.   The monomer was then distilled, with the first and last portions of distillate discarded.

3.1.2 Polymerisation of Homopolymers and Copolymers[114]

All polymerisations were carried out in a two-necked, round bottomed flask, fitted with a condenser and silica gel drying tube. Nitrogen gas was bubbled through the reaction solution.   The flask was heated in a thermostatically controlled water bath.   The apparatus is shown diagrammatically in figure 3.1.   Polymers were isolated by precipitating in the appropriate chilled non-solvent, before being purified by redissolving in a minimum amount of the polymerisation solvent, reprecipitating and drying in a vacuum oven at 60°C to constant weight.   The details for each reaction are shown in tables 3.1 and 3.2.   Samples of low molecular weight poly (n-butyl

Figure 3.1
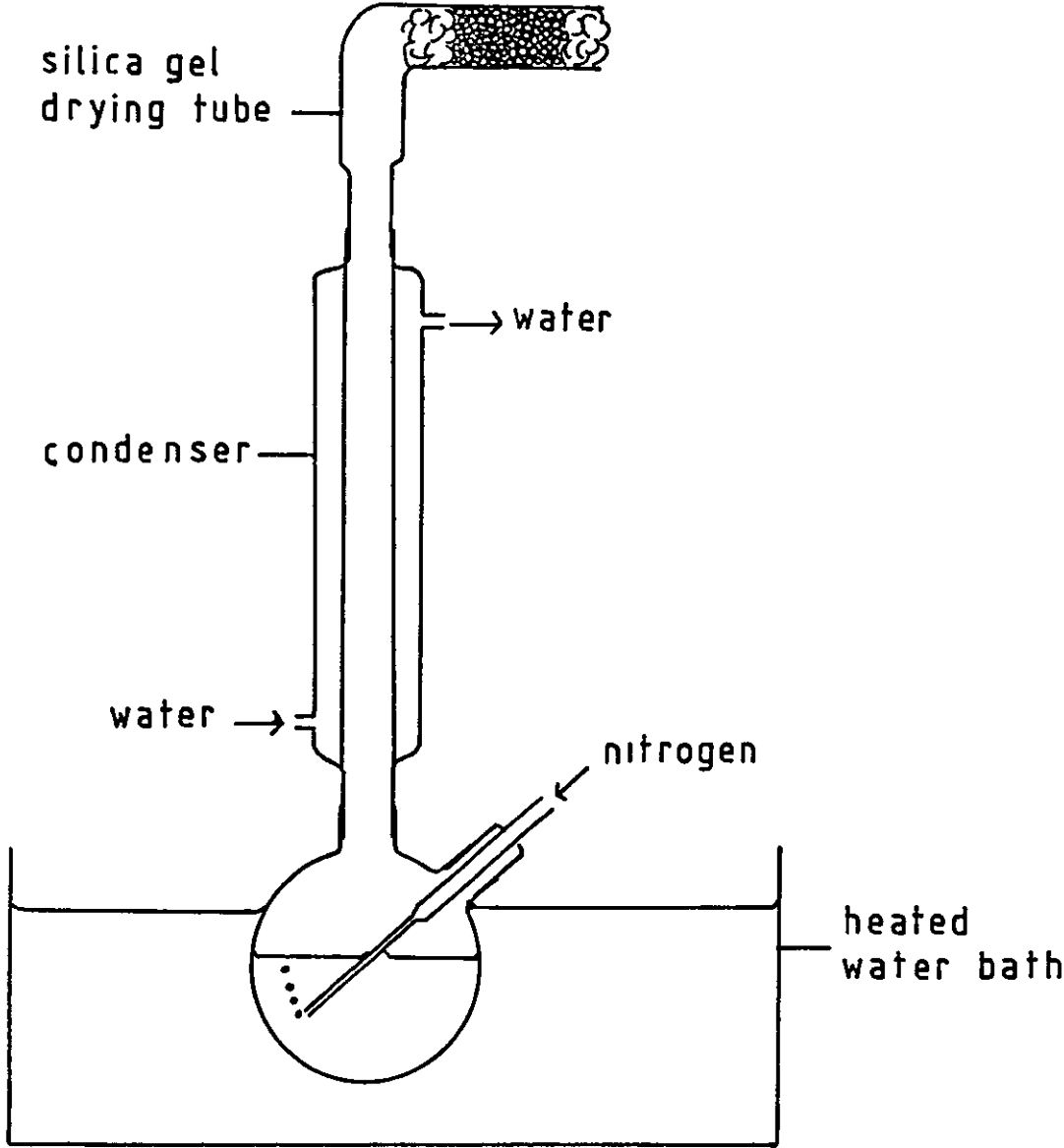Apparatus Used for Solution Polymerisation

silica gel
drying tube

condenser

water →

water →

nitrogen

heated
water bath

Table 3.1   Homopolymerisations

Monomer (abbreviation) (source)	Solvent	T/°C	t/hours	[solvent]/ [monomer]	Initiator (A.I.B.N.) concentration	Yield wt.%	Non-Solvent for precipitation
n-butyl acrylate (BA) (Aldrich Chemical Co.)	1-methoxy propan-2-ol	60	17	5	3% of monomer weight	72.1	Methanol
dimethylaminoethyl methacrylate (DMAEMA) (Aldrich Chemical Co.)	"	60	17	5	"	52.8	diethylether
2-hydroxyethyl methacrylate (HEMA) (Aldrich Chemical Co.)	"	60	17	5	"	60.1	40/60 petroleum ether
n-butyl methacrylate (BMA) (Koch-Light Labs. Ltd)	"	60	4	5	"	47.6	methanol
methyl acrylate (MA) (Aldrich Chemical Co)	"	60	17	5	"	82.4	methanol
methacrylic acid (MAA) (Aldrich Chemical Co.)	"	70	1.67	5	"	45.7	n-heptane
styrene (ST) (Aldrich Chemical Co.)	"	70	24	5	"	56.6	n-heptane

Table 3.2   Styrene-Methacrylic Acid Copolymerisations

Product Number	monomer proportions/ mole % ST	MAA	Reaction solvent	T/°C	t/hours	[solvent]/ [monomer]	AIBN concentration	Yield wt.%	Non-solvent for precipitation
7	25	75	1-methoxy propan-2-ol	70	24	5	3% of monomer wt	97.5	n-heptane
8	50	50	"	"	"	"	"	82.5	"
9	75	25	"	"	"	"	"	53.8	"
29	90	10	"	"	"	"	"	47.0	"
30	95	5	"	"	"	"	"	30.0	"
163	95.6	5.4	"	60	4	"	"	16.7	"

Note: AIBN – azobisisobutyronitrile (initiator)

acrylate) were prepared using a chain transfer agent, using the formulations as shown in table 3.3.

The polymers provided by L.V.H. Coatings Ltd are described below, whilst the structural formulae of all other polymers used for blending are shown in table 3.4.

3.1.3 Polymers Supplied by L.V.H. Coatings Ltd

Lumiflon LF200

Lumiflon LF200 is one of a series of soluble fluoro-resins developed by Asahi Glass Co. Ltd, and marketed in the United Kingdom by I C I plc. It is designed to be a high performance surface coating material. The structural formula is as follows:

$$\left[\begin{array}{c} F\ F \\ |\ \ | \\ C-C \\ |\ \ | \\ F\ Cl \end{array}\right]_w \left[\begin{array}{c} H\ H \\ |\ \ | \\ C-C \\ |\ \ | \\ H\ O \end{array}\right]_x \left[\begin{array}{c} H\ H \\ |\ \ | \\ C-C \\ |\ \ | \\ H\ O \end{array}\right]_y \left[\begin{array}{c} H\ H \\ |\ \ | \\ C-C \\ |\ \ | \\ H\ O \end{array}\right]_z$$
$$\quad\quad\quad\quad R_1 \quad\quad\quad R_2 \quad\quad\quad R_3OH$$
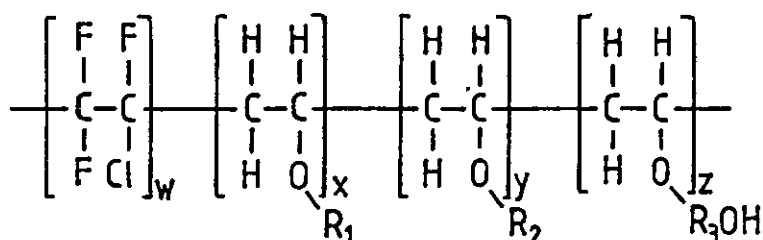
Where R_1 - Cyclohexyl group (C_6H_{11})

R_2 - C_2H_5

R_3 - C_4H_8

LF200 has an OH value (mg KOH/g) of 32.

CM03

This a terpolymer made by reacting the following monomers in the proportions indicated;

Methacrylic acid,	17% by weight
2-hydroxyethyl acrylate,	17% by weight
Butyl acrylate,	66% by weight

Table 3.3

Preparation of low molecular weight poly(butyl acrylate)

.

	T/°C	t/hrs	solvent	[S]/[M]	ACVA concentration	Thioglycolic Acid concentration	Yield wt.%	M̄n
PBA(2)	77	1	ethyl acetate	11	0.8% of monomer wt.	2.5% of monomer wt.	9	1926
PBA(3)	"	"	"	"	"	1.1% of monomer wt.	19	5204

Note: ACVA = azobisisocyanovaleric acid.

Thioglycolic acid - chain transfer agent.

Note: The number average molecular weight (M̄n) was determined by GPC.

Table 3.4   Repeat Unit Structures of Polymers and Copolymers

Polymer	Structure of Repeat Unit
Poly(styrene) (PST)	$-CH-CH_2-$ $\mid$ C_6H_5
Poly(methacrylic acid) (PMAA)	CH_3 $\mid$ $-CH_2-C-$ $\mid$ $C = O$ $/$ HO
Poly(n-butyl acrylate) (PBA)	$-CH_2-CH-$ $\mid$ $C=O$ $/$ C_4H_9-O
Poly(n-butyl methacrylate) (PBMA)	CH_3 $\mid$ $-CH_2-C-$ $\mid$ $C=O$ $/$ C_4H_9-O
Poly(2-hydroxyethyl methacrylate) (PHEMA)	CH_3 $\mid$ $-CH_2-C-$ $\mid$ $C=O$ $/$ $HO(CH_2)_2-O$
Poly(methyl acrylate) (PMA)	$-CH_2-CH-$ $\mid$ $C=O$ $/$ H_3C-O

Table 3.4 Continued

Polymer	Structure of Repeat Unit

Poly(methyl methacrylate)

(PMMA)

$$\begin{array}{c} CH_3 \\ | \\ -CH_2-C- \\ | \\ C=O \\ / \\ H_3C-O \end{array}$$

Poly(dimethylaminoethyl methacrylate)

(PDMAEMA)

$$\begin{array}{c} CH_3 \\ | \\ -CH_2-C- \\ | \\ C=O \\ / \\ N-(CH_2)_2-O \end{array}$$

H$_3$C, H$_3$C — N

Poly(vinyl acetate)

(PVAc)

$$\begin{array}{c} -CH_2-CH- \\ | \\ O \\ \backslash \\ C=O \\ / \\ H_3C \end{array}$$

Poly(ethylene glycol)

(PEG)

$-CH_2-CH_2-O-$

Poly(propylene glycol)

(PPG)

$$\begin{array}{c} H \\ | \\ -CH_2-O-C \\ | \\ CH_3 \end{array}$$

Poly(propylene adipate)

(PPA)

$$\begin{array}{c} O \\ \| \\ -(CH_2)_3-O-C- \end{array}$$

Table 3.4 Continued

Polymer   Structure of Repeat Unit

Ethylene-vinyl acetate copolymer $-(CH_2-CH_2)_{\overline{x}}(CH_2-CH)_y$

(EVA) O

                                                                          $\backslash$

                                                                          $C=O$

                                                                          $/$

                                                                    H_3C

Styrene - acrylonitrile copolymer $(CH_2-CH)_{\overline{x}}(CH_2-CH)_y$

(SAN) C_6H_5 CN
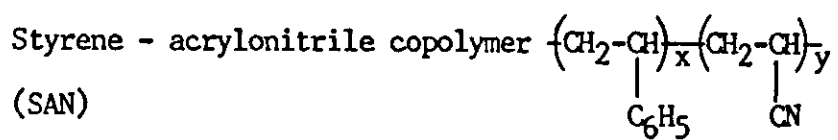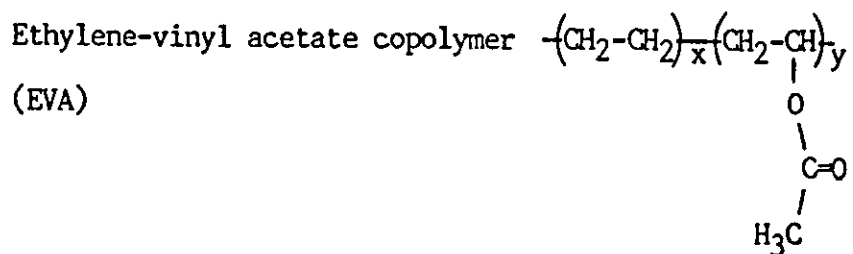
Xenacryl 9A/303

This is a polymer differing from CM03 by the inclusion of a fourth monomer, TONE M-100, a caprolactone having an acrylic double bond and a hydroxyl group. The proportion of monomer units used in the polymerisation mixture is as follows;

Methacrylic acid   17%   by weight

2-hydroxyethyl acrylate   12.7% by weight

Butyl acrylate   57.6% by weight

TONE M-100   12.7% by weight

Setal 1711

This is a saturated aliphatic polyester. The structural formula was not supplied however, the infrared spectrum has been obtained and as shown in appendix 3.

LF200, CM03 and 9A/303 have all been characterised using gel permeation chromatography (GPC), nuclear magnetic resonance spectroscopy (NMR) and fourier transform infrared spectroscopy (FTIR).

3.2   Characterisation of Blend Components

3.2.1 Nuclear Magnetic Resonance (N M R)

This technique was used to determine the composition of the styrene-methacrylic acid copolymers, in addition to investigating the structural detail of other polymers used for blending. The proton NMR spectra were obtained using an EM-360 60MH$_z$ spectrometer. All samples were prepared by dissolving approximately 0.1g of polymer in 1-2 ml of deuterated solvent d-chloroform containing 1% of tetramethyl siloxane (TMS) as internal standard was used for all polymers, except the ST/MAA copolymers having high proportions of MAA, where it was necessary to use a mixture of deuterated chloroform

and deuterated dimethyl sulphoxide (again with 1% T.M.S.).

The NMR spectra of the ST/MAA copolymers revealed a well separated resonance at 6-7 δ due to the five aromatic protons of styrene. If the integrated area of the styrene aromatic protons is found, then the integrated area of the remaining peaks is due to the 3 non-aromatic styrene protons and the 5 protons of methacrylic acid (not including the acid proton, which appears at around 12 δ and is not required for the calculation). The copolymer composition can then be calculated. The copolymer contains M_1 moles of styrene units (each having 8 protons) and M_2 moles of methacrylic acid units (each having 5 protons, not counting the acid proton). So the total integrated height of the spectrum (H_T) represents the resonance of the 5 styrene aromatic protons (H_S), plus the remaining 3 styrene protons and the 5 protons of methacrylic acid (H_T-H_S). So the proportion of M_1 and M_2 units can be found by

$$\frac{M_1}{M_2} = \frac{H_s/5}{\left(H_T - \frac{8H_s}{5}\right)/5} \qquad \frac{H_s}{H_T - \frac{8H_s}{5}}$$

3.2.2 Gel Permeation Chromatography (GPC)

Gel permeation chromatography[117] separates molecules on the basis of size alone. The separation takes place in a column packed with beads of a rigid porous gel (usually highly crosslinked polystyrene). The pores in the gel are of similar dimensions to the polymer molecules. A sample of the polymer in dilute solution is introduced into a solvent stream flowing through the column. As the polymer molecules flow past the porous beads, they can diffuse into the pores of the gel to an extent that depends on their size and the size distribution of the pores. Smaller molecules are able to

diffuse into the pores to a greater extent than larger molecules and are, therefore, retained on the column for longer times. That is, larger molecules pass from the column first and have shorter retention times than smaller molecules.

Polymers were characterised using the following procedure. Solutions of the polymers in destabilised tetrahydrofuran (Aldrich Chemical Co.), having a concentration of 0.1% (W/V) were prepared, incorporating a small amount of toluene as a reference. The solutions were loaded into a 6-part injection valve having a 100 ml loop. The polymers were eluted with tetrahydrofuran using a Knauer High Performance Liquid Chromatography Pump 64 at a flow rate of 1.0 ml per minute. Chromatograms were obtained by means of a Knauer differential refractometer connected to a J.J. Chart recorder (using a chart speed of 20 mm/minute). Two columns were used, both obtained from Polymer Laboratories Ltd. One column was filled with polystyrene beads with a particle size of 10 μm. The columns were calibrated by polystyrene standards (Polymer Laboratories Ltd). Values for the number average and weight average molecular weight were obtained using a computer program, from values of peak heights over a range of elution times.

3.3   Blending of Polymers

3.3.1 Solution Blending

All the blends were prepared by dissolving the various components in a common solvent, in most cases chloroform, although 1-methoxy propan-2-ol and tetrahydrofuran have also been used. Typically 0.8-1g total weight of polymers was dissolved in approximately 15 ml of solvent. The mixtures were shaken for several hours to produce homogeneous transparent solutions, before being cast into a crystallising dish and left in a fume cupboard at room

- 69 -

temperature for the solvent to evaporate. To ensure the films were completely dry, they were placed in a vacuum oven at several degrees above the Tg of the highest Tg component for a few hours.

3.3.2 Reaction Blending

A series of blends were produced by copolymerising styrene and methacrylic acid in a solution of LF200 in 1-methoxy propan-2-ol (MP). The reactions were carried out at 60 or 70°C for 16 - 24 hours, with 2.5% azobisisobutyronitrile (A.I.B.N.) as initiator. The reaction mixture in each case was precipitated into chilled n-heptane. The blends were purified by redissolving in M.P., and reprecipitating in n-heptane, before being dried to constant weight, in a vacuum oven at around 60°C.

3.4 Techniques Used to Investigate Miscibility and Polymer-Polymer Interactions

Miscibility
3.4.1 Film Appearance

For all the blends produced, the appearance of the solvent cast film were observed. It is generally the case that totally miscible blends are transparent, that is, they contain no microscopic phases that scatter light. Clearly, there is a threshold size of phase, below which light will not be scattered, but nevertheless, transparency is quite a good indication of miscibility. However, if the refractive indices of two polymers in a blend are the same or very close then, even if two phases do exist, the blend film will appear transparent. So transparency can never be taken to be conclusive proof of miscibility. The blends produced were classified

as either transparent (totally clear), translucent (allows light to pass through without being clear), or opaque (appearing white). The observation of film appearance were taken in conjunction with results obtained using dynamic mechanical thermal analysis to determine the miscibility, or otherwise, of the blends produced.

3.4.2 Dynamic Mechanical Thermal Analysis (DMTA)

All of the polymers used for blending and the resultant blends were studied using a Polymer Laboratories Dynamic Mechanical Thermal Analyser (DMTA).

The dual cantilever bending mode was used to study the samples. This involves clamping a rectangular sample (usually a bar of approximate dimensions 40mm x 11mm x 2.5mm) onto a fixed frame (Figure 3.2(a)). The sample is then oscillated at it's centre via a clamp attached to a drive shaft linked to a mechanical oscillator. The amplitude (strain) and frequency of oscillation are set on the instrument, along with the temperature range to be studied and the heating rate.

The resistance to the applied sinusoidal displacement is recorded as a function of the phase and magnitude of the displacement. The instrument converts these signals to yield the dynamic storage modulus. The glass transition of the polymer is characterised by a damping effect, resulting in a peak in the tan δ curve and a corresponding drop in the modulus, which is due to the softening of the polymer at this point. A diagram of the DMTA head is shown in figure 3.2(b).

Many of the blends and blend components studied are soft at room temperature, if not actually liquid, and so instead of using the usual bar-type sample, which would have been impractical, the polymers were impregnated into filter paper.
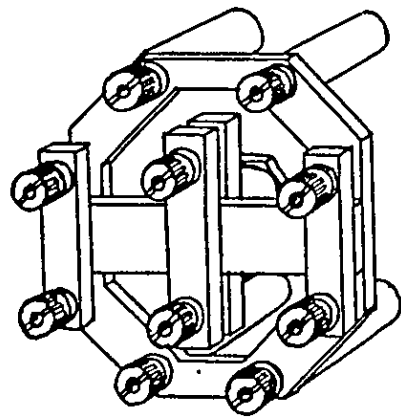
Figure 32(a)

Dual Cantilever
Clamping Arrangement

Vibrator

Displacement
Transducer

Temperature
Enclosure

Sample

Liquid
Nitrogen

Drive Shaft   Clamps
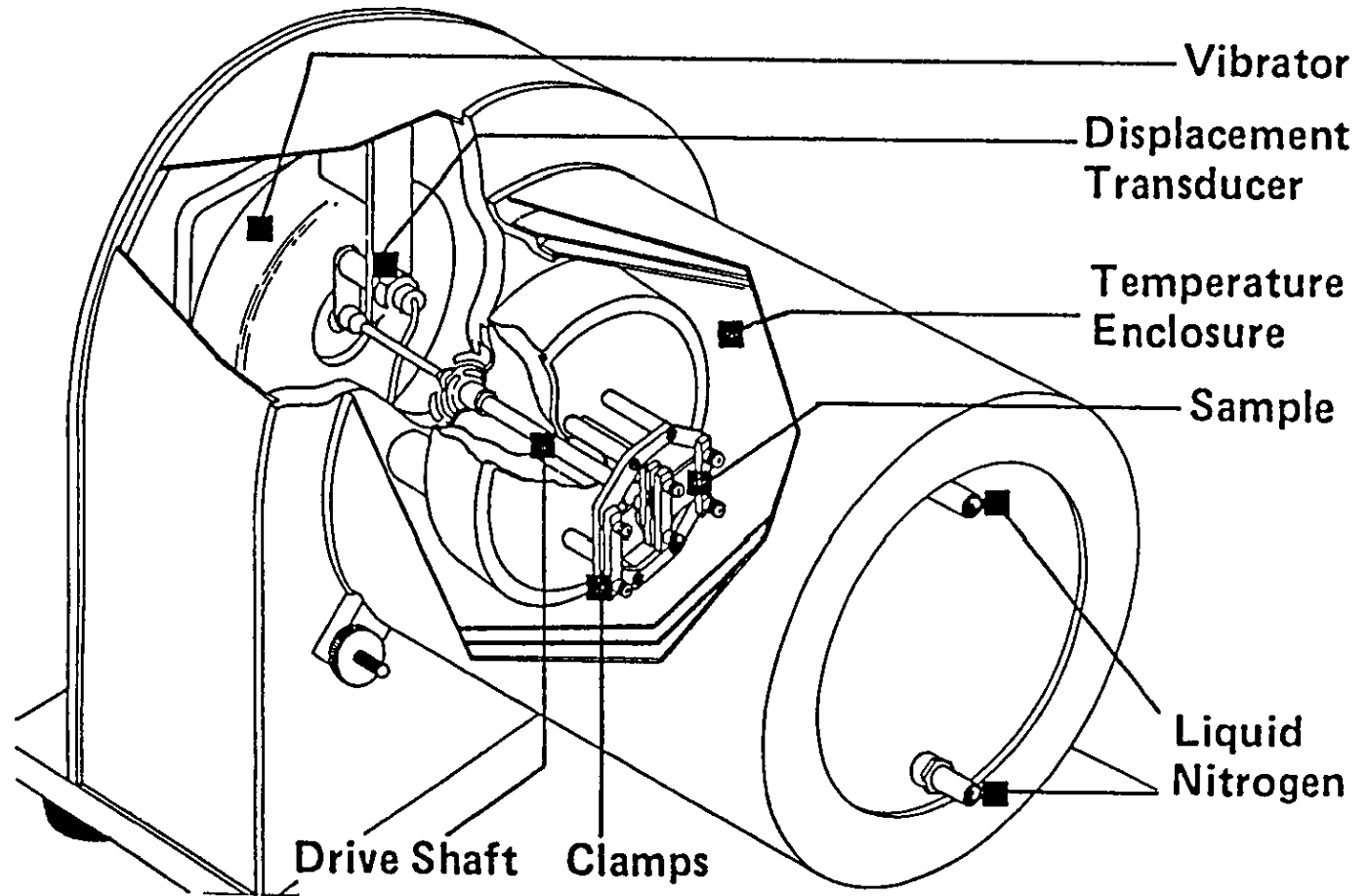
Figure 3.2(b)

DMTA Measuring Head

The samples were prepared on a heated press, at a temperature 10 to 20°C above the glass transition temperature (Tg) of the component having the highest Tg. A sandwich of polymer and filter paper, between two pieces of mould-release film was pressed for a few seconds at a pressure of 300 p.s.i.

The suitability of the filter paper as an inert support was checked by carrying out an analysis using filter paper alone, under the same conditions as used for the impregnated polymer samples. There was no significant damping behaviour observed over the temperature range investigated (-80°C to 200°C), except for a very small tan δ peak, sometimes observed at around 15°C. It is suspected that this may be due to melting of ice, from moisture absorbed by the paper. This effect can be minimised by drying the filter paper in an oven before impregnating with polymer , and by keeping prepared samples in a dessicator before use. For consistency, impregnated samples were left for 24 hours in a dessicator before being run on the DMTA. Reproducibility has been checked and confirmed by repeating a number of samples, and by comparing impregnated filter paper results to those obtained using a standard bar sample (see the DMTA plot in appendix 5).

Samples were securely clamped onto the clamping frame, and were cooled to at least 30°C below the Tg of the component having the lowest Tg, by passing liquid nitrogen through the cooling coils of the furnace arrangement of the DMTA measuring head. All samples were heated at 4°C/minute, at a frequency of 1 H_z and a strain of X4 (equivalent to a displacement of 40μm).

This technique was preferred to differential scanning calorimetry (DSC), because of the much higher sensitivity to the glass transition, and the comparative ease with which two or more

glass transitions can be resolved in immiscible blends (provided they are sufficiently separated in temperature).

3.4.3 Scanning Electron Microscopy (SEM)

Scanning electron microscopy (SEM) was chosen instead of transmission electron microscopy (TEM) for two main reasons. Firstly, it would have proved very difficult to produce thin films of the blends, since at room temperature many are soft, making sectioning difficult. An attempt was made to embed the samples in an epoxy resin prior to low temperature sectioning, but mixing of the blend sample with the epoxy could not be prevented at the elevated temperatures used for curing the epoxy. Secondly, had it been possible to produce thin films by sectioning, they would have required staining to enable observation of any phase separation present. This would have meant selectively staining one or other of the two phases, by using a staining agent specific to the functional groups in one phase but not the other. The blends to be studied, however, had hydroxyl groups in each of the two major components, and a staining agent specific to the relatively small percentage of carboxylic acid groups in the acrylic component would have been needed. This was a requirement that could not be met by the usual staining compounds.

The preparation of specimens for SEM presents fewer problems, and so this technique was chosen to probe the bulk internal structure of a number of blends, both miscible and immiscible (as determined by DMTA). To observe the internal structure, blend films produced by solution casting or melt pressing (between mould-release film at 300 psi) were fractured at liquid nitrogen temperatures. A small fragment was then mounted onto a metal holder or stub, using an electrically conducting adhesive (silver dag). To reduce damage by

Figure 3.3

Apparatus Used for Sputter-Coating Samples for SEM

Vacuum Chamber

Electron Deflecting Magnet

Target (-ve)

Specimen Table(+ve)

Specimen

To pump
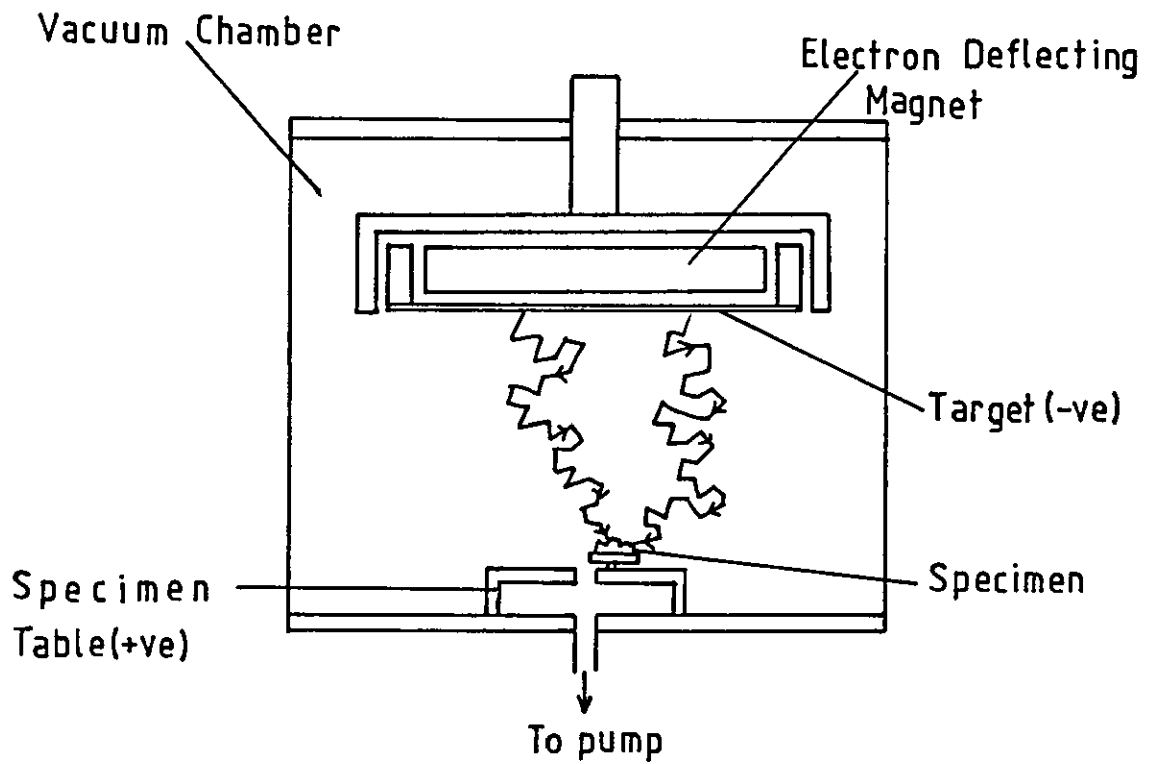
the electron beam, the specimen has to be coated with a thin layer (~10nm) of an electrically conducting material, in this case, gold. Figure 3.3. shows the apparatus used for sputter coating the specimen. Once coated the specimens were then placed into the electron microscope and the fracture surfaces observed. The process involves scanning a fine beam of electrons across the surface of the specimen. Secondary electrons, back-scattered electrons and x-ray photons emitted when the beam hits the specimen, are collected to provide a signal, used to modulate the intensity of the electron beam in a television tube, scanning in synchronisation with the microscope beam.

The fracture surfaces of the films were observed at magnifications of 1000 to 20,000, and photographs taken of the images produced. Only a limited number of blend films could be studied, because the films had to be rigid enough to be easily handled and to be self-supporting when mounted edgeways on the holder. It was found that only samples having D.M.T.A. Tgs of around 35°C and above were rigid enough. Blends having Tgs lower than this were too soft or sticky to be studied.

3.4.4 Investigations of Specific Interactions

Fourier Transform Infrared Spectroscopy (FTIR)

A Nicolet 20DXC Fourier Transform Infrared Spectrometer was used to investigate the presence of specific interactions in the blends, by observing any shifts in the position of peaks, corresponding to the functional groups involved in the interactions.

The samples were all cast from chloroform onto a slab of sodium chloride, yielding thin films, which were dried using a hot air blower. The samples were scanned 50 times at a resolution of 1 wavenumber and the resulting averaged spectra were stored on

microfloppy disks. By taking 50 scans the signal to noise ratio was improved, thereby increasing the sensitivity.

Figure 3.4 shows the layout of a typical FTIR spectrometer. There are three basic components, a source, a Michelson Interferometer (consisting of a beam splitter, a fixed mirror) and a detector. The principle of operation is as follows: Collimated radiation from the broad-band source is directed into the interferometer and impinges on the beamsplitter. Approximately 50% of the light is transmitted through the beamsplitter and is directed onto the fixed mirror. The remainder of the light reflects off the beamsplitter and is directed onto the moving mirror. The beams reflect off the surfaces of the two mirrors and recombine at the beamsplitter. Here, constructive and destructive interference occur, depending on the position of the moving mirror relative to the fixed mirror. The resulting beam passes through the sample where selective absorption takes place, and then continues onto the detector. In simple terms, what is happening is that the interferometer encodes the initial frequencies (by optically taking the Fourier transformation of the incoming signal) into a special form that the detector can observe in time. The inverse Fourier transformation is a mathematical means of resorting the individual frequencies for the final presentation of the infrared spectrum.
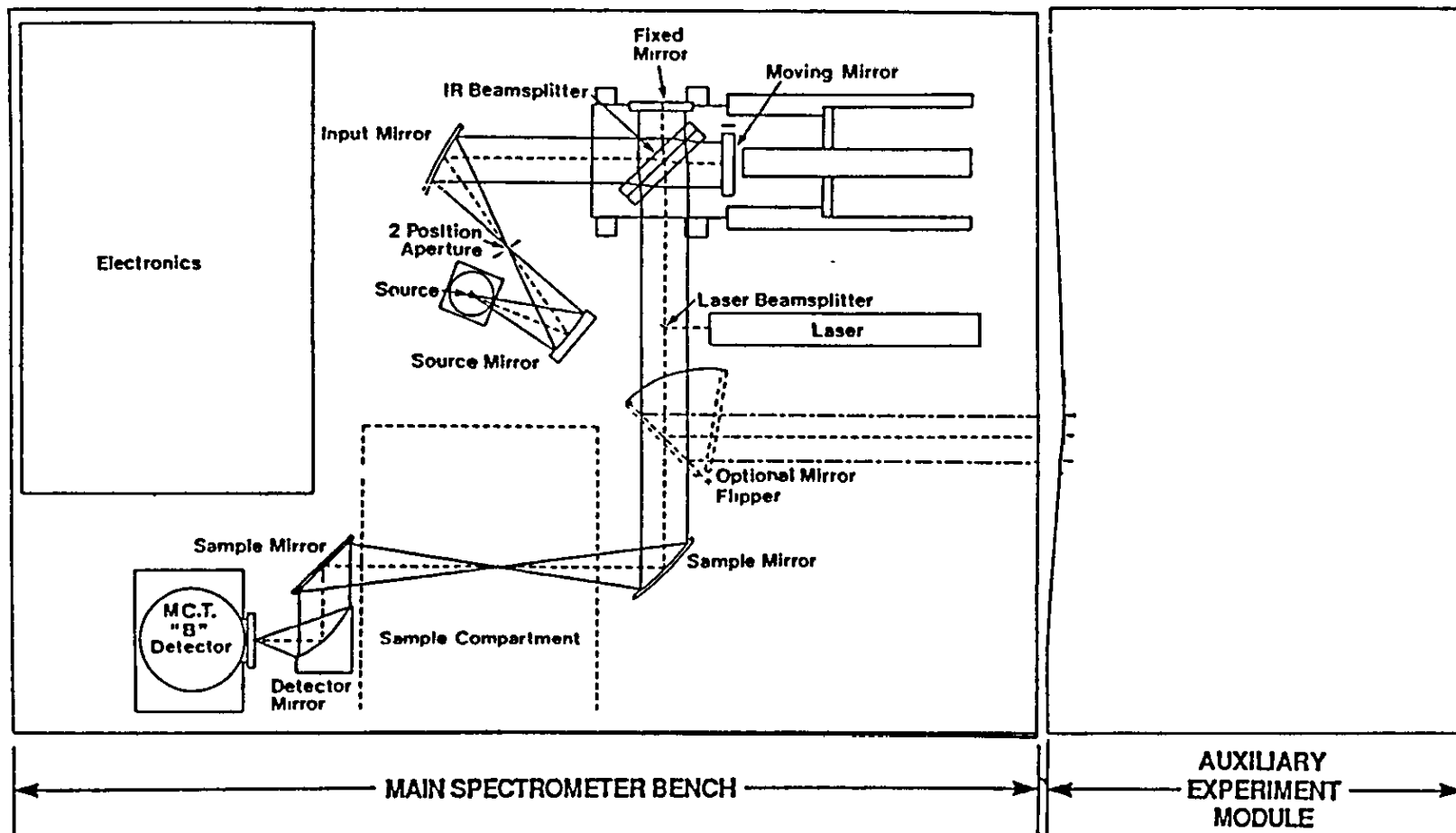
Figure 3.4

Layout of FTIR Spectrometer

4.0   Results and Discussion

4.1   Styrene/Methacrylic Acid Copolymer Blends

4.1.1 Characterisations and Composition Determination of ST/MAA Copolymers

(i) Reactivity Ratios

The reactivity ratios of styrene and methacrylic acid have been shown to vary with the particular reaction solvent used,[115] ranging from 0.06 for ST and 0.54 for MAA in chloroform, to 0.65 for ST and 0.43 for MAA in acetone. However, values of 0.18 and 0.65 for ST and MAA respectively have been obtained using 2-ethoxy ethanol as solvent.[116]   Since this is very similar in nature to 1-methoxy propan-2-ol , these reactivity ratios were used when determining the monomer feed ratios necessary to obtain a particular copolymer composition,   using equation (2.96).   It is important to remember however, that this equation only applies to monomer conversions of 10% or less.[107]   Since all of the copolymers produced have higher conversions than this, the implications relating to copolymer composition and distribution of monomer units should be considered. Assuming the reactivity ratios for ST and MAA in 2-ethoxy ethanol are a reasonable estimate of those in 1-methoxy propan-2-ol, it is clear that there is a tendency towards alternation ($r_1 r_2 \ll 1.0$), with MAA being the more reactive monomer.   This means that MAA will be consumed more quickly than ST in the copolymerisation reaction. Consider, for example, a reaction aiming to produce a 50:50 ratio of monomer units in the copolymer.   Since MAA is the more reactive monomer, a higher proportion of ST than MAA will be required in the initial mixture to counteract this.   In the early stages of the reaction, chains tending to have alternation of monomer units will be

- 76 -

formed, but after a time, the proportion of MAA in the mixture will decrease due to it's greater reactivity, leading to an increased tendency towards the formation of ST sequences; the further the reaction proceeds, the greater this tendency. If the reaction is allowed to go to high conversion, the proportion of ST units incorporated into the polymer chains will be greater than that predicted by the copolymer equation, because more ST units were present in the starting mixture than MAA units. So to obtain an approximately alternating copolymer of the desired composition, it is wise to limit the conversion to 10% or less. The copolymers 7, 8, 9, 29 and 30 were nevertheless, produced to high conversion as models for the polymers CMO3 and 9A/303, which were also produced to high conversion. (See Chapter 3).

(ii) Copolymer Composition

The composition of each copolymer produced was found from results of proton NMR spectroscopy, the method being outlined in section 3.2.1. The results are shown in table 4.1. along with the DMTA Tg values obtained for each copolymer. The NMR plots for the copolymers are shown in appendix 1. Figure 4.1 is a plot of copolymer composition vs Tg.

(iii) Molecular Weight

Copolymers 29 and 163 were eluted on a mixed gel GPC column in order to estimate the number and weight average molecular weights (see section 3.2.2.), the results are given in table 4.2., and the chromatograms shown in appendix 2.

(iv) Infrared Spectroscopy

The infrared spectra of copolymers 29 and 163 were obtained

- 77 -

Table 4.1 NMR and DMTA Results of ST/MAA Copolymers

(a) High Conversion Copolymers

Product	Monomer Feed Ratio (moles %)		Copolymer Composition from NMR (moles %)		DMTA Tg/°C
	ST	MAA	ST	MAA	
PMAA	0	100	0	100	189
7	25	75	35	65	180
8	50	50	49	51	155
9	75	25	54	46	143
29	90	10	84	16	120
30	95	5	88	12	112
PS	100	0	100	0	101

(b) Low Conversion Copolymer

Product	Monomer Feed Ratio (moles %)		Copolymer Composition from NMR (moles %)		DMTA Tg/°C
	ST	MAA	ST	MAA	
163	95	5	81	19	115

Note: All percentage coversions are given in table 3.2.

Figure 4.1
Composition vs Tg for ST/MAA Copolymers
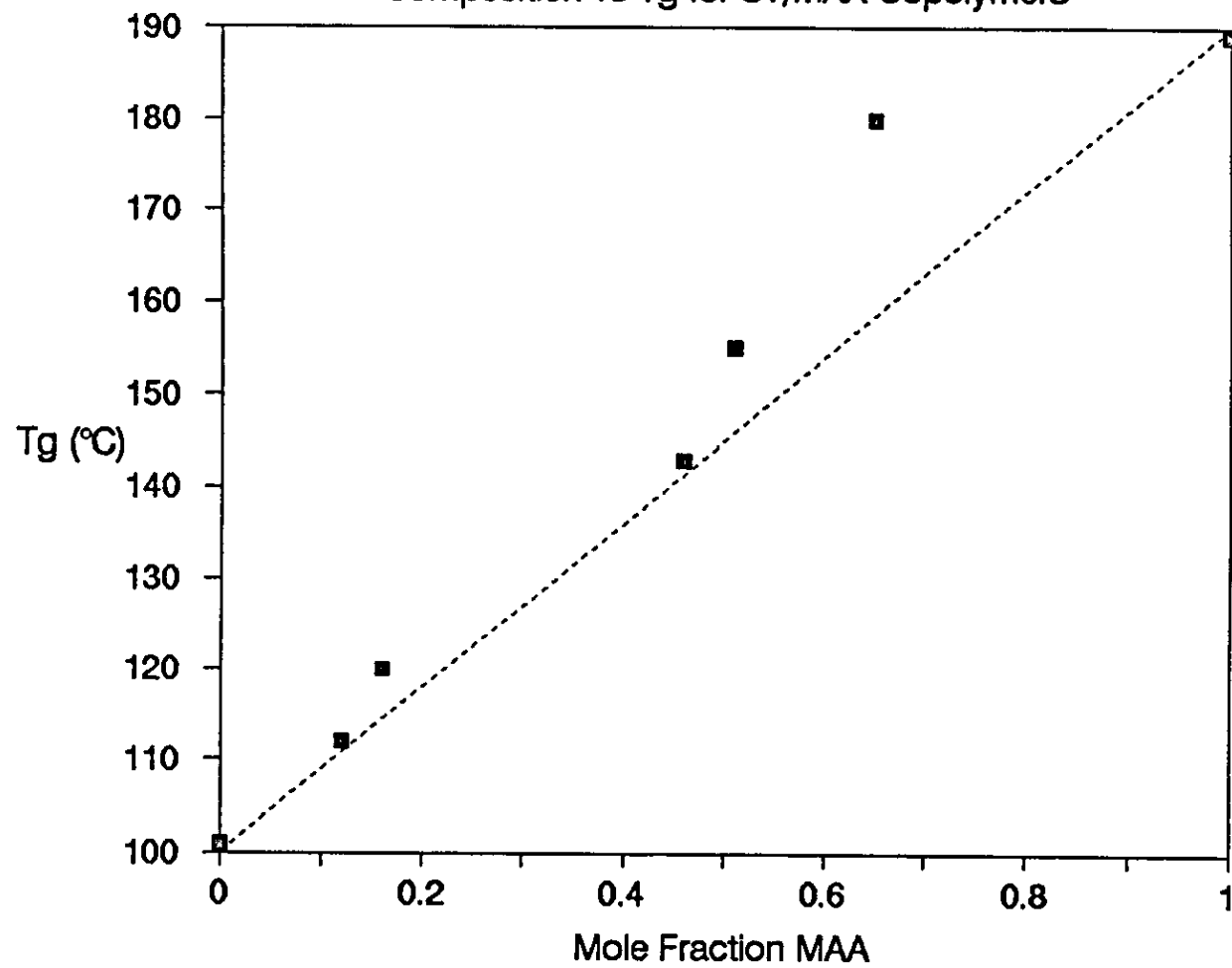
Table 4.2 GPC Results

Polymer	Source	Column	$\bar{M}n$	$\bar{M}w$	$\bar{M}w/\bar{M}n$	$\bar{M}p$
PBA(1)	Solution polymerisation	500Å	1749	2768	1.58	2200
PBA(2)	"	Mixed gel.	6757	20105	2.98	11655
PBA(3)	"	500 Å	5201	8231	1.58	6543
PPG(1)	Aldrich Chemical Co.	500 Å	9491	9900	1.04	9693
PPG(2)	"	500 Å	2769	2918	1.05	2843
LF200	LVH Coatings Ltd.	Mixed gel.	/	/	/	28793
CM03	"	Mixed gel.	/	/	/	19724
9A/303	"	Mixed gel.	/	/	/	19055
29 ST/MAA	Solution polymerisation	Mixed gel.	5996	11428	1.91	8278
163 ST/MAA	"	Mixed gel.	8141	16011	1.97	11417
PBMA	"	Mixed gel.	31315	53713	1.72	41012
PDMAEMA	"	Mixed gel.	4759	10546	2.22	7085
PPA	Victor Wolf Ltd.	Mixed gel.	5734	11600	2.02	8156

Note: ST/MAA copolymers 7, 8 and 9 were not analysed by GPC because they were not soluble in the chromatographic eluent THF, due to their relatively high MAA content.

using a Nicolet FTIR spectrometer (see section 3.4.4.) and are shown in appendix 3. Both spectra show characteristic peaks as expected for a combination of the two monomers ST and MAA.

(v) Characterisation of Lumiflon LF200

LF200 was found to have a glass transition temperature of 49°C by DMTA. The transition occurred over a narrow temperature range, the peak having a width of half height ($W_{h\frac{1}{2}}$) of 16°. The material was also characterised by NMR, GPC, FTIR and SEM, the results being shown in appendices 1, 2, 3, and 4 respectively.

4.1.2 Solution Blends

The blends were prepared as described in section 3.3.1, using tetrahydrofuran (THF) as solvent. In each case, the appearance of the dried blend film was noted, prior to each blend being studied by DMTA and FTIR. The results of these analyses are shown in table 4.3. Also shown are the values of Tg predicted by the Fox equation (2.77) and by the rule of mixtures:[101]

$$T_g = W_1 T_{g_1} + W_2 T_{g_2} + W_i T_{g_i} \quad (4.1),$$ W_i is the weight fraction of the repeat units of component i, whose homopolymer has glass transition temperature T_{g_i}. It is clear that from the film appearance and the occurrence of two glass transitions for each of the blends that all are immiscible in the proportions prepared. The opacity of the films is due to the presence of two separate phases corresponding to the two components of the mixture, which have different refractive indices and are sufficiently large to cause the scattering of light.[9] The two phase nature of the ST/MAA – LF200 blends is strongly confirmed by the presence of two glass transition temperatures for each of the blends, close to the temperatures at which transitions are observed for the unmixed copolymers and pure

- 78 -

Table 4.3   2 Component ST/MAA Copolymer Blends with LF200

Blend Number	Copolymer No. (wt. % in blend)	Film Appearance	DMTA Tg/°C	Fox Eqn. Tg/°C	Rule of Mixtures Tg/°C	FTIR Result
13	7 (25)	opaque	32,200	74	82	No Peak
12	7 (50)	"	46,189	103	115	Shifts
14	7 (75)	"	42,204	138	147	Observed
16	8 (25)	"	40,177	70	76	"
15	8 (50)	"	43,177	95	102	"
17	8 (75)	"	47,180	122	129	"
18	9 (25)	"	38,137	68	73	"
19	9 (50)	"	48,119	90	96	"
20	9 (75)	"	36,129	115	120	"
34	29 (25)	"	51,122	64	67	"
45	29 (50)	"	53,123	81	85	"
46	29 (75)	"	52,110	99	102	"
50	30 (25)	"	43,95	63	65	"
33	30 (50)	"	47,110	78	81	"
51	30 (75)	"	48,111	94	96	"
113	163 (25)	"	58,120	63	66	"
112	163 (50)	"	58,117	79	82	"

| LF200 | – | transparent | 49 | – | – | – |

LF200. Had the blends been miscible, transitions may have been expected in the region of the temperatures predicted by the rule of mixtures and the Fox equation. Figures 4.2 to 4.6 clearly show the two phase nature of these blends, both by the double Tg transitions and by the corresponding falls in the log modulus (E').

Fourier transform infrared spectroscopy (FTIR) was used to determine whether any specific interactions were present in the mixtures, between the functional groups of the two components. The only group of the copolymer likely to be involved in such interactions is the carboxylic acid group. LF200 is a polymer comprising four monomer units (see section 3.1.3), two of which have ether side groups and one which has a hydroxy-butyl group linked to the backbone by another ether oxygen. The most likely interaction therefore, is that between the methacrylic acid group and the hydroxyl group of LF200. If such an interaction is present in the blend, it might be expected to have some effect on the bond lengths between the atoms of the groups involved. This would in turn lead to a change in the vibrational frequency of these blends, which could then be observed as a change in the position of the infrared band corresponding to that group. However, no noticeable change occurred in the position of the acid carbonyl band at around 1700 cm^{-1}, nor could any other band shifts be detected in the spectra of the blends. The peak at 1700 cm^{-1} is in fact due to the dimer formed by the intermolecular hydrogen bonding interaction between carboxylic acid groups. It seems that this interaction is sufficiently strong as to occur preferentially to any interactions between the acid group and the hydroxyl group of LF200. The apparent lack of any specific interactions for this system could be one reason for the observed immiscibility. Many miscible blends studied recently by FTIR have been shown to have interactions between the components and this has

Figure   4.2

DMTA Results for ST/MAA – LF200 Solution Blends (Table 4.3)
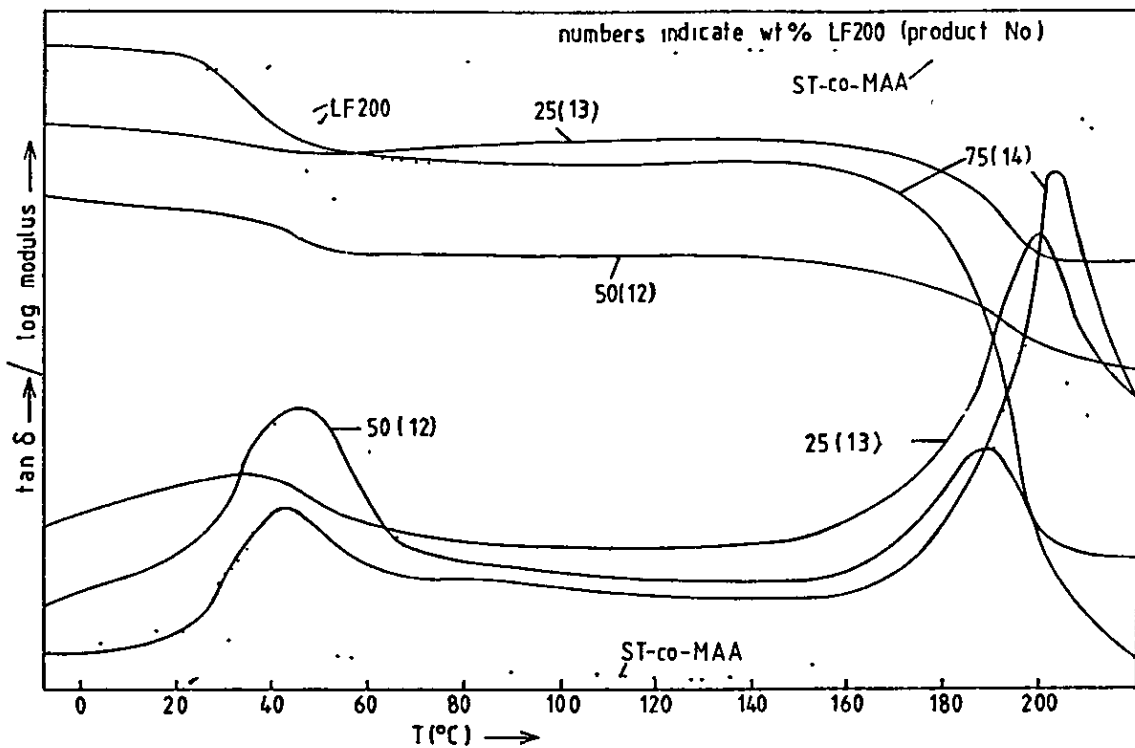
Figure   4.3

DMTA Results for ST/MAA – LF200 Solution Blends (Table 4.3)
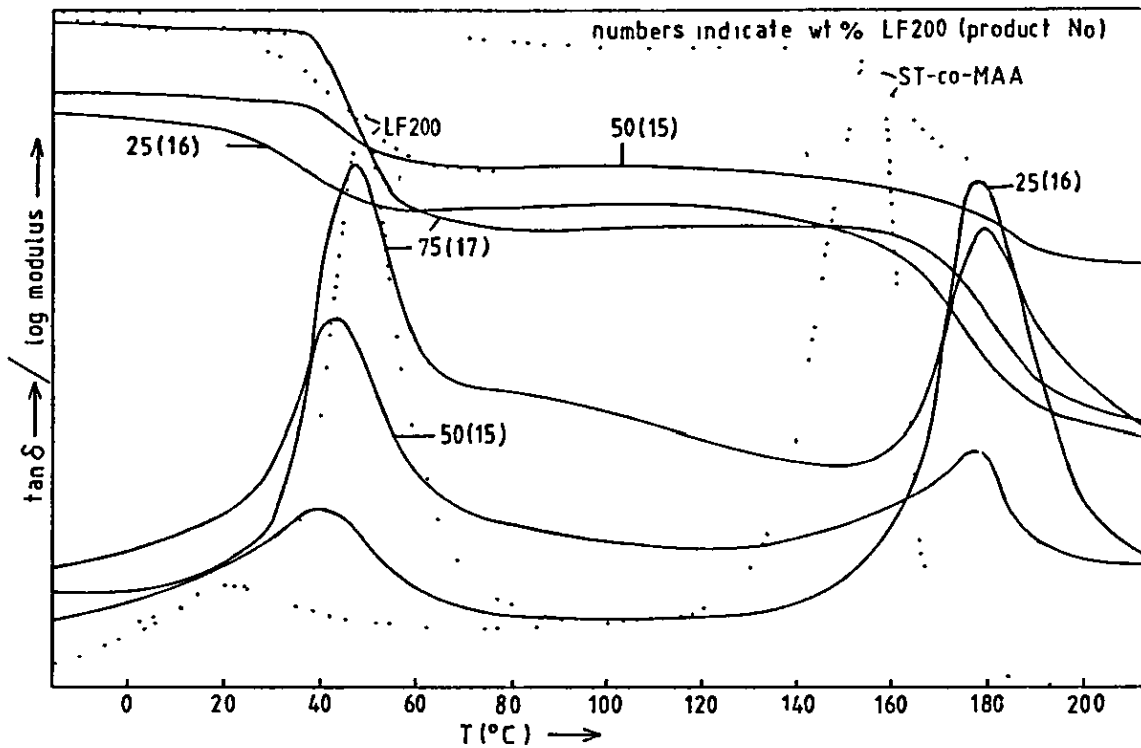
Figure 4.4

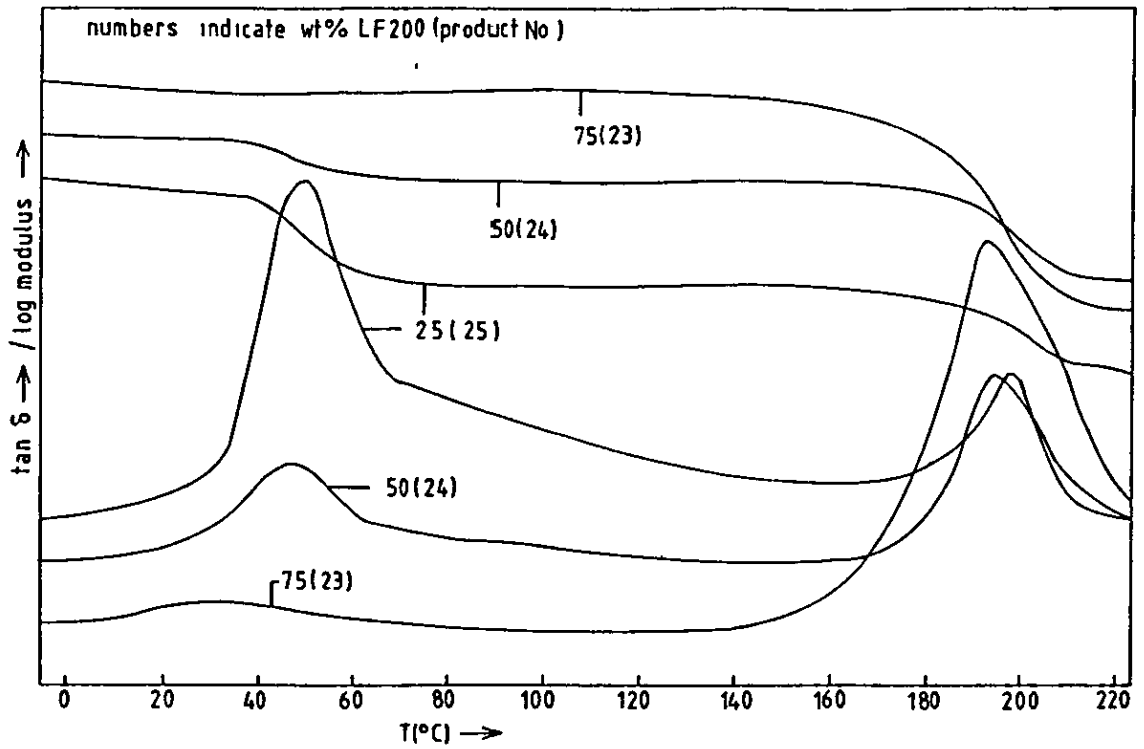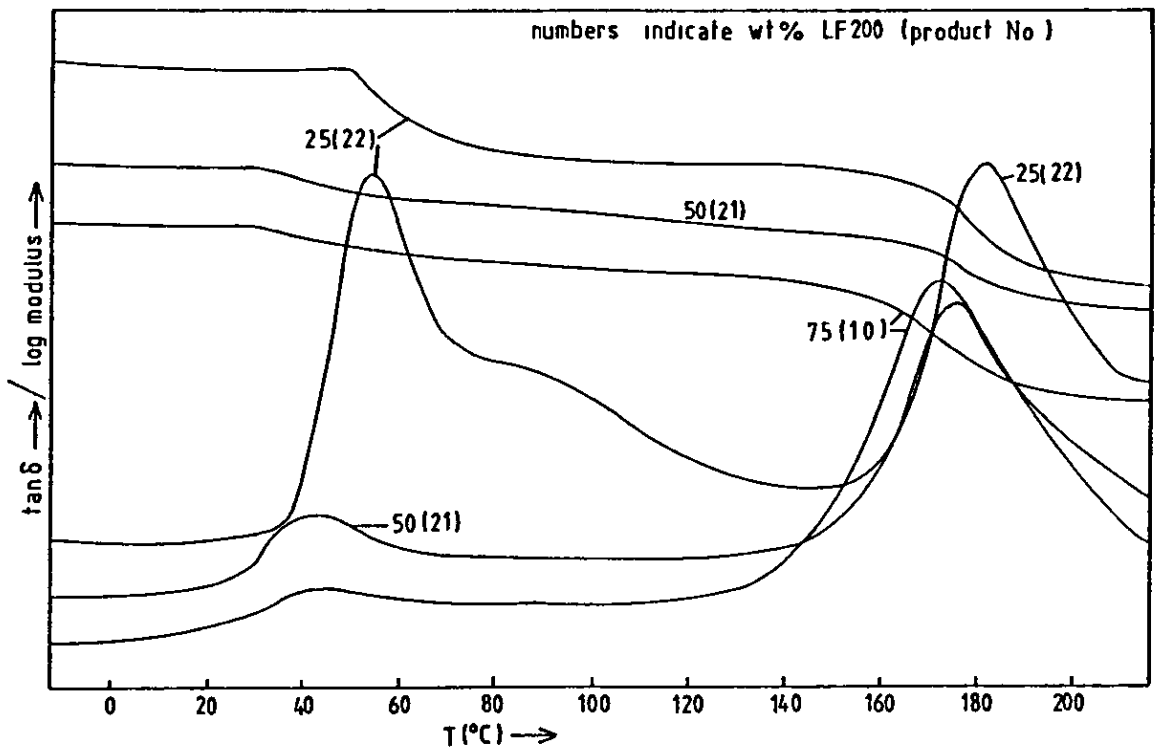DMTA Results for ST/MAA – LF200 Solution Blends (Table 4.3)
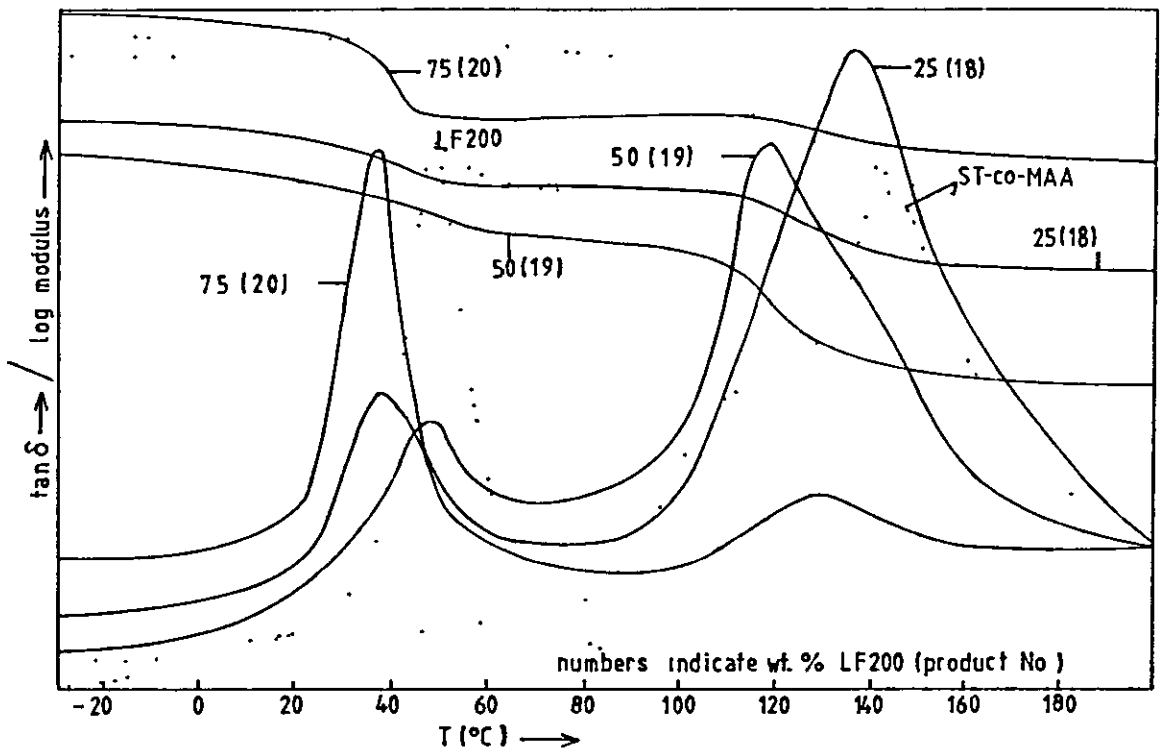
Figure 4.5

DMTA Results for ST/MAA – LF200 Solution Blends (Table 4.3)
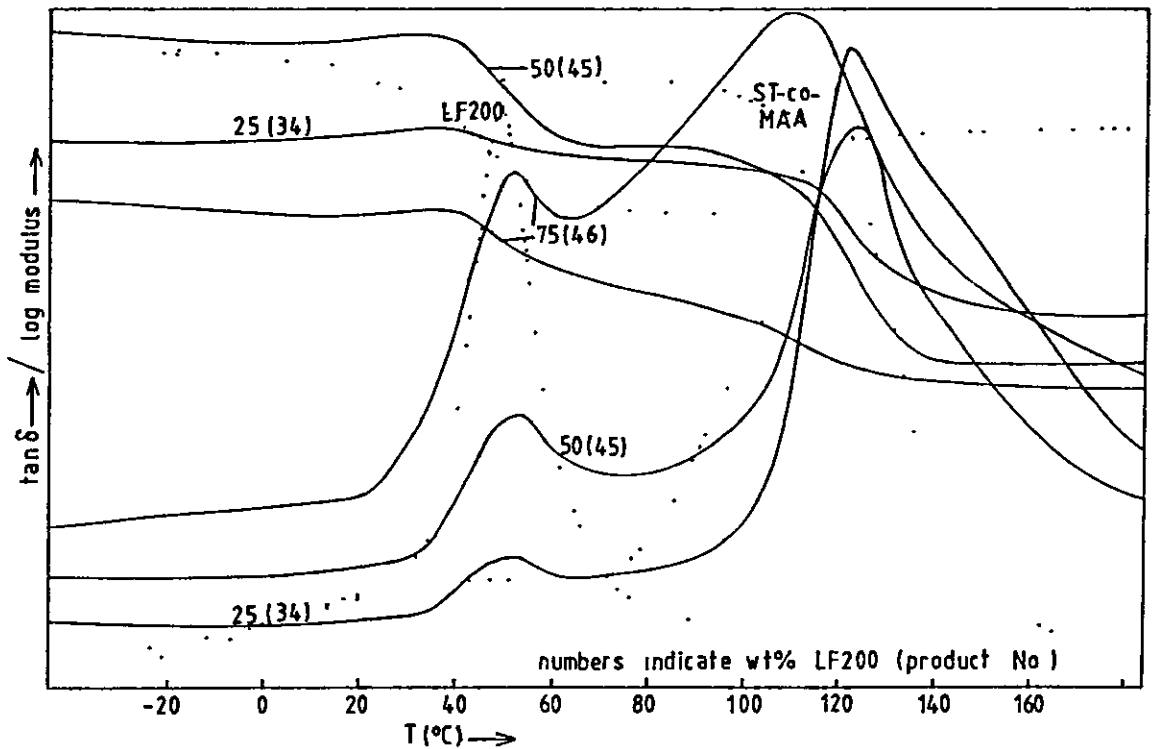
Figure 4.6

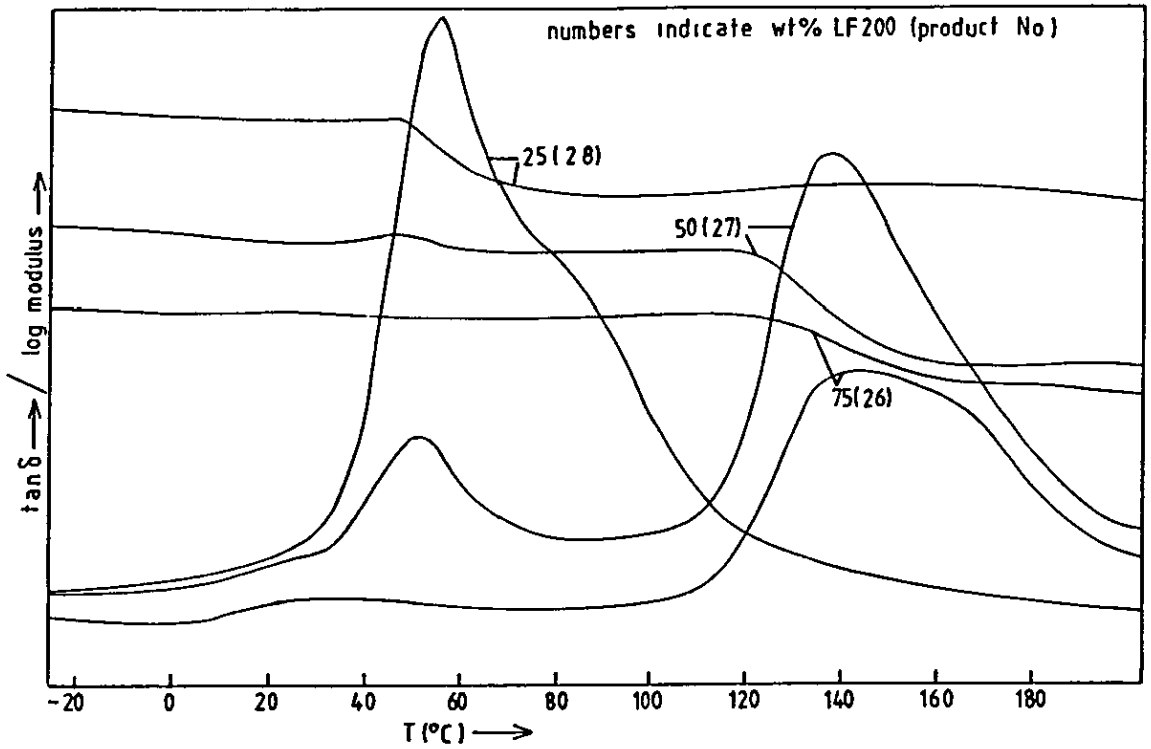DMTA Results for ST/MAA - LF200 Solution Blends (Table 4.3)
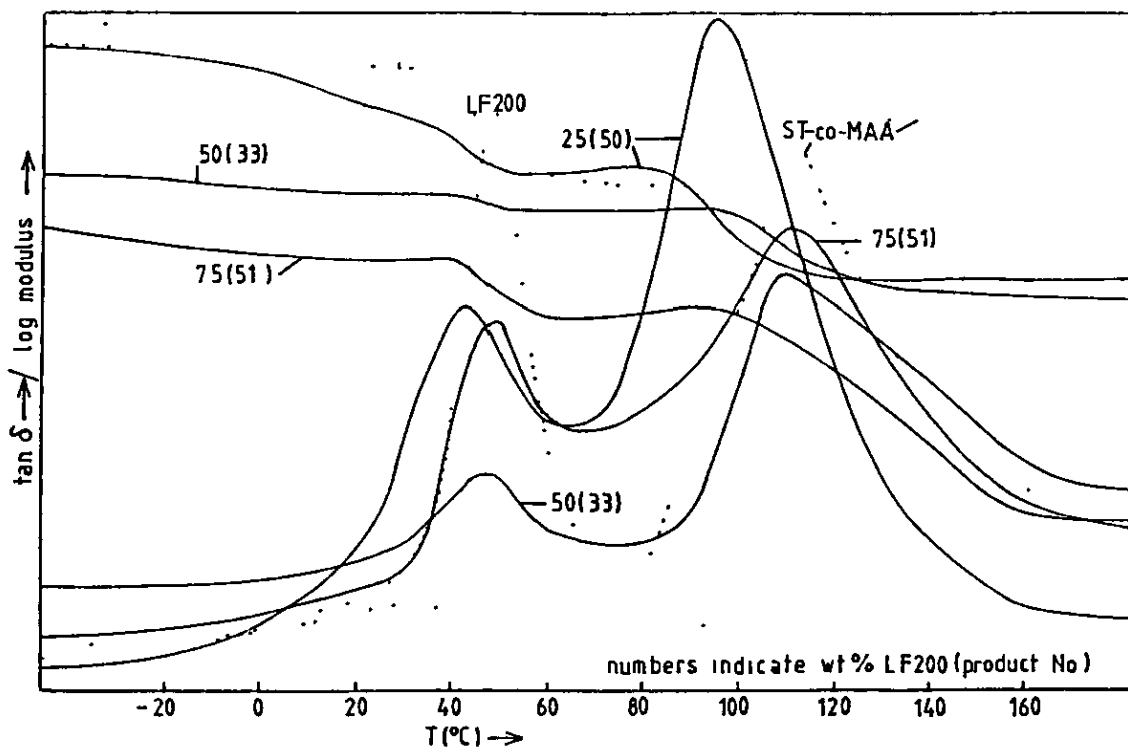
been suggested as a major factor which enhances polymer-polymer miscibility.[111,112,118-121]

Another factor which may have influenced the mixing behaviour of the two components, could be the choice of solvent used for the solution blending procedure. Tetrahydrofuran (THF) was chosen because it appeared to be a good solvent for all of the copolymers, including those with a high proportion of MAA units (poly(methacrylic acid) is soluble in few organic solvents) and also LF200. It also had the advantage of being quite volatile, making it's evaporation quite rapid and the drying of subsequent blend films easier. It has been suggested,[122] that the nature of the solvent used to mix two polymers has an important effect with regard to the miscibility of the blend. The extent to which the solvent influences the final miscibility, depends on the nature and strength of the various interactions between the components of the solution, prior to and during the evaporation of the solvent. If for example, the solvent is a good one for both polymers, then the two polymer chains will have significant coil extension which will promote good contacts between potential interaction sites, leading to a miscible blend. On the other hand, if the solvent is a bad one for the two polymers, the chains of each polymer will tend to coil up and contract, giving few opportunities for interfacial contacts. In the case of a system where strong polymer-solvent interactions exist, the polymer chains will be tightly solvated by solvent molecules which would hinder interactions between the unlike chains, thereby reducing the eventual blend miscibility.

For the system involving ST/MAA copolymer, LF200 and THF as solvent, interactions are possible between the copolymer carboxylic acid groups and the ether oxygen of the THF. This can be observed by FTIR spectroscopy. If a ST/MAA film is cast from THF, but is not

completely dry, a second acid carbonyl peak appears at around 1728 cm^{-1}, alongside the peak at 1700 cm^{-1}, due to the hydrogen bonding interactions between the acid group and the ether oxygen of the solvent. For this reason, films for FTIR analysis were cast from chloroform instead of THF wherever possible. The existence of this polymer-solvent interaction could be one possible explanation for this systems lack of miscibility, by preventing any possible interactions between the carboxylic acid groups of MAA and the hydroxyl or ether groups of LF200. However, it may just be that the groups on LF200 are not sufficiently polar or electronegative to be susceptible to hydrogen bonding interactions.

4.1.3 Reaction Blends

Following the unsuccessful attempts to produce a miscible blend by solution casting, a series of experiments was carried out to see if miscibility could be improved by employing a different preparation technique. It was decided to polymerise the two monomers ST and MAA in a solution of LF200 in 1-methoxy propan-2-ol at 60 - 70°C, this method was termed "reaction blending" (see section 3.3.2). Since the LF200 was present in the polymerisation solvent and the reaction was carried out at elevated temperatures, there was the potential for an interaction between the acid monomer and the hydroxyl containing LF200, especially in the early stages of the reaction when short chain molecules containing the MAA unit were present in the solution. The small chain molecules would also have had a greater mobility and easier accessibility to potential interaction sites on the LF200 chains. It was hoped that these factors would help to improve the blend miscibility. However, this was not the case, as can be seen from the results in table 4.4 and from figures 4.7 to 4.10. All the blends formed by this method are clearly two phase, being opaque in

- 81 -

Table 4.4 DMTA Results for LF200 - ST/MAA Reaction Blends

Product Number	Monomer Ratio (moles %)		Ratio of LF200 to total monomer		DMTA Tgs/°C
	ST	MAA	LF200	Total Monomer	
23	25	75	75	25	35,193
24	25	75	50	50	48,195
25	25	75	25	75	49,198
10	50	50	75	25	45,172
21	50	50	50	50	42,176
22	50	50	25	75	54,182
26	75	25	75	25	40,141
27	75	25	50	50	52,138
28	75	25	25	75	55,(85)
81	90	10	30	70	47,112
82	95	5	30	70	50,120

Figure   4.7

DMTA Results for ST/MAA − LF200 Reaction Blends (Table 4.4)

Figure   4.8

DMTA Results for ST/MAA − LF200 Reaction Blends (Table 4.4)

Figure 4.9

DMTA Results for ST/MAA — LF200 Reaction Blends (Table 4.4)

Figure 4.10

DMTA Results for ST/MAA — LF200 Reaction Blends (Table 4.4)
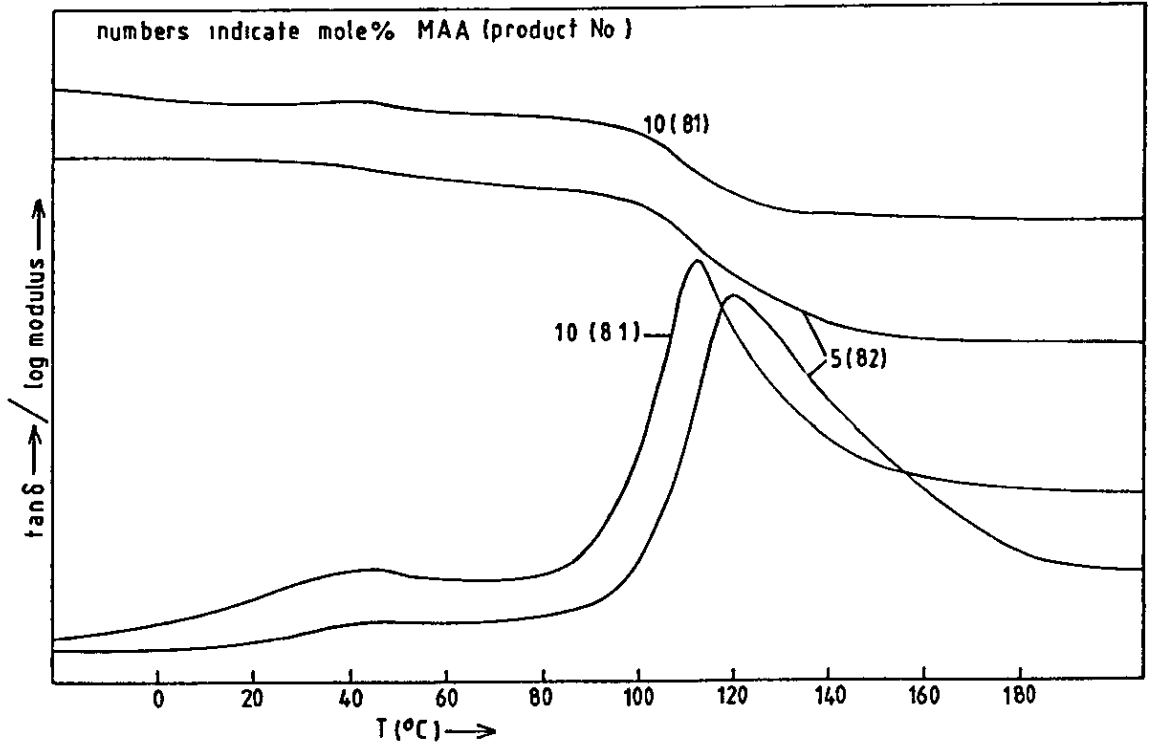
appearance when dry, with two well separated glass transitions for each of the phases. It appears therefore, that this method offers no improvement with regard to improving miscibility compared to the usual solution blending procedure, for this system at least. The actual positions of the observed glass transition temperatures varied slightly, but not significantly from those observed in the previous experiments. The fact that a different solvent was used and that the solutions containing the polymerised monomers and the LF200 were precipitated into n-heptane instead of the solvent being evaporated, appeared to have little or no effect on the miscibility of the blends.

4.1.4   ST/MAA - LF200 Blends - Summary and Conclusions

All of the blends produced were clearly immiscible regardless of composition or method of preparation, as indicated by their opacity and by the DMTA glass transition results. It seems therefore, that the copolymer of ST and MAA was a poor choice for a model system for the LVH coatings polymers CM03 and 9A/303. Neither were any specific interactions identified, nor were any miscible blends produced. At this point it was decided to investigate the miscibility of LF200 with a range of homopolymers and copolymers, in order to discover what type of polymer it may be miscible with.

4.2   Solution Blends of LF200 with a Variety of Polymers

Table 4.5 shows the series of blends produced, describing the optical appearance of the films along with the transitions observed by DMTA. An indication of the Tg transition width is given where appropriate. Conclusions regarding miscibility are also included in

Table 4.5 Solution Blends of LF200 with Various Polymers

Product Number	Blend Composition	Appearance of Blend Film	DMTA Tg/°C	Wh½	Inference
	100% PBA(2)		−24	17°	
78	LF200/PBA(2) 25:75	transparent	−18, 32	−	partially miscible
79	LF200/PBA(2) 50:50	transparent	8	34°	miscible
80	LF200/PBA(2) 75:25	transparent	35	39°	miscible
	100% PBMA		59	68°	
43	LF200/PBMA 25:75	transparent	50	41°	inconclusive
36	LF200/PBMA 50:50	transparent	46	58°	''
62	LF200/PBMA 75:25	transparent	49	22°	''
	100% PMA		17	14°	
59	LF200/PMA 25:75	transparent	20,36,(63)	−	immiscible
37	LF200/PMA 50:50	transparent	23, 47	−	immiscible
44	LF200/PMA 75:25	transparent	17, 47	−	immiscible
	100% PMMA		100		
47	LF200/PMMA 25:75	translucent	37, 103	−	immiscible
38	LF200/PMMA 50:50	translucent	33, 83	−	immiscible
58	LF200/PMMA 75:25	translucent	44, 95	−	immiscible
	100% PHEMA		53 (33)	−	
75	LF200/PHEMA 25:75	translucent	37, 53, 77	−	inconclusive
76	LF200/PHEMA 50:50	translucent	42, 86	−	''
77	LF200/PHEMA 75:25	translucent	(39), 66	(100°)	''
	100% PDMAEMA		43	39°	
83	LF200/PDMAEMA 25:75	translucent	43	34°	inconclusive
84	LF200/PDMAEMA 50·50	translucent	43	26°	''
85	LF200/PDMAEMA 75:25	translucent	52	24°	''
	100% PST		101	43°	
49	LF200/PST 25:75	opaque	44, 91	−	immiscible
39	LF200/PST 50:50	opaque	45, 89	−	immiscible
48	LF200/PST 75:25	opaque	49, 93	−	immiscible

	100% LF200		49	16°	

Table 4.5 (continued) Solution Blends of LF200 with Various Polymers

Product Number	Blend Composition	Appearance of Blend Film	DMTA Tg/°C	Wh½	Inference
	100% SAN		114	20°	
52	LF200/SAN 25:75	opaque	43, 87	–	immiscible
53	LF200/SAN 50:50	opaque	42, 91	–	immiscible
54	LF200/SAN 75:25	opaque	47	22°	miscible
	100% PVAc		47	21°	
63	LF200/PVAc 25:75	transparent	48	24°	inconclusive
64	LF200/PVAc 50:50	transparent	45	22°	"
65	LF200/PVAc 75:25	transparent	44	21°	"
	100% EVA		–14(Tg),51(Tm)	–	
55	LF200/EVA 25:75	transparent	1, 47	–	inconclusive
56	LF200/EVA 50:50	transparent	10, (20–65)	(74°)	"
57	LF200/EVA 75:25	transparent	30	39	miscible
	100% PEG		–11, 20, 58	–	
41	LF200/PEG 25:75	transparent at 60°C, opaque patches at R.T.	(–20), 44	(33°)	inconclusive
40	LF200/PEG 50:50	"	48, (15)	26°	"
42	LF200/PEG 75:25	"	48	51°	miscible

the table. The DMTA results are shown in figures 4.11 to 4.21. All blends were prepared as described in section 3.3.1 using tetrahydrofuran as solvent, unless otherwise stated.

LF200 - Poly(n-butyl acrylate) (2) (PBA(2))

The poly(n-butyl acrylate) used was prepared as described in section 3.1.2 and table 3.1, and had a number average molecular weight ($\bar{M}n$) of 6757 as determined by gel permeation chromatography (see table 4.2). The DMTA plots for this blend are shown in figure 4.11. The dried blend films for each of the three compositions were completely transparent, which is often, although not always, a good indication of miscibility. The single phase nature of this blend is strongly confirmed by the DMTA results, for the compositions having 25% and 50% by weight of PBA(2), showing single Tg transitions at 35°C and 8°C respectively. The blend having 75% PBA(2) does not show a single Tg transition, but has a more complex tanδ curve, which probably suggests a certain degree of partial miscibility. In each case the tanδ curves are mirrored closely by the log modulus (E') curves, which show a reduction in log modulus at the glass transition temperature as would be expected. If the widths of the peaks at half height are considered, it can be seen that the tanδ peaks relating to the 25% and 50% PBA(2) blends are broader than the peaks corresponding to the glass transitions of the unmixed component polymers. This may be an indication that these blends are not completely miscible, but that depends on the definition of miscibility. Kaplan[8] has suggested that a domain or phase size of 15 nm is required to contain a "universal" segmental length associated with the glass transition. That is, if larger phases than this exist, then two transitions will be observed, below this size a single transition. However, it is likely that there will be a range

- 83 -

Figure 4.11
DMTA Results for LF200 – PBA(2) Blends (Table 4.5)
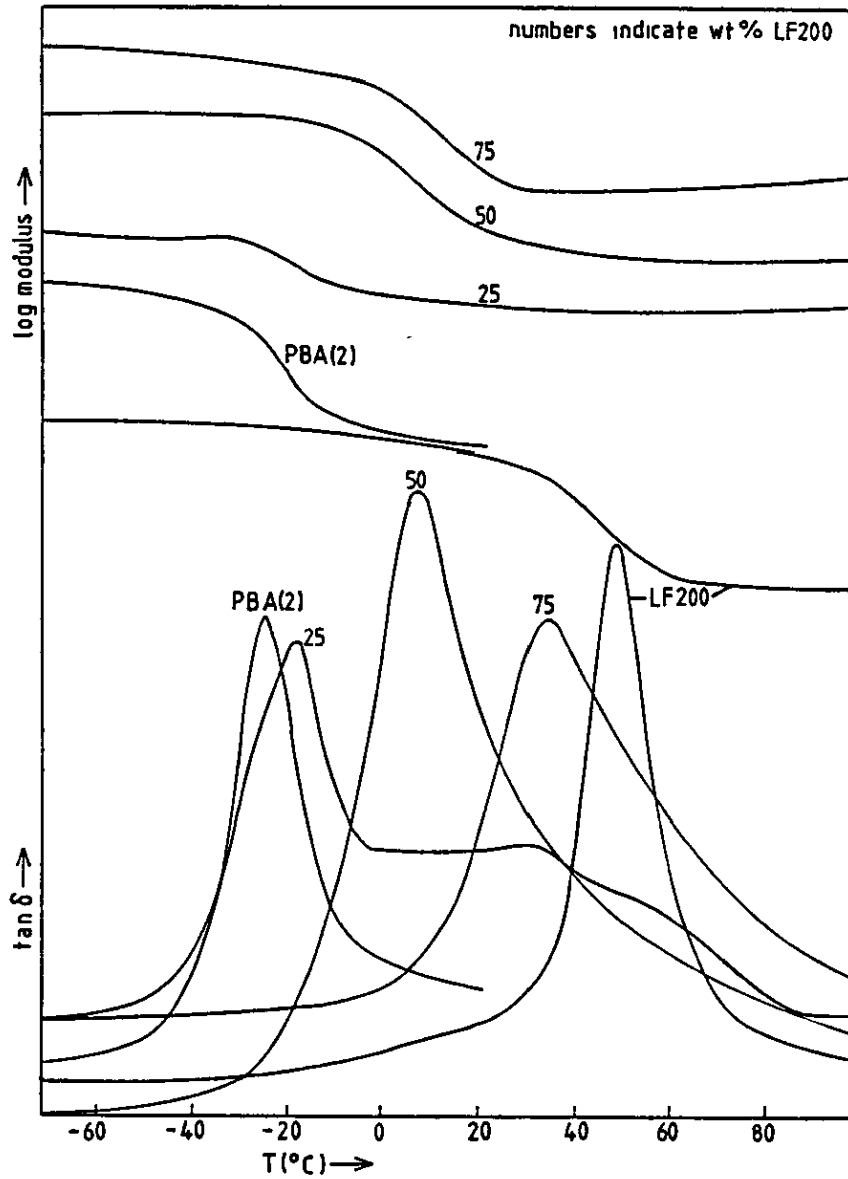
Figure 4.12
DMTA Results for LF200 – PBMA Blends (Table 4.5)
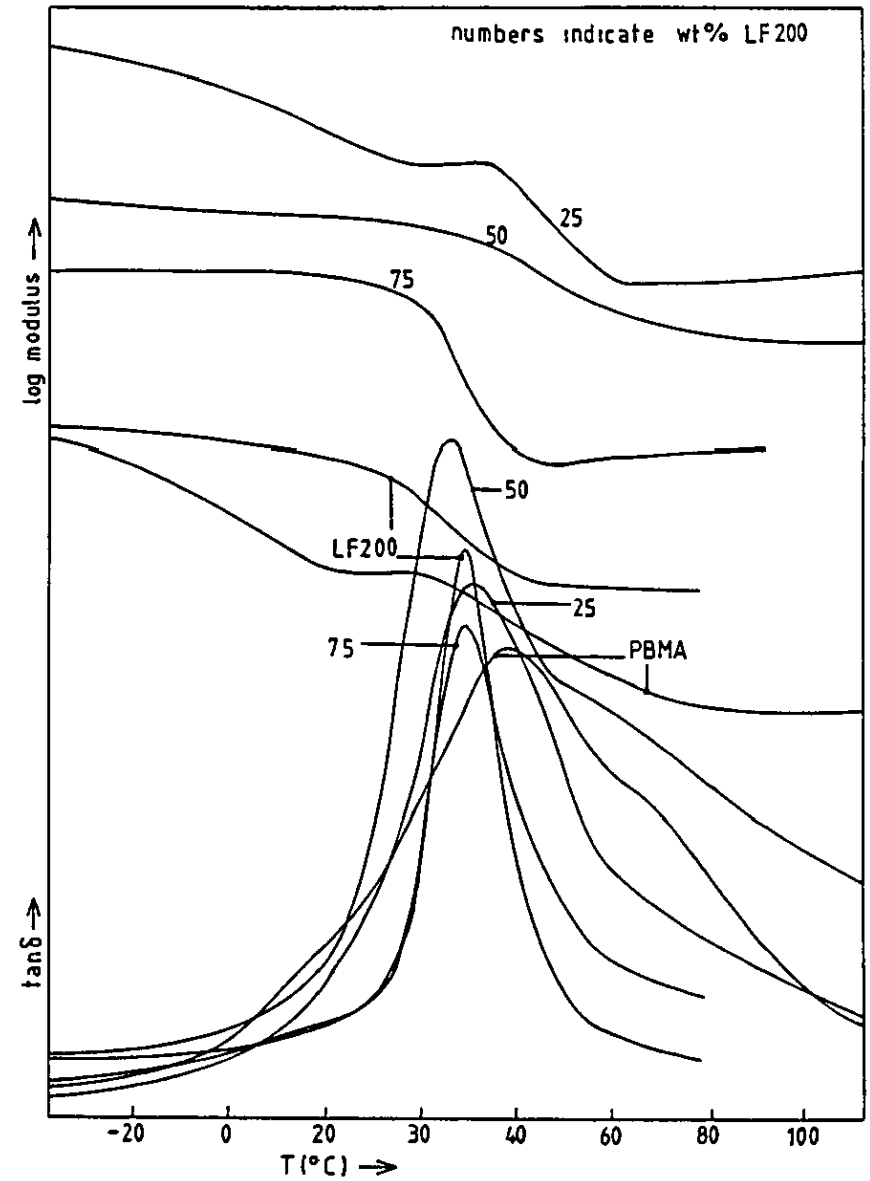
of domain sizes in the region of 15 nm which are borderline between miscibility and immiscibility, as defined in terms of a single glass transition. The definition of miscibility therefore, usually depends on the method by which it is observed. A system that is indicated to be miscible by DMTA or some other technique, may not be completely thermodynamically miscible, if such a state exists.

In this case it is reasonable to conclude that PBA(2) is miscible in the compositions having 25% and 50% by weight of PBA(2), as indicated by optical clarity and single glass transitions.

LF200 - Poly(n-butyl methacrylate) (PBMA)

The DMTA results (figure 4.12) for these blends highlight one of the limitations of the technique of assigning the state of mixing using glass transitions. LF200 has a Tg of 49°C and PBMA which has an $\bar{M}n$ of 31300 (table 4.2), has a Tg of 59°C, so it is inevitable that there will be considerable overlap of the transitions of these polymers. Dynamic mechanical analysis can really only resolve transitions which are separated by 20°C or more, the resolution often depending on the peak widths.

The three compositions of LF200 and PBMA each yield a single Tg, but this is not surprising, because of the proximity of their respective Tg transitions. It would be unwise in this case therefore, to attempt to draw conclusions on the miscibility of the blend based on DMTA results alone. Each of the blend films however,was transparent and this may be an indication of miscibility, provided the two components have different refractive indices. To be able to make definite conclusions about the state of mixing of LF200-PBMA blends another technique such as electron microscopy perhaps,[123] would be required to confirm the tentative conclusion of miscibility based solely on optical clarity.

LF200 - Poly(methyl acrylate) (PMA)

The DMTA plots for these blends are shown in figure 4.13 and from the presence of two glass transitions for each composition, it is clear that they are immiscible. The blends having 50% and 75% LF200 each show two tanδ peaks with some overlap between them, the peaks appearing close to the temperatures at which the peaks for PMA and LF200 are to be found. The log modulus curves for these two compositions each show two falls in value and confirm the existence of two separate glass transitions. The blend containing 25% LF200 has a more complex tanδ curve, having what appears to be three peaks, although largely overlapped. This could be an indication of three phases which could conceivably be, a phase rich in PMA, a phase rich in LF200 and a third mixed phase comprising both components. If the transition at 36°C truly represents a mixed phase, then it could be that some degree of partial miscibility exists for this blend composition. It may be that with a still smaller proportion of LF200, a greater degree of miscibility might be achieved.

The optical clarity of these three blends, contradicts with their apparent lack of miscibility, as indicated by their multiple glass transitions. It could be in this case that the refractive indices of the two polymers are very close, leading to optical clarity despite the fact that they do not mix. This is the reason why transparency alone should never lead to firm conclusions regarding the miscibility of polymer blends.

LF200 - Poly(methyl methacrylate) (PMMA)

The PMMA used was supplied by Aldrich and had a molecular weight ($\bar{M}_n$) of 12000. The DMTA plots are shown in figure 4.14 and the curves for each composition indicate two well separated glass transitions. The glass transition temperatures of LF200 and PMMA,

Figure 4.13
DMTA Results for LF200 – PMA Blends (Table 4.5)
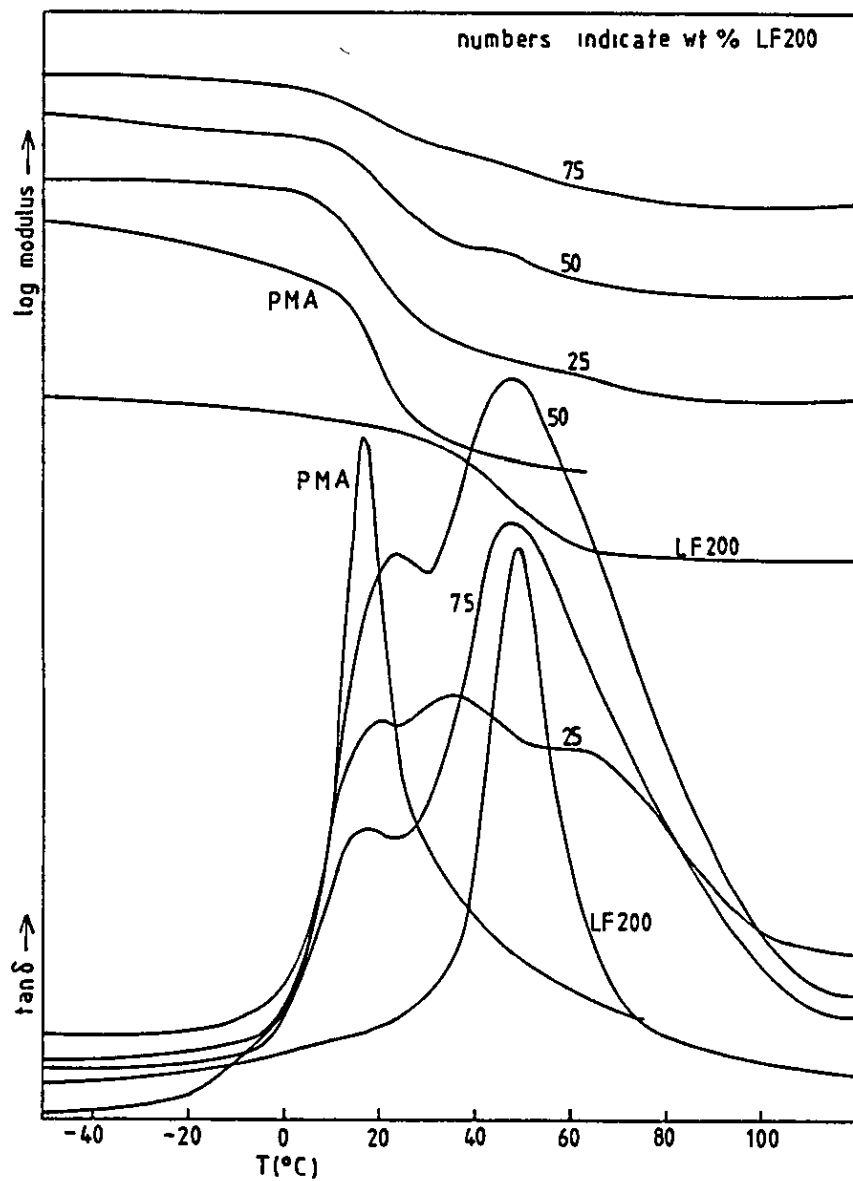
Figure 4.14
DMTA Results for LF200 – PMMA Blends (Table 4.5)
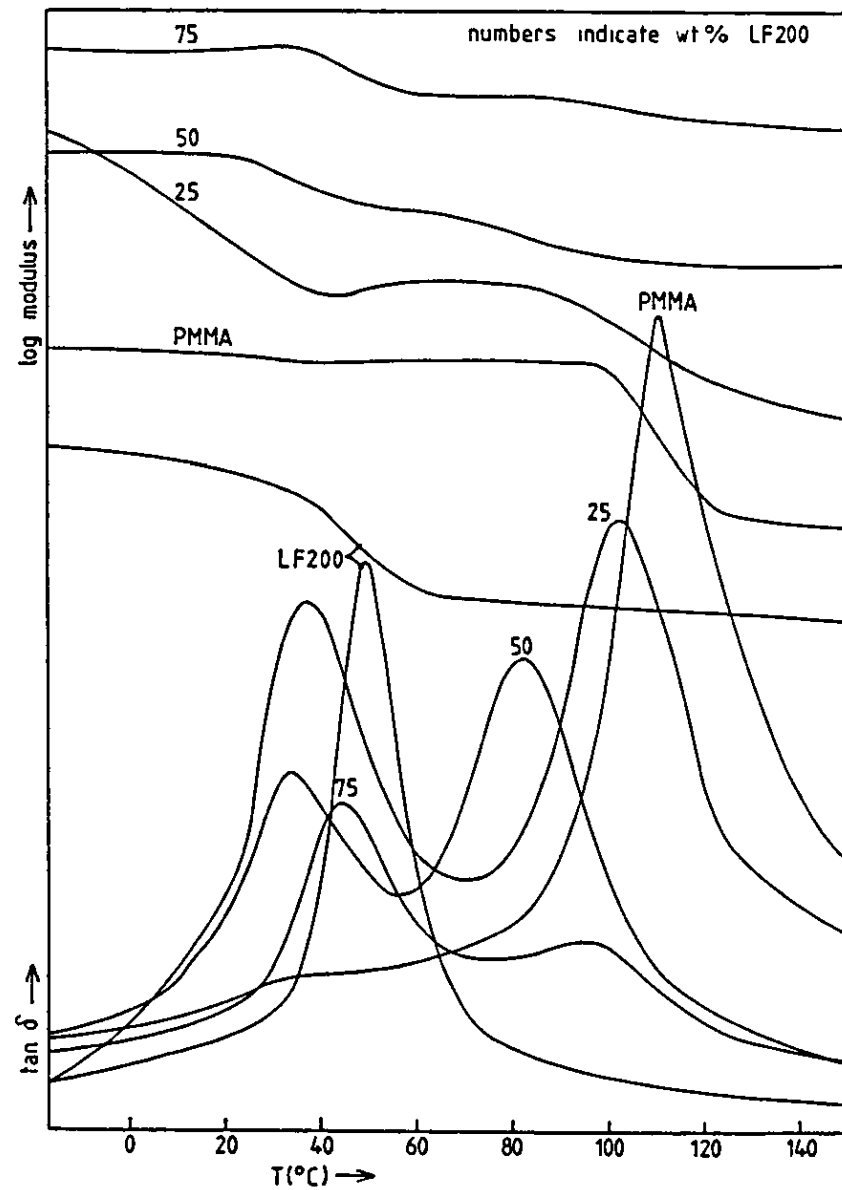
being 49°C and 100°C respectively ensure that the conclusion of immiscibility is unambiguous. It is noticeable that the tanδ peaks for the three blend compositions show some displacement from the positions at which the transitions appear for the pure unmixed components. The reason for this is not obvious. Partial miscibility is not indicated by this observation, since in this case the peaks tend to be shifted towards one another (see section 2.9.1 and figure 2.12). One possible explanation could be that the blends were not completely dried and that some solvent (THF) remained after the samples were melt pressed. It is unlikely that much THF could be retained after this procedure, but it might explain the shifts of the two tanδ peaks for each composition, to lower temperatures than expected, by acting as a plasticiser. If solvent were still present in the blend films it would also perhaps, explain the translucence of the films. Whatever the explanation for these observations, it still remains clear that PMMA and LF200 do not mix in the proportions tried.

LF200 - Poly(2-hydroxyethyl methacrylate) (PHEMA)

PHEMA was found to be insoluble in THF and so 1-methoxy propan-2-ol was used as solvent. Again there is the problem that the glass transitions of the two polymers are very close, this time separated by only 4°C, so it is impossible to make any firm conclusions about the miscibility of the blends from DMTA results alone. As can be seen from figure 4.16 the tanδ curves for PHEMA itself and for the three blends with LF200 are all of a rather complex shape, each showing two or three peaks or "shoulders". It seems that there is some interaction between the two components, but it is very unclear what this might be. It is very unusual to produce a transition in a blend of two polymers, which is significantly higher than the

- 86 -

Figure 4.15

DMTA Results for LF200 – PDMAEMA Blends (Table 4.5)
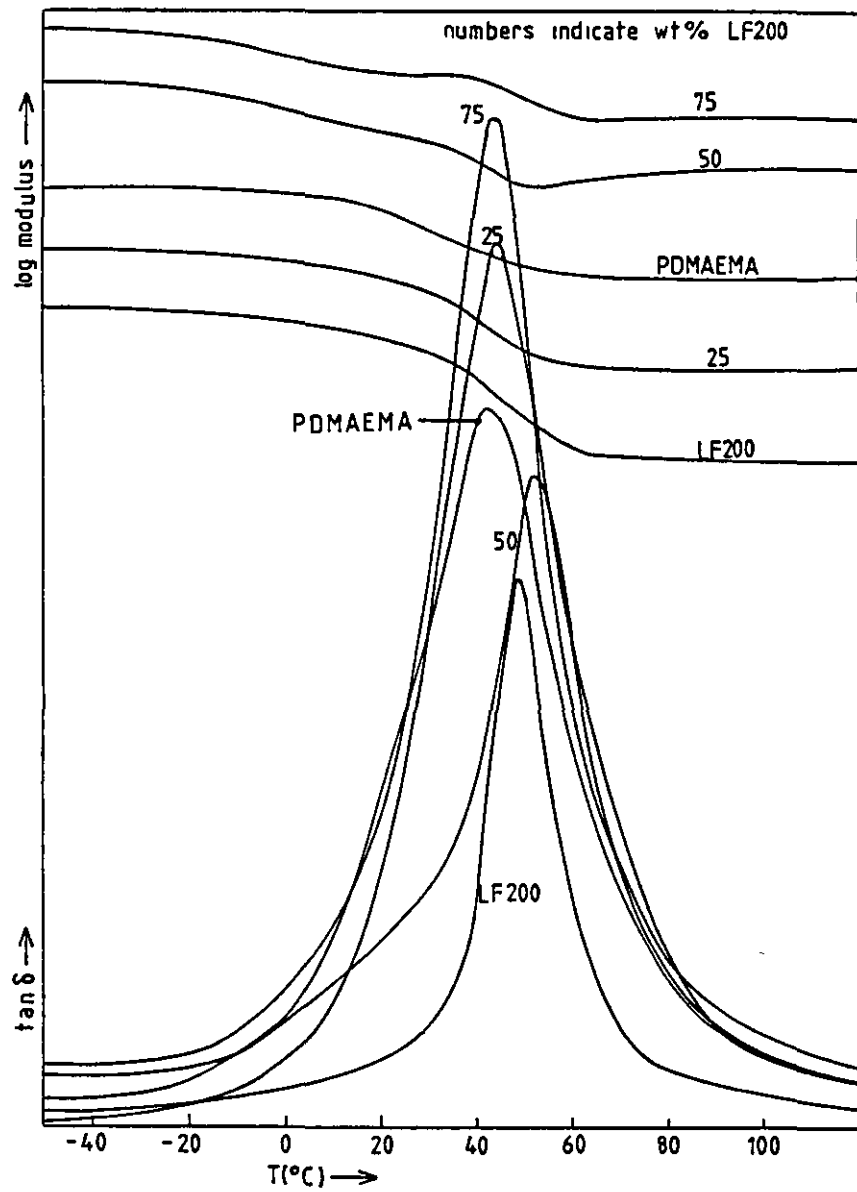
Figure 4.16

DMTA Results for LF200 – PHEMA Blends (Table 4.5)
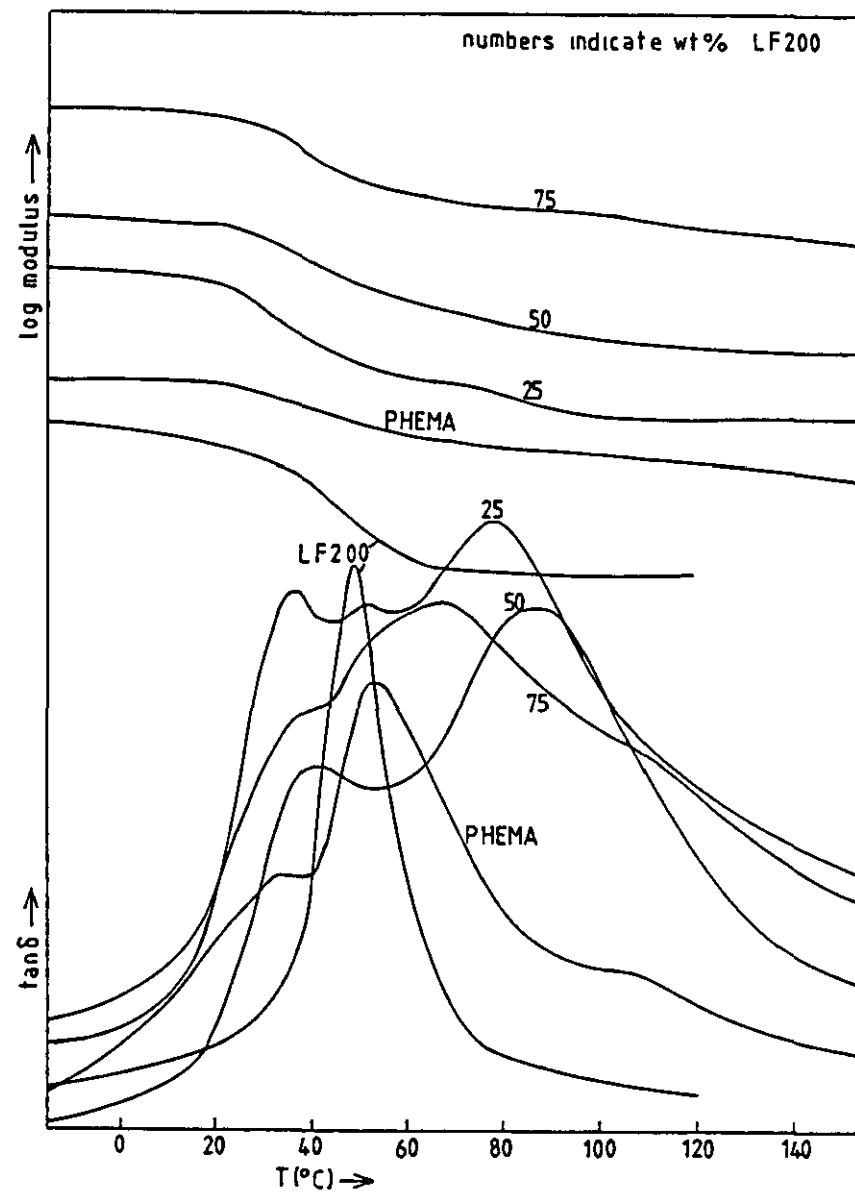
transitions of either component, as is the case here. It can only be speculated that the interaction between LF200 and PHEMA if in fact one exists, causes some hindrance to rotation about the backbone chain of one or both components, manifested in an increase in the observed glass transition of the blend. It is unclear in the first instance why PHEMA, a homopolymer, should have a multiple tanδ transition. This, along with the complex nature of the blend tan δ curves, make it difficult to understand the behaviour in this system. The log modulus curves shed little light on the problem, showing either one or two transitions depending on the composition. The translucent appearance of the blend films, complete the very inconclusive results for this blend system.

LF200 - Poly(dimethylaminoethyl methacrylate) (PDMAEMA)

The solution polymerised PDMAEMA was found by GPC to have $\bar{M}_n$ = 4759 (table 4.2), and by DMTA to have a Tg of 43°C. The proximity of this Tg value to that of LF200, again prevents any definite conclusions being drawn from the DMTA results of the blends produced. As can be seen from figure 4.15 the tanδ curves for LF200, PDMAEMA and the three blends thereof, virtually coincide at around 40 - 50°C. The widths of the blend peaks at half height are intermediate between those for LF200 and PDMAEMA and this could be a reflection of simple additivity. Again, the translucent appearance of the films does not aid the assignment of a state of mixing to this blend. Obviously the results are inconclusive and the system would have to be studied by another technique in order to prove or disprove miscibility.

LF200 - Polystyrene (PST)

The solution polymerised PST was found to have a glass

- 87 -

transition temperature of 101°C. The DMTA results of the blends produced are shown in figure 4.17 and clearly indicate that these two polymers are immiscible, each blend having two tanδ peaks relating to the Tg transitions of the PST and LF200 components in the blend. The opacity of the blend films leads to an unambiguous conclusion of immiscibility for the blend system. These results may explain in part why the copolymer of styrene and methacrylic acid was also immiscible with LF200 since all of the copolymers had a styrene content of at least 35% (moles) (see section 4.1.1).

LF200 - Styrene/Acrylonitrile Copolymer (SAN) (Monsanto)

The SAN copolymer used had an 60:40 ratio of ST:AN units (as determined by NMR, see appendix 1) and a recorded Tg of 114°C. The DMTA results for the LF200-SAN blends are shown in figure 4.18. Blends containing 25% and 50% by weight of LF200 show double tanδ transitions indicating two separate phases. In each case the higher temperature transition appears at a lower temperature than would be expected for pure SAN alone, so it may be that the tanδ peaks at 87° and 91° represent some sort of mixed phase containing some proportion of LF200. Alternatively, there may be another mechanism which is causing the shift to lower temperature, although what this might be is uncertain. The blend containing 75% by weight of LF200 shows only a single tanδ transition and implies that this blend composition is miscible. The peak does however, have a long "tail" and this may be due to incomplete mixing of some sort, but it may be the case that compositions having low SAN content and hence, low ST content are more likely to be miscible. The apparent miscibility of the blend with 75% LF200 is contradicted by the opacity of the blend film. The other two blend compositions are opaque as expected.

- 88 -

Figure 4.17

DMTA Results for LF200 – PST Blends (Table 4.5)
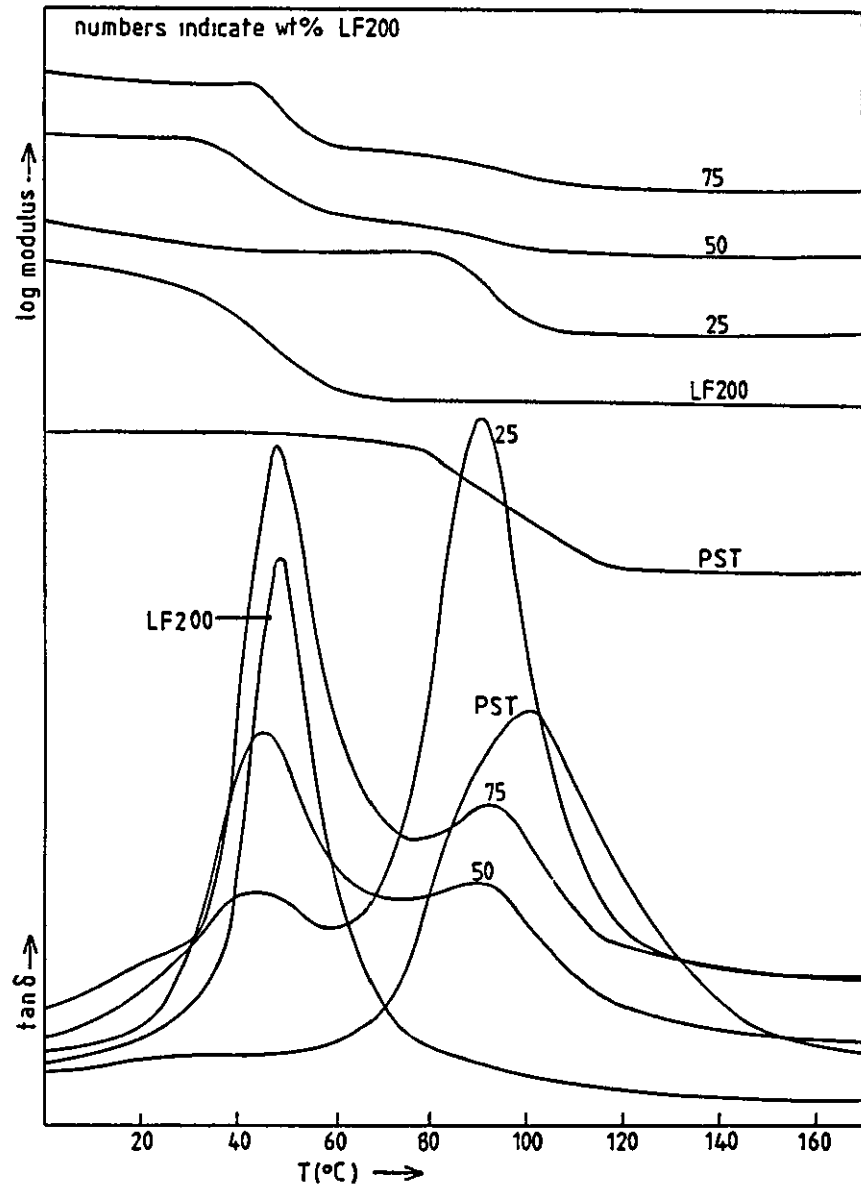
Figure 4.18

DMTA Results for LF200 – SAN Blends (Table 4.5)
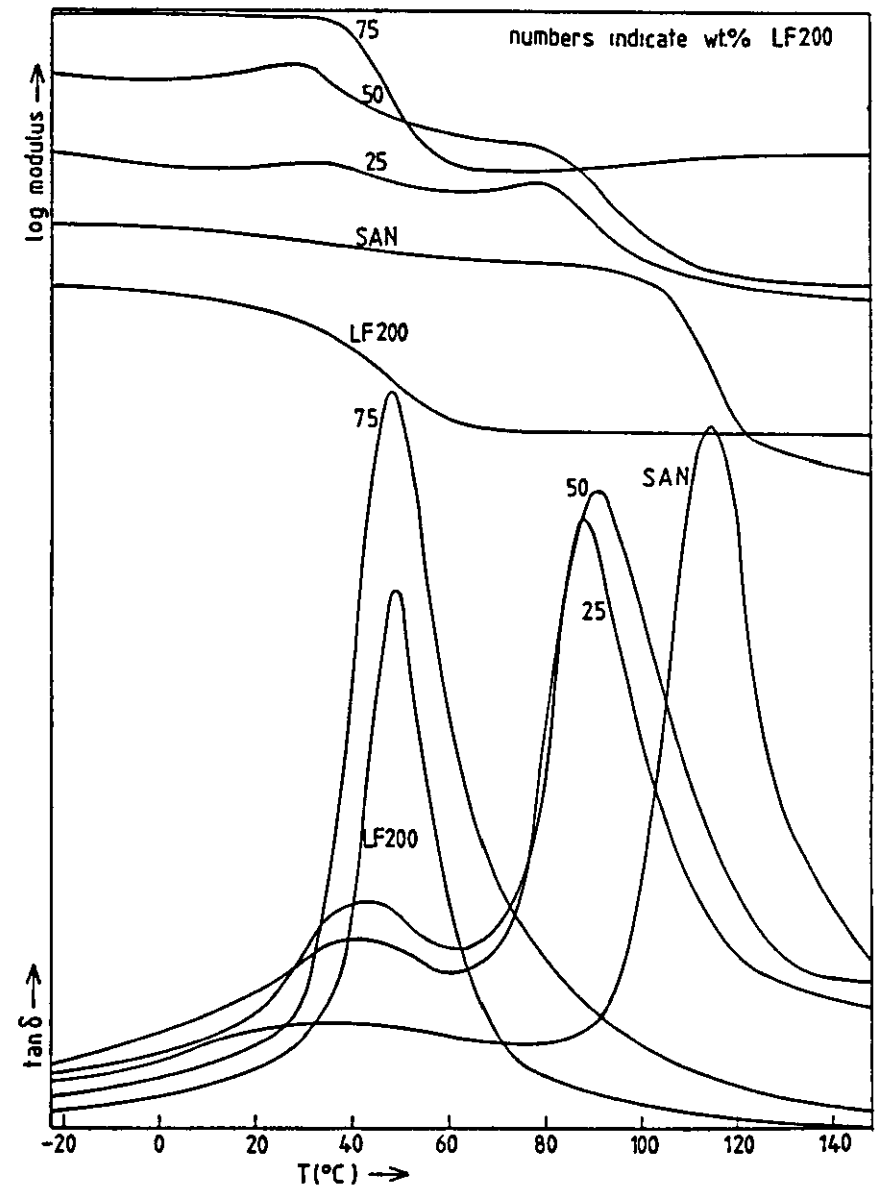
LF200 - Poly(vinyl acetate) (PVAc)

The PVAc was supplied by BDH Chemicals Ltd and had a molecular weight of 160,000, with a DMTA Tg of 47°C, again leading to the problem of the tan δ peak overlapping with that of LF200. The transparency of the blend films is the only indication of miscibility, because, as can be seen from the tanδ curves of the blends (figure 4.19), the glass transitions all coincide at around 47°C, making any conclusions regarding miscibility impossible.

LF200 - Ethylene/Vinyl Acetate Copolymer (EVA)

The EVA copolymer was supplied by ICI and had a vinyl acetate content of 41.4% (by moles). This blend system is complicated by the crystallinity of the EVA, which is observed as a very broad tanδ peak in figure 4.20. It is interesting to note that the log modulus curve of EVA drops at the lower Tg transition at -14°C, but remains fairly constant during the melting transition which peaks at 51°C. This implies that whilst the modulus (E') decreases during the Tg process, it does not significantly change during the melting process. The presence of the crystallinity makes the understanding of the DMTA results quite difficult, because, certainly for blends having 50% and 75%, there are 3 possible transitions to be resolved. There does however, seem to be a trend in the results. As the content of EVA decreases, the crystallisable content of the blend also decreases. This results in the tanδ curves moving away from the situation where there are two separate transitions, representing the Tg of the EVA and the melting transition of the EVA along with the Tg of LF200. So, at 75% LF200 only a single transition is observed, at a point in between the temperatures at which the Tg transitions of the pure unmixed components appear. What appears to be happening is that the components become more miscible as the EVA

Figure 4.19
DMTA Results for LF200 - PVAc Blends (Table 4.5)
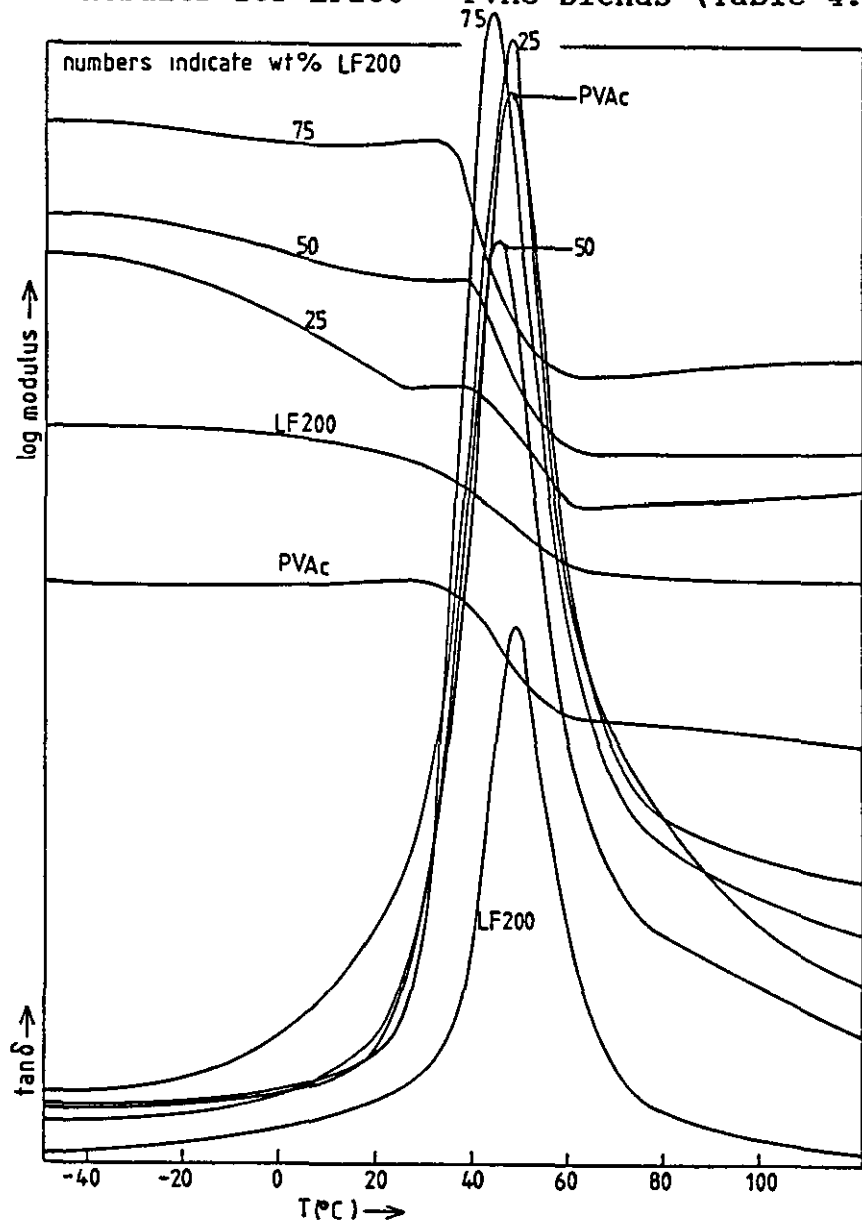
Figure 4.20
DMTA Results for LF200 - EVA Blends (Table 4.5)
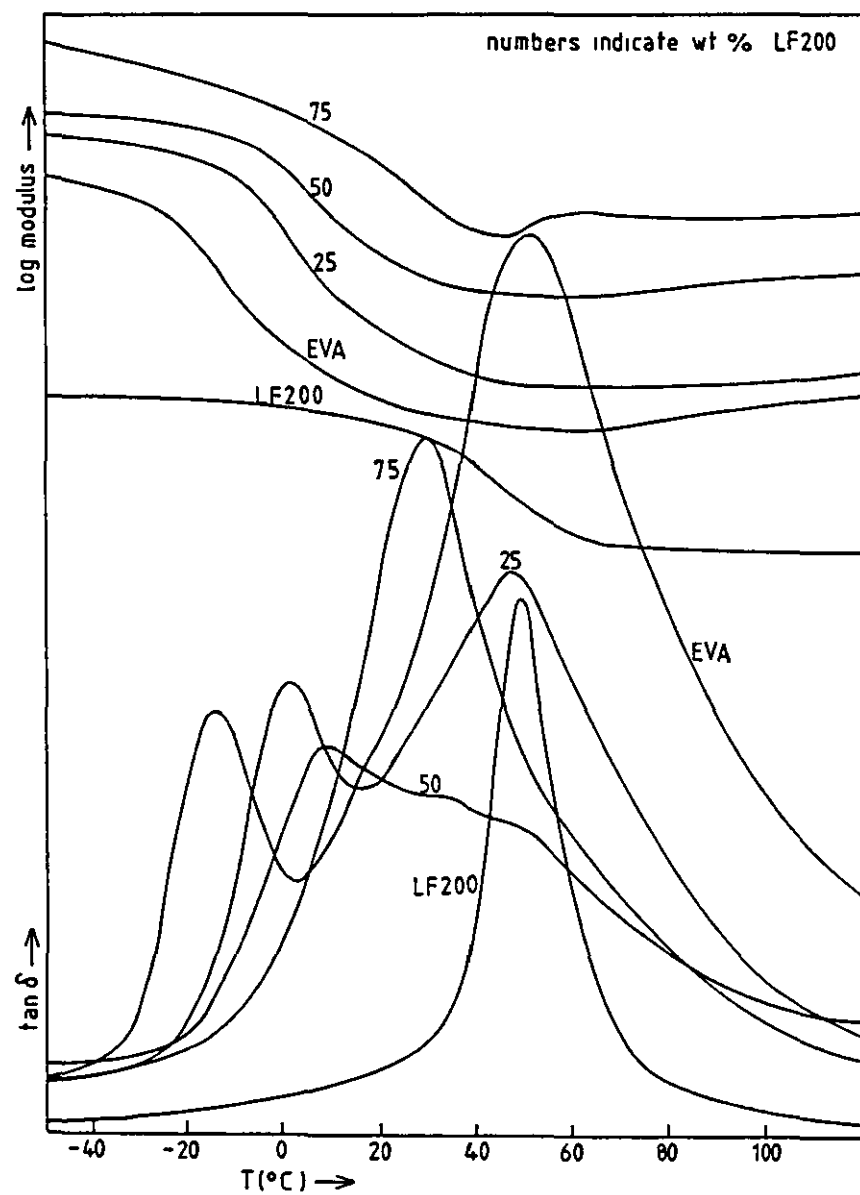
content is reduced. The blend is miscible at 75% LF200, whereas at 50% LF200, three transitions can be detected; these could correspond to some unmixed EVA, reflected in the Tg of the amorphous regions at 10°C and the Tm of the crystalline regions at around 55°C, and a mixed phase consisting of amorphous EVA and LF200, with a transition appearing at around 35°C. At 25% LF200 two peaks are observed, the one at 47°C corresponding to the melting of the crystalline regions of EVA and the one at 1°C perhaps indicating a partially mixed phase of LF200 and amorphous EVA. It is also interesting to note that the blend films are all transparent, despite the crystallinity of the EVA. It is probably reasonable to conclude that some mixing of the amorphous region of EVA and LF200 occurs, especially in compositions having a lower EVA content. The occurance of miscibility in blends having one or more crystalline components often results in the depression of the observed melting transition temperature of the crystalline phase(s) and this can be taken in part as an indication of such miscibility.[124,125] Although it is not easy to see this effect in the blend of EVA and LF200, the melting point depression phenomenon should be taken into consideration. These comments also apply to the following blend.

LF200 - Poly(ethylene glycol) (PEG)

The PEG was supplied by BDH Chemicals Ltd and had a molecular weight of 6000 (table 4.2). Again this system is complicated by the crystallinity of the PEG (more so than for EVA). From the DMTA results in figure 4.21, it is uncertain which peaks to assign to Tg transitions and which to assign to Tm transitions. It seems likely that the peaks at 20°C and 58°C correspond to some sort of melting phenomena (notice the unusual appearance of the log modules curve for PEG). All that can be concluded with any certainty for this system

Figure 4.21
DMTA Results for LF200 – PEG Blends (Table 4.5)
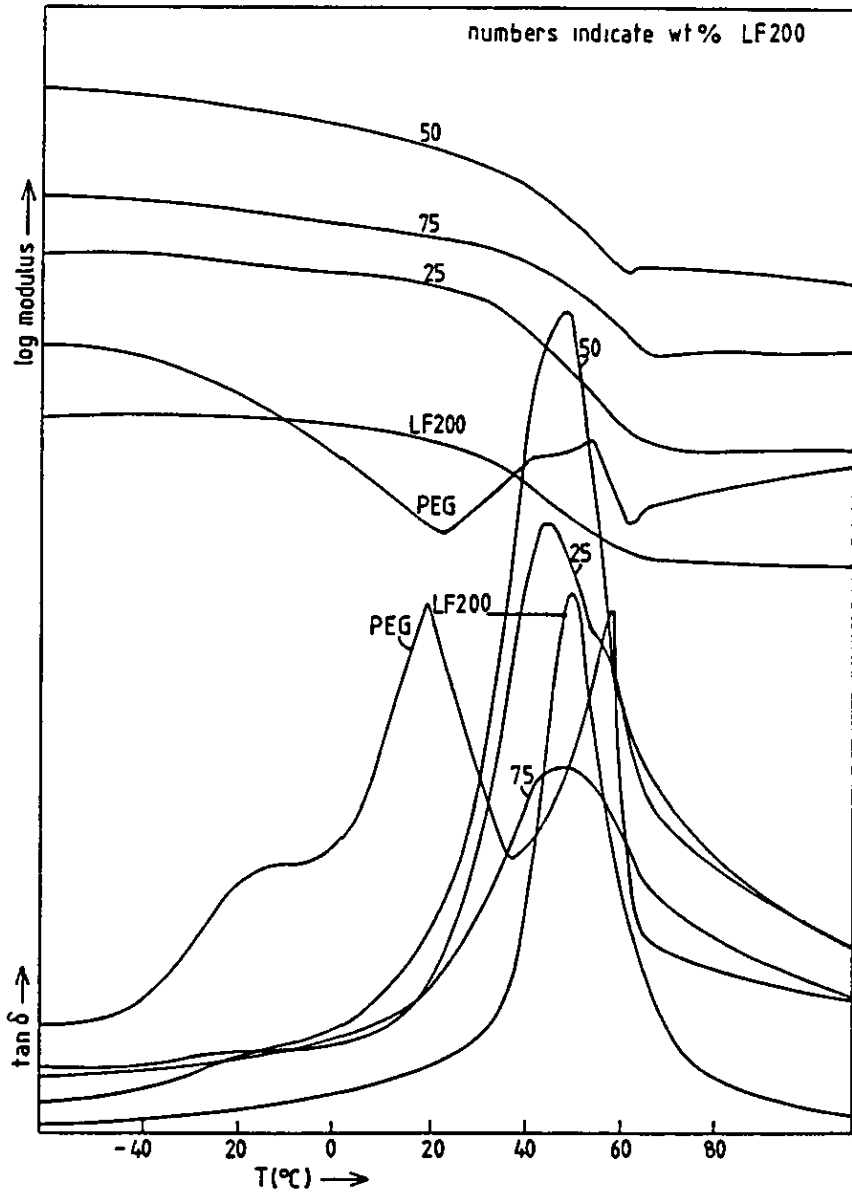
is that, at 75% LF200 the blend appears to be miscible, showing a single tanδ peak at 48°C. At 50% and 25% LF200 it is very difficult to say what the DMTA results represent.

For this system, the optical appearance is quite informative. All three blends had a transparent appearance at 60°C, above the melting region of PEG, whilst at room temperature the films had small opaque spots, evidently due to crystallisation of the PEG. So, it may well be the case that at temperatures above 60°C LF200 and PEG are miscible, whilst at room temperature there is some degree of mixing between LF200 and the amorphous phase of PEG, especially at low PEG contents.

Summary

From the selection of polymers chosen to investigate the miscibility of LF200, one or two have been successful in producing single phase blends, whilst others have shown immiscibility or given inconclusive results. The blend having perhaps the greatest extent of miscibility was that between LF200 and PBA(2), and blends involving PBA will be investigated further. Poly(ethylene glycol) appeared to show some miscibility in blends with LF200 and also warrants further investigation (see section 4.3). Several other systems were possibly miscible, but because of the problem of the proximity of the Tg transitions to that of LF200, no firm conclusion could be made. It would be interesting to look into these systems further, using a technique which did not rely on differences between glass transitions as a means of observing miscibility. However, such investigations are outside the objectives of this work.

The next section aims to look at the possible role of compatibilising agents in the miscibility enhancement of immiscible

polymer pairs, starting with the ST/MAA - LF200 system. Low molecular weight PBA will be studied further along with other poly(ethers).

4.3 Blends of LF200 with Potential Compatibilisers

A compatibilising agent is a third component, which when added to an immiscible polymer pair, leads to improvement in the overall miscibility of the system. Compatibilisers can be of several types and a recent review by Xanthos[14] outlines some of them. Block copolymers[126] are one type of compatibilising agent, which are being used increasingly to produce miscible systems. Usually, a block copolymer is prepared, which is made up of blocks of the two immiscible polymers with which it is to be blended. Another type of additive which enhances miscibility is one which, when added to the system induces crosslinking or grafting reactions, for example. Such materials are usually low molecular weight compounds. However, very little attention has been paid to the use of a third polymer as compatibilising agent,[130,131] and very few ternary blends have been investigated thoroughly.[127,131] To date, no examples of low molecular weight polymers being employed as compatibilisers have been found in the literature, although recently, the effect of homopolymer molecular weight on the miscibility of binary polymer blends has been studied.[132]

This section investigates the miscibility of a number of potential, low molecular weight, polymeric compatibilising agents with LF200.

Table 4.6 shows the results of a study of the blends involving the low molecular weight polymers chosen, including film appearance and the results of DMTA and FTIR analyses. The width at half height

Table 4.6   LF200 - Compatibiliser Blends

Product No.	Blend Composition	Film Appearance	DMTA Tg/°C	$W_{h\frac{1}{2}}$	Fox Eqn Tg/°C	Rule of Mixtures	FTIR Result
198	LF200/PPG(1) 25:75	transparent	-40	45°	-28	-22	no peak shifts
112	LF200/PPG(1) 50:50	translucent	-16 (-40)	(44°)	-7	2	"
199	LF200/PPG(1) 75:25	transparent	20	24°	19	25	"
193	LF200/PPG(2) 25:75	transparent	-49	24°	-32	-26	"
194	LF200/PPG(2) 50:50	transparent	-14	47°	-10	-1	"
195	LF200/PPG(2) 75:25	transparent	18	27°	16	24	"
197	LF200/PBA(1) 25:75	translucent	-9	29°	-17	-13	"
122	LF200/PBA(1) 50:50	translucent	4	18°	2	8	"
196	LF200/PBA(1) 75:25	translucent	38	17°	24	29	"
78	LF200/PBA(2) 25:75	transparent	-18,32	-	-9	-6	"
79	LF200/PBA(2) 50:50	transparent	8	34°	8	13	"
80	LF200/PBA(2) 75:25	transparent	35	39°	27	31	"
244	LF200/PBA(3) 50:50	transparent	37	75°	6	11	"
245	LF200/PBA(3) 75:25	transparent	39	35°	26	30	"

Table 4.6 (continued) <u>LF200 - Compatibiliser Blends</u>

Product No.	Blend Composition	Film Appearance	DMTA Tg/°C	$W_{h\frac{1}{2}}$	Fox Eqn Tg/°C	Rule of Mixtures	FTIR Result
132	LF200/Setal 25:75	translucent	26 (80)	(39°)	39	39	no peak shifts
131	LF200/Setal 50:50	translucent	25,44	-	42	43	"
130	LF200/Setal 75:25	translucent	24,50	-	46	46	"
233	LF200/PPA 25:75	translucent	-21,13, 47	-	-7	-4	"
231	LF200/PPA 50:50	translucent	-24,14 55	-	10	14	"
232	LF200/PPA 75:25	translucent	-16,19 50	-	28	32	"

of tanδ peaks is shown where appropriate, along with the values of Tg predicted for miscible blends, by the rule of mixtures and by the Fox equation. Before discussing the results, it is appropriate to give reasons for the choice of the low molecular weight polymers. Poly(n-butyl acrylate) has already been shown to be miscible with LF200, and it was decided to see what effect molecular weight might have on the miscibility of this system. Poly(propylene glycol)(PPG) was chosen instead of poly(ethylene glycol) (PEG) for three reasons; firstly for its similarity to PEG, with the hope that it too would be miscible to LF200, secondly because there are no complications caused by crystallinity and finally because of the possible end use of the material in a system used for surface coatings, which would necessitate an insolubility in water. Setal 1711 is a saturated aliphatic polyester, the NMR and FTIR characterisation of which appear in appendices 1 and 3 respectively, and which was supplied by LVH Coatings Ltd. Setal 1711 and poly(propylene adipate)(PPA) were chosen because they have applications as polymeric plasticisers. It will also be interesting to compare their miscibility with LF200 to that of PVAc and EVA which showed signs of being miscible (see section 4.2). The comparison therefore, is between polyesters having the ester group along the backbone and polymers having ester functionality on the side group.

LF200 - PPG(1)

PPG(1) was found to have a molecular weight ($\bar{M}n$) of 9500 as determined by GPC (see table 4.2) and a glass transition temperature of -46°C. The results shown in table 4.6 indicate that the blend with LF200 is miscible at levels of 25% and 75% by weight, exhibiting a single glass transition and transparent films when cast from chloroform. The blend containing a 50% by weight mixture of the two

components has a main Tg transition at -16°C with a shoulder at -40°C, and this suggests a mixed phase of LF200 and PPG(1) having a Tg at -16°C along with some unmixed PPG(1) represented by the shoulder at -40°C. Figure 4.22 shows DMTA results for the blend of 75% LF200 and 25% PPG(1) with a relatively sharp tan δ transition and corresponding drop in log E'. It is interesting to compare the Tg values obtained from DMTA to those predicted by the rule of mixtures and the Fox equation (2.77). The blend having 25% by weight of PPG(1) has a Tg very close to that calculated using the Fox equation and is only 5°C from that predicted by the rule of mixtures. At higher proportions of PPG(1), there is a greater negative deviation of actual Tg values from those predicted. One reason for this could be the fact that the blends were prepared by weight. For example, consider a 50:50 blend by weight. Since PPG(1) has a much lower $\bar{M}n$ than LF200, more chains of PPG(1) will be present than would have been the case had the molecular weights of the two polymers been similar. This means that there will be a greater proportion of free volume in this system, caused by a larger number of PPG(1) chain ends and this leads to a decrease in the observed Tg. The higher the proportion of PPG(1) in the blend, the more pronounced is this effect.

The infrared analysis of these blends did not show any noticeable band shifts due to intermolecular interactions. This is perhaps not surprising, since both polymers contain the ether functionality. This in fact, could be a reason why the blends are miscible in certain proportions, on the simplistic basis of like mixing with like. On the other hand, the miscibility may be a function of the low molecular weight of the PPG(1). In order to see the effect that changing the molecular weight of PPG might have, a lower molecular weight sample was tried (PPG(2)).

Figure 4.22   (Table 4.6)
DMTA Results for LF200 – PPG(1) Blends
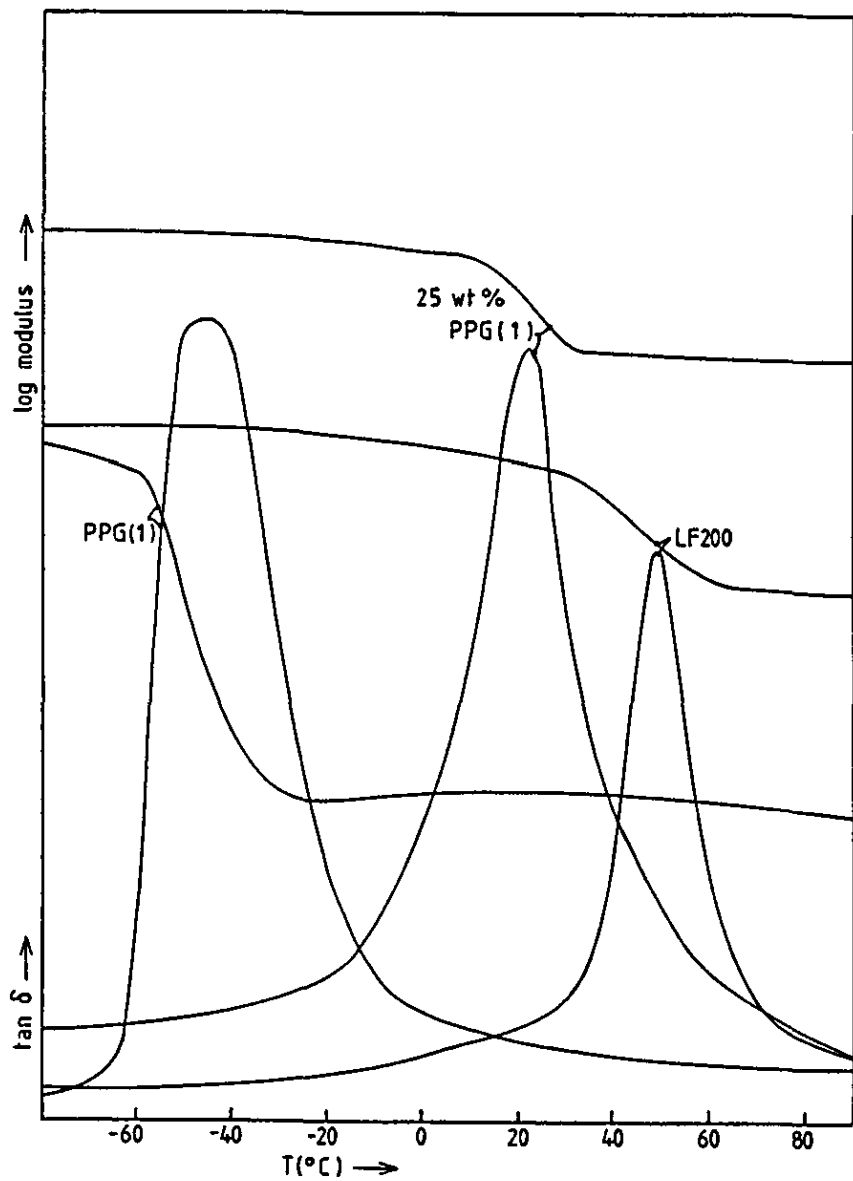
Figure 4.23   (Table 4.6)
DMTA Results for LF200 – PPG(2) Blends
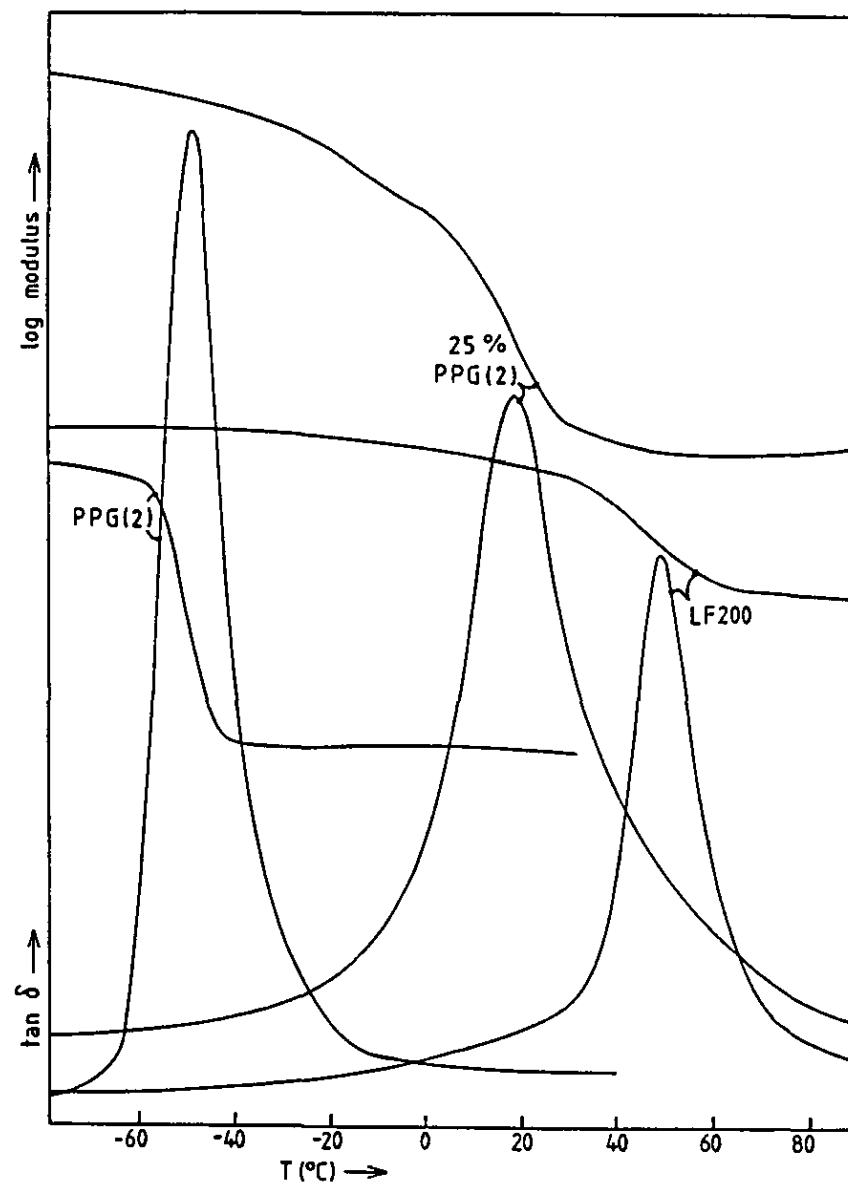
<u>LF200 - PPG(2)</u>

The lower molecular weight material, PPG(2) was found to have a molecular weight ($\bar{M}n$) of 2769, as determined by GPC (table 4.2) and a glass transition temperature of -15°C. All three blend compositions yielded single glass transition temperatures and transparent films, and if anything, appeared from these results to be slightly more miscible than the blends involving PPG(1). The DMTA result of the 25% PPG(2) blends is shown in figure 4.23. The trend relating the experimental and predicted Tg values is similar to that for the PPG(1) blends discussed above; the Tg of the composition having 75% PPG(2) being furthest from the predicted values, presumably for the same reason as mentioned above. This can be seen graphically in figure 4.24.

No band shifts were observed in the infrared spectra of the blends, compared to the spectra of the unmixed components. The FTIR spectrum of PPG(2) is shown in appendix 3.

<u>LF200 - PBA(1)</u>

PBA(1) was prepared using a chain transfer agent, as described in section 3.1.2 and table 3.3, and was found to have a molecular weight ($\bar{M}n$) of 1749 by GPC and a Tg of -33°C. The results for this blend are shown in table 4.6 and figure 4.25, which is the DMTA tanδ and log modulus curves for the blend having 25% of PBA(1). The DMTA results all yielded tanδ curves indicating single glass transitions and suggested an improved miscibility compared to the higher molecular weight PBA(2) ($\bar{M}n$ 6757). This suggestion of improved miscibility is supported by the narrow widths of the blend tanδ Tg peaks. Figure 4.26 shows the relationship between the experimentally observed Tg and those predicted by the rule of mixtures and the Fox

Figure 4.24   Variation of Blend Tg with PPG(2) Content
for LF200/PPG(2) Blends

- Experimental Tg
+ Fox Equation
◇ Rule of Mixtures

Tg (°C)

Weight Percent of PPG(2)
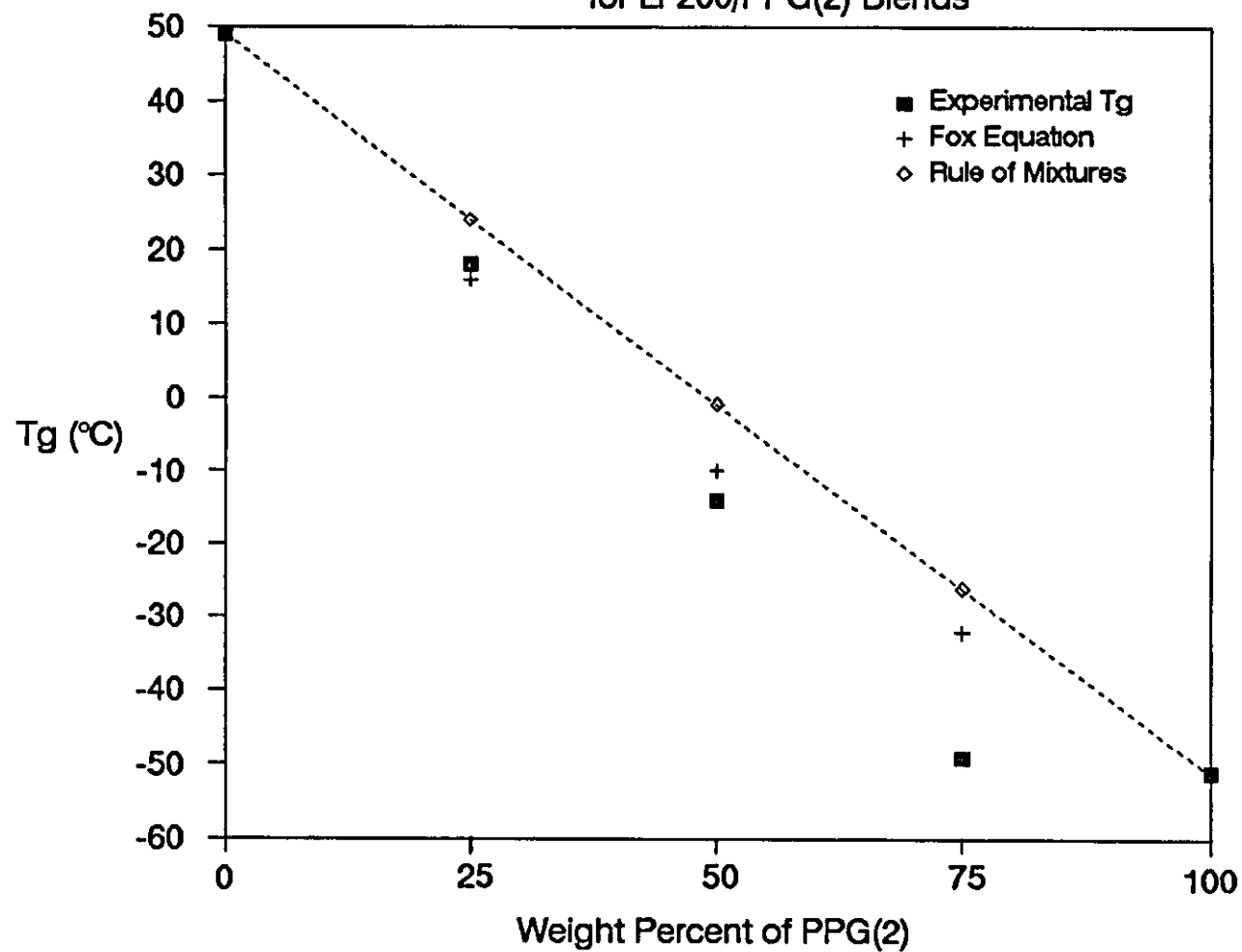
Figure 4.25

DMTA Results for LF200 - PBA(1) Blends (Table 4.6)
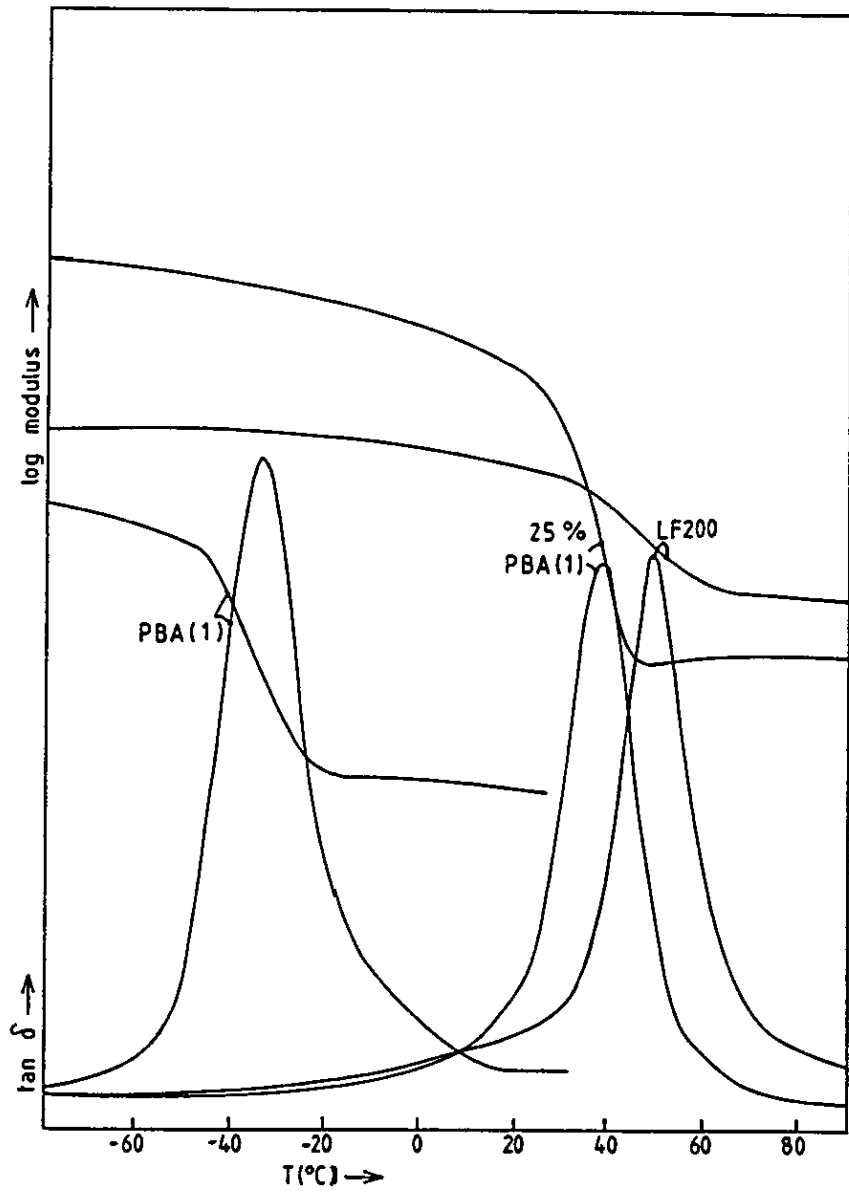
Figure 4.26   Variation of Blend Tg with PBA(1) Content for LF200/PBA(1) Blends
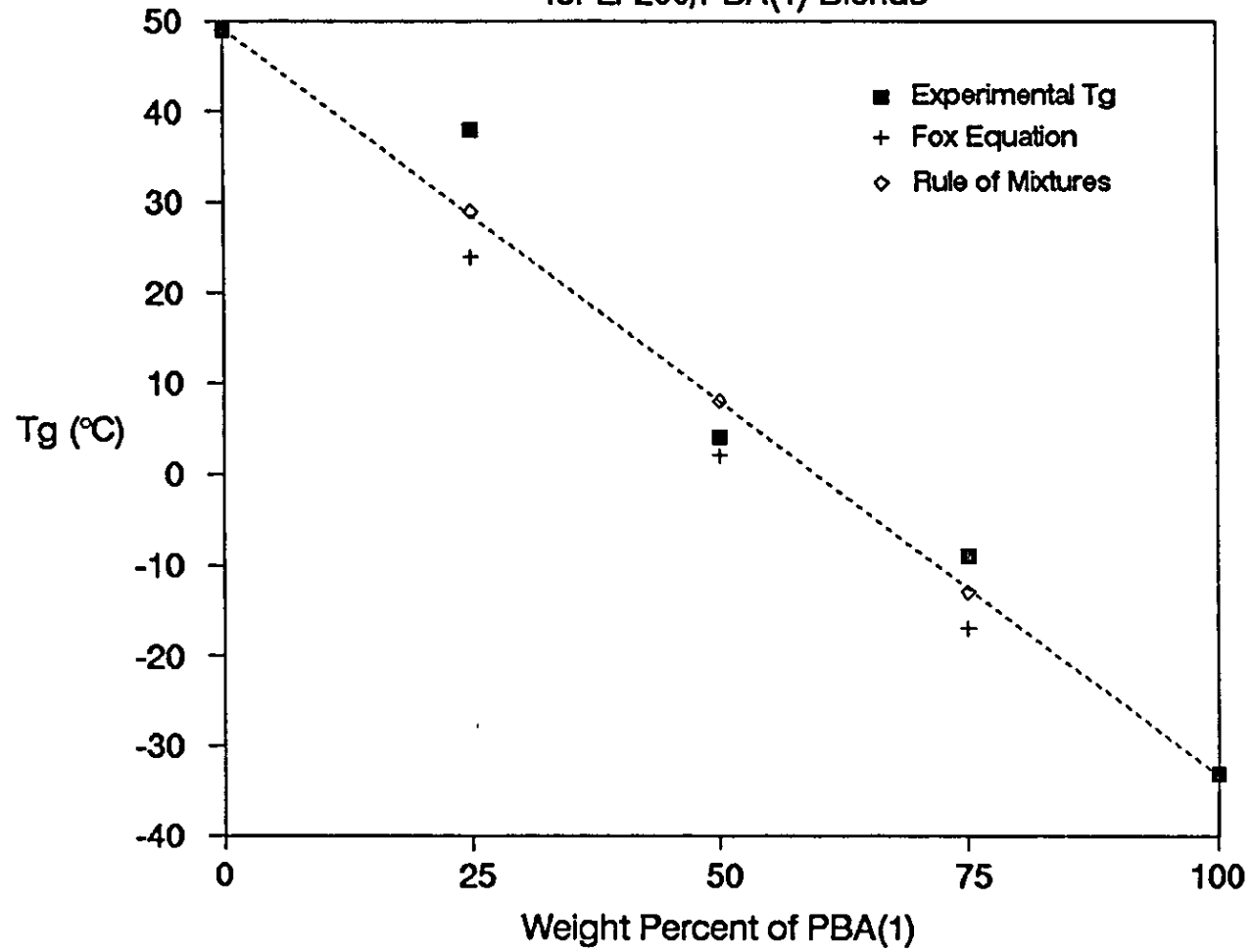
equation, as a function of blend composition. The translucency of the blend films may be due to a small amount of residual solvent, or due to the evaporation procedure, but should not detract from the DMTA results. No interactions between the functional groups of LF200 and PBA(1) were detected by FTIR, so the driving force for miscibility appears to be something other than specific interactions. It is conceivable that the low molecular weight PBA(1) is acting as a plasticiser, but whether that could explain such large decreases in the Tg value of blends containing 50% and 75% of PBA(1) is open to debate. It might also be expected that if this was the case, that separate peaks due to the presence of excess PBA(1) would be observed in the DMTA plots of the blends rich in PBA(1).

LF200 - PBA(2)

These results have been discussed in the previous section (4.2), but the results are summarised in table 4.6 and should be compared to those for the other two PBA polymers.

LF200 - PBA(3)

PBA(3), which was polymerised using a chain transfer agent under the conditions described in table 3.3, was found to have a molecular weight ($\bar{M}n$) of 5200 and Tg of -27°C. Compositions having 50 and 25% by weight of PBA(3) were prepared and the results of DMTA and FTIR analyses are shown in table 4.6. Before looking at the results of these two blends, it is interesting to compare the peak widths of the pure PBA homopolymers. PBA(1) and PBA(2) have quite narrow Tg transitions (20° and 17° at half height), whereas PBA(3) has a broader tanδ peak of 39° at half height. This is a little unexpected as the tanδ peaks ought to have been of a similar width to that of PBA(1), since the method of preparation was the same.

Both of the blends give single Tg transitions as observed by DMTA, but the width of the $\tan\delta$ peak for the 50% PBA(3) blend is very wide, 75° at half height. Such wide transitions are sometimes associated with the presence of a number of overlapping, partially mixed phases within the blend. The 50% blend is transparent, indicating miscibility, but it is also interesting to note that the Tg of 37°C is significantly different from that predicted by the rule of mixtures or the Fox equation. The 25% PBA(3) blend is also transparent, but has a comparatively narrow transition width and is clearly miscible. The Tg of 39°C is however, somewhat different from that predicted, but not so much as for the 50% blend. It appears overall though, that PBA(3) is not as miscible as PBA(1), but perhaps slightly more so than PBA(2), with LF200.

LF200 - Setal 1711

Setal 1711 is a saturated aliphatic polyester whose structural formula was not supplied. The NMR and infrared spectra are however, shown in appendices 1 and 3 respectively. Little attention will be paid to these blends as the results obtained by DMTA indicate clearly that all compositions are immiscible. No specific interactions between Setal 1711 and LF200 could be identified by FTIR. It is unlikely that this material would be of any great use as a compatibilising agent, since for the systems being studied some extent of miscibility with LF200 would be desirable for this.

LF200 - Poly(propylene adipate) (PPA)

This polymer (PPA) was supplied by Victor Wolf Ltd., and was found to have a molecular weight ($\bar{M}n$) of 5734 and Tg of -21°C. Judging by the DMTA results shown in table 4.6, it appears that there may be a slight degree of miscibility of PPA with LF200. This is

indicated by the appearance of a third Tg between the positions of the transitions relating to the unmixed components. These transitions at 13°C, 14°C and 19°C in the 25, 50 and 75% LF200 blends respectively, are probably representative of a mixed phase composed of some combination of the two components. Coupled with the blends translucent appearance, partial miscibility seems to be the case for these blends. Again, no specific interactions were detected by FTIR.

4.4 Blends of ST/MAA Copolymers with Potential Compatibilising Agents

Following the study of the blends of potential compatibilisers with LF200, it was decided to look at the miscibility of these polymers with copolymers of ST and MAA, with the aim of hopefully finding one which would enhance the miscibility of the ST/MAA - LF200 system. Table 4.7 shows the DMTA and FTIR results of the blends studied, along with the optical appearance of each blend film.

ST/MAA Copolymer 29 - Poly(ethylene glycol) (PEG)

Copolymer 29, which was polymerised as described in section 3.1.2 using the conditions shown in table 3.2, has a methacrylic acid content of 84% and a Tg of 120°C. The PEG used is the same as that previously blended with LF200 (see section 4.2, table 4.5) and has a molecular weight of 6000.

This blend is of particular interest, because there are similarities between this pair of polymers and a system which has been shown to be miscible, with hydrogen-bonding interactions existing between the two components. The system in question is that of Poly(ethylene-co-methacrylic acid) (EMAA) blended with each of the polyethers, poly(vinyl methyl ether) (PVME) and a copolymer of

- 98 -

Table 4.7 Blends of ST/MAA Copolymers with Potential Compatibilising Agents

Product No.	Blend Composition	Film Appearance	DMTA Tg/°C	$W_{h\frac{1}{2}}$	Fox Eqn Tg/°C	Rule of Mixtures	FTIR Result
105	29/PEG 50:50	transparent	25,52	44°	-	-	carbonyl shift
110	29/PPG(1) 50:50	transparent	18	44°	15	37	carbonyl shift
125	29/PBA(1) 50:50	transparent	26	73°	25	44	incon-clusive
211	29/PBA(2) 50:50	transparent	-25,19 119	-	32	48	incon-clusive
216	163/PPG(1) 50:50	transparent	75	52°	57	75	carbonyl shift
217	163/PPG(1) 50:50	transparent	30, (-30)	(62°)	13	35	carbonyl shift

Note: Blend 105 shows two tanδ peaks at 25°C and 52°C which are probably due to crystalline melting transitions.

ethylene oxide and propylene oxide (EP)). It was found that EMAA copolymers are strongly self-associated, via the formation of intermolecular carboxylic acid dimers. However, in blends of the EMAA copolymer with the polyethers,[111,112] there was found to be a strong association between the two components in the form of intermolecular hydrogen bonds, between the carboxylic acid and ether oxygen groups. These conclusions were drawn, by the observation of a shift in the position of the acid carbonyl peak in the infrared spectra of the blends, compared to it's position in spectra of the pure copolymer. The carbonyl stretching band corresponding to the acid dimer appears at 1700cm^{-1}, whilst in blends of the EMAA copolymer and the polyethers, a second peak appears at 1728cm^{-1} which is assigned to the carbonyl stretching vibration when the acid group is involved in hydrogen bonding with the ether oxygen. This can be illustrated as follows:

CH₃ structure — hydrogen bonding — acid copolymer blended with EPO or PVME

acid dimer: 1700cm^{-1}
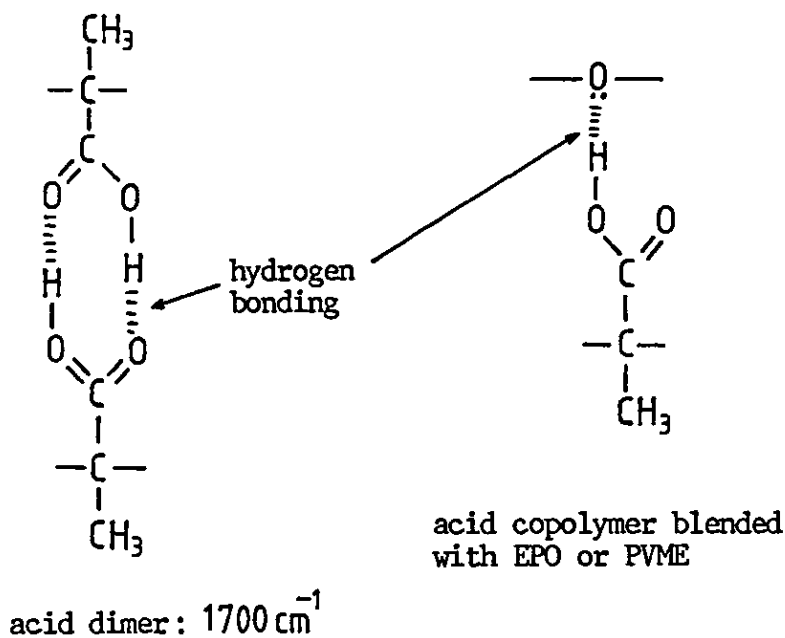
Judging by these recently published results, it seems likely that a similar interaction may well be present in the blend of the ST/MAA copolymer with PEG. This is indeed the case, as can be seen in figure 4.28. There is every reason to believe that hydrogen

bonding is the cause of this shift and that the illustration above is equally applicable to this system. It is however, more difficult to come to any firm conclusions regarding the miscibility of the blend. The transparency of the blend films is a pointer towards miscibility, but as in blends of LF200 with PEG, the crystallinity of the PEG makes the interpretation of the DMTA results complicated. The transitions that appear at 25 and 52°C are similar to those observed for pure PEG and probably represent melting transitions. However, because of the apparently strong hydrogen bonding interactions present, the optical clarity of the blend and the similarity between the blend and the EMAA - EPO/PVME system,[112] it is likely that some degree of miscibility exists between the blend components.

ST/MAA Copolymer 29 - PPG(1)

The PPG(1) material has been found to be largely miscible with LF200, and it was hoped that any miscibility between the ST/MAA and PPG(1) would lead to a miscible ternary blend of the three components, with the polyether acting as compatibiliser. In the light of the results of the blend of PEG with the same copolymer, it was to be expected that hydrogen bonding interactions exist between the acid component of the copolymer and the ether oxygen of the PPG(1). The results of the DMTA and FTIR analyses of this blend indicate both miscibility and hydrogen bonding interactions (table 4.7). The 50% blend by weight of the two components forms a transparent film, having a single glass transition at 18°C, close to that predicted by the Fox equation and a shift of the acid carbonyl in the infrared spectrum similar to that observed for the PEG - ST/MAA copolymer system. A portion of the infrared spectrum is shown in figure 4.29. By comparison, figure 4.27 shows that no similar interactions exists between a similar ST/MAA copolymer (163)

Figure 4.27

The Infrared Carbonyl Band for
Copolymer 163 – LF200 Blend
(Table 4.3)
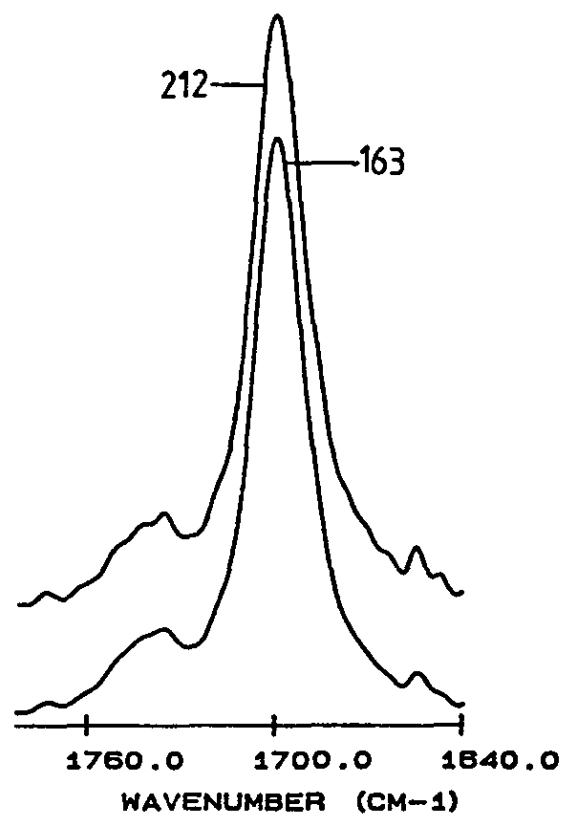
Figure 4.28

The Infrared Carbonyl Band for
Copolymer 29 – PEG Blend
(Table 4.7)
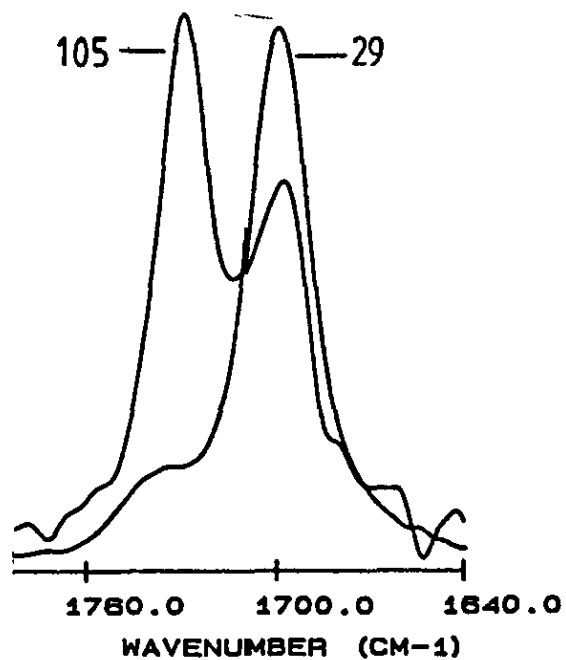
Figure 4.29

The Infrared Carbonyl Band for
Copolymer 29 – PPG(1) Blends
(Table 4.7)
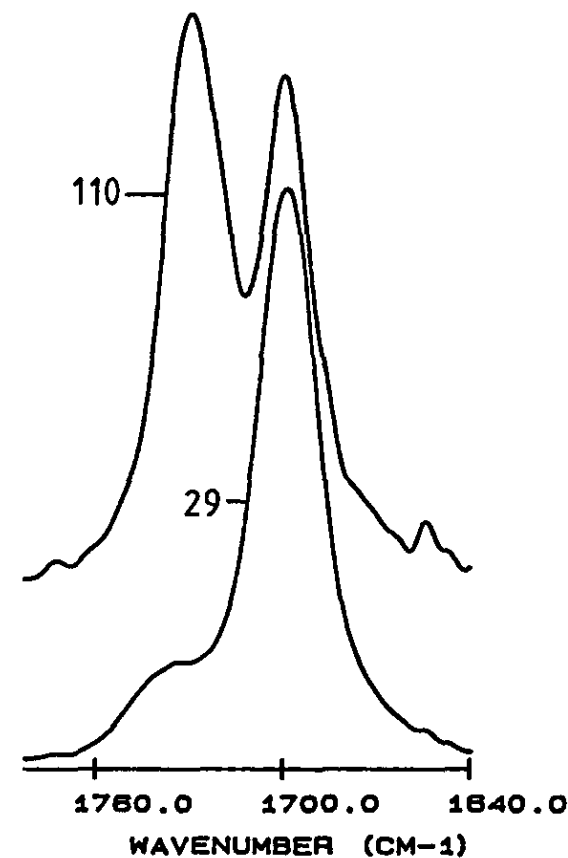
and LF200, the carbonyl peak in the blend being almost identical to that in the pure polymer.

Although both PEG and PPG(1) form blends with copolymer 29, in which hydrogen bonding interactions are encountered and are probably both miscible (not conclusively in the case of PEG, due to its crystallinity), because of the reasons discussed earlier (section 4.3) relating to the crystallinity and water solubility of PEG, PPG(1) is probably the better choice as compatibilising agent for the ST/MAA - LF200 blend system. The results of the study of such blends will be discussed in the next section (4.5).

ST/MAA Copolymer 29 - PBA(1)

PBA(1), when blended with copolymer 29 forms a transparent film and a single glass transition at 26°C, albeit very broad, close to that predicted by the Fox equation. Whether a tanδ peak of such large width (73° at half height) can be attributed to a completely miscible blend is debatable, but it is clear that some miscibility between the components exists.

The infrared analysis of this blend was not straightforward, being complicated by the fact that both components have carbonyl groups whose infrared bonds overlap to a large degree. The acid carbonyl peak usually appears at 1700 cm^{-1} and the acrylate carbonyl at around 1735 cm^{-1}. If, for example, hydrogen bonding were to exist between the two groups then, by comparison with the blends of the ST/MAA copolymer with PEG and PPG(1), it might be expected that the acid carbonyl would be shifted to 1728 cm^{-1}. This would obviously coincide almost exactly with the acrylate carbonyl at 1735 cm^{-1}. It is for this reason that such an interaction would be difficult to detect. Despite spectra being derived from the subtraction of the spectra of the two components from that of the blend, and despite

using a wavenumber resolution of 1 cm^{-1}, no such shifts and hence, interactions were found. However, there is an example in the literature involving the related blend system of styrene/acrylic acid copolymer with poly(methyl methacrylate), in which just such interactions have been observed, using the spectral subtraction of spectra obtained by FTIR. It may be therefore, that given a more thorough investigation of the PBA(1)-ST/MAA system, hydrogen bonding interactions may be observed for certain blend compositions. On the other hand, it could be the case that such interactions are not active in this particular blend. Either way, the low molecular weight PBA(1) is still a potential compatibiliser for the ST/MAA - LF200 system, showing some miscibility with both of the components.

ST/MAA Copolymer 29 - PBA(2)

Much of the discussion relating to the blend of copolymer 29 with PBA(1) is relevant to this blend also, and will not be repeated. It is worthwhile noting however, that this blend does not seem to be as miscible as the one just discussed, having three tanδ transitions, probably indicative of some degree of partial miscibility. The blend film does though, exhibit optical clarity. From these results it is difficult to draw conclusions about the effect of PBA molecular weight on the miscibility of blends with copolymer 29.

ST/MAA Copolymer 163-PPG(1)

Copolymer 163 was prepared as described in section 3.1.2 and table 3.2 and has a Tg of 115°C. Two blend compositions were produced containing 25 and 50% by weight of PPG(1) respectively and both formed transparent films. The DMTA results are shown in table

4.7 and graphically in figure 4.30. The blend having 25% PPG(1) appears to be the more miscible, having a single Tg transition at 75°C (the same value as predicted by the rule of mixtures equation), although it is quite broad. Still broader is the transition observed for the 50% blend, probably indicating an incomplete miscibility.

The infrared spectra of the two blends (figures 4.31 and 4.32) both show carbonyl shifts, due to the hydrogen bonding interaction between the ether oxygen of PPG(1) and the acid carbonyl of the copolymer. This confirms the existence of such interactions, as found for the other ST/MAA copolymer PPG(1) blend discussed earlier. It should be noted, that the effect is slightly more pronounced in the blend of copolymer 29 with PEG than with blends involving PPG(1). This is probably due to some hindrance caused by the methyl group on the carbon atom adjacent to the ether oxygen, towards the acid group of the copolymer.

4.5 ST/MAA Copolymer Ternary Blends

From the results of the last section in which ST/MAA copolymers were blended with potential compatibilising agents, it was concluded that PPG(1) was probably the more miscible of the low molecular weight polymers used. For this reason, this section will concentrate on the three component system of ST/MAA copolymer - PPG(1) - LF200, with the aim of discovering whether the PPG(1) component has the effect of enhancing the miscibility of the other two components.

ST/MAA Copolymers (163) - PPG(1) - LF200 Blends

Table 4.9 shows the compositions of the blends studied, along with the results of the DMTA and FTIR analyses. Figure 4.33 shows the $\tan\delta$ and log modulus curves for blends in which the ratio of

Figure 4.30

DMTA Results for Copolymer 163 - PPG(1) Blends (Table 4.7)
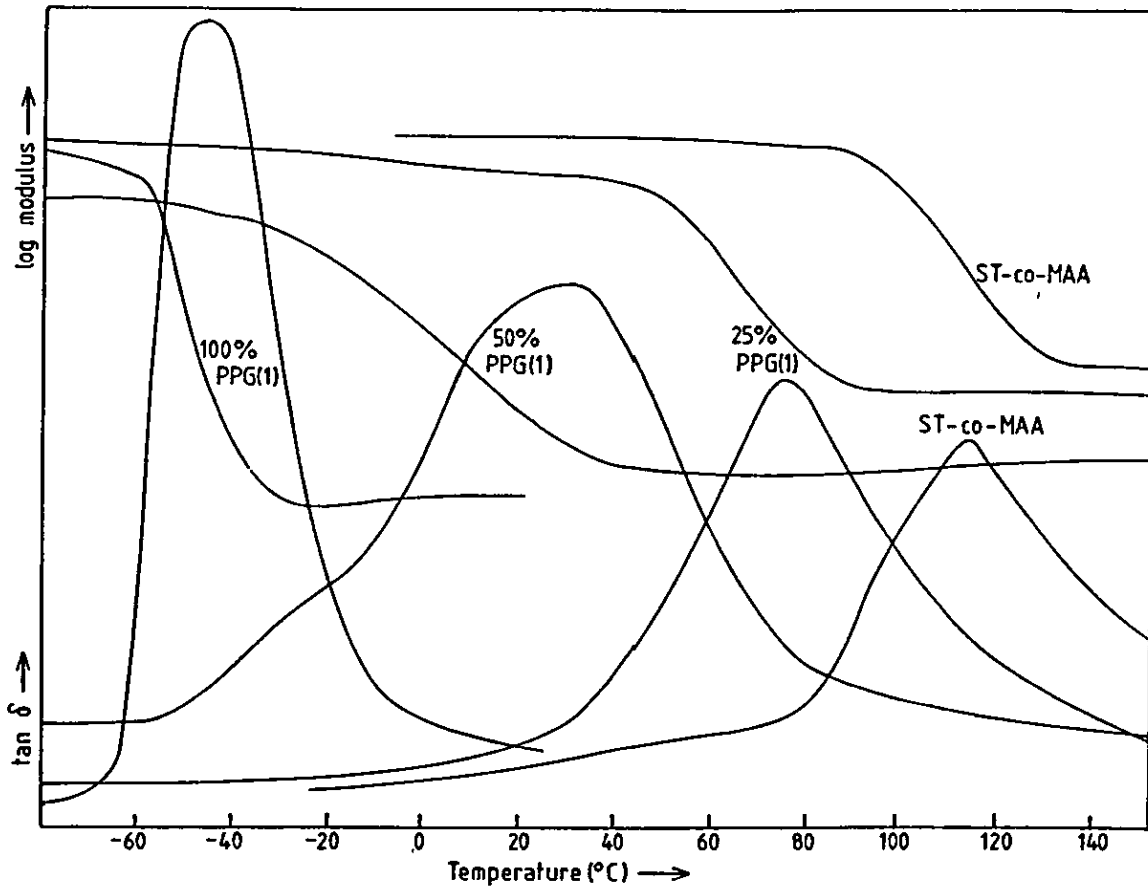
Figure 4.31

The Infrared Carbonyl Band for

Copolymer 163 - PPG(1) Blend

(Table 4.7)

216⌐ 163⌐

1820.0   1760.0   1700.0   1640.0

WAVENUMBER (CM-1)
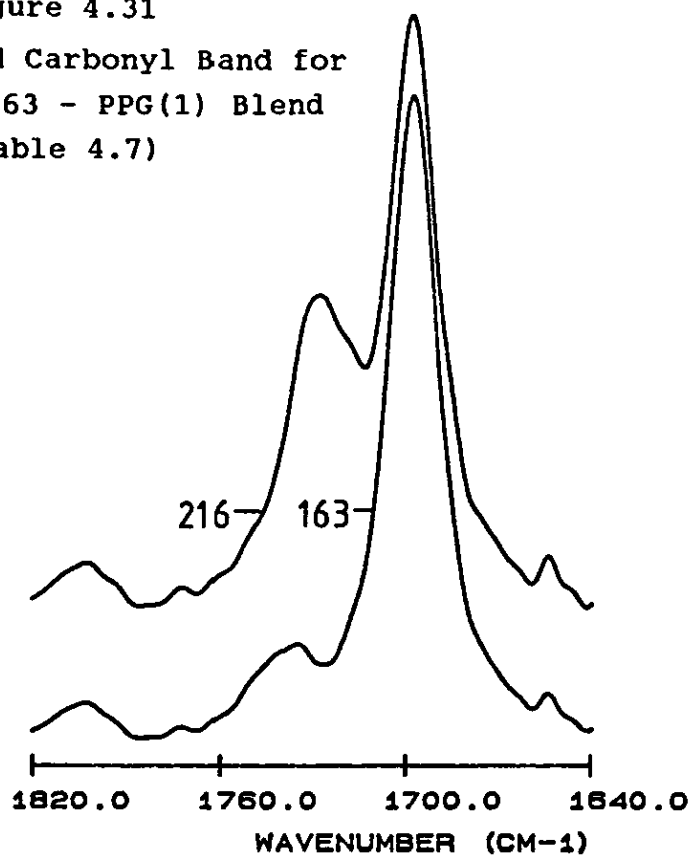
Figure 4.32

The Infrared Carbonyl Band for

Copolymer 163 - PPG(1) Blend

(Table 4.7)

⌐217

163⌐

1820.0   1760.0   1700.0   1640.0

WAVENUMBER (CM-1)
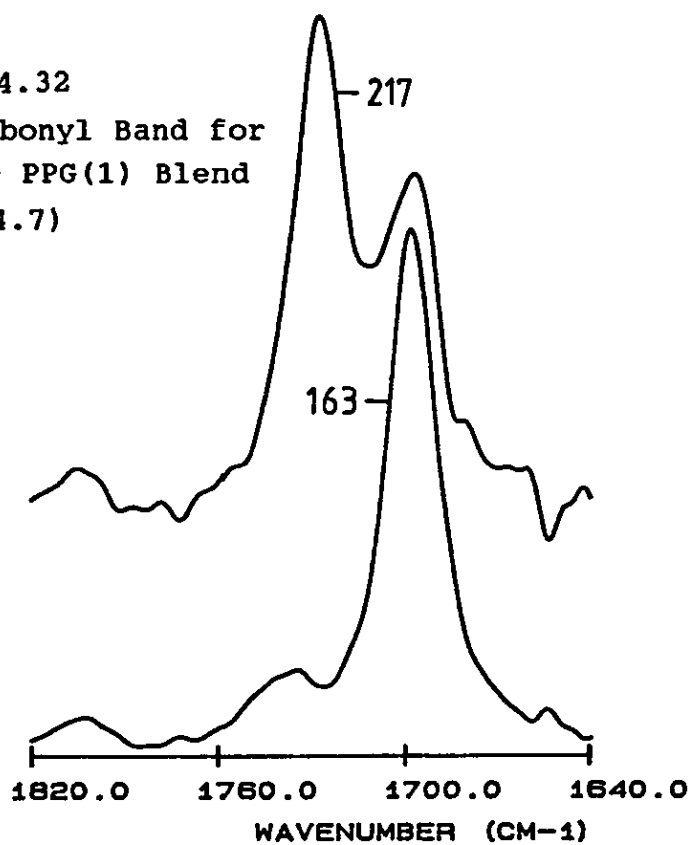
Figure 4.33   DMTA Results for Copolymer 163 - PPG(1) Blends
with 1:1 Ratio of 163:PPG(1)   (Table 4.8)
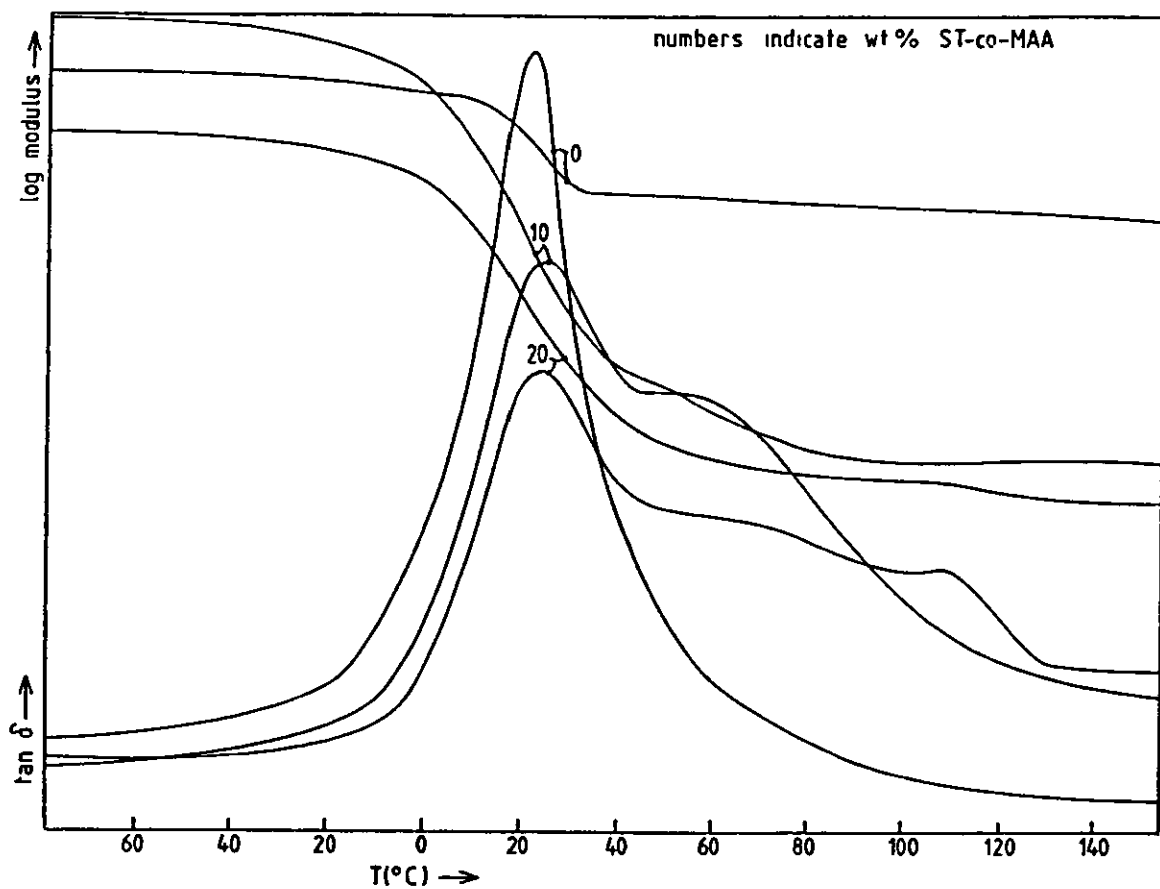
Figure 4.34   DMTA Results for Copolymer 163 - PPG(1) Blends
with 3:1 Ratio of 163:PPG(1)   (Table 4.8)
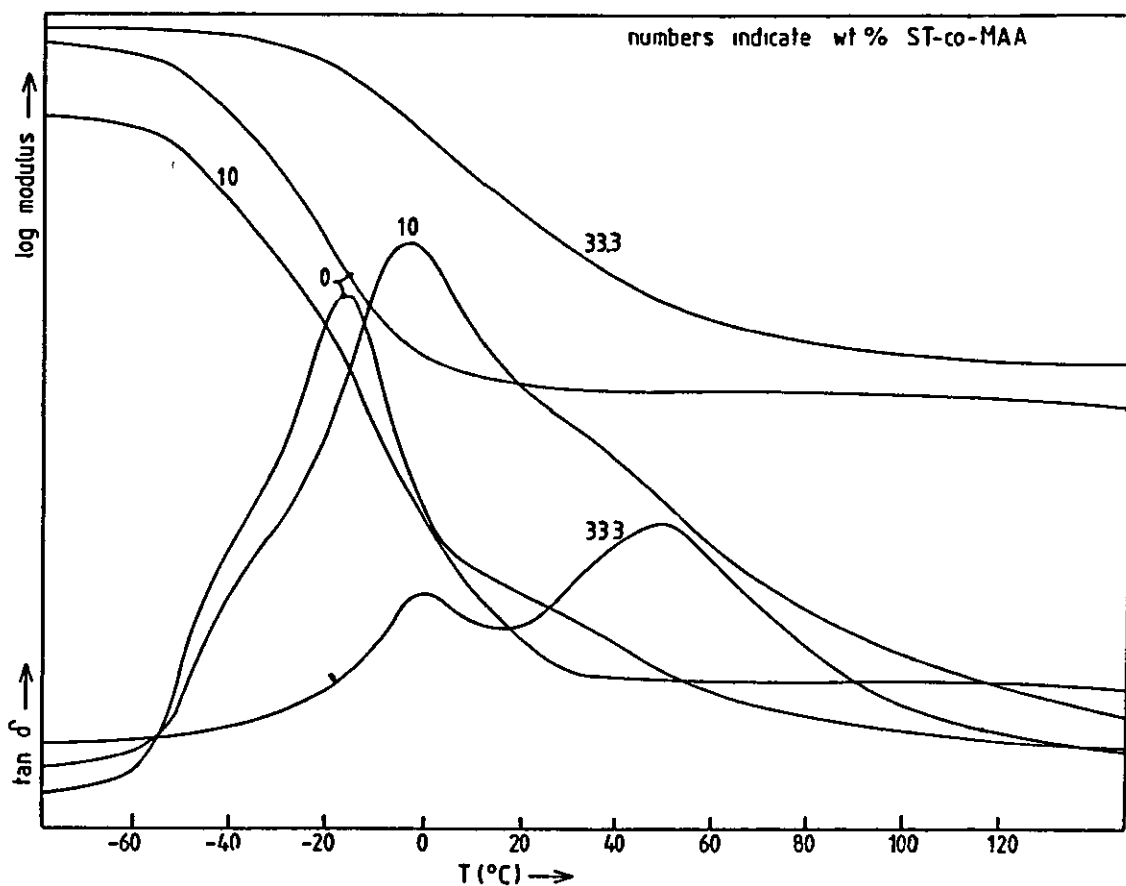
Table 4.8   A Summary of the Tg Values for Components Used in Ternary Blends

Blend Component	DMTA Tg(°C)	Peak Width at Half Height (Wh½)
LF200	49	16°
ST/MAA Copolymer 29	120	35°
ST/MAA Copolymer 163	115	50°
PBA(1)	-33	20°
PBA(2)	-24	17°
PBA(3)	-27	39°
PPG(1)	-46	30°
PPG(2)	-51	15°
PPA	-21	17°
Setal 1711	36	48°
CM03	36	37°
9A/303	25	48°

Table 4.9 3-Component ST/MAA Copolymer Blends

Product/No.	Blend Composition	Film Appearance	DMTA Tg/°C	W½ m½	Fox Eqn Tg/°C	Rule of Mixtures	FTIR Result
214	163/PPG(1)/LF200 20: 20 : 60	opaque	24,(70) (108)	-	43	34	slight carbonyl shift
219	163/PPG(1)/LF200 10: 22.5 : 67.5	opaque	25, 55	-	34	26	slight carbonyl shift
221	163/PPG(1)/LF200 33.3: 33.3 : 33.3	opaque	0, 50	-	39	24	carbonyl shift
222	163/PPG(1)/LF200 10 : 45 : 45	opaque	-3,(-35)	-	13	2	carbonyl shift

LF200 to PPG(1) is 3:1, whilst the proportion of the copolymer is varied from 0% to 10% and 20%. From the tanδ curves it appears that the higher the proportion of copolymer, the more immiscible the system. Care must be taken though in interpreting DMTA results of ternary blends, because the situation is obviously more complicated than for binary blends. For example, consider the tanδ curve for the blend having 20% copolymer, which exhibits one main peak at 24°C and two minor peaks or shoulders at around 70°C and 108°C. The glass transition of the individual components are summarised in table 4.8 and are as follows, PPG(1), -46°C; copolymer 163, 115°C and LF200, 49°C. It is clear therefore, that the blend transition at 24°C is not due to any of the three components alone in a single unmixed phase. However, this transition appears at almost exactly the same temperature as the tanδ transition for the blend containing 0% copolymer, that is the blend of LF200 and PPG(1) in the ratio of 75:25 weight percent (see table 4.6). It seems likely then, that the peak at 24°C in blend number 214 (20% copolymer), and also the peak at 25°C in blend number 219 (10% copolymer) are due to a mixed phase consisting largely of LF200 and PPG(1). The tanδ curve for the 20% copolymer blend then tails-off slowly until ending in a small peak around 108°C. It is probable that this small transition corresponds largely to, unmixed copolymer, being only a few degrees lower than the glass transition temperature of pure copolymer (Tg 115°C). Between the major transition at 24°C and the minor one at 108°C is a broad plateau which is more difficult to assign. It is probably due to some kind of mixed phase or a series of overlapping mixed phases consisting of all three components. So despite the opacity of the blend film, it appears from the DMTA plot that some degree of miscibility exists in the system, even though several phases are present.

Blend 219, containing 10% copolymer, exhibits only two tan-δ transitions in the DMTA plot, one at 25°C presumably due to a mixed phase of LF200 and PPG(1) and one at 55°C. This second transition could well be an indication of a mixed phase consisting of copolymer and PPG(1). Blends of ST/MAA copolymers and PPG(1) discussed in the previous section (4.4) showed some degree of miscibility, so it is likely that the tanδ peak is a mixed phase of these two components.

The FTIR results (figures 4.35 and 4.36) indicate that some specific interactions are in operation in both of the blends, 214 and 219, because of a change in the appearance of the carbonyl peaks in the infrared spectra of the blends, compared to the spectrum of pure copolymer. The copolymer acid carbonyl appears at 1700 cm^{-1} as discussed in the previous section and when involved in hydrogen bonding interactions shifts to 1728 cm^{-1}. This appears to be what is happening, although to a much smaller extent to what was observed in the previous section (4.4). It is fairly certain that the interactions are between the ether oxygen of the PPG(1) and the acid carbonyl of the copolymer as before, the peak at 1728 cm^{-1} being much smaller in this case, due to the smaller proportions of these two components in the ternary blends.

Blends 221 and 222 have a 1:1 ratio of LF200 and PPG(1), whilst the copolymer content is 33.3% and 10% by weight overall. The DMTA plots are shown in figure 4.34, along with the tanδ and log modulus curves for the 1:1 blend PPG(1) and LF200 (see blend 112 in table 4.6). The two component blend has a tanδ peak at -16°C, but shows signs of only partial miscibility, because of the "shoulders" that can be seen either side of the main peak. Adding 10% ST/MAA copolymer to form a ternary blend (222) shifts the peak of the main transition to -3°C, whilst still retaining shoulders either side of

The Infrared Carbonyl Band for
Copolymer 163 – PPG(1) – LF200 Blends (Table 4.9)

Figure 4.35

214

163

1760.0   1700.0   1640.0
WAVENUMBER (CM-1)

Figure 4.36

219

163

1760.0   1700.0   1640.0
WAVENUMBER (CM-1)

Figure 4.37

221

163

1760.0   1700.0   1640.0
WAVENUMBER (CM-1)

Figure 4.38

222

163

1760.0   1700.0   1640.0
WAVENUMBER (CM-1)
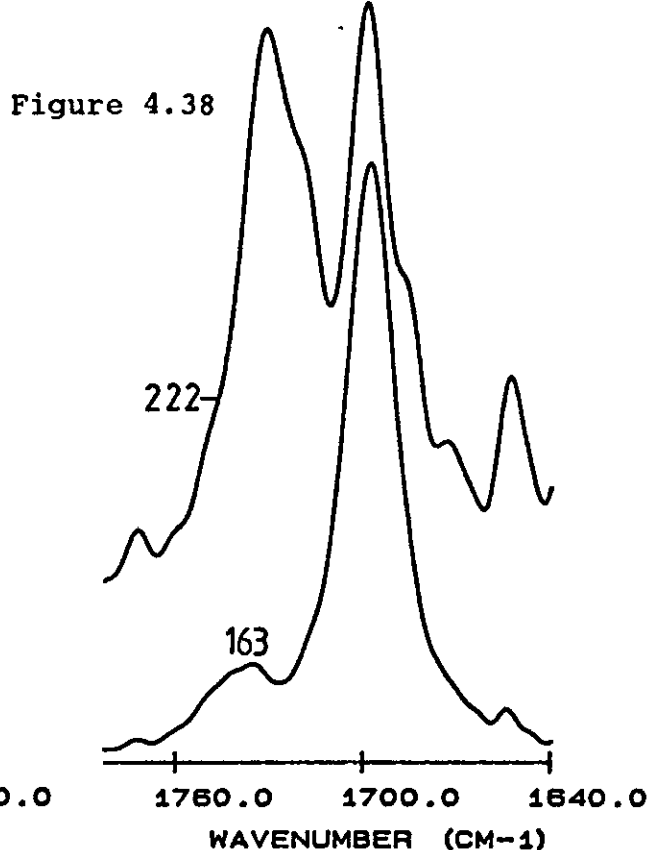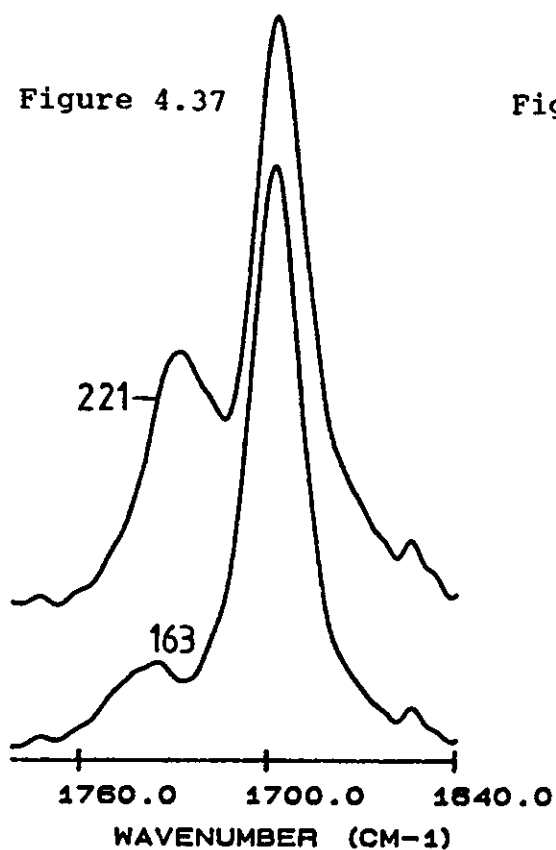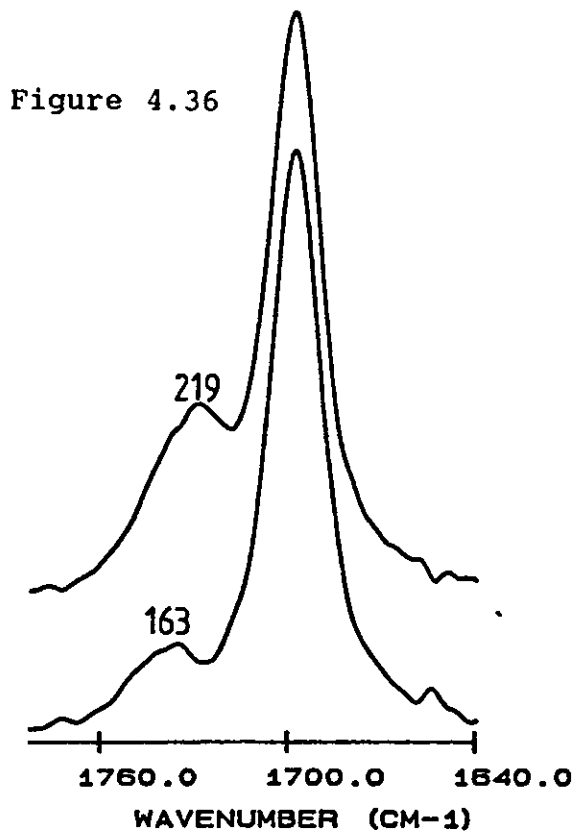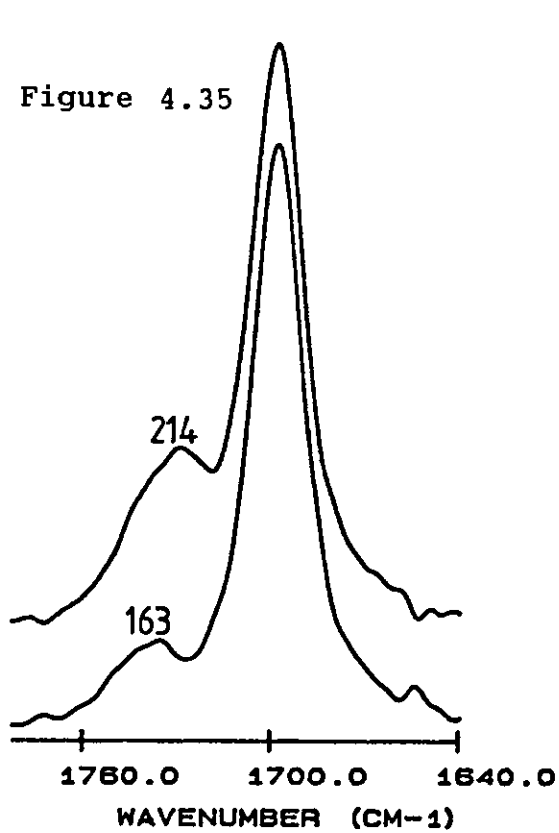
this peak. It terms of assigning the peaks, it is probably a fair assumption that the shoulder observed at around -40°C, relates the tanδ transition due to unmixed PPG(1). The large transition at 0°C is probably composed of a predominantly mixed phase of LF200 and PPG(1), but perhaps with a small amount of the copolymer also. This would account for the shift of the transition to higher temperature, compared to the binary blend of LF200 and PPG(1). The shoulder on the higher temperature side of the main peak, at around 40°C could well be due to a mixed or partially mixed phase of the copolymer and PPG(1). A mixed phase of just copolymer and LF200 would be very unlikely (see section 4.1) to be miscible, and in any case would appear at a higher temperature than 40°C. Blend 221, containing 33.3% of copolymer, clearly exhibits two separate glass transition temperatures at 0°C and 50°C. The lower temperature transition again almost certainly corresponds to a mixed phase of PPG(1) and LF200, whilst the higher temperature transition at 50°C seems likely to be the result of a mixed phase of PPG(1) and ST/MAA copolymer. The fact that some degree of mixing is achieved between the copolymer and the PPG(1), is confirmed by the appearance of a carbonyl peak at 1728 cm^{-1}

in the infrared spectrum of blend 221 (see figure 4.37). It is apparent also, that the higher the proportion of PPG(1) in the system, the stronger the interaction with the acid group of the copolymer. Blend 222 having 33.3% PPG(1) exhibits a larger peak, proportionally, at 1728 cm^{-1} than the blend 221 having only 10% PPG(1), compare figures 4.37 and 4.38. Note that all the infrared spectra were scaled, such that the carbonyl peaks were of approximately the same size, for comparison purposes. The absorbance scale will therefore, be different for each trace.

Summarising the results of this ternary blend system, it is apparent that whilst mixed phases are obtained between PPG(1) and

each of the other two components, no overall mixed phase is produced, nor it seems, any mixed phase of ST/MAA copolymer with LF200. It must be concluded therefore, that PPG(1) fails to enhance the miscibility of LF200 and the ST/MAA copolymer to any large extent.

Blends Involving Polymers Supplied by LVH Coatings Ltd

The next four sections detail the results and discussion of solution blends which involve the acrylic polymers CM03 and 9A/303 (see section 3.1.3). The results of both binary and ternary blends of each polymer will be discussed in turn.

4.6   Binary CM03 Blends

4.6.1 The Characterisation of CM03

CM03 is a terpolymer made by reacting the monomers methacrylic acid (MMA), 2-hydroxy-ethyl acrylate (2-HEA) and n-butyl acrylate (BA) in the ratio of 17:17:66 percent by weight. The material was characterised by GPC, NMR and FTIR, the graphical results being shown in appendices 2, 1 and 3 respectively. The peak molecular weight (Mp) was found to be 19700 by GPC using a mixed gel column (table 4.2). The shape of the chromatogram is probably indicative of the way in which the terpolymer was produced, i.e. a large scale batch reaction to high conversion, although precise details of the process have not been supplied.

4.6.2 Binary Solution Blend Results and Discussion

All blends were prepared as described in section 3.3.1 using chloroform as solvent and were studied by DMTA and FTIR with each blend film appearance being noted.

CM03 - LF200 Blends

Before discussing the results of the analyses of these blends, it is perhaps appropriate to discuss a little of the background to the reasons for wanting to blend these two commercial materials. Lumiflon LF200 is a high performance and hence, high cost surface coating material (see Introduction) and the aim was to incorporate this material into the acrylic coating composition CM03, in order to improve the overall physical properties of the acrylic system and to produce a coating material intermediate in performance and cost between LF200 and CM03. It was found however, that mixtures of these two components lacked miscibility. In order to more fully understand the interaction, or lack of it, between LF200 and CM03, the model system of ST/MAA was used to investigate the potential for specific interactions, between LF200 and the MAA component of the copolymer, (the MAA content in the copolymers 29 and 163, and in CM03 is very similar). Also investigated was the possibility of enhancing the miscibility of LF200 and the copolymer using low molecular weight compatibilisers. The results of these experiments and others involving LF200 and various other polymers, although not always entirely successful in terms of producing miscibility, provided a lot of information about the potential for interactions with LF200 and information about the types of polymers likely to be miscible with LF200. Given this information, binary and ternary blends of CM03 were studied, and the results discussed in this section, starting first of all with the blends of LF200 with CM03.

The glass transition temperature of CM03 was found by DMTA to be 36°C (see table 4.8) and immediately, we are faced with the problem that this transition is only 13°C below that of LF200. Quite obviously this makes the DMTA analysis of LF200-CM03 blends difficult, with the technique unable to resolve the two Tg

transitions. Table 4.10 shows the results of the DMTA analysis of 25, 50 and 75% blends of CM03 with LF200. Figure 4.39 shows the tan δ and log modulus curves from which these T_g values were obtained. Blend 99 (75% LF200) shows a single T_g of narrow width at 43°C, giving the false impression of miscibility at this composition. The immiscibility of the two components is more evident at the compositions of 50 and 25% LF200, with shoulders being observed on the tan δ peaks for these blends. Not so much in these binary blends, but in the ternary blends of CM03, the width of the blend tan δ transitions, becomes more important in the assessment of whether miscibility exists. The ternary blends will be discussed in the next section, but before that, the results of binary blends of CM03 involving potential compatibilising agents will be discussed.

CM03 - PPG(1) Blends

In section 4.3 it was found that there was a significant degree of miscibility between PPG(1) and LF200 and in section 4.4 that there was also some extent of miscibility between PPG(1) and the copolymer of ST and MAA. Ternary blends results (section 4.5) however, showed that PPG(1) failed to significantly improve the miscibility of LF200 and the ST/MAA copolymer. Nevertheless, the miscibility of PPG(1) with CM03 was investigated with the results being shown in table 4.10 and graphically in figures 4.40 and 4.41. All three blends formed transparent films when cast from chloroform, an encouraging sign with regards to miscibility. The blends containing 75 and 25% PPG(1) yielded single glass transition temperatures, with narrow tan δ peak widths. The tan δ and log modulus curves for the 25% PPG(1) blend are shown in figure 4.40 and is really a perfect example of the result expected for a miscible blend. The DMTA result of the 50:50 blends is perhaps a typical example of a partially miscible

Table 4.10   2-Component CM03 Blends

Product No.	Blend Composition	Film Appearance	DMTA Tg/°C	W_{1h2}	Fox Eqn Tg/°C	Rule of Mixtures	FTIR Result
99	CM03/LF200 25:75	translucent	43	24°	46	46	no peak shifts
98	CM03/LF200 50:50	translucent	48, (30)	40°	42	43	"
97	CM03/LF200 75:25	translucent	44, (-1)	38°	39	39	"
138	CM03/PPG(1) 25:75	transparent	-49	32°	-30	-26	carbonyl shift
118	CM03/PPG(1) 50:50	transparent	-26, 10	-	-11	-5	"
121	CM03/PPG(1) 75:25	transparent	1	20°	10	16	"
177	CM03/PPG(2) 25:75	transparent	-45	27°	-34	-29	"
178	CM03/PPG(2) 50:50	transparent	-22	36°	-15	-8	"
179	CM03/PPG(2) 75:25	transparent	3	34°	8	14	"
127	CM03/PBA(1) 25:75	transparent	-30, 20	-	-19	-16	inconclusive
123	CM03/PBA(1) 50:50	transparent	-33, 12	-	-3	2	"
128	CM03/PBA(1) 75:25	transparent	29	24°	15	19	"
172	CM03/PBA(2) 25:75	translucent	-26, 18,40	-	-11	-9	"
115	CM03/PBA(2) 50:50	translucent	-28, 24,55	-	3	6	"
173	CM03/PBA(2) 75:25	translucent	-32, 38	-	18	21	"

Table 4.10 (continued)   2-Component CM03 Blends

Product No.	Blend Composition	Film Appearance	DMTA Tg/°C	W₁/₂	Fox Eqn Tg/°C	Rule of Mixtures	FTIR Result
246	CM03/PBA(3) 50:50	translucent	-33, 51	-	1	5	inconclusive
247	CM03/PBA(3) 75:25	translucent	-33, 51	-	17	20	"
237	CM03/PPA 50:50	almost transparent	-29, 20	-	5	8	no peak shift
117	CM03/PEG 50:50	opaque	18, (50)	-	-	-	carbonyl shift
257	CM03/163 25:75	opaque	32,120 (57)	-	53	56	inconclusive
258	CM03/163 50:50	opaque	32,121	-	71	76	"
259	CM03/163 75:25	opaque	32,117	-	92	95	"

Figure 4.39
DMTA Results for CMO3 - LF200 Blends (Table 4.10)
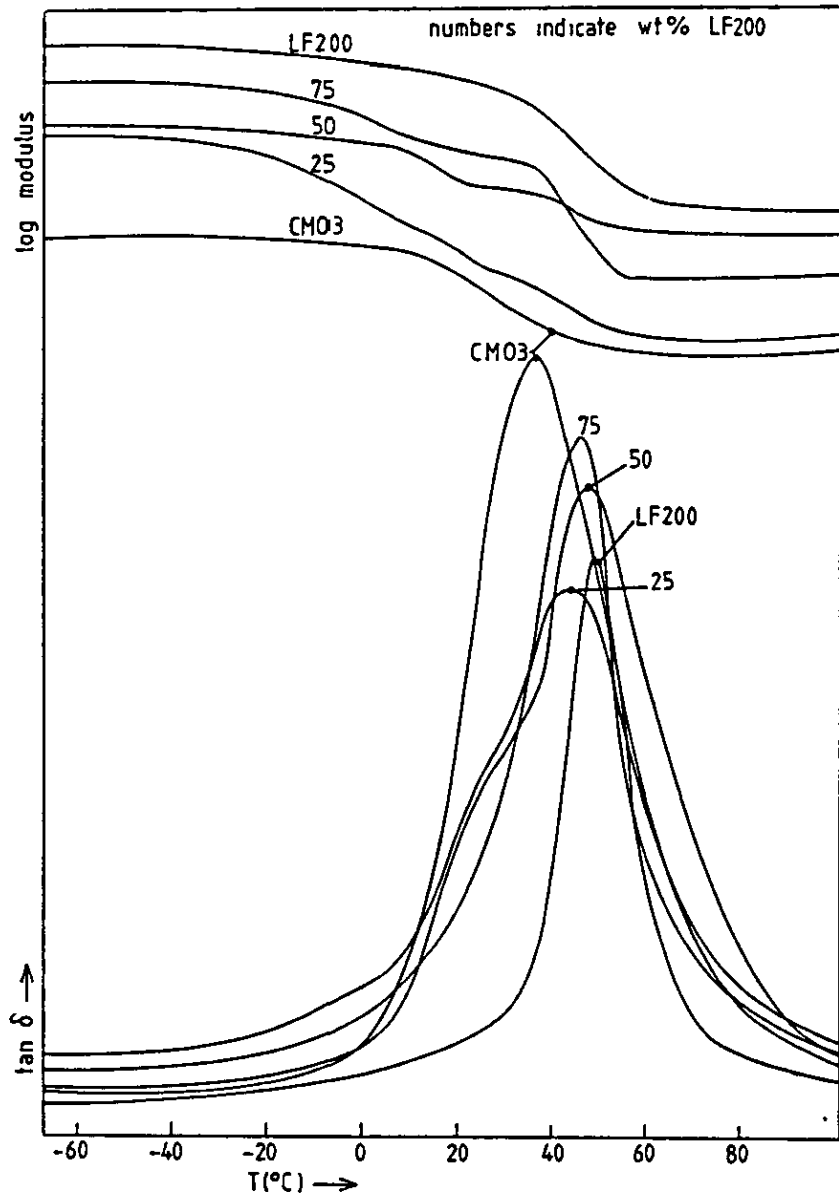
Figure 4.40

DMTA Results for CMO3 – PPG(1) Blends (Table 4.10)
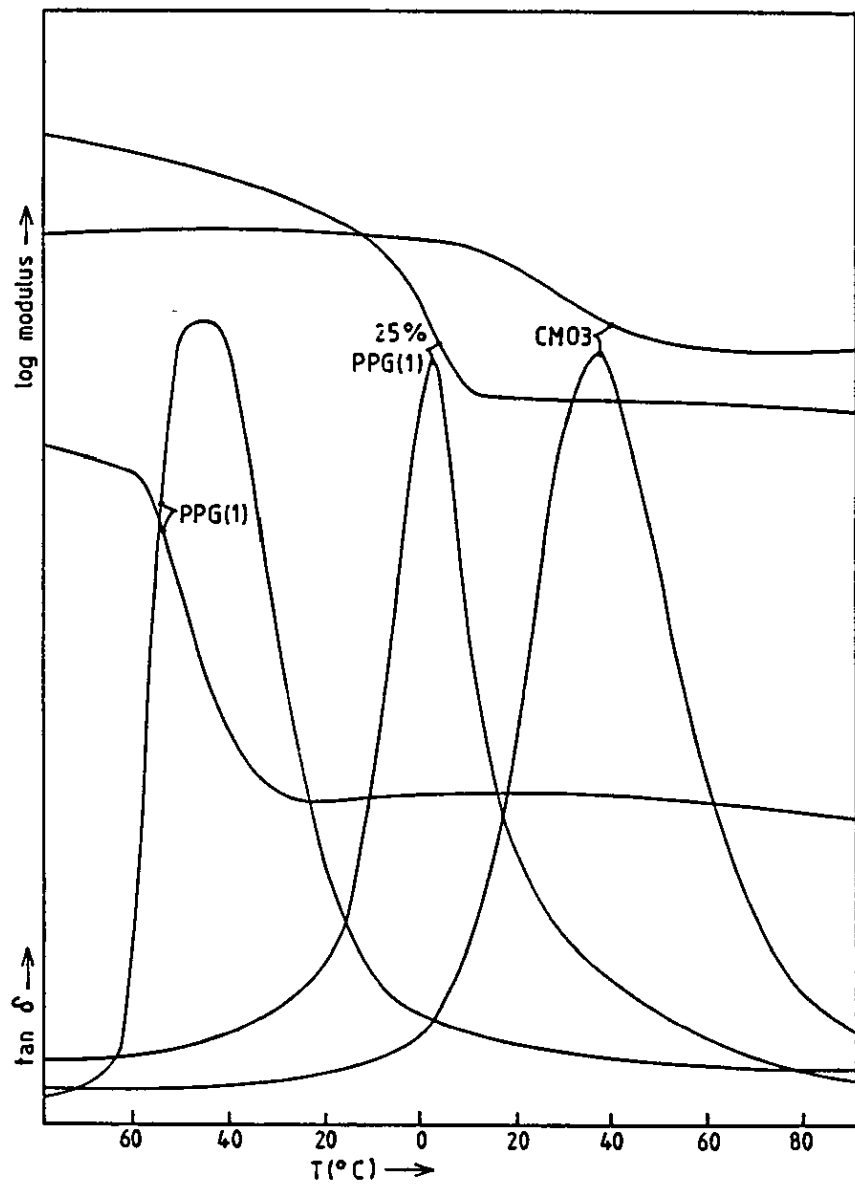
Figure 4.41

DMTA Results for CMO3 – PPG(2) Blends (Table 4.10)
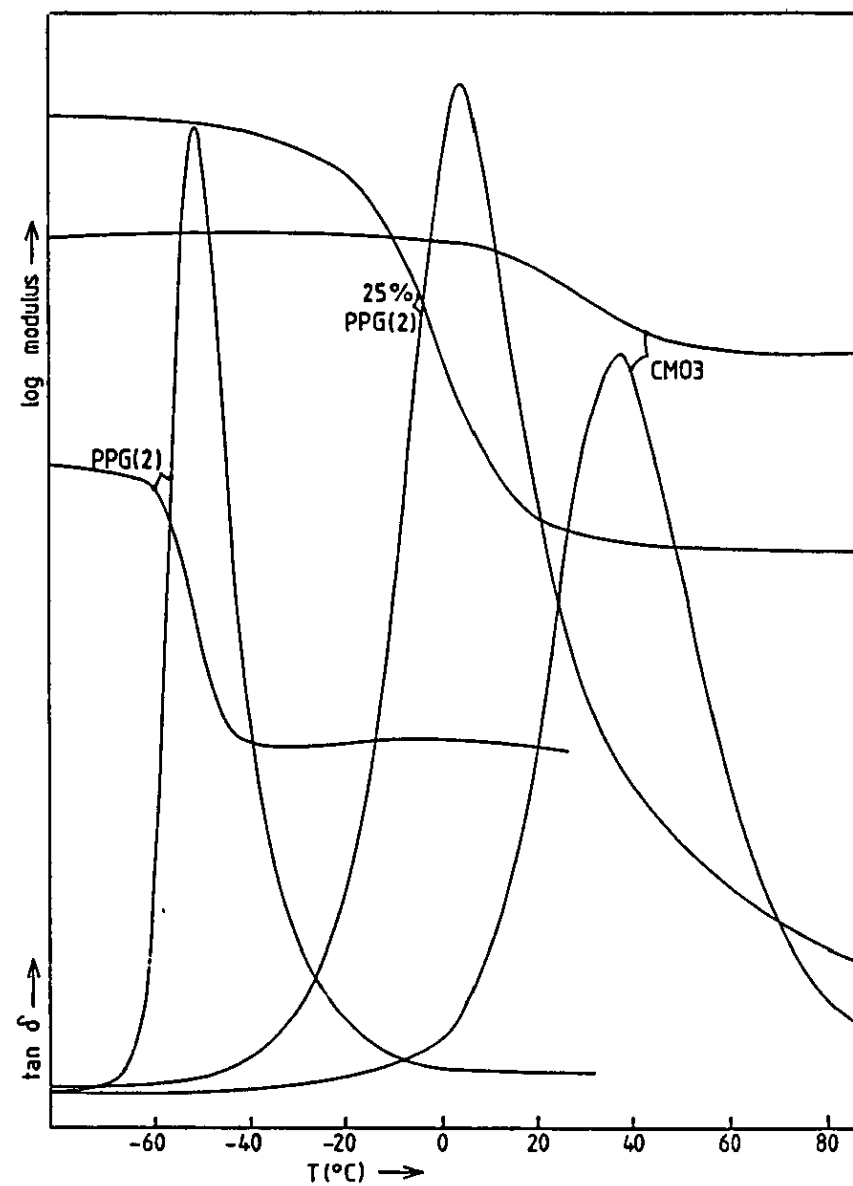
system, with the Tg transitions of the two components moving towards one another relative to the peak positions for each pure component. This is indicative of a partial mixing of the components, although not sufficient to yield a single transition. The Tg values predicted by the Fox equation and the rule of mixtures are somewhat different to those actually observed. This could be due to the difference in molecular weight of the two components, as suggested previously (section 4.4). Since PPG(1) has a much lower molecular weight than CM03, more chains of PPG(1) are present proportionally, than would have been true if the polymers were of similar molecular weight. More chains ends mean a greater free volume and this leads to a decrease in the Tg of the blend (see section 2.8.3).

Figure 4.43 shows the carbonyl region of the infrared spectrum of CM03 and of the three blend compositions. Consider first, the carbonyl band of pure CM03, which appears to be composed of two unresolved bands, the stronger of which peaks at a wavenumber value of around 1735 cm^{-1}. CM03 is composed of three monomer units, all of which have carbonyl groups. The main component of CM03 is BA (66 weight percent, in the reaction mixture) and the homopolymer of BA has a carbonyl group which appears at 1735 cm^{-1} in the infrared spectrum, which therefore, accounts for the strong band at 1735 cm^{-1} in CM03. The acid carbonyl of MAA appears at 1700 cm^{-1}, and explains the unresolved shoulder observed in the spectrum of CM03 at around 1700 cm^{-1}, being less intense, because of the corresponding smaller proportion of MAA units in the terpolymer. It seems likely that the carbonyl peak due to 2-HEA is obscured by the BA carbonyl at around 1735 cm^{-1}. It is now possible to more easily understand what might be happening as indicated by the carbonyl bands in the infrared spectra of the blends of CM03 and PPG(1) (figure 4.43). There appears to be a clear trend in the infrared spectra going from pure

Figure 4.43
The Infrared Carbonyl Band for
CMO3 - PPG(1) Blends

75% PPG(1)

50% PPG(1)

25% PPG(1)

CMO3

1820.0   1775.0   1730.0   1685.0   1640.0
WAVENUMBER (CM-1)
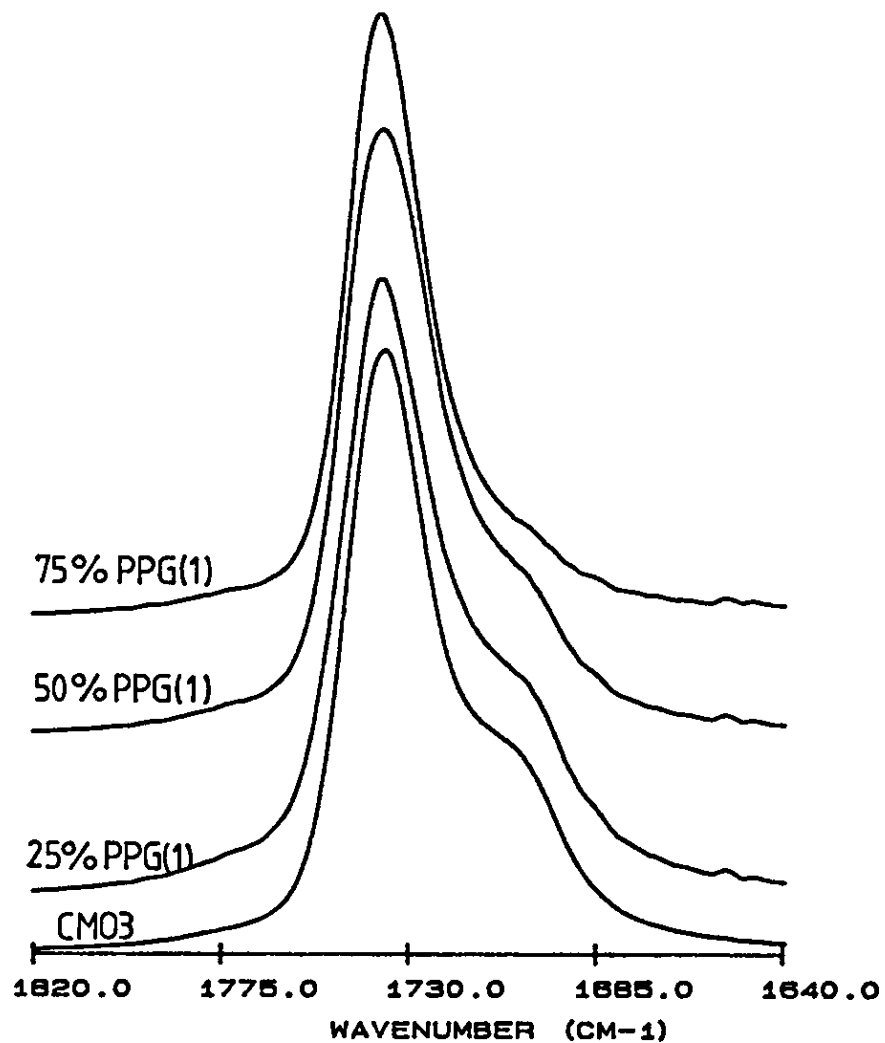
Figure 4.44
The Infrared Carbonyl Band for
CMO3 - PPG(2) Blends

75% PPG(2)

50% PPG(2)

25% PPG(2)

CMO3

1820.0   1775.0   1730.0   1685.0   1640.0
WAVENUMBER (CM-1)
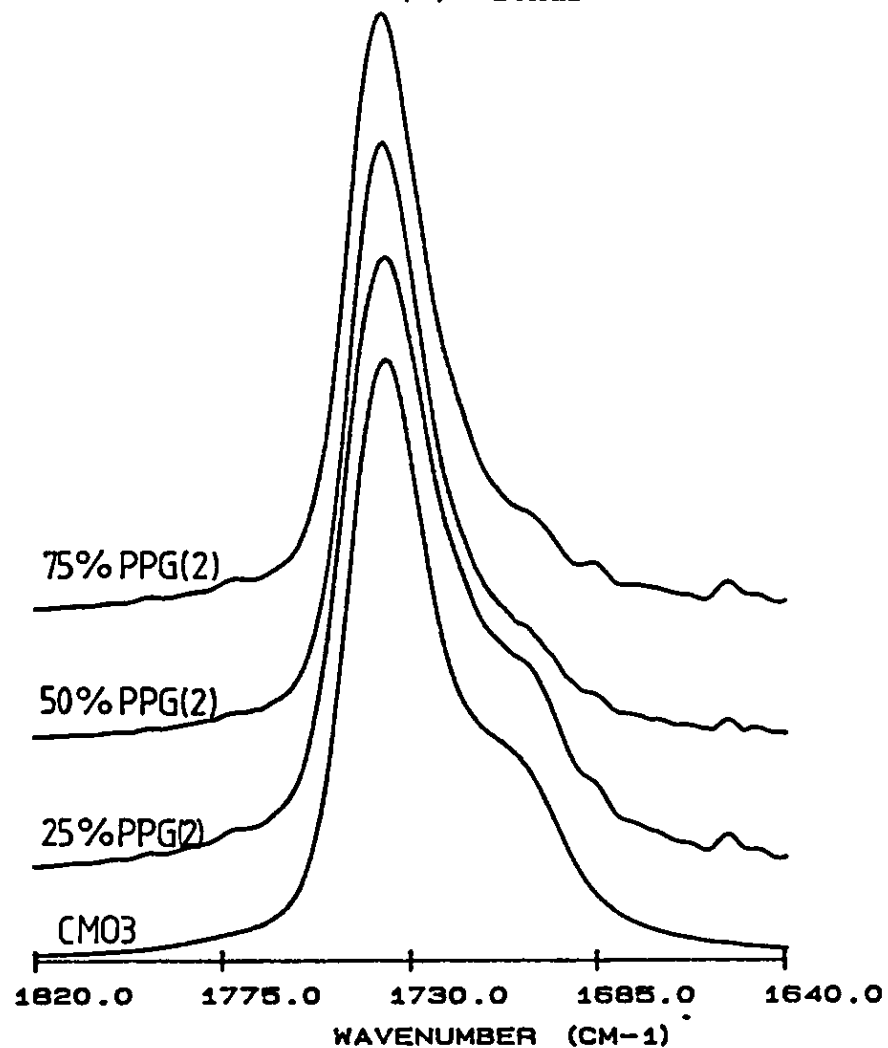
CM03 to blend 138 (75% PPG(1)). The higher the proportion of PPG(1) in the blend, the smaller the shoulder on the side of the more intense band becomes. Bearing in mind the fact that the carbonyl peaks for each blend were rescaled for comparison purposes, the relative intensities of the main band and the shoulder are clearly changing. This indicates that as more PPG(1) is introduced into the system, the less intense the band due to the acid dimer at 1700 cm^{-1} becomes. By comparison with the infrared results for ST/MAA - polyether blends discussed in previous sections, it seems plausible that a similar interaction is in operation here. That is, a hydrogen bonding interaction between the acid carbonyl and the ether oxygen of the PPG(1). This time though, the position at which the hydrogen bonded acid carbonyl appears, i.e. 1728 cm^{-1}, is close to that for the acrylate carbonyls of BA and 2-HEA and is therefore, almost completely obscured.

CM03 - PPG(2) Blends

PPG(2) has a number average molecular weight (Mn) of 2769 as determined by GPC, with a Tg of - 51°C. Blends of PPG(2) with LF200 (table 4.6) were shown to be miscible, perhaps slightly more so than the blends involving LF200 and PPG(1). This also seems to be the case here, PPG(2) appears to have slightly greater miscibility with CM03 than PPG(1), all three blend compositions giving single glass transitions (figure 4.41). Apart from a slightly improved miscibility, there seems to be little difference between the blends of PPG(1) and PPG(2) with CM03. The infrared results for this blend are very similar to those for the PPG(1) blends and the same comments apply (figure 4.44).

CM03 -PBA(1) Blends

The blends of CM03 with the lowest molecular weight PBA studied (Mn, 1749) all produced transparent films, yet only one composition showed a single glass transition temperature. Blends having 75% and 50% PBA(1) both exhibited two $\tan\delta$ peaks. Both of these compositions yielded a $\tan\delta$ peak close to the position at which the Tg of pure PBA(1) is normally observed, indicating some unmixed PBA(1) in these blends. The second transition in each of the blends occurred at a temperature intermediate to the Tg values of the two pure components and therefore, indicted a partially mixed phase of PBA(1) and CM03. The 25% PBA(1) blend (figure 4.45) has a single Tg indicated by a narrow $\tan\delta$ peak at 29°C and may be considered to be miscible.

The infrared spectra of these blends are difficult to interpret in terms of carbonyl shifts. There are a total of four monomer units in the blends each with a carbonyl group, all of which overlap in the region of 1700 - 1735 cm^{-1}. It would be almost impossible to resolve and assign the various bands, even with the help of computer-aided spectral subtraction.

Overall, it is interesting that only partial miscibility is observed for this system, with the possible exception of the 25% PBA(1) blend, since BA units are common to both the terpolymer and homopolymer involved in the blend. This might conceivably have been a factor which would have been expected to favour the miscibility of the blend. In other words, a greater extent of miscibility might have been expected than was obtained, because of the high proportion of BA units in CM03.

Figure 4.45
DMTA Results for CMO3 - PBA(1) Blends (Table 4.10)
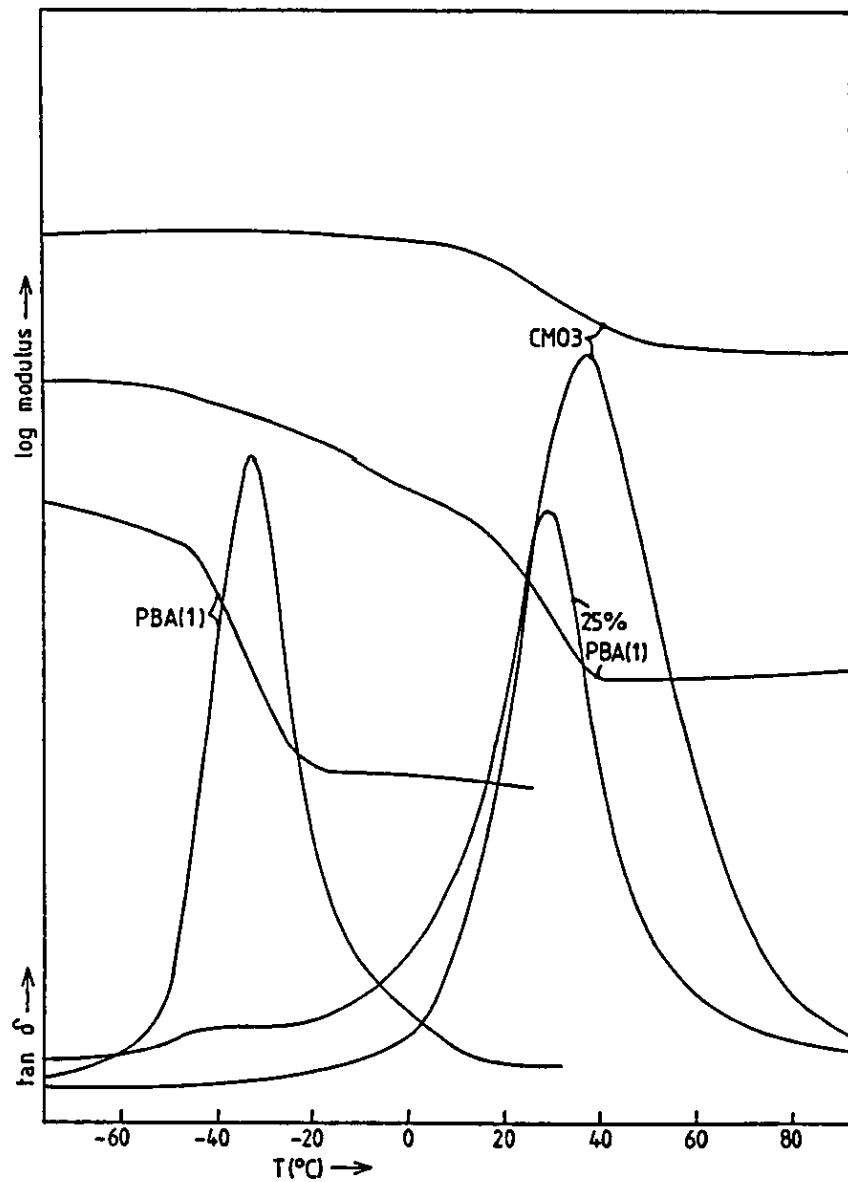
Figure 4.46
DMTA Results for CMO3 - PBA(2) Blends (Table 4.10)
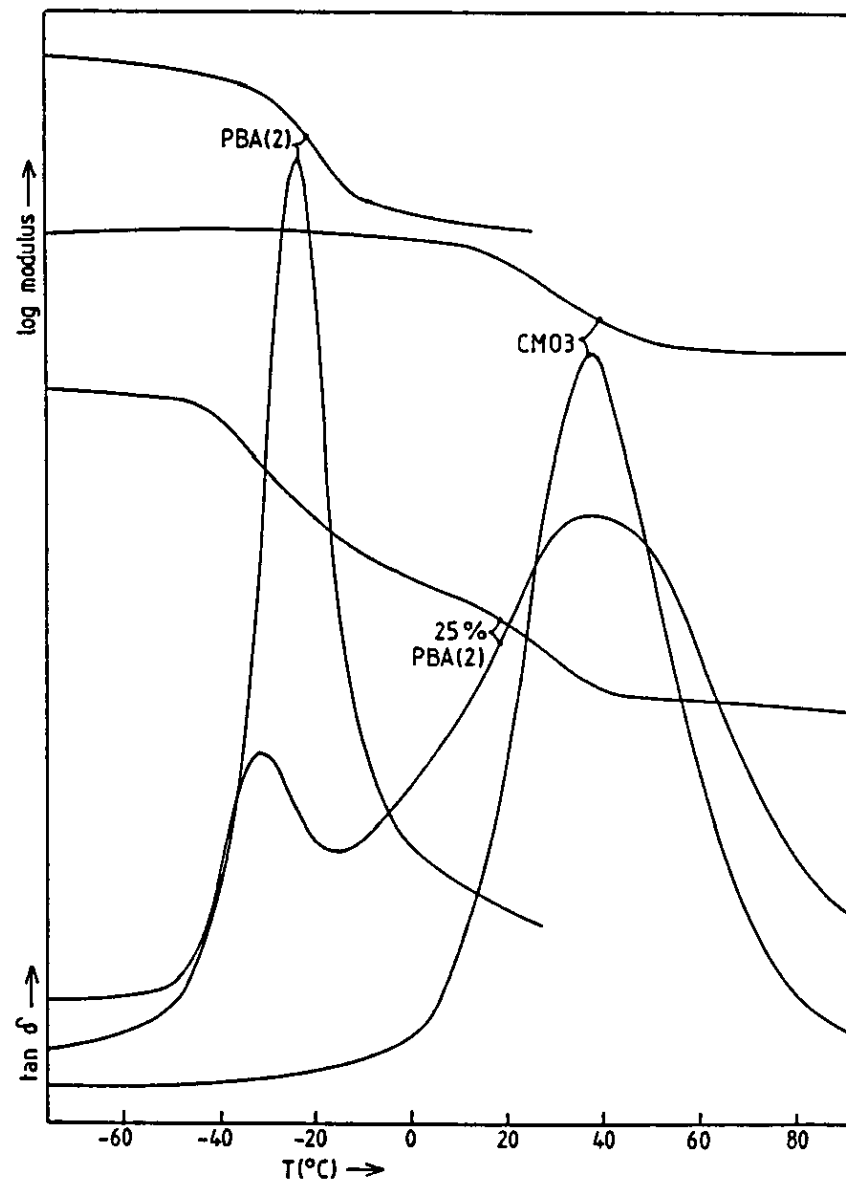
CM03 - PBA(2) Blends

The blends between CM03 and PBA(2) (Mn, 6757) appear at best to be partially miscible and at worst completely immiscible. Blends having 75% and 50% PBA(2) exhibit three $\tan \delta$ transitions, due probably to an unmixed phase of each of the two components, together with a mixed or partially mixed phase intermediate to the other transitions. The blend of 25% PBA(2) with CM03 has two well separated $\tan \delta$ transitions which occur close to the temperatures of the pure component Tg transitions (see figure 4.46). This is a strong indication of immiscibility. The same comments are true about the infrared analysis of this blend system as for the PBA(1) - CM03 system. Overall, PBA(2) appears to be less miscible with CM03 than PBA(1).

CM03 - PBA(3) Blends

PBA(3) was prepared using a chain transfer agent under the conditions described in table 3.3 and has a number average molecular weight of 5200. The glass transition temperature of PBA(3) was found to be -27°C by DMTA. Two blend compositions were produced with each showing two $\tan \delta$ Tg transitions corresponding to the unmixed components, leading to the conclusion of immiscibility for these blends.

By comparing the results of the CM03 blends with each of the three PBA polymers, it is possible to rank the different PBAs in order of their miscibility with CM03. This order is as follows; PBA(1) is the most miscible followed by PBA(2) and then PBA(3). This order does not correspond to the change in molecular weight of the PBA polymers, as may have been expected. None of the three PBA

polymers are completely miscible with CM03 however, and are noticeably less miscible than PPG(1) and PPG(2).

CM03 - PPA Blends

Despite the near-transparent appearance of the blend film, the DMTA result showing two well separated Tg transitions suggests that this is an immiscible blend. No specific interactions were indicated by shifts in bands in the infrared spectrum of the blend.

CM03 - PEG Blend

As discussed earlier, the crystallinity of PEG hinders the analysis of miscibility using DMTA. However, as might have been expected from the infrared results of the CM03 - PPG blends, a carbonyl shift was observed in the IR spectrum of this blend. This again, is almost certainly indicative of a hydrogen bonding interaction between the ether oxygen of the PEG and the acid carbonyl of the MAA units in the terpolymer.

CM03 - ST/MAA Copolymer 163 Blends

CM03 was blended with the copolymer which had been chosen as a model system for the terpolymer, ST-co-MAA. However, as can be seen from the results in table 4.10, opaque films were formed and immiscibility was confirmed by each blend composition showing two well separated glass transitions, relating to the unmixed component phases. The small transition at 57°C in the blend containing 75% copolymer may indicate a small amount of mixing between the phases, although probably minimal. Analysis of the FTIR results would not be practical, because of the complexity caused by the number of overlapping carbonyl bands observed in the infrared spectrum of these blends, between 1700 and 1735 cm^{-1}.

4.7 Ternary CM03 Blends

Table 4.11 lists the series of CM03-LF200 blends in which a third component is incorporated, in an attempt to improve the miscibility of the system. The results of DMTA and FTIR analyses are summarised along with an indication of the optical appearance of blend films.

The interpretation of DMTA results for ternary polymer mixtures is more complicated than for binary blends, due of course to the third component. Consider firstly, the two extreme cases with regards to miscibility that is, a completely mixed single phase consisting of all three components and yielding a single Tg, and conversely a completely immiscible system composed of three separate phases, made up of the three unmixed components in the blend, each exhibiting a characteristic Tg. Provided that the three blend components each have Tg transitions well separated from one another, it might be expected that the observation of either a single Tg, or three separate Tg transitions for a ternary blend, would be reasonably unambiguous. This however is not entirely true, as can be seen if the intermediate cases of miscibility are considered. For a ternary system made up of components A, B and C (each having different Tgs), there are a number of possibilities with regards to miscibility. For example, A may be miscible with B, but not with C. This would lead to a transition due to the mixed phase AB and a separate one for phase C. Another possibility is that B is miscible with both A and C, whilst A and C are themselves immiscible. This would yield two Tg transitions, one for the mixed phase AB and one for the mixed phase BC, the temperatures at which these occur depending on the proportions of A:B and B:C and of A:B:C overall. The various possibilities can be summarised as follows, taking into

Table 4.11   3-Component CM03 Blends

Product No.	Blend Composition	Film Appearance	DMTA $T_g/°C$	$W_{1/2}$	Fox Eqn $T_g/°C$	Rule of Mixtures	FTIR Result
119	CM03/PPG(1)/LF200 33.3 : 33.3 : 33.3	translucent	-3	44°	6	13	carbonyl shift
164	CM03/PPG(1)/LF200 40 : 20 : 40	translucent	20	42°	20	25	"
166	CM03/PPG(1)/LF200 45 : 10 : 45	translucent	32	24°	31	34	"
191	CM03/PPG(1)/LF200 17.5 : 30 : 52.5	translucent	16	52°	11	18	"
141	CM03/PPG(1)/LF200 20 : 20 : 60	translucent	22	19°	22	27	"
154	CM03/PPG(1)/LF200 22.5 : 10 : 67.5	translucent	36	20°	33	37	"
181	CM03/PPG(2)/LF200 33.3 : 33.3 : 33.3	translucent	10(-10) (30)	(65°)	4	11	"
182	CM03/PPG(2)/LF200 20 : 20 : 60	translucent	26	30°	20	26	"
116	CM03/PBA(1)/LF200 33.3 : 33.3 : 33.3	translucent	18	46°	13	17	inconclusive
165	CM03/PBA(1)/LF200 40 : 20 : 40	translucent	32	31°	24	27	"
167	CM03/PBA(1)/LF200 45 : 10 : 45	translucent	37	19°	33	35	"
192	CM03/PBA(1)/LF200 17.5 : 30 : 52.5	translucent	25	30°	17	22	"
143	CM03/PBA(1)/LF200 20 : 20 : 60	translucent	29	20°	26	30	"
155	CM03/PBA(1)/LF200 22.5 : 10 : 67.5	translucent	45(20-25)	(25°)	36	38	"

Table 4.11 (continued)   3-Component CM03 Blends

Product No.	Blend Composition	Film Appearance	DMTA $T_g/°C$	$W_{\frac{1}{2}}$	Fox Eqn $T_g/°C$	Rule of Mixtures	FTIR Result
185	CM03/PBA(2)/LF200 33.3 : 33.3 : 33.3	translucent	-5,34	-	17	20	inconclusive
186	CM03/PBA(2)/LF200 20 : 20 : 60	translucent	34	24°	29	32	"
250	CM03/PBA(3)/LF200 45 : 10 : 45	translucent	43	32°	34	36	"
251	CM03/PBA(3)/LF200 20 : 20 : 60	translucent	40	25°	28	31	"
238	CM03/PPA/LF200 20 : 20: 60	translucent	-26,52	-	30	32	no peak shifts
239	CM03/PPA/LF200 33.3 :33.3:33.3	translucent	-18,51	-	18	21	"

account only complete miscibility between the mixed components of a given phase:

ABC   : mixed phase showing single Tg

A + B + C   : three unmixed phases, three Tgs

AB + C   ⎫

A + BC   ⎬   : two of the three components

AC + B   ⎭   miscible, two Tgs

AB + BC   ⎫   one component miscible with the two

AC + AB   ⎬ : other components (which are

CA + CB   ⎭   themselves immiscible), two Tgs.

The picture is complicated further when partial miscibility is taken into account, there probably being an infinite number of possibilities. For example, A could be partially miscible with B and immiscible with C. This would probably yield a Tg for unmixed A, a Tg for unmixed C, and one or two Tgs for the partially mixed phase of A and B. It is obvious therefore, that the interpretation of DMTA results may not be clearcut for ternary blends and it is quite likely that tan δ transitions will overlap, and hence, will be misleading. If the glass transitions of two or more of the components are close, then the interpretation will be further complicated. Prior knowledge of the miscibility of pairs of components in the three component blend from previous experiments, may however, be helpful in deciphering the DMTA results of the ternary systems.

CM03 - PPG(1) - LF200 Blends

Six ternary blend compositions were prepared in total, three having equal proportions of LF200 and CM03 and three having a 3:1

ratio of LF200 and CM03. The overall percentage of PPG(1) was varied between 10, 20 and 30 (or 33.3) for each ratio of the other two components. The DMTA plots for these blends are shown in figures 4.47 and 4.48, and portions of the infrared spectra are shown in figures 4.50 and 4.51.

Consider first of all, the blends having an equal proportion of LF200 and CM03 (119, 164 and 166). All three compositions exhibit single glass transitions as can be seen from the single tan δ peaks in figure 4.47. This appears to indicate a mixed phase of all three components for each blend, but the question to consider is whether these results could be explained in another way. For example, the tan δ peak at 20°C for blend 164 could in fact be due to overlapping peaks corresponding to partially mixed phases of LF200 and CM03 with PPG(1), whilst LF200 and CM03 remain themselves, unmixed. This could be a plausible explanation given that CM03 and LF200 both show miscibility, with PPG(1) in binary blends, whilst CM03 and are not miscible. However, the most likely explanation for the observation of single tan δ peaks is of a single mixed phase, since all of the blend transitions are smooth and show no sign of shoulders to indicate overlapping peaks, and the appearance of the log modulus curves by and large correspond well with the conclusion of miscibility. Only the log modulus curve for the 10% PPG(1) blend shows any sign of two transitions, contradicting with the smooth, narrow tan δ curve for that blend. When studying the curves for the ternary blends, it is wise to compare them with those for the binary CM03-LF200 blend, which has a shoulder on the tan δ - peak and two falls in the log modulus curve (0% blend).

Another reason for concluding that those blends are miscible, is the good agreement at 10 and 20% PPG(1) levels, between the observed Tg values and those predicted by the Fox equation (2.77) and

-117-

Figure 4.47   DMTA Results for PPG(1) Blends
1:1 Ratio of LF200 : CM03   (Table 4.11)

numbers indicate wt% PPG(1)

log modulus →

0
10
20
33.3

tan δ →

33.3
20
10
0

T(°C) →

-60   -40   -20   0   20   40   60   80
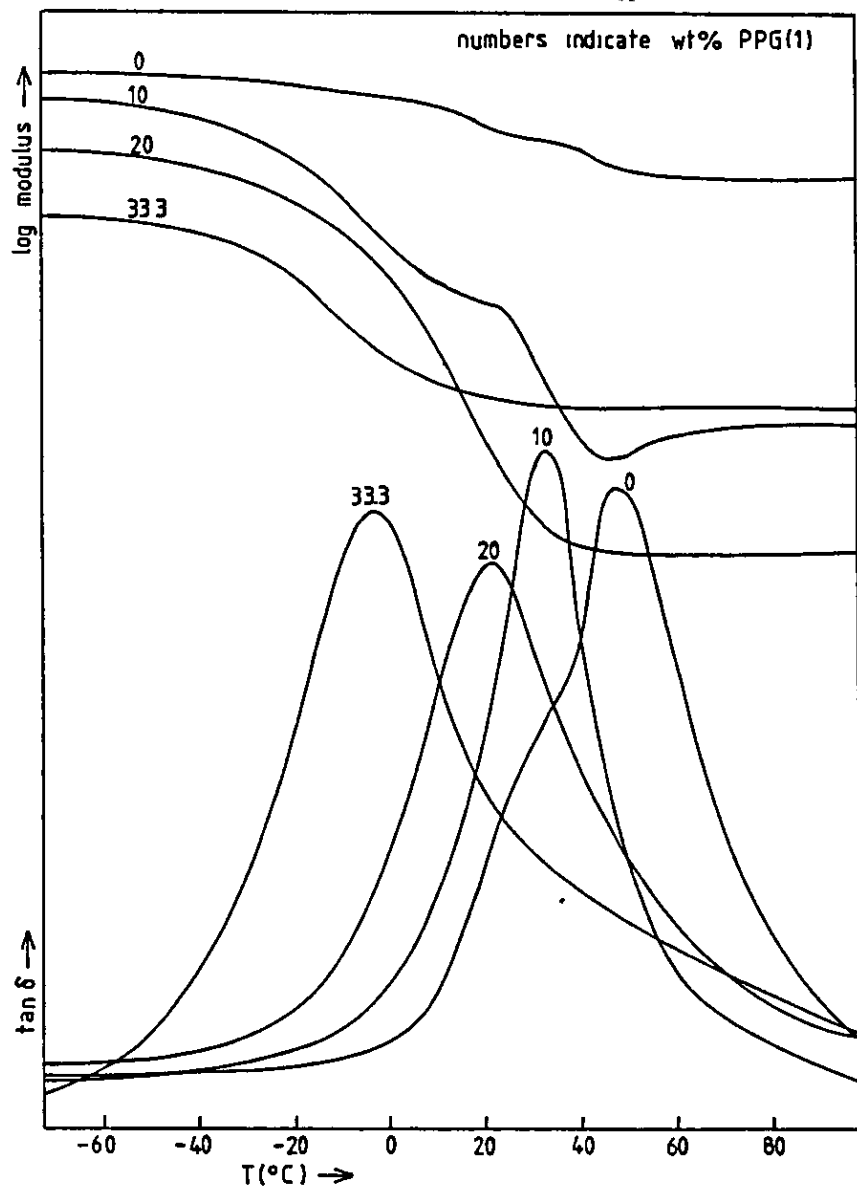
Figure 4.48   DMTA Results for PPG(1) Blends
3:1 Ratio of LF200 : CM03   (Table 4.11)

numbers indicate wt%   PPG(1)

log modulus →

0
20
10
20
30

tan δ →

30
10
0

T(°C) →

-40   -20   0   20   40   60   80   100
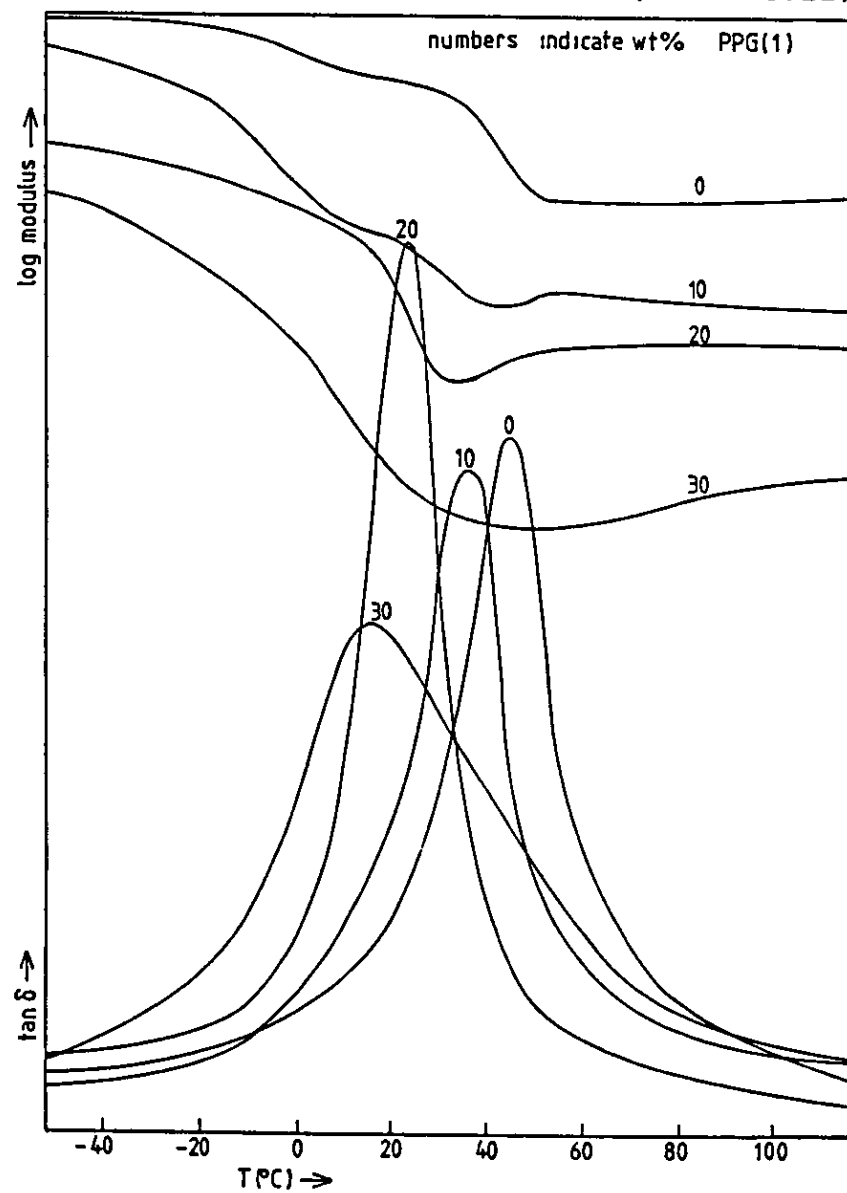
the rule of mixtures equation (4.1), as can be seen graphically in figure 4.49. The only exception to this is for the blend having 33.3% PPG(1). The observation of translucency for these three blends, neither strongly confirms nor contradicts the inference of miscibility.

The infrared results appear to indicate a slight specific interaction involving the carbonyl group(s) of one or more of the blend components. From the FTIR analyses of CM03-PPG(1) blends, it is likely that a similar hydrogen bonding type interaction is in operation in the ternary blends, although in this case the carbonyl shift is only very slight and only really becomes noticeable for the blend having 33.3% PPG(1), see figure 4.50. The interaction in question is that between the ether oxygen of PPG(1) and the acid carbonyl of the MAA component of CM03. It makes sense therefore, that at low proportions of PPG(1), the interaction can barely be detected.

The three blends in which the CM03:LF200 ratio is 1:3, follow the same pattern as for the blends just discussed and the same conclusion is applicable. The tanδ curve for the binary blend of 25% CM03, 75% LF200 exhibits only a single peak, giving the impression of miscibility, this being due to the proximity of the glass transitions of the two polymers (figure 4.48). However, the very narrow tanδ peaks at 22°C and 36°C must surely indicate miscibility for the blends containing 20 and 10% PPG(1) respectively.

The overall impression for all six ternary blends is that 10 or 20% PPG(1) leads to the narrowest tanδ curves, presumably indicating the greatest degree of miscibility at these blend proportions. The conclusion of miscibility cannot be totally certain, because of the reasons discussed earlier and would need to be confirmed by another technique, not relying on glass transitions temperatures.

Figure 4.49

Effect of PPG(1) Content on the Tg of a Ternary Blend with LF200 and CM03
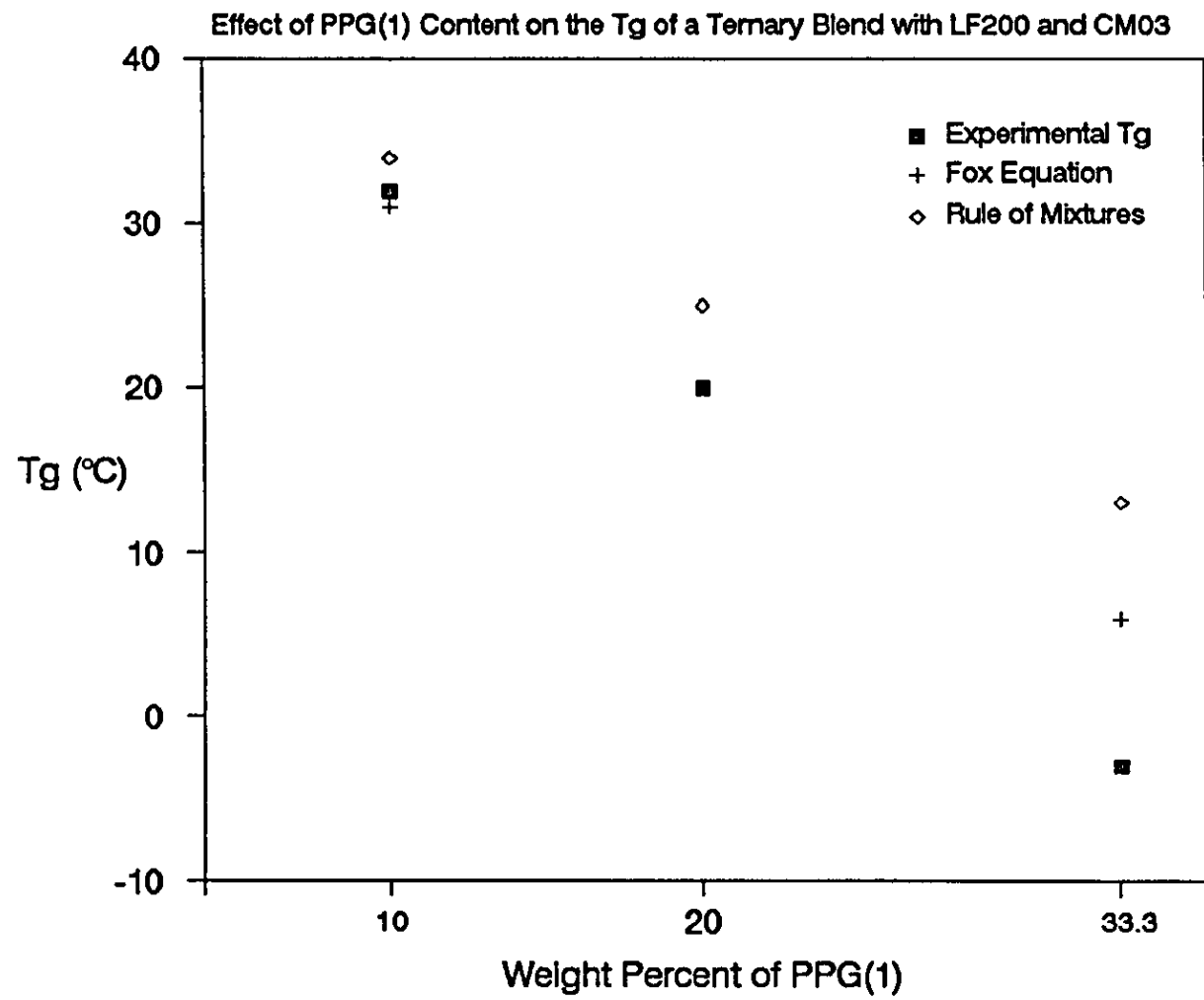
Figure 4.50
The Infrared Carbonyl Band for
CMO3 – PPG(1) – LF200 Blends

wt.% PPG(1)

33.3

20

10

CMO3

1820.0   1775.0   1730.0   1685.0   1640.0
WAVENUMBER (CM–1)
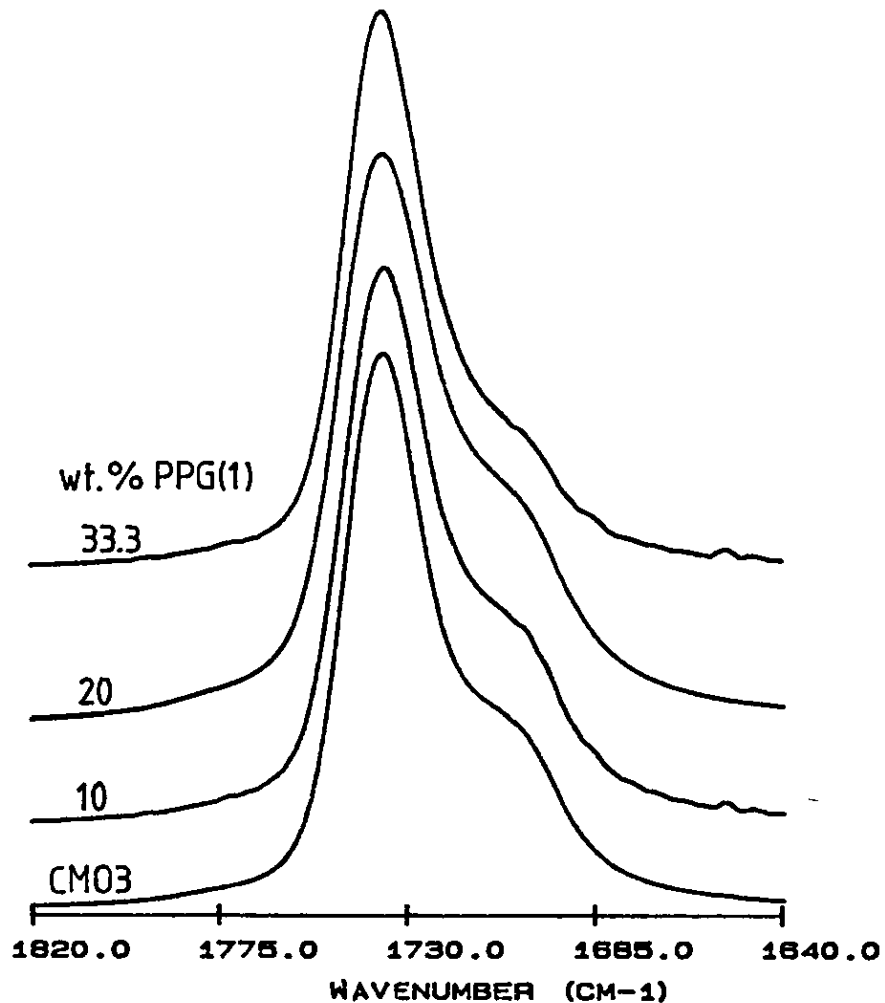
Figure 4.51
The Infrared Carbonyl Band for
CMO3 – PPG(1) – LF200 Blends

wt. % PPG(1)

30

20

10

CMO3

1820.0   1775.0   1730.0   1685.0   1640.0
WAVENUMBER (CM–1)
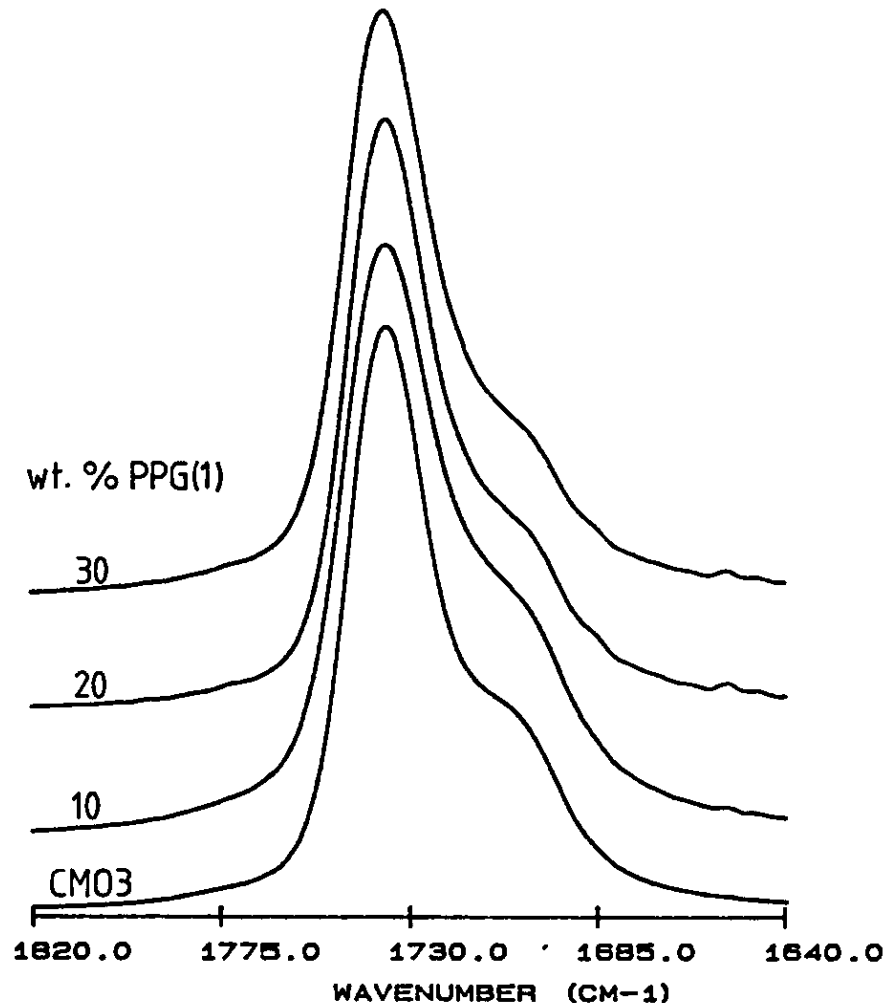
CM03 - PPG(2) - LF200 Blends

These blends were prepared to compare the effectiveness of PPG(2) to that of PPG(1) in enhancing the miscibility of LF200 and CM03. Blends 181 and 182 can be directly compared to the PPG(1) equivalents 119 and 141 respectively. Blend 181, having 33.3% PPG(2) exhibits a multiple $\tan\delta$ transition with a main peak at 10°C and unresolved minor peaks (shoulders) at around -10°C and 30°C (see figure 4.52). This blend composition, therefore, lacks complete miscibility and compares unfavourably with the corresponding blend involving PPG(1) (119). Blend 182 (figure 4.53) has a single glass transition like the corresponding PPG(1) blend 141, with a narrower $\tan\delta$ transition ($W_{h\frac{1}{2}}$=30° compared 42° for 141). Taken together, these blend results do not clearly indicate either a definite improvement or otherwise, in the miscibility enhancement achieved by the use of PPG(2) relative to PPG(1).

The infrared spectrum of 181 (figure 4.54) shows a similar slight carbonyl shift as observed in the PPG(1) ternary blends, suggesting that a small extent of hydrogen bonding is present in the system, the explanation for which has already been discussed.

CM03 - PBA(1) - LF200 Blends

As for PPG(1), six blends were prepared, three having equal proportions of LF200 and CM03, and three having a ratio of LF200:CM03 of 3:1. Considering the first three compositions first, all produced translucent films and gave single $\tan\delta$ Tg peaks when analysed by DMTA (figure 4.55). The blends containing 10 and 20% PBA(1) exhibited narrow $\tan\delta$ transitions at 37°C and 32°C respectively, close to the temperatures predicted by the rule of mixtures. The transition for the 33.3% PBA(1) blend was broader (broad peaks were similarly observed for 33.3% PPG(1) ternary blends), whilst again

Figure 4.52   DMTA Results for PPG(2) Blends
1:1 Ratio of LF200 : CM03   (Table 4.11)

numbers indicate wt% PPG(2)
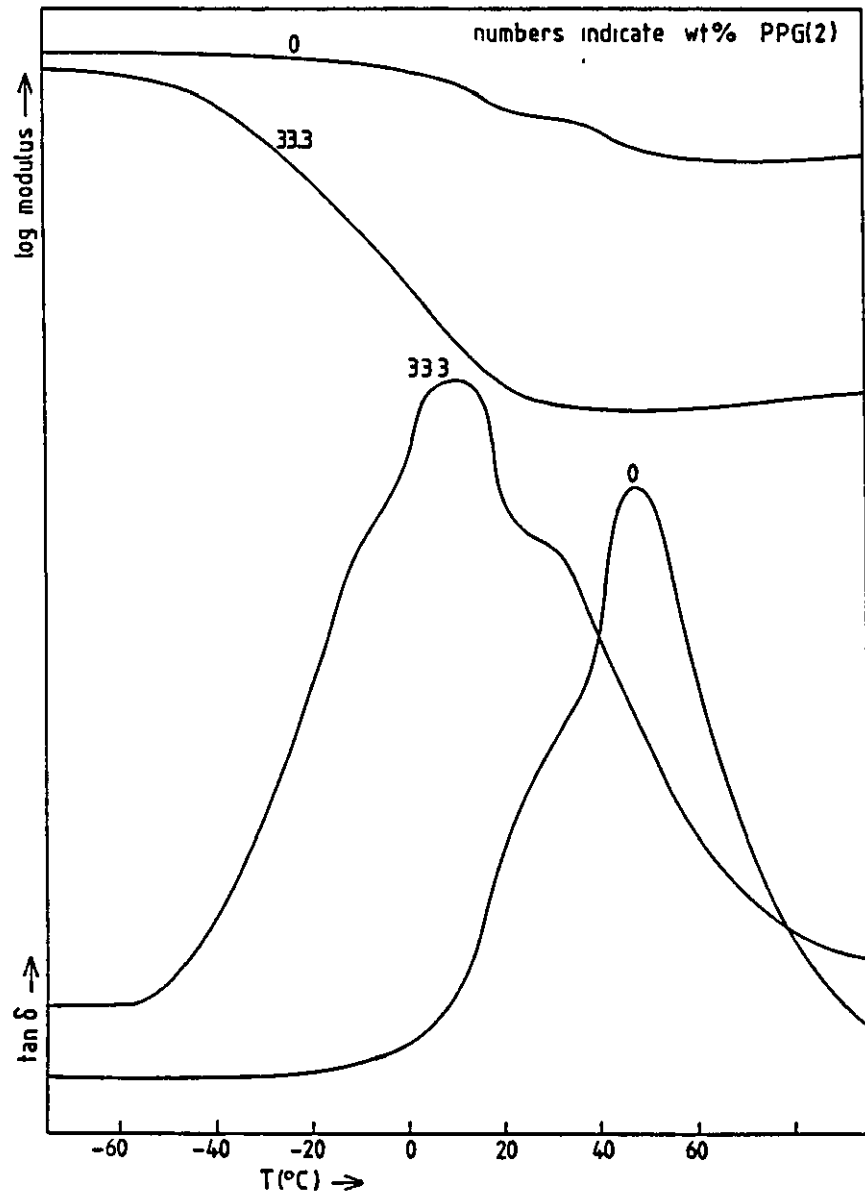
Figure 4.53   DMTA Results for PPG(2) Blends
3:1 Ratio of LF200 : CM03   (Table 4.11)

numbers indicate wt% PPG(2)
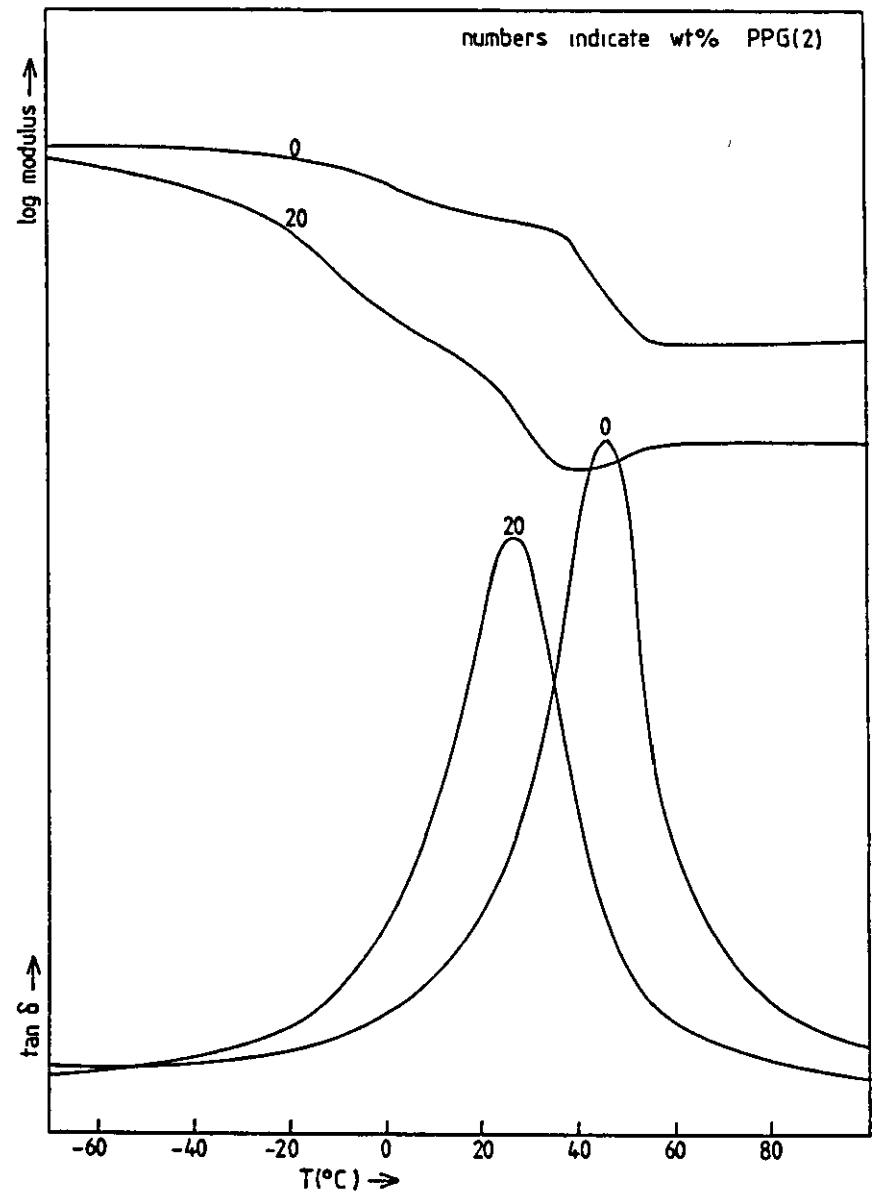
Figure 4.54
The Infrared Carbonyl Band for
CMO3 - PPG(2) - LF200 Blend
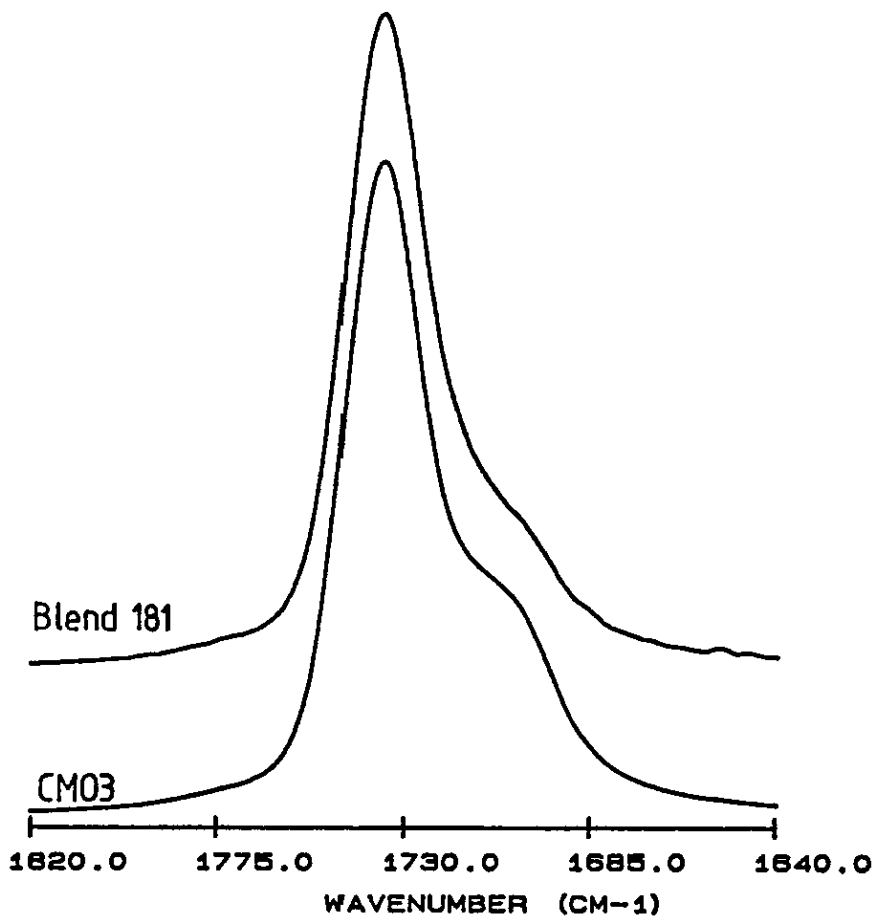
Figure 4.55 DMTA Results for PBA(1) Blends
1:1 Ratio of LF200 : CM03 (Table 4.11)
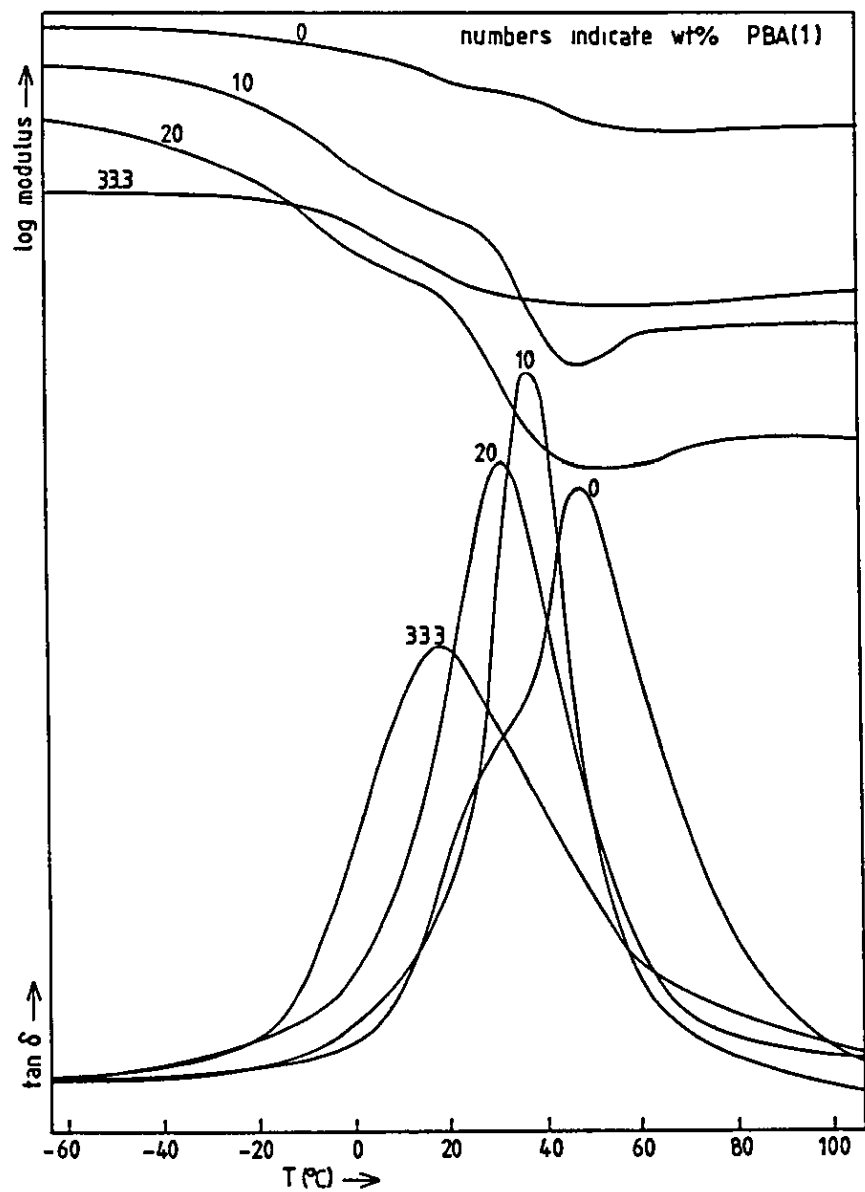
Figure 4.56 DMTA Results for PBA(1) Blends
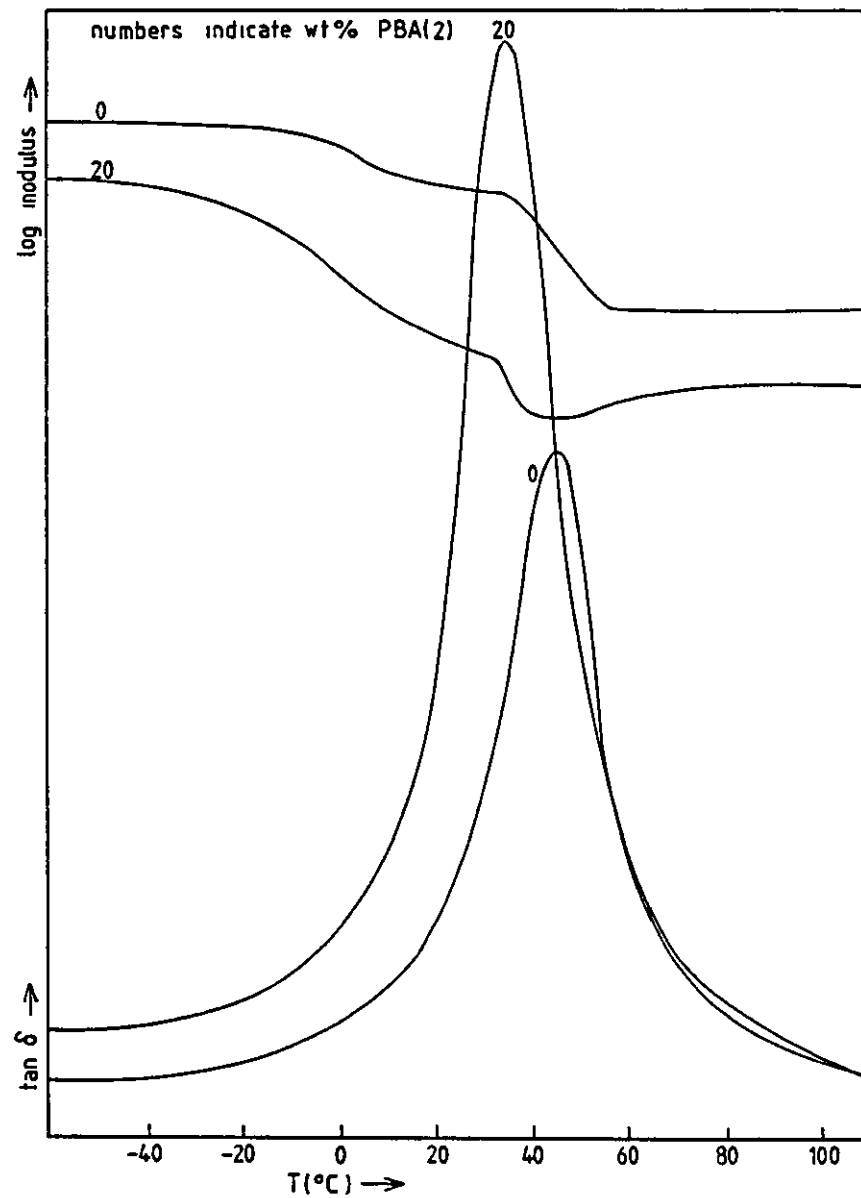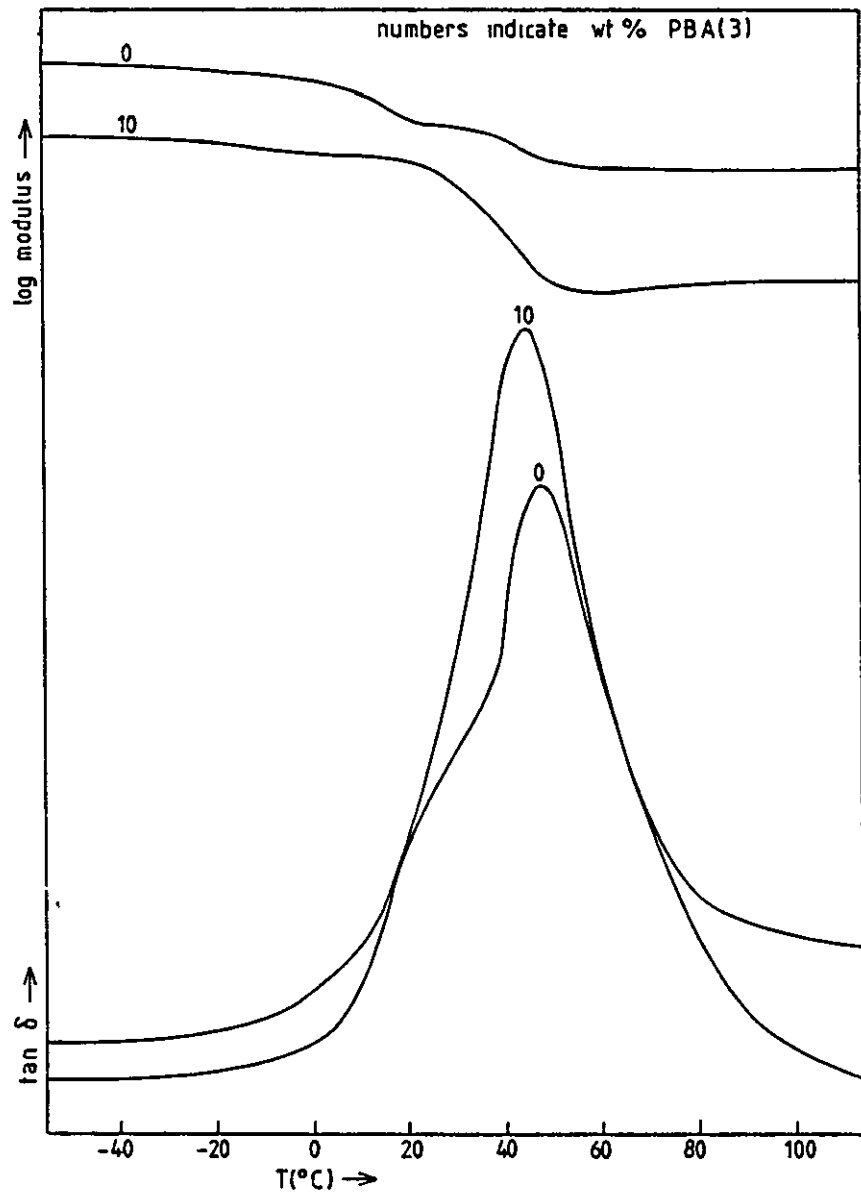3:1 Ratio of LF200 : CM03 (Table 4.11)
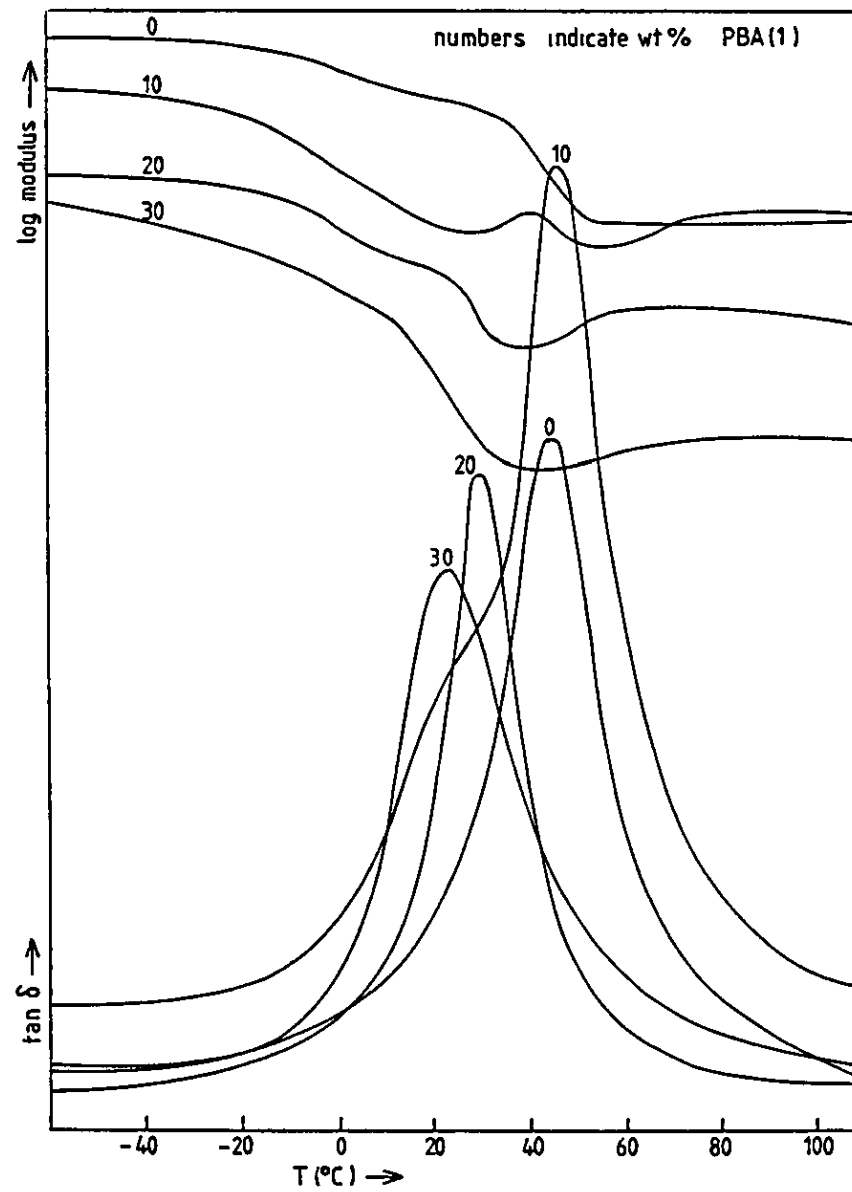
appearing close to the temperature predicted by the rule of mixtures. Figure 4.57 shows the relationship between the experimentally observed Tg values, and those predicted by the Fox and rule of mixtures equations. (2.77 and 4.1 respectively). It is interesting, if not somewhat contradictory, that the log modulus curves corresponding to the blends having narrow $\tan\delta$ peaks, show two falls in value, whilst the log modulus curve corresponding to the blend having a broader $\tan\delta$ curve shows a single sharp fall in value. This is a somewhat unexpected result and the reasons for it are not obvious.

The DMTA results of blends 192, 143 and 155 having a 3:1 ratio of LF200:CM03 are shown in figure 4.56. Again all blends had a translucent film appearance. The blends having 20 and 30% by weight of PBA(1) exhibited single $\tan\delta$ transitions at 29°C and 25°C respectively, each having a narrow transition width. The 10% PBA(1) blend however, showed two unresolved transitions, the main one peaking at 45°C, with an unresolved peak (shoulder) at 20-25°C. The larger peak probably corresponds to overlapping transitions due to unmixed LF200 and CM03 (see 0% PBA(1) curve), whilst the shoulder is due to a mixed phase of PBA(1) with one of the other components, probably LF200, since these two materials show miscibility in binary blends (see section 4.3).

Apart from the isolated result (blend 155), PBA(1) appears to have a similar effectiveness as PPG(1) in enhancing the miscibility of the system. The infrared results proved to be inconclusive in terms of identifying any specific interactions between the blend components. The reason for this has been discussed previously in section 4.6, that is, the difficulty in resolving the carbonyl bands for each of the acrylic-based components of the blend.

Figure 4.57

Effect of PBA(1) Content on the Tg of a Ternary Blend with LF200 and CM03
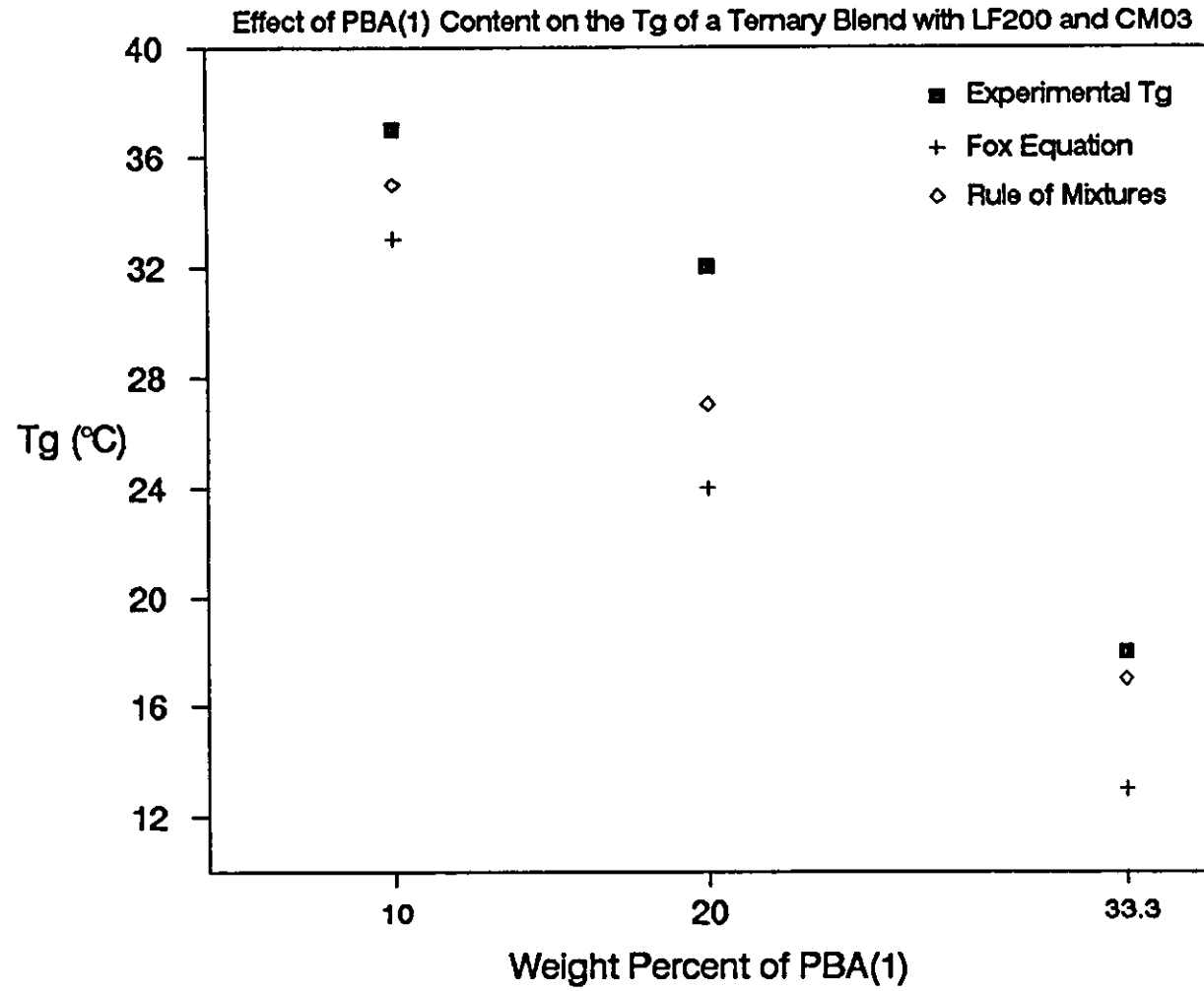
CM03 - PBA(2) - LF200 Blends

Figure 4.58 shows the DMTA plots for the blend having equal proportions by weight of the three components, and figure 4.59 shows the plots for a blend having a 20:20:60 percentage ratio of CM03, PBA and LF200. It appears that the addition of 33.3% PBA(2) to the 50:50 blend of CM03 and LF200 does not improve the overall miscibility of the system, with the observation of two separate tanδ peaks. However, it is possible that a certain amount of mixing has occurred judging by the temperatures at which the peaks occur, although it is not easy to assign these transitions to particular mixed or partially mixed phases.

Figure 4.59 does not provide conclusive evidence for or against miscibility, since the CM03-LF200 blend (0% PBA(2)) gives a single tanδ transition, due to the proximity of the glass transition temperatures of the two polymers. Addition of an overall 20% of PBA(2) still yields a single peak, but it is hard to say whether there has been an overall improvement of the miscibility of the system. It is likely that a certain amount of mixing between the phases exists since no peak due to unmixed PBA(2) can be observed.

CM03 - PBA(3) - LF200 Blends

Figure 4.61 shows the DMTA plots for the blend having a 20:20:60 percentage ratio of the components, compared to the plots for the 25:75 % blend of CM03 and LF200. The results for this blend are very similar to the corresponding PBA(2) blend (figure 4.55) and the same comments apply; that there is some mixing between the PBA(3) and the other two components, but it is unclear whether the overall miscibility has been improved compared to the two component blend.

Figure 4.60 shows the log modulus and tanδ curves for the 50:50 blend of LF200 and CM03 and the ternary blend incorporating 10%

-121-

Figure 4.58   DMTA Results for PBA(2) Blends
1:1 Ratio of LF200 : CM03   (Table 4.11)
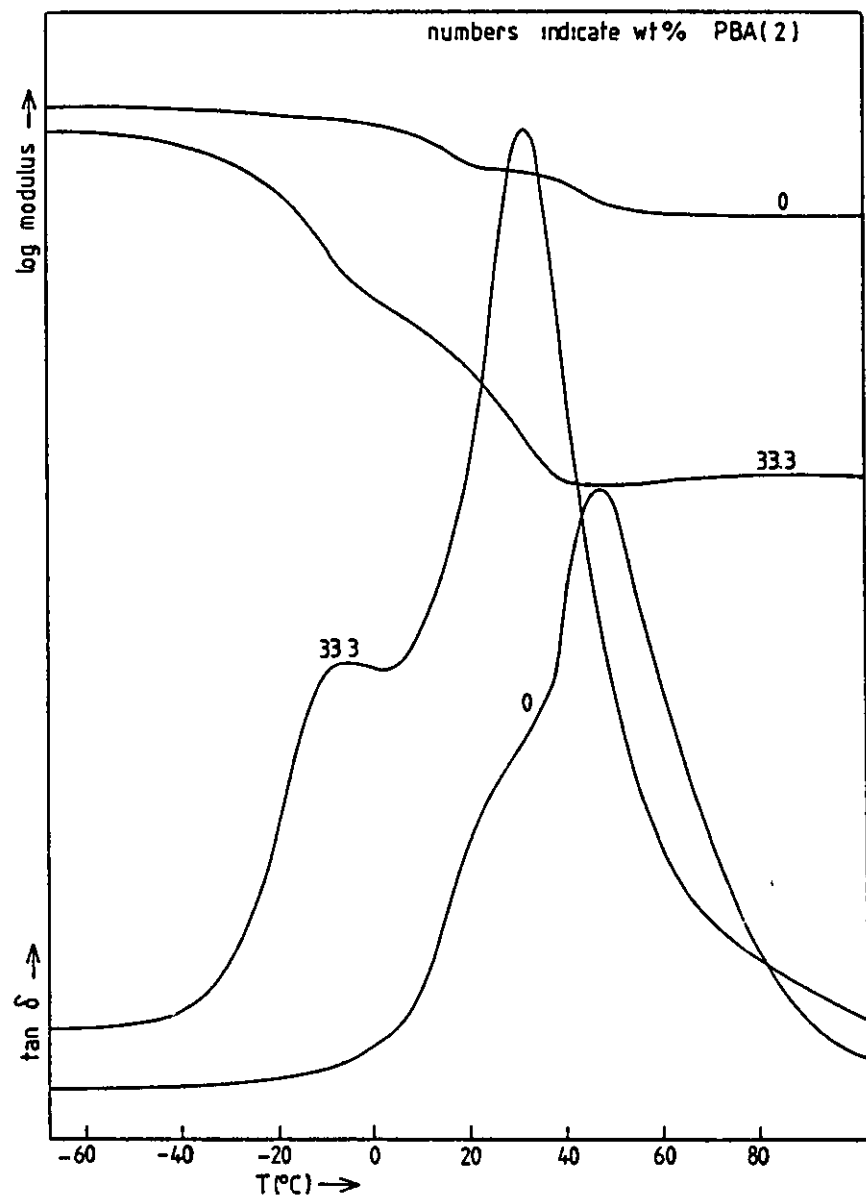
Figure 4.59   DMTA Results for PBA(2) Blends
3:1 Ratio of LF200 : CM03   (Table 4.11)

Figure 4.60   DMTA Results for PBA(3) Blends
1:1 Ratio of LF200 : CM03   (Table 4.11)

numbers indicate wt% PBA(3)

Figure 4.61   DMTA Results for PBA(3) Blends
3:1 Ratio of LF200 : CM03   (Table 4.11)

numbers indicate wt% PBA(3)
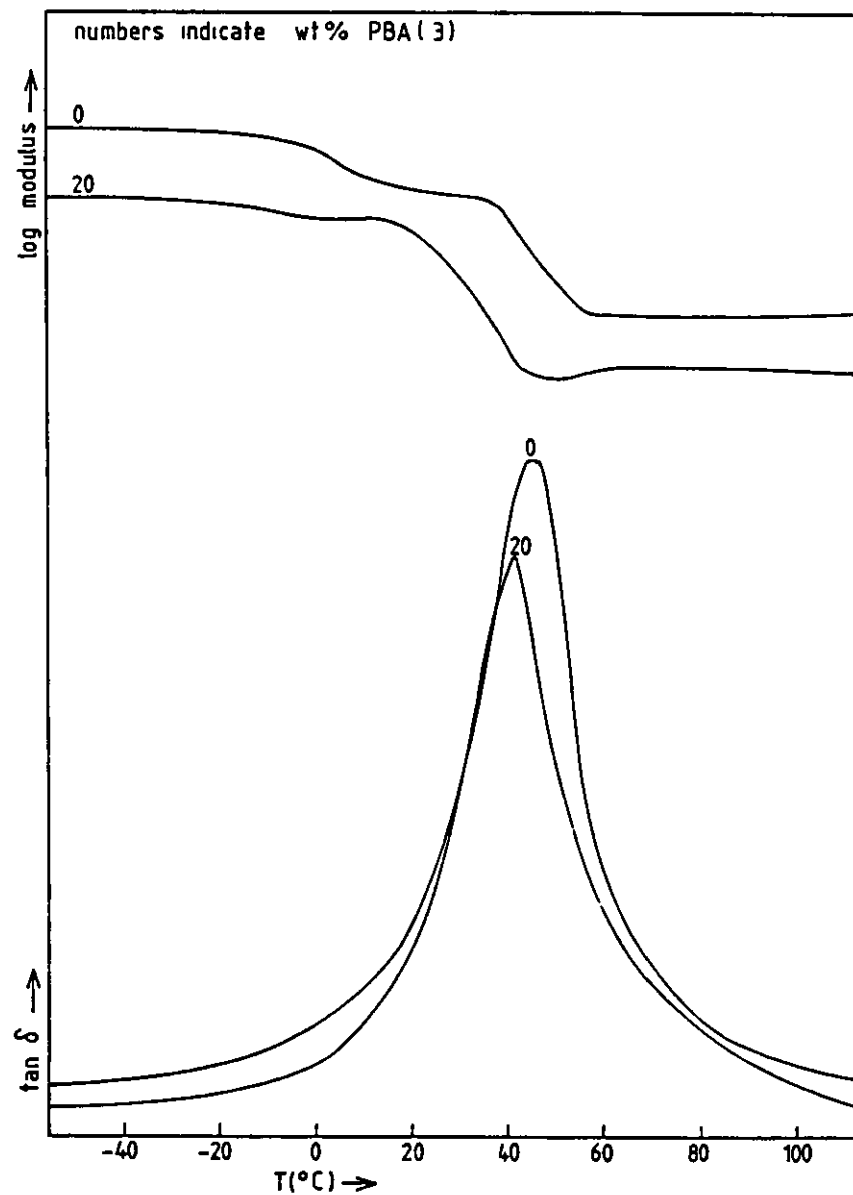
by weight of PBA(3). Both the tan δ and log modulus curves appear to indicate an improvement in miscibility on addition of PBA(3), although the transition still occurs at approximately the same temperature.

The problem caused by the proximity of the Tg transitions of LF200 and CM03 makes it difficult to compare the effect of the molecular weight of the poly(butyl acrylate) on the material's ability to promote miscibility between LF200 and CM03. However, it is fair to say from the results obtained, that there appears to be no significant difference in the miscibility enhancing ability of the three poly(butyl acrylates) used.

CM03 - PPA - LF200

Figures 4.62 and 4.63 appear to indicate that PPA is a poor compatibilising agent for LF200 and CM03, in the two blend proportions employed. In each case, tan δ peaks at sub-zero temperatures indicate unmixed PPA and overall, the tan δ curves appear broader suggesting poor miscibility.

The infrared spectra of the blends showed no peak shifts which might have indicated specific interactions between the blend components.

4.8   Binary 9A/303 Blends

4.8.1 Characterisation of 9A/303

9A/303 differs from CM03 by the inclusion of a fourth monomer, TONE M-100, a caprolactone having an acrylic double bond and an hydroxyl group, which effectively introduces hydroxyl terminated pendant groups into the polymer. The starting proportions of the four monomers in the polymerization are given in section 3.2.

-122-

Figure 4.62 DMTA Results for PPA Blends
1:1 Ratio of LF200 : CM03 (Table 4.11)

numbers indicate wt % PPA

log modulus

0

20

tan δ

0

20

T(°C) ⟶
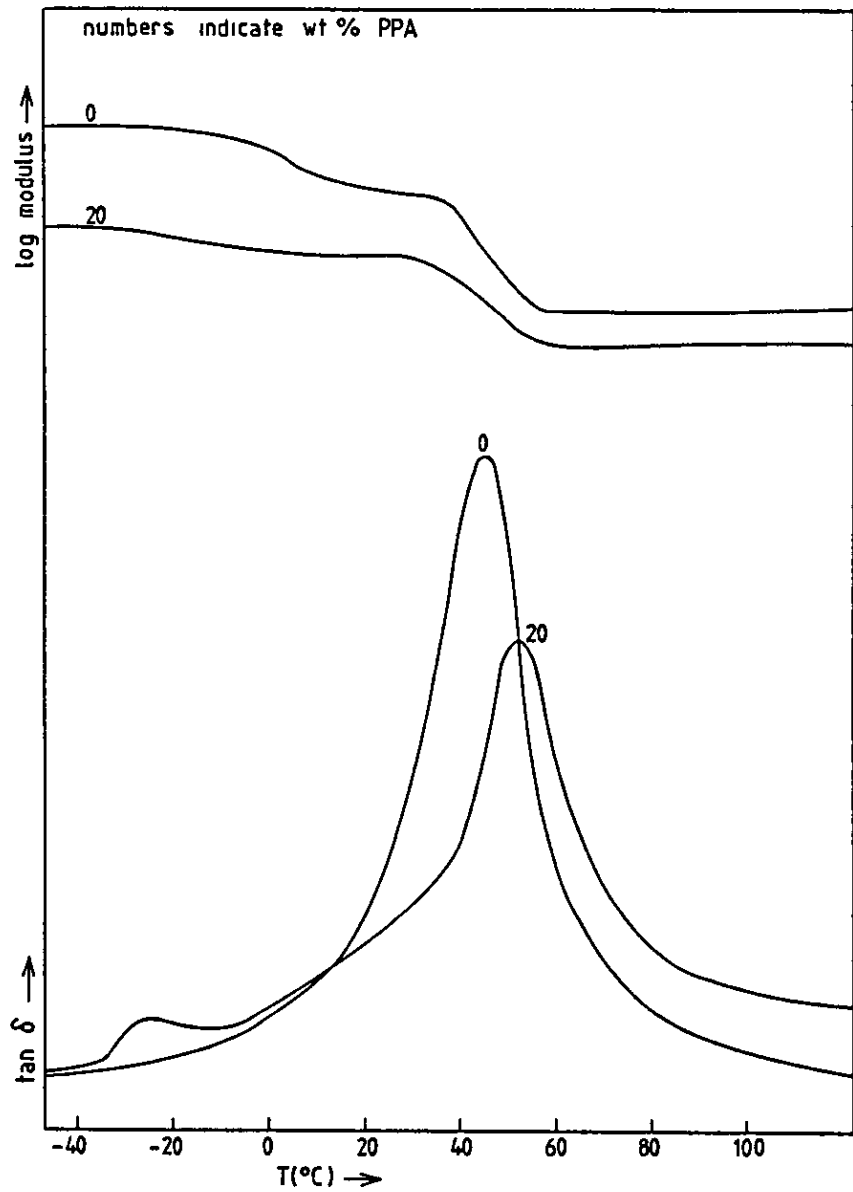
Figure 4.63 DMTA Results for PPA Blends
3:1 Ratio of LF200 : CM03 (Table 4.11)

numbers indicate wt % PPA

log modulus

0

33 3

tan δ

0

33 3

T(°C) ⟶
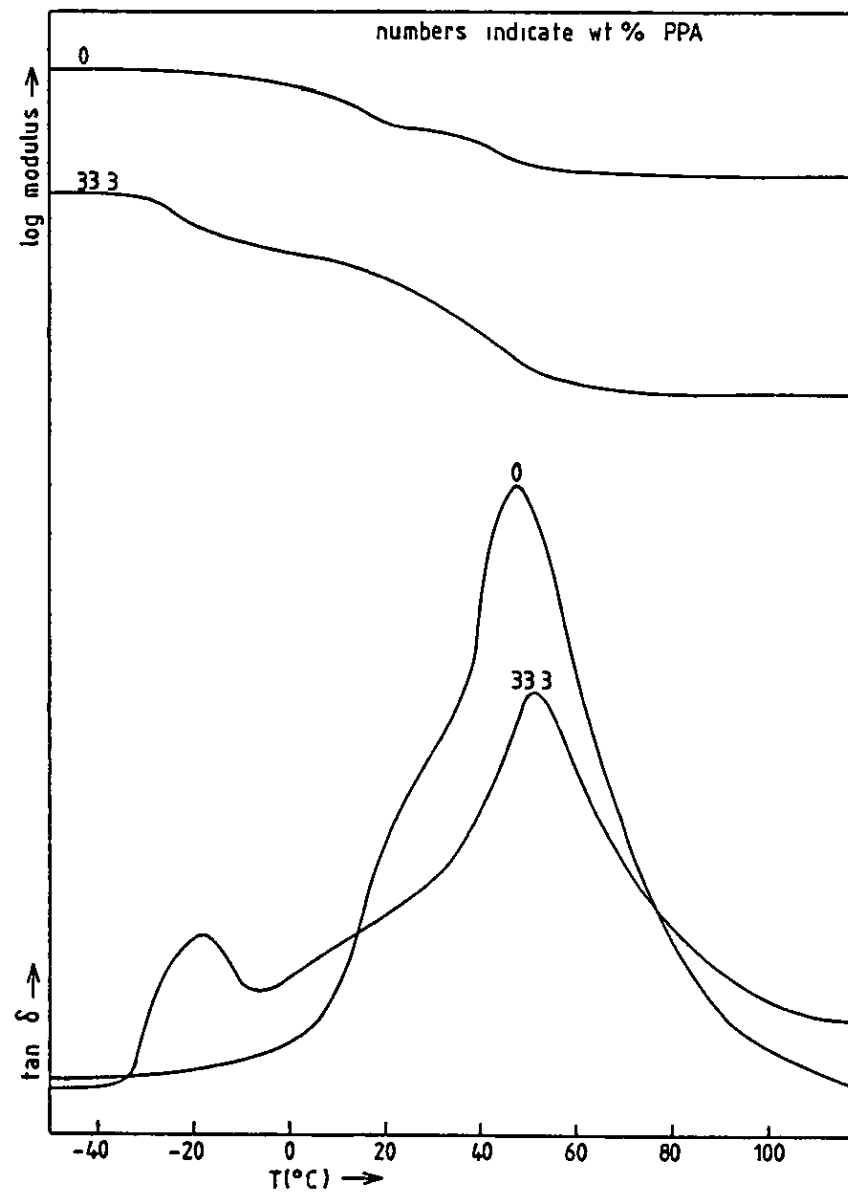
9A/303 was found to have a glass transition temperature of 25°C by DMTA. The polymer was also characterised by GPC, NMR and FTIR, the graphical results being shown in appendices 2, 1 and 3 respectively. The peak molecular weight was found to be 19055 by GPC using a mixed gel column (table 4.2). The shape of the chromatogram peak is probably indicative of the way in which the material was manufactured, and indicates polymer chains having a wide range of molecular weights.

4.8.2 Binary Solution Blends

All of the blends were prepared as described in section 3.3.1 using chloroform as solvent and were studied by DMTA and FTIR with each blend film appearance being noted.

9A/303 - LF200 Blends

Table 4.12 shows the results of DMTA and FTIR analysis of the three 9A/303-LF200 blends, along with the appearance of the blend films. Systems involving 9A/303 rather than CM03 with LF200 have the advantage that there is larger difference between the glass transition temperatures of the two polymers, facilitating study by DMTA. Whereas LF200-CM03 blends show poor separation of the two $\tan \delta$ Tg transitions, the corresponding 9A/303 blends are characterised by two $\tan \delta$ peaks or a definite shoulder in the case of the 50:50 blend. Figure 4.64 illustrates the immiscibility of the two polymers, showing two Tg peaks each for the 25:75 and the 75:25 blends. All three blend compositions formed translucent films, and exhibited no infrared band shifts in a similar way to the corresponding CM03 blends.

It will now be interesting to compare the miscibility of the blends of 9A/303 with the various compatibilisers, to the miscibility

-123-

Table 4.12   2-Component 9A/303 Blends

Product No.	Blend Composition	Film Appearance	DMTA Tg/°C	$W_{h\frac{1}{2}}$	Fox Eqn Tg/°C	Rule of Mixtures	FTIR Result
102	(9A/303)/LF200 25:75	translucent	22,50	-	43	43	no peak shift
101	(9A/303)/LF200 50:50	translucent	47(20)	(44°)	37	37	"
100	(9A/303)/LF200 75:25	translucent	29,50	-	31	31	"
137	(9A/303)/PPG(1) 25:75	translucent	-46,-6	-	-32	-28	carbonyl shift
120	(9A/303)/PPG(1) 50:50	translucent	-19	34°	-15	-11	"
136	(9A/303)/PPG(1) 75:25	translucent	4	34°	3	7	"
180	(9A/303)/PPG(2) 25:75	transparent	-44	36°	-36	-32	"
168	(9A/303)/PPG(2) 50:50	transparent	-19	17°	-19	-13	"
169	(9A/303)/PPG(2) 75:25	transparent	0	18°	2	6	"
135	(9A/303)/PBA(1) 25:75	transparent	-32,21	-	-21	-19	incon-clusive
133	(9A/303)/PBA(1) 50:50	translucent	-33,22	-	-7	-4	"
134	(9A/303)/PBA(1) 75:25	translucent	22 (-35)	(21°)	8	11	"
174	(9A/303)/PBA(2) 25:75	translucent	-27,14	-	-13	-12	"
175	(9A/303)/PBA(2) 50:50	translucent	-26,17 43	-	-2	1	"
171	(9A/303)/PBA(2) 75:25	translucent	-26,26	-	11	13	"

Table 4.12 (continued) 2-Component 9A/303 Blends

Product No.	Blend Composition	Film Appearance	DMTA Tg/°C	$W_{n_{\frac{1}{2}}}$	Fox Eqn Tg/°C	Rule of Mixtures	FTIR Result
248	(9A/303)/PBA(3) 50:50	translucent	-32,35	-	-3	-1	incon-clusive
249	(9A/303)/PBA(3) 75:25	translucent	-35,41	-	10	12	"
236	(9A/303)/PPA 50:50	translucent	-20,32	-	0	2	no peak shifts
254	(9A/303)/163 25:75	opaque	35,112	-	88	93	incon-clusive
255	(9A/303)/163 50:50	opaque	30,113	-	64	70	"
256	(9A/303)/163 75:25	opaque	30,114	-	43	48	"

Figure 4.64

DMTA Results for 9A\303 - LF200 Blends
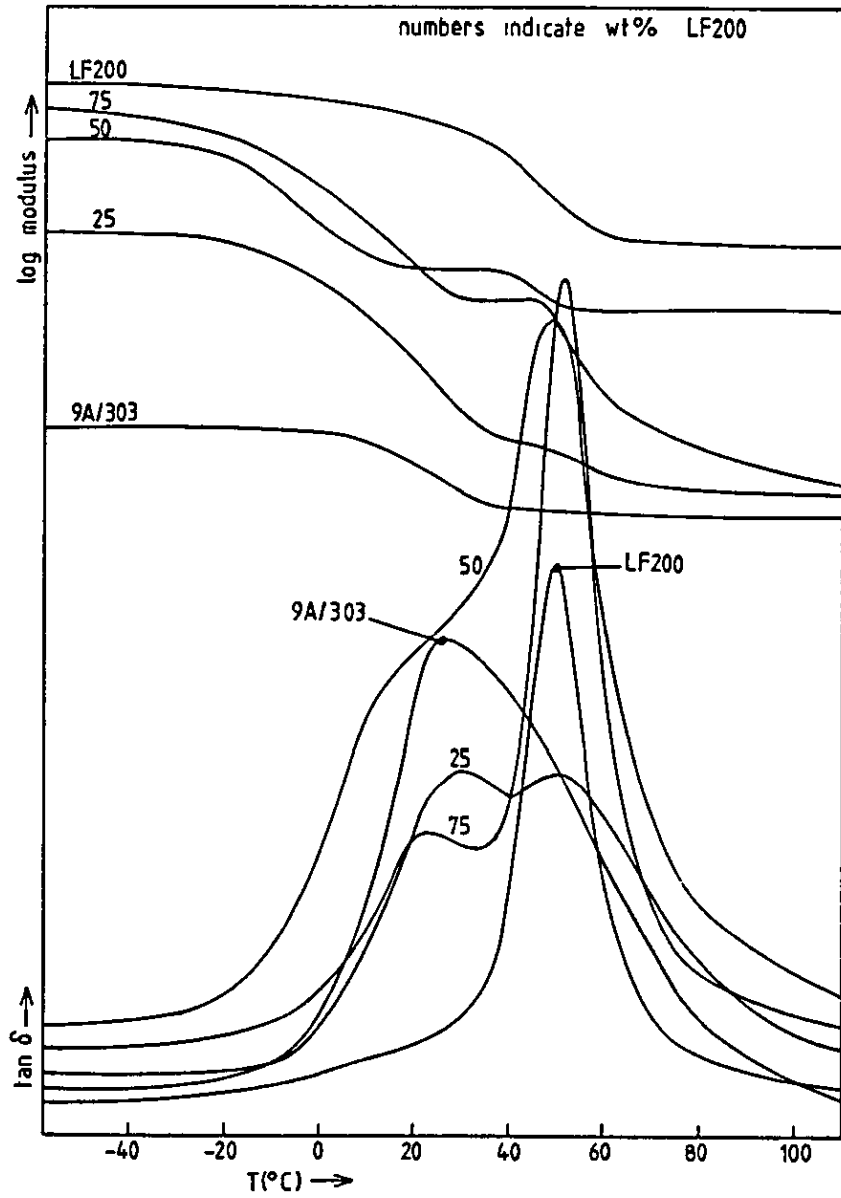
of the corresponding CM03 blends, to see if there is any significant difference between the behaviour of the two acrylic polymers.

9A/303 - PPG(1) Blends

Table 4.12 summarises the results of the analyses of the three blend compositions, whilst figure 4.65 shows the DMTA plots for the 25% PPG(1) blend. Both the 50% and 25% PPG(1) blends clearly exhibit single tan δ transitions characteristic of single mixed phases. The temperatures at which the transitions occur in each case are close to the temperature predicted by the rule of mixtures and the Fox equation. The blend containing 75% PPG(1) does, however, show two separate glass transitions. The temperatures at which the tan δ

peaks occur tend to suggest residual unmixed PPG(1), giving a transition at -46°C and, a mixed phase of 9A/303 and PPG(1) at -6°C. It does seem likely that some mixing of the two polymers has occurred. Comparing these observations to those for the CM03-PPG(1) blends discussed in the previous section, it appears that CM03 and 9A/303 mix to a similar extent with the PPG(1) each showing two miscible blends and one partially miscible blend, as indicated by the DMTA results.

Infrared analysis of the blends indicated a similar carbonyl band shift as had been observed for the CM03 blends. Presumably, the reason for this shift is the same, that is, the presence of a hydrogen bonding interaction between the carboxylic acid component of the 9A/303 and the ether oxygen of the polyether. This interaction is illustrated in figure 4.67 by the decrease in the size of the carbonyl band at around 1700 cm^{-1}, as the proportion of PPG(1) increases. As has been discussed earlier, this is due to a decrease in the proportion of carboxylic acid dimers present, corresponding to

Figure 4.65
DMTA Results for 9A\303 – PPG(1) Blends (Table 4.12)
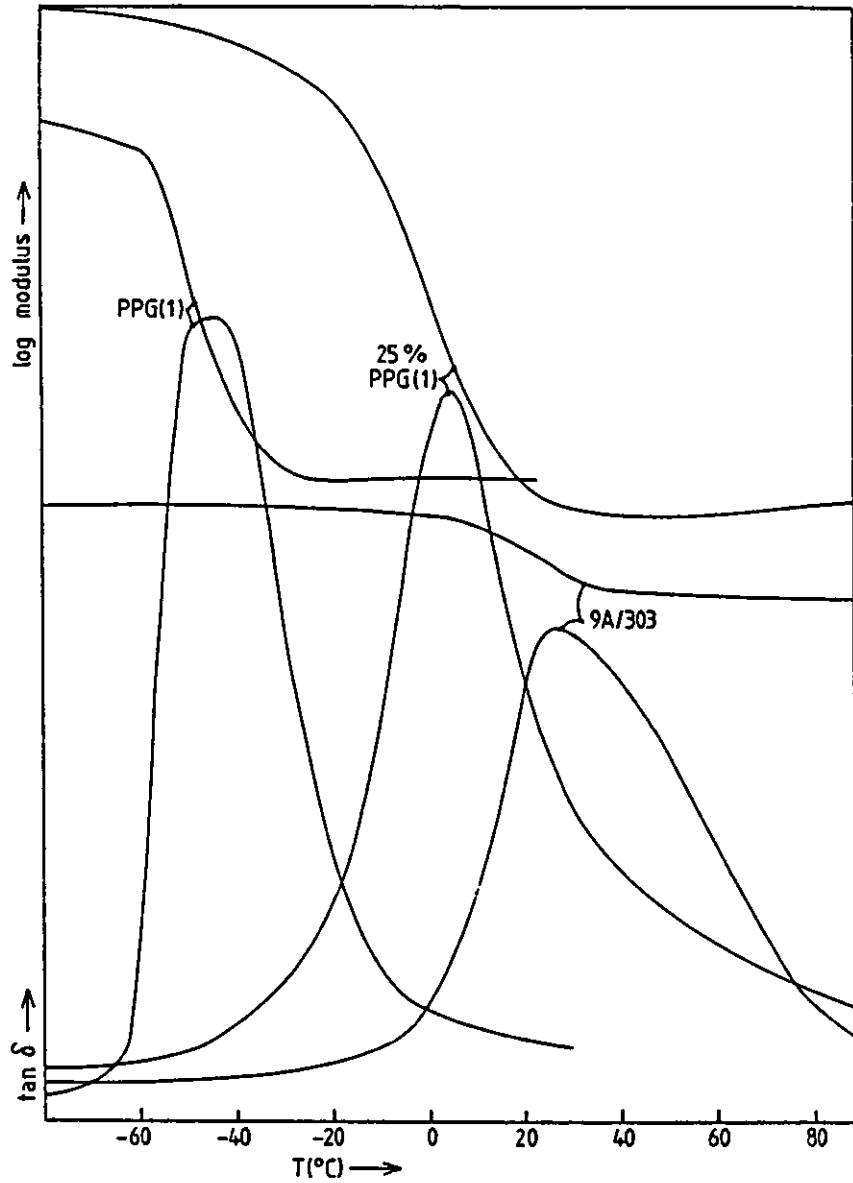
Figure 4.66
DMTA Results for 9A\303 – PPG(2) Blends (Table 4.12)
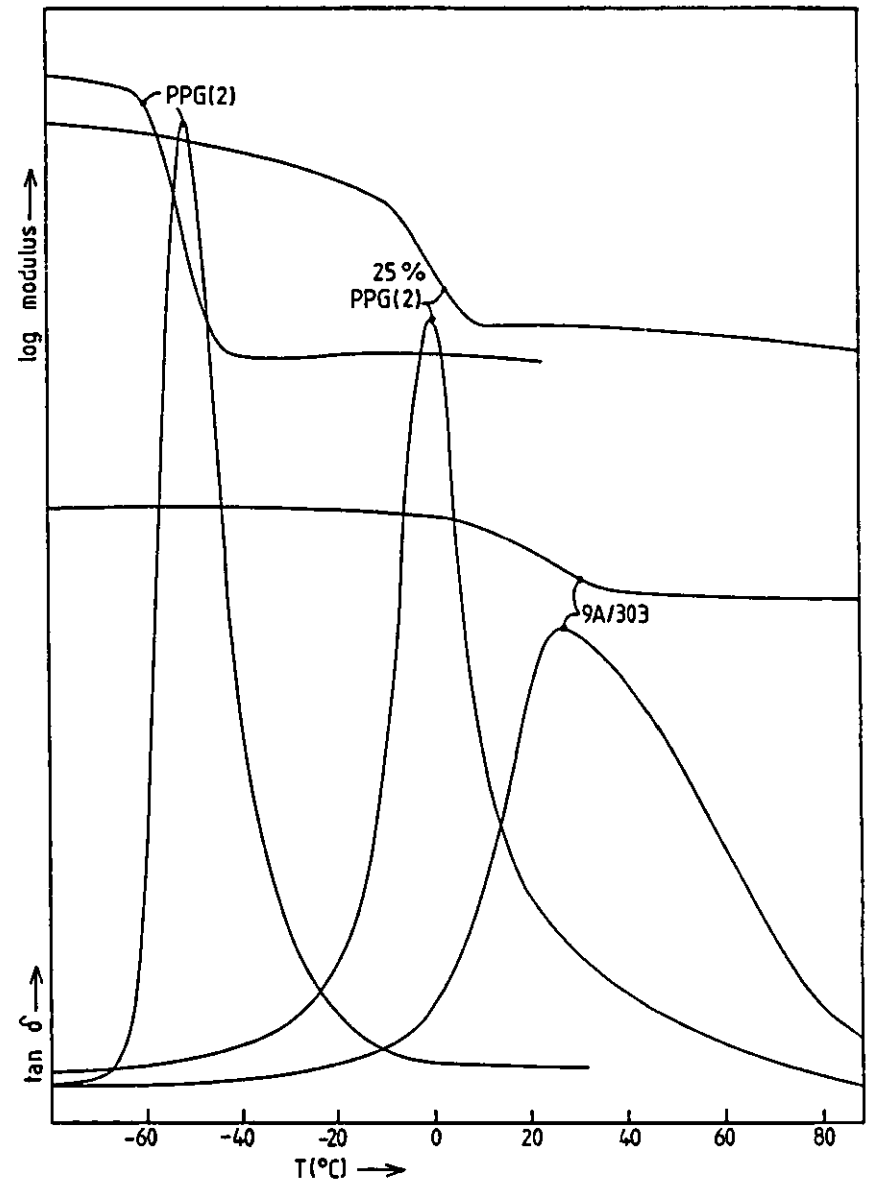
Figure 4.67
The Infrared Carbonyl Band for
9A/303 – PPG(1) Blends (Table 4.12)
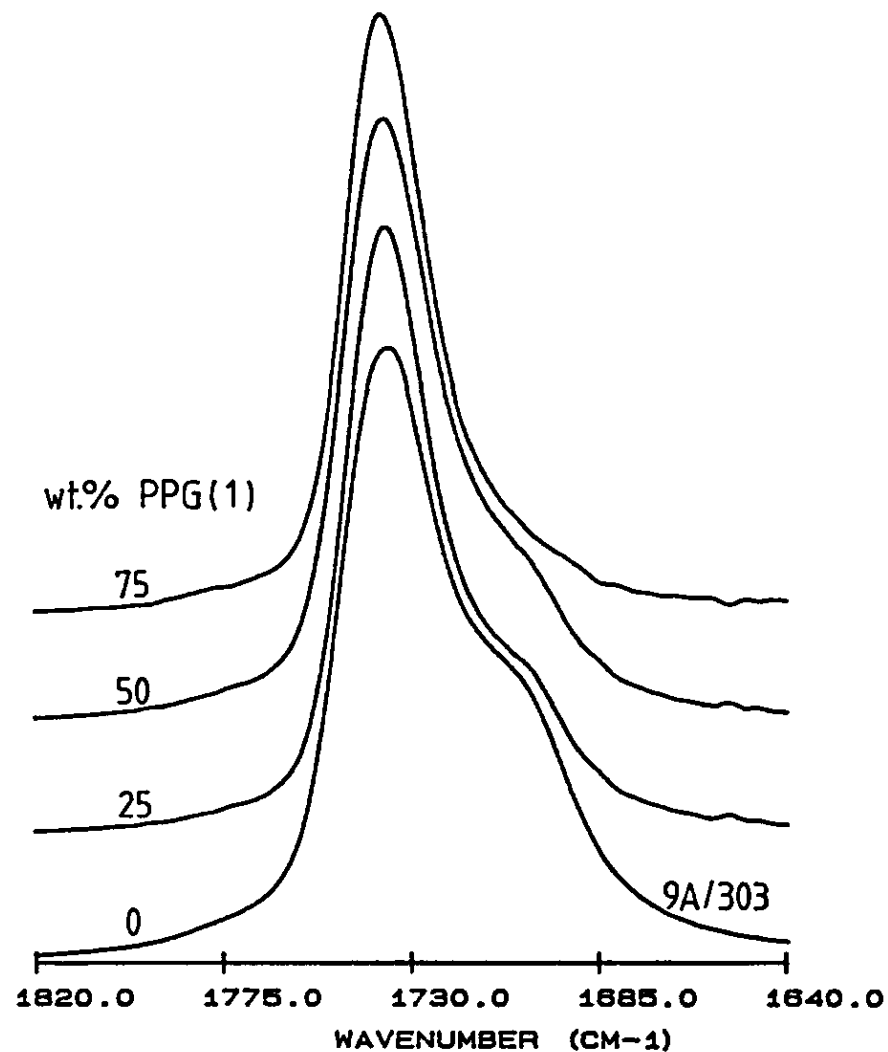
Figure 4.68
The Infrared Carbonyl Band for
9A/303 – PPG(2) Blends (Table 4.12)
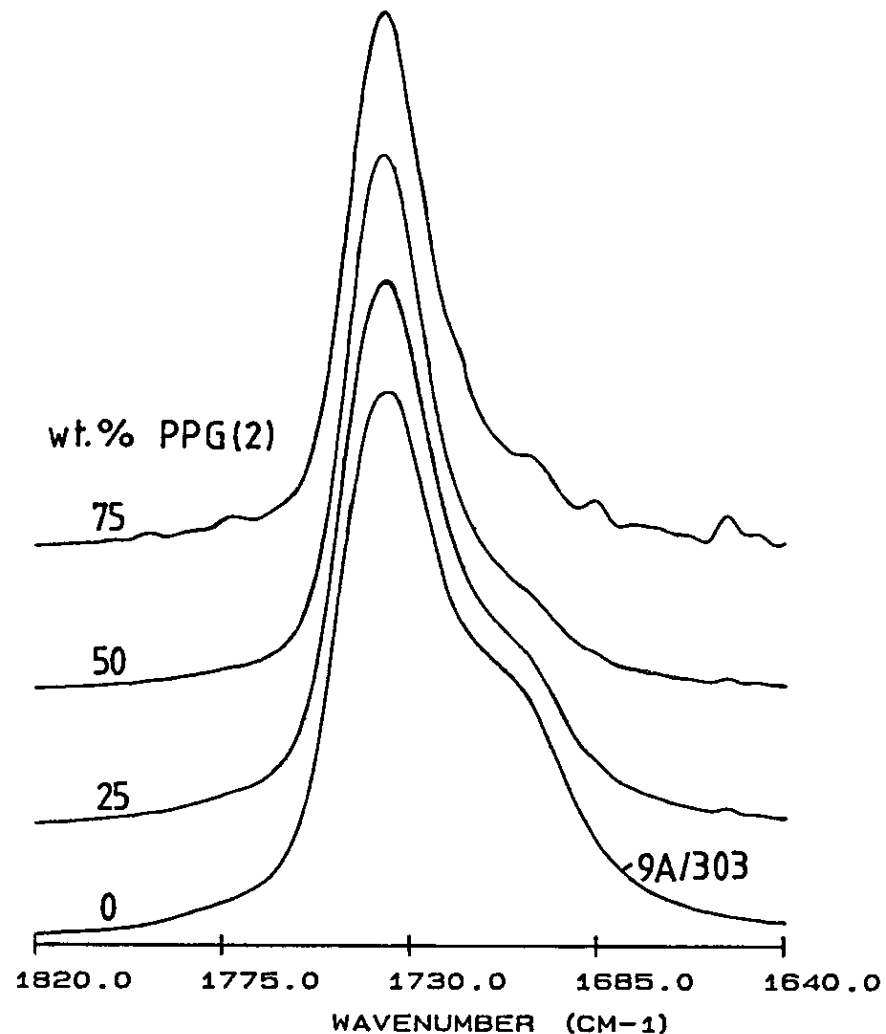
an increase in intermolecular hydrogen bonded carboxylic acid groups, which appear at around 1730 cm^{-1} in the spectrum.

9A/303 - PPG(2) Blends

The DMTA results for the three blend compositions are detailed in table 4.12, with figure 4.66 showing the plots for the 25% PPG(2) blend. All three blends exhibited single glass transitions indicating a good degree of miscibility for this system, with the 50 and 25% PPG(2) blends having particularly narrow tan δ peak widths.

The infrared results are very similar to those obtained for the corresponding PPG(1) blends, as would be expected, and need not be discussed further. Figure 4.68 shows the carbonyl peaks for the three blends compared to that of pure 9A/303.

There seems to be little difference between the results for these blends compared to the corresponding CM03 blends, both giving transparent blend films and single glass transitions. If anything, the 9A/303 blends show narrower tan δ peak widths, but this is a minor point.

9A/303 - PBA(1) Blends

The DMTA results as shown in table 4.12 indicate that PBA(1) is not miscible with 9A/303 in the proportions tried. The blends having 75 and 50% by weight of PBA(1) both exhibit two glass transitions, whilst the blend having 25% PBA(1) has a small second tan δ peak or shoulder at -35°C. (figure 4.69).

The DMTA results for this blend are similar to those for the corresponding CM03 system with the exception that the 25:75 PBA(1) - CM03 blend yielded a single tan δ transition. It seems, therefore, that 9A/303 is slightly less miscible with PBA(1) than CM03.

The infrared spectra of the three blends do not yield any

Figure 4.69
DMTA Results for 9A\303 – PBA(1) Blends (Table 4.12)
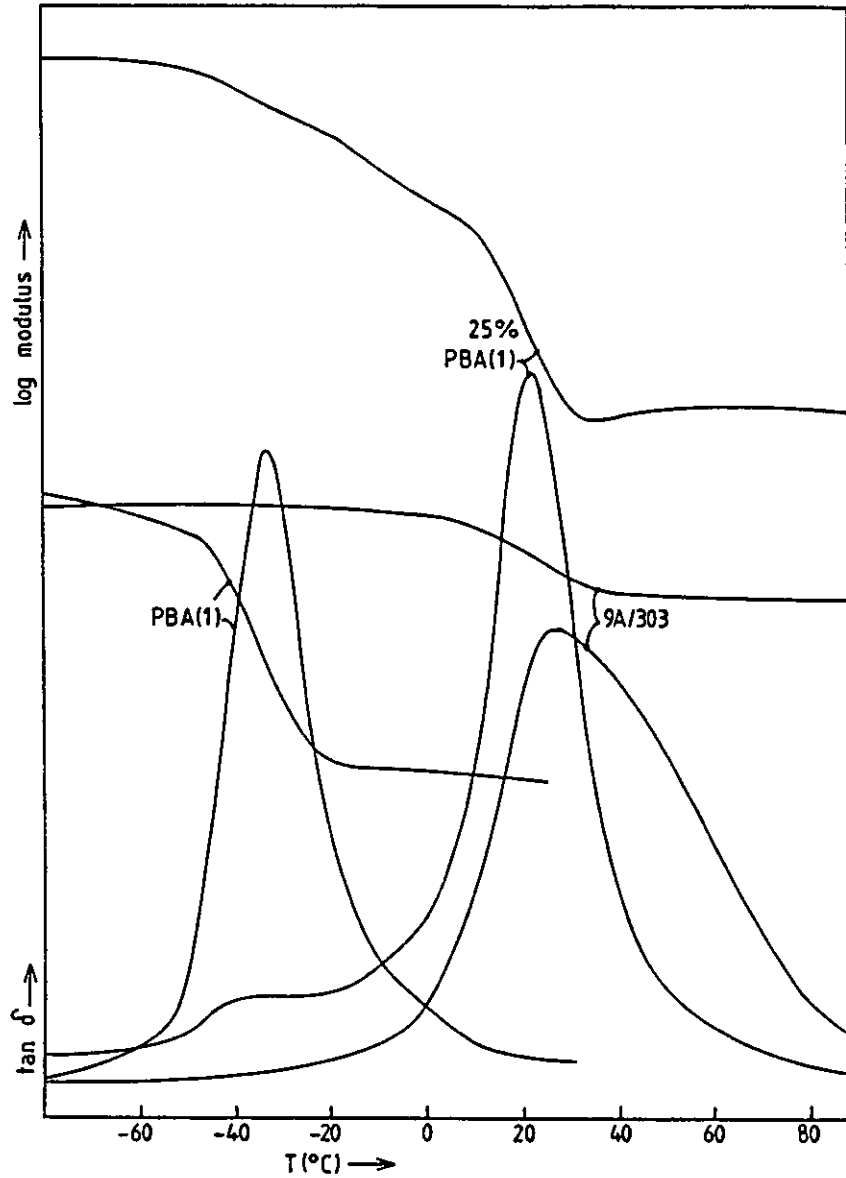
Figure 4.70
DMTA Results for 9A/303 – PBA(2) Blends (Table 4.12)
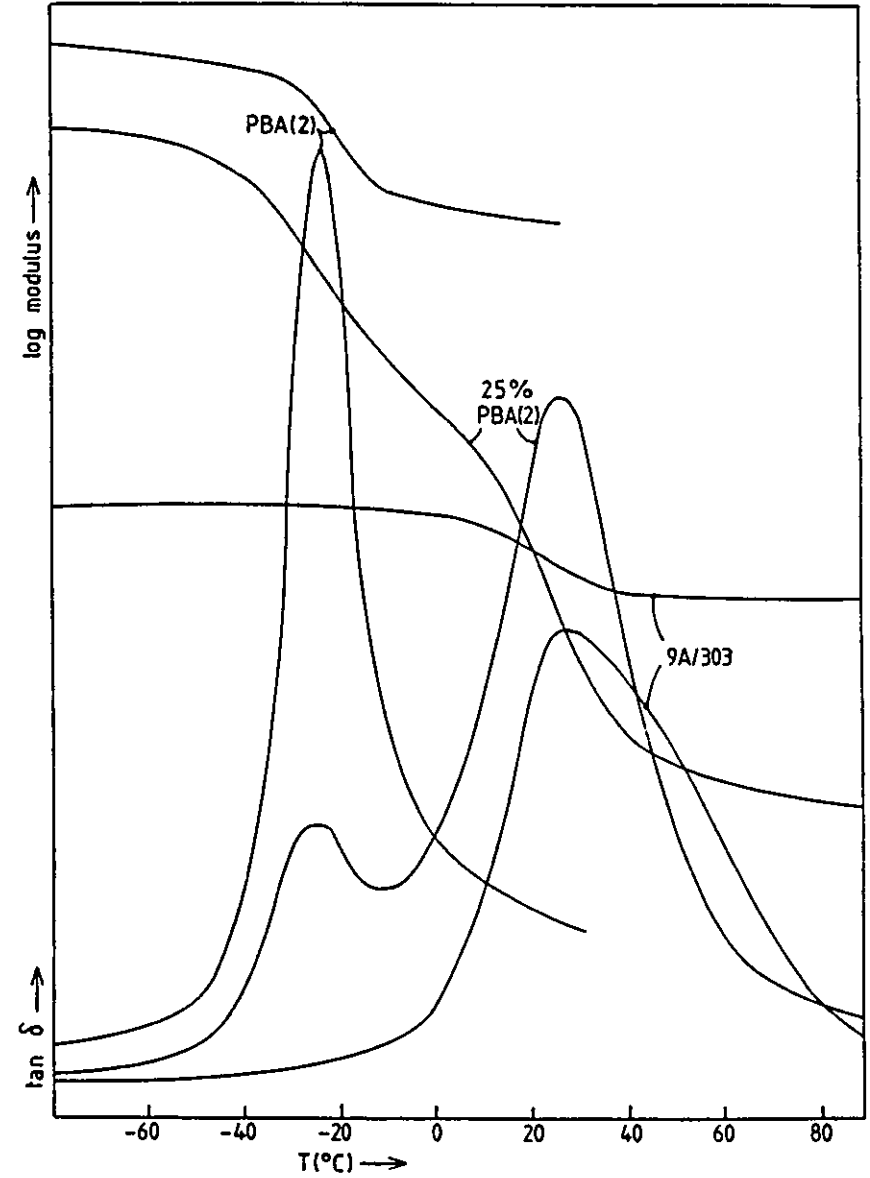
information about the presence of specific interactions, because of the complex nature of the carbonyl band, being made up of several groups of the different acrylic and methacrylic units within the system.

9A/303 - PBA(2) Blends

The DMTA results given in table 4.12 and the plots shown in figure 4.70, clearly show that these two polymers are also immiscible, as were the PBA(1) blends. The compositions having 25 and 75% by weight of PBA(2) each gave two well separated glass transitions. The 50% blend, did however, show a third peak intermediate between the other two, perhaps indicating some extent of mixing between the components. These observations are again similar to those for the CMO3 PBA(2) system.

It is clear from these results that poly(propylene glycol) is more miscible with both CMO3 and 9A/303 than either PBA(1) or PBA(2). It also appears that PPG(2) ($\bar{M}$n:2770) is slightly more miscible with 9A/303 than PPG(1) ($\bar{M}$n:9500).

9A/303 - PBA(3) Blends

From the results of the blends of 9A/303 with PBA(1) and PBA(1) it is of no surprise that PBA(3) is also immiscible with 9A/303. It also seems that the molecular weight (table 4.2) of the poly(butyl acrylate) has no effect on the miscibility of the system.

9A/303 - PPA Blends

The 50:50 blend yielded two glass transitions by DMTA and was clearly immiscible. The same was true for the corresponding CMO3 blend. Again, no band shifts were observed by FTIR.

9A/303 - ST/MAA Copolymer 163 Blends

The results for this blend are very similar to those obtained for the corresponding CM03 blend, that is, that the blend is immiscible in all proportions, exhibiting two glass transitions and opaque blend films. The FTIR analysis again proved to be inconclusive for the same reason mentioned before.

4.9 Ternary 9A/303 Blends

Table 4.13 shows the results of the DMTA and infrared analysis of the various ternary 9A/303 blends, some of which are shown pictorially in figure 4.71 and onwards. Each blend system will now be discussed in turn and compared to the corresponding CM03 blends where appropriate.

9A/303 - PPG(1) - LF200 Blends

Six blends were prepared in all, three having a 1:1 ratio of 9A/303 and LF200, and three having a 1:3 ratio. Figure 4.71 is an illustration of the DMTA results for the first three blends, 140, 159 and 161. It can be clearly seen that the 50:50 blend of 9A/303 and LF200 exhibits a large shoulder on the main $\tan \delta$ peak, indicating immiscibility. It is equally apparent that incorporation of 10, 20 and 33.3% PPG(1) into the system leads to the appearance of single $\tan \delta$ Tg peak suggesting a considerable improvement in miscibility. The blend having 10% PPG(1) has the narrowest $\tan \delta$ transition with a width at half-height of 32°. The 33.3% PPG(1) peak is noticeably broader with a slight shoulder at around 30°C, probably due to an extent of partial or incomplete miscibility. The temperatures at which the transitions occur are in each case quite close to those predicted by the Fox equation (2.77) and the rule of mixtures (4.1),

Table 4.13 3-Component 9A/303 Blends

Product No.	Blend Composition	Film Appearance	DMTA Tg/°C	W_{m2}^{-1}	Fox Eqn Tg/°C	Rule of Mixtures	FTIR Result
140	9A/303/PPG(1)/LF200 33.3 :33.3 :33.3	translucent	2	52°	3	9	carbonyl shifts
159	9A/303/PPG(1)/LF200 40 : 20 : 40	translucent	22	45°	16	20	"
161	9A/303/PPG(1)/LF200 45 : 10 : 45	translucent	31	32°	29	22	"
189	9A/303/PPG(1)/LF200 17.5 : 30 : 52.5	translucent	14	58°	10	16	"
142	9A/303/PPG(1)/LF200 20 : 20 : 60	translucent	19	26°	20	25	"
156	9A/303/PPG(1)/LF200 22.5 : 10 : 67.5	translucent	35	35°	31	34	"
183	9A/303/PPG(2)/LF200 33.3 : 33.3 :33.3	translucent	24	25°	1	8	"
184	9A/303/PPG(2)/LF200 20 : 20 : 60	translucent	24	23°	18	24	"
139	9A/303/PBA(1)/LF200 33.3 :33.3 :33.3	translucent	20	37°	14	9	inconclusive
160	9A/303/PBA(1)/LF200 40 : 20 : 40	translucent	26	49°	20	23	"
162	9A/303/PBA(1)/LF200 45 : 10 : 45	translucent	36	38°	28	30	"
190	9A/303/PBA(1)/LF200 17.5 : 30 : 52.5	translucent	24	22°	15	20	"
144	9A/303/PBA(1)/LF200 20 : 20 : 60	translucent	31	24°	24	28	"
157	9A/303/PBA(1)/LF200 22.5 : 10 :67.5	translucent	40	32°	33	35	"

Table 4.13 (continued) 3-Component 9A/303 Blends

Product No.	Blend Composition	Film Appearance	DMTA $T_g/°C$	$W_{\frac{1}{2}}$	Fox Eqn $T_g/°C$	Rule of Mixtures	FTIR Result
187	9A/303/PBA(2)/LF200 33.3 : 33.3 :33.3	translucent	(0),30	40°	13	17	inconclusive
188	9A/303/PBA(2)/LF200 20 : 20 :60	translucent	33	22°	27	30	"
252	9A/303/PBA(3)/LF200 33.3 : 33.3 :33.3	translucent	38	40°	29	31	"
253	9A/303/PBA(3)/LF200 20 : 20 : 60	translucent	38	28°	26	29	"
240	9A/303/PPA/LF200 20 :20: 60	translucent	-20,25, 51	-	27	30	no peak shift
241	9A/303/PPA/LF200 33.3 :33.3:33.3	translucent	-20,51	-	15	18	"

Figure 4.71   DMTA Results for PPG(1) Blends
1:1 Ratio of LF200 : 9A/303   (Table 4.13)
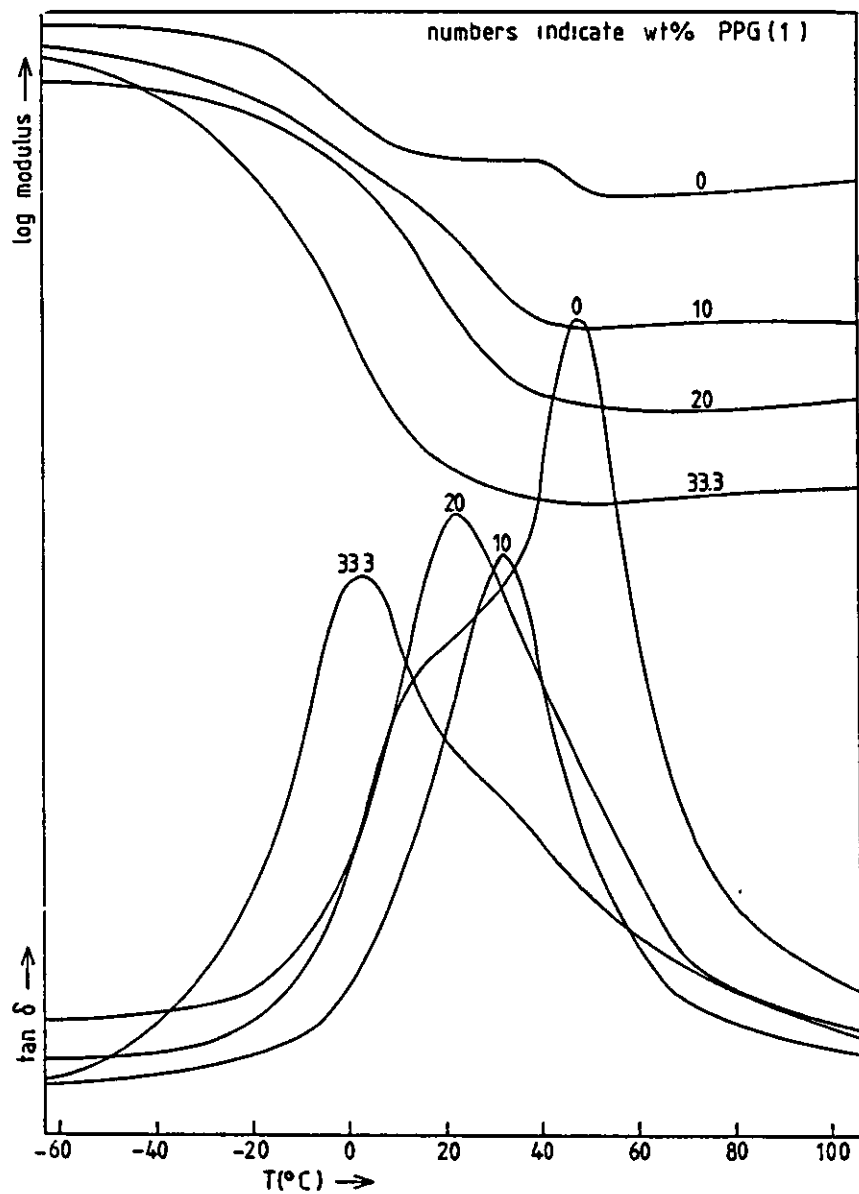
Figure 4.72   DMTA Results for PPG(1) Blends
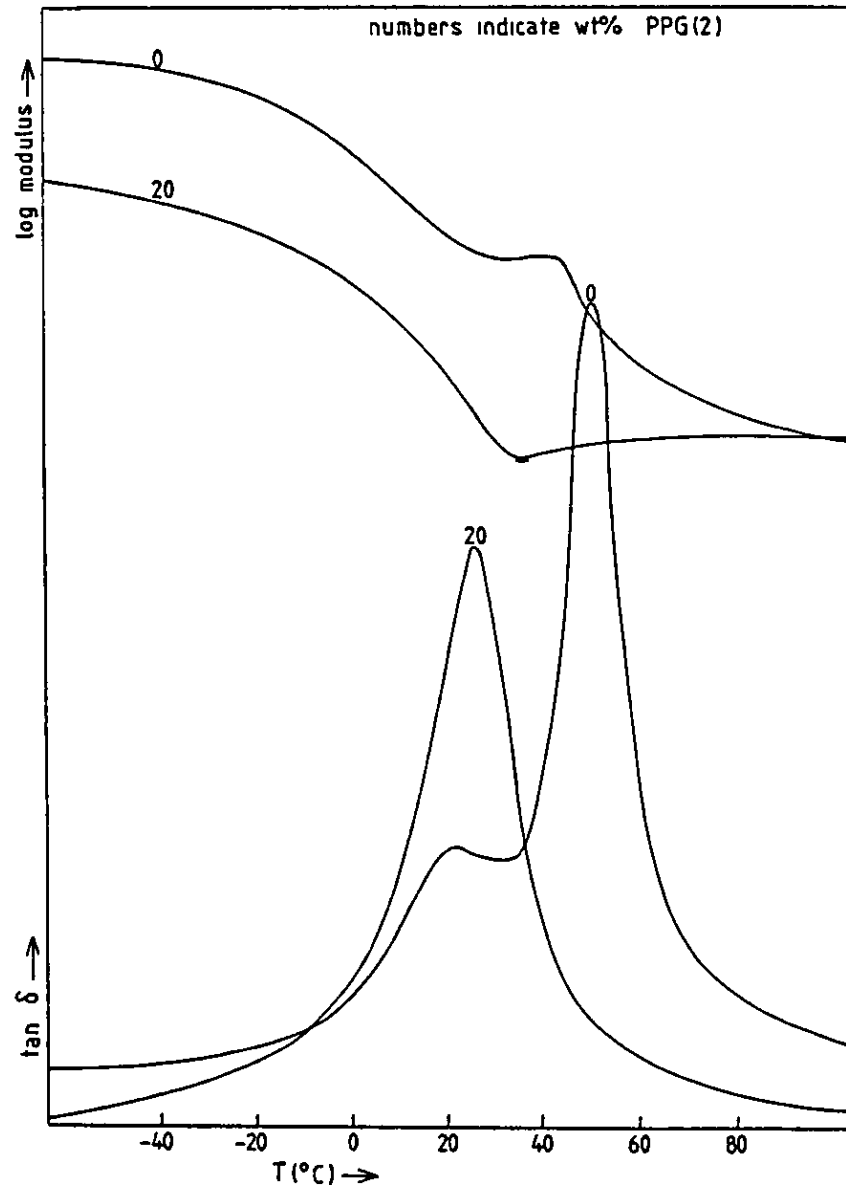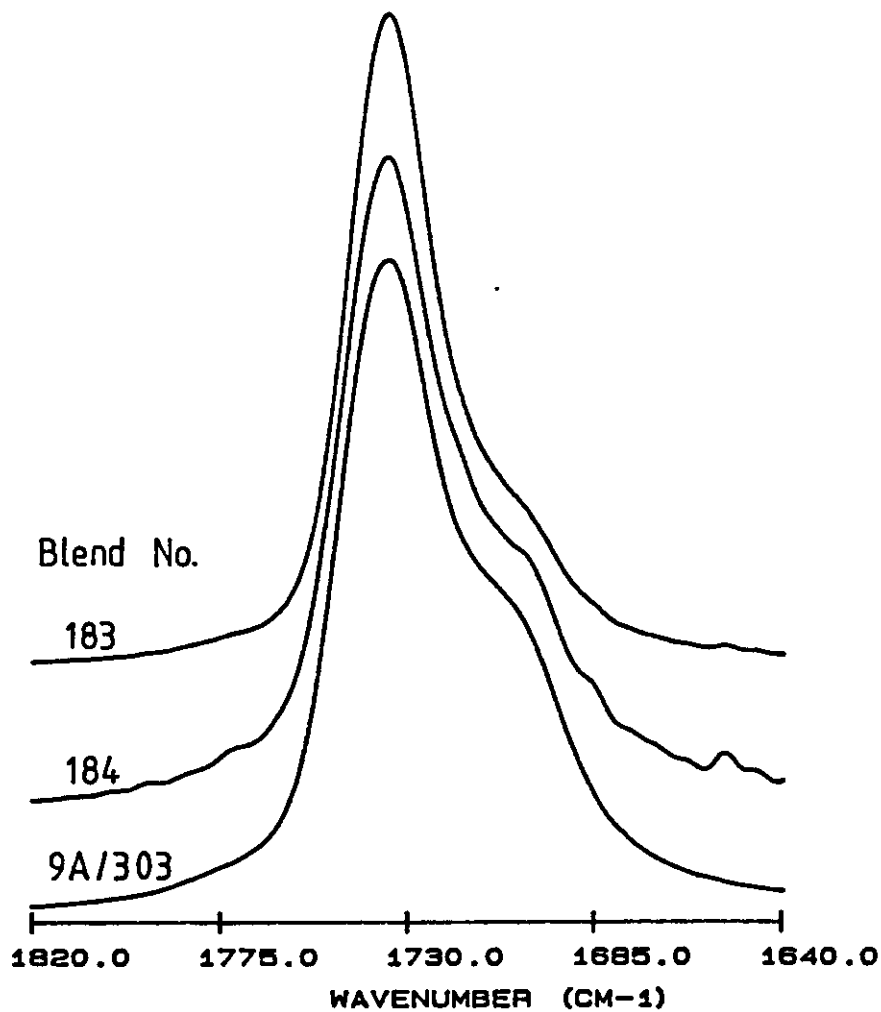3:1 Ratio of LF200 : 9A/303   (Table 4.13)
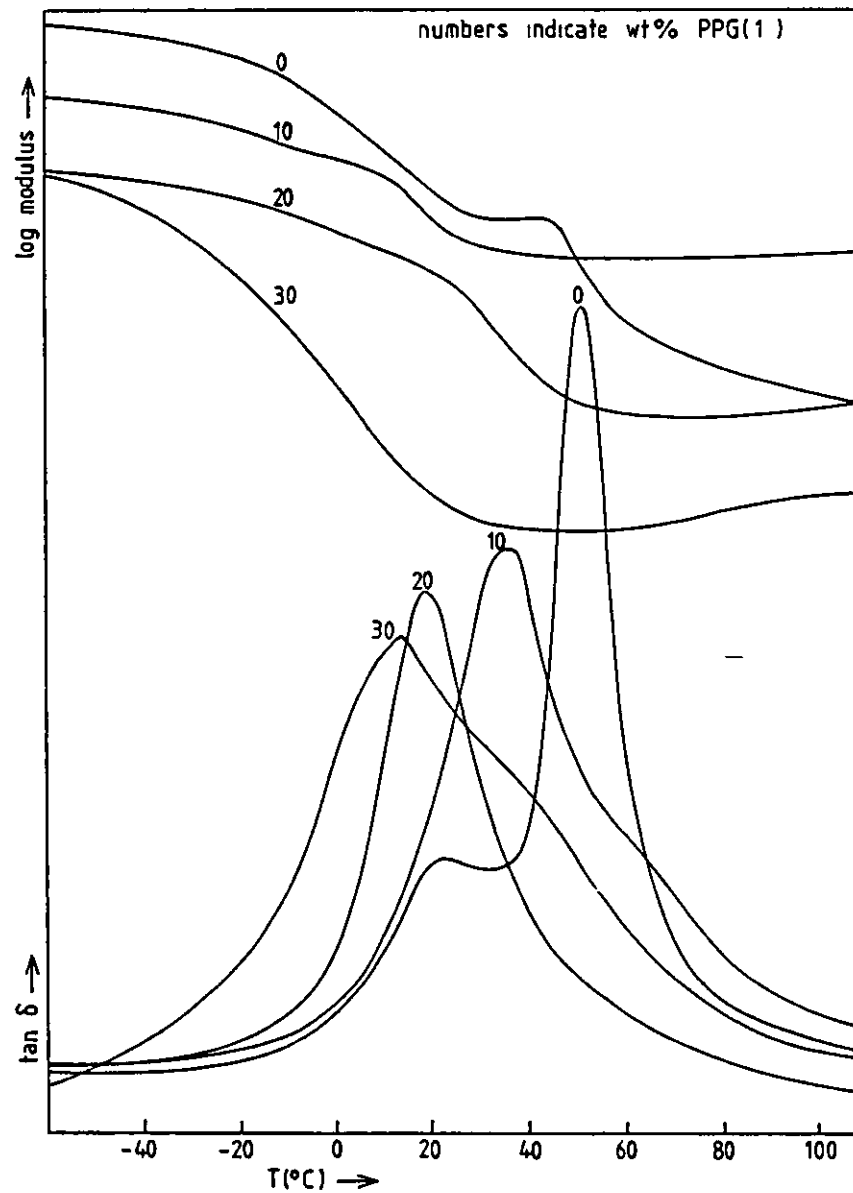
sometimes one equation giving a closer prediction, sometimes than the other. This is illustrated graphically in figure 4.73.

Figure 4.72 shows the DMTA results for the blends having a 1:3 ratio of 9A/303 to LF200. The immiscibility of LF200 and 9A/303 is even more clearly indicated by the tan δ curve of the blend containing 0% PPG(1), showing two peaks relating to the two individual glass transitions. In this ternary system, it is the blend containing 20% PPG(1) which has the narrower tanδ peak, with a half height width of 26°. It is therefore, this blend proportion which appears to produce the greatest extent of miscibility between the components. Both the blend containing 10% PPG(1) and the blend containing 30% PPG(1) have peaks which appear to have unresolved "shoulders", perhaps relating to a lesser extent of mixing between two or more of the components. It is difficult to say very much about the extent or nature of the immiscibility present, but it may be fair to assume that the lack of intimate mixing is between 9A/303 and LF200.

The infrared results obtained are very similar to the analogous CM03 ternary blends and can be seen in figures 4.74 and 4.75. The reason for the diminishing band at 1700 cm^{-1} as the proportion of PPG(1) increases has been discussed before and need not be mentioned again in detail. The results confirm the presence of a hydrogen bonding interaction between the ether oxygen of the polyether and the acid carbonyl group of the MAA component of 9A/303. (See section 4.7 and 4.5)

9A/303 - PPG(2) - LF200 Blends

The two blends were prepared in order to compare the effect of PPG(2) to PPG(1) on the miscibility of the system. Blend 183 containing an equal proportion of the components can be directly

Figure 4.73

Effect of PPG Content on the Tg of a Ternary Blend with LF200 and 9A/303
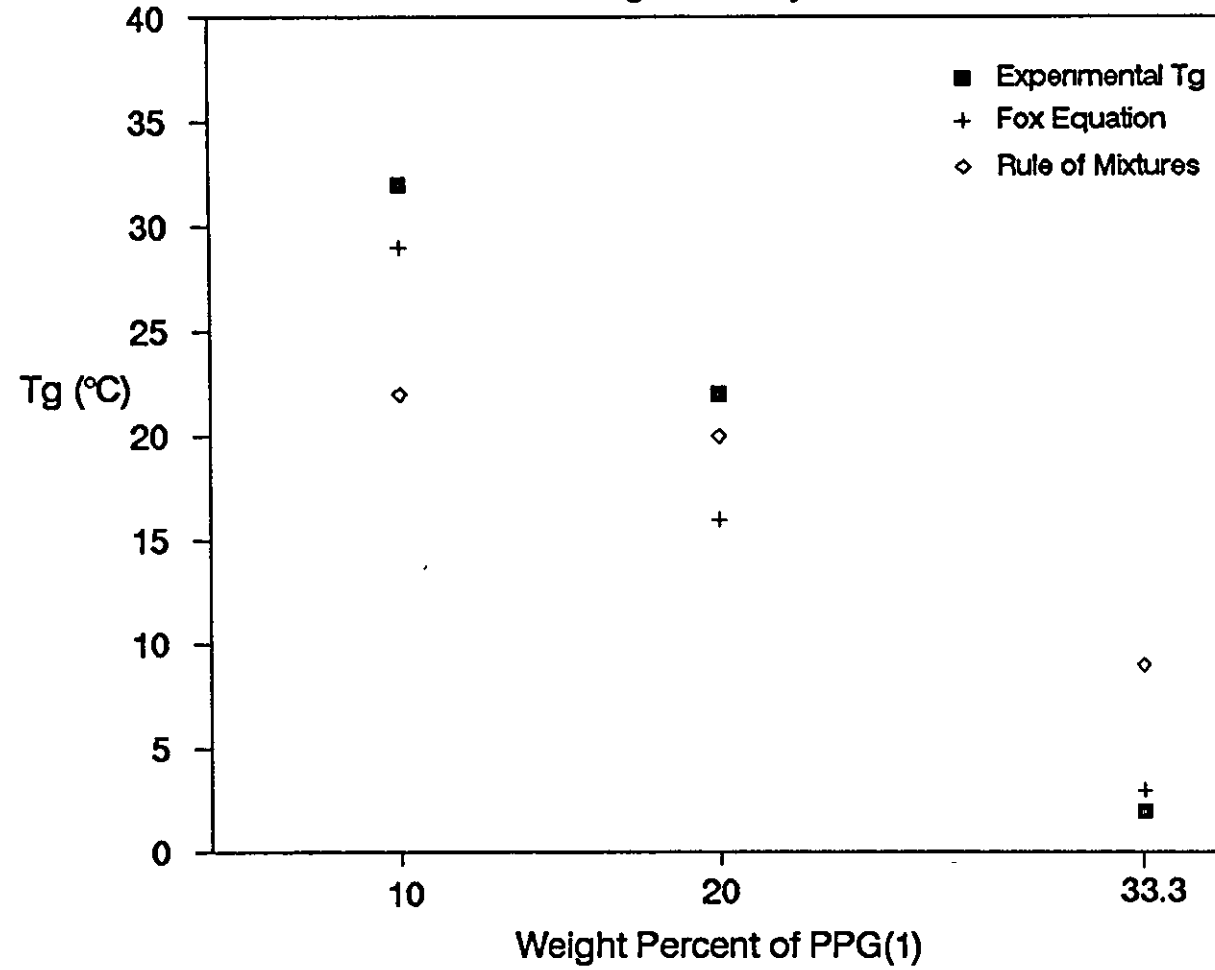
Figure 4.74
The Infrared Carbonyl Band for
9A/303 – PPG(1) – LF200 Blends

wt.% PPG(1)

33.3

20

10

9A/303

1820.0   1775.0   1730.0   1685.0   1640.0
WAVENUMBER (CM-1)
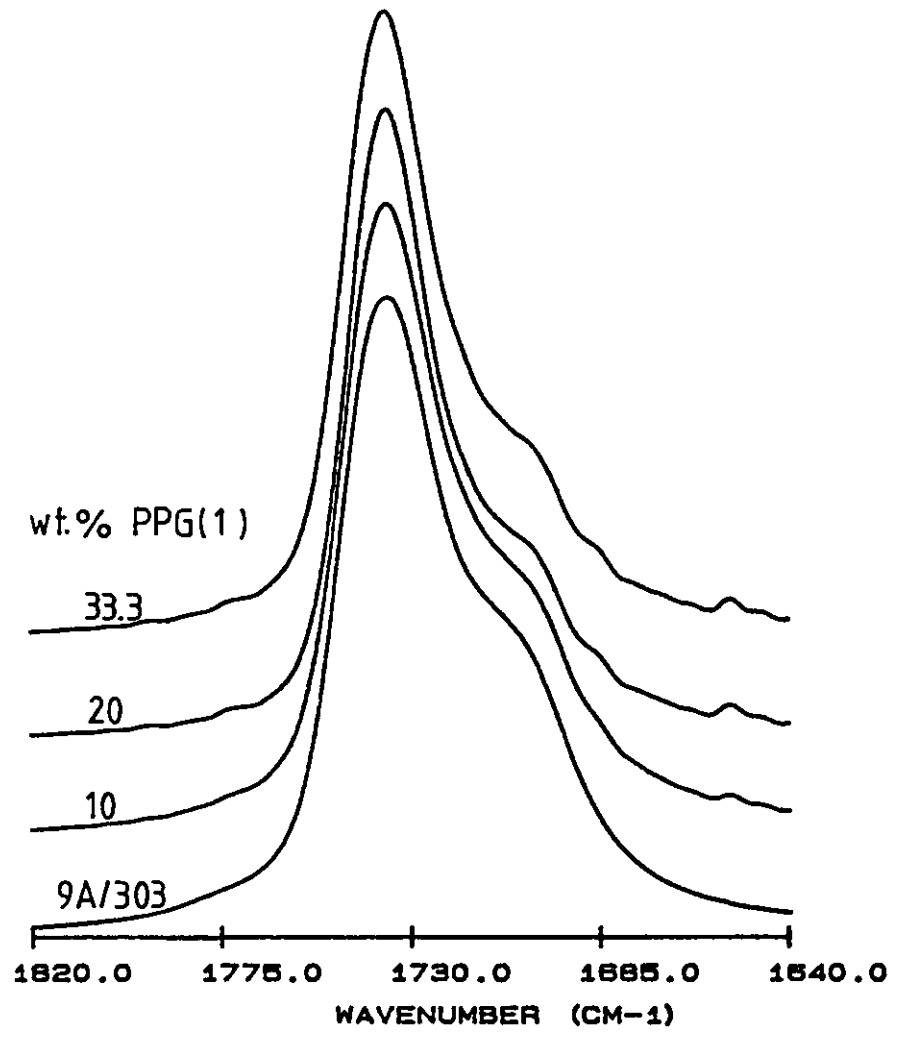
Figure 4.75
The Infrared Carbonyl Band for
9A/303 – PPG(1) – LF200 Blends

wt.% PPG(1)

30

20

10

9A/303

1820.0   1775.0   1730.0   1685.0   1640.0
WAVENUMBER (CM-1)
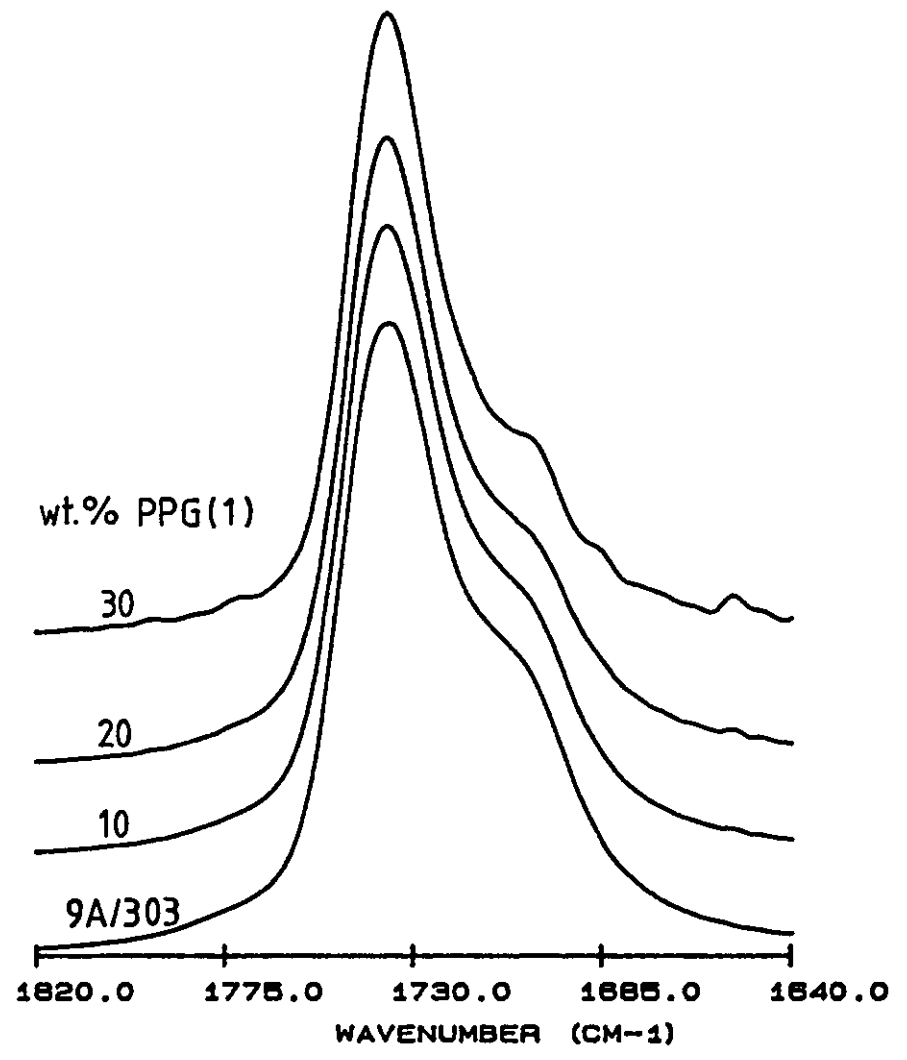
compared to the PPG(1) equivalent, blend 140. Figure 4.76 shows that the addition of 33.3% PPG(2) leads to a reasonably narrow $\tan\delta$ peak ($W_{h\frac{1}{2}}=25°$), which suggests an improvement in miscibility compared with the corresponding PPG(1) blend which has a broader transition. Figure 4.77 shows the DMTA curves for the 20:20:60 blend, again yielding a sharp narrow tan peak, comparable to the peak for the PPG(1) blend 142 (figure 4.72). It is interesting to note that the observed DMTA Tg for blend 183 (33.3:33.3:33.3 blend) is considerably different to that predicted, being around 20°C higher. The reason for this is not apparent.

The infrared results, showing the carbonyl band region are shown in figure 4.78. As expected there is a reduction in the height of the band at 1700 cm^{-1} due to the previously discussed hydrogen bonding interaction.

9A/303 - PBA(1) - LF200 Blends

Six blends were prepared, in the same proportions as the PPG(1) blends discussed above, substituting PBA(1) (Mn 1750). The DMTA curves for the three blends having equal proportions of LF200 and 9A/303 are shown in figure 4.79. All three ternary blends appear to have an improved overall miscibility compared to the 50:50 9A/303 - LF200 blend (0% PBA(1)). Figure 4.81 shows the variation of blend Tg with composition, comparing the experimentally determined Tg values to those predicted by the Fox equation and the rule of mixtures. The same is true for the three blends having a 1:3 ratio of 9A/303 and LF200, the 20 and 30% PBA(1) blends having especially narrow transition widths. The blend containing 10% PBA(1) (157, figure 4.80) has quite a broad $\tan\delta$ peak, over the range 10-80°C, making definite conclusions about the miscibility difficult, although it is likely that some degree of partial miscibility is present.

Figure 4.76   DMTA Results for PPG(2) Blends
1:1 Ratio of LF200 : 9A/303   (Table 4.13)
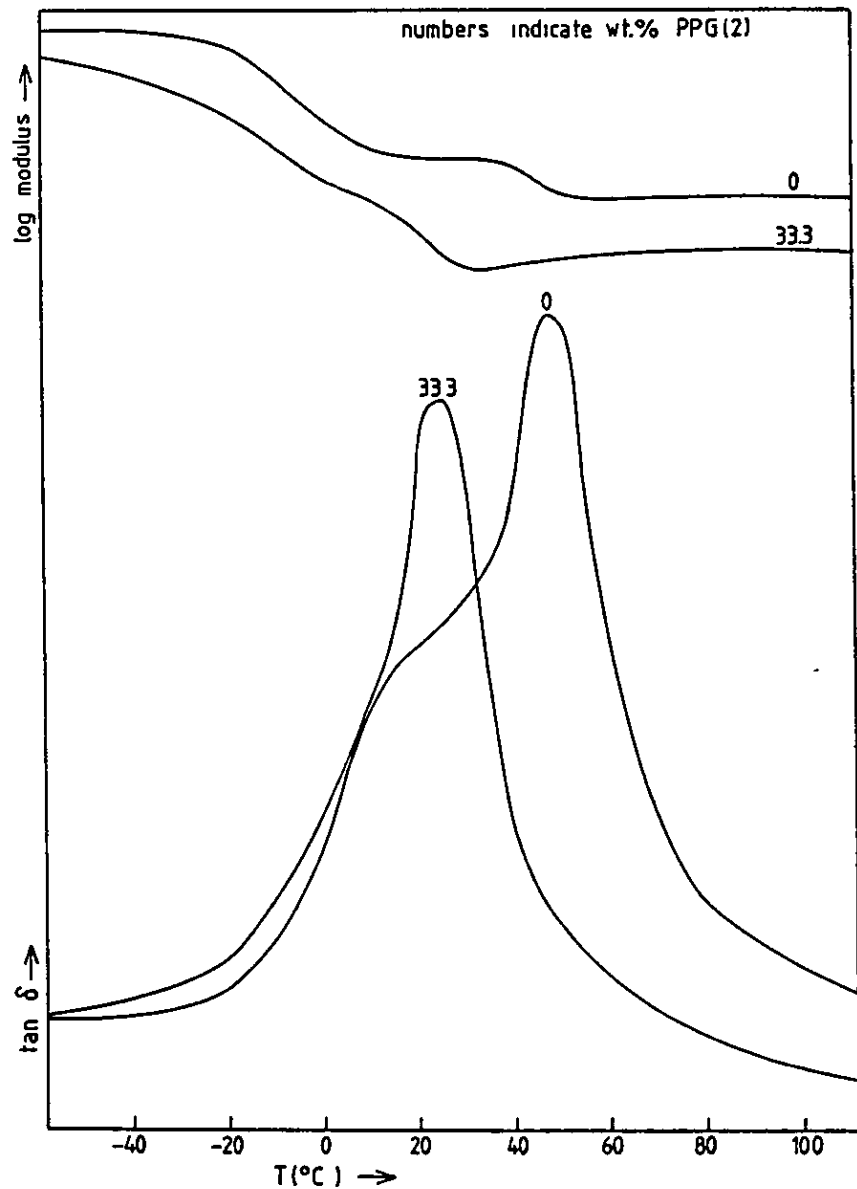
Figure 4.77   DMTA Results for PPG(2) Blends
3:1 Ratio of LF200 : 9A/303   (Table 4.13)

Figure 4.78
The Infrared Carbonyl Band for
9A/303 − PPG(2) − LF200 Blends

Blend No.

183

184

9A/303

1820.0   1775.0   1730.0   1685.0   1640.0
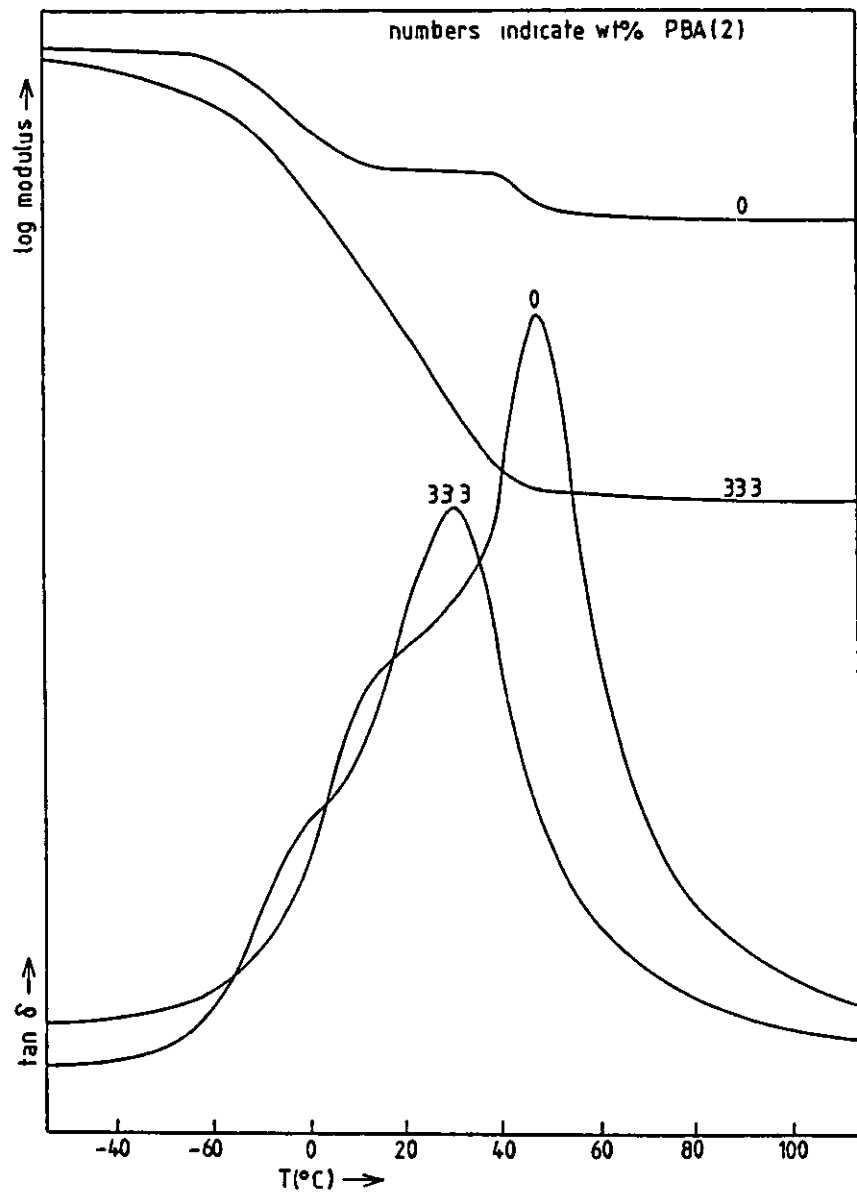
WAVENUMBER (CM−1)

Figure 4.79   DMTA Results for PBA(1) Blends
1:1 Ratio of LF200 : 9A/303   (Table 4.13)
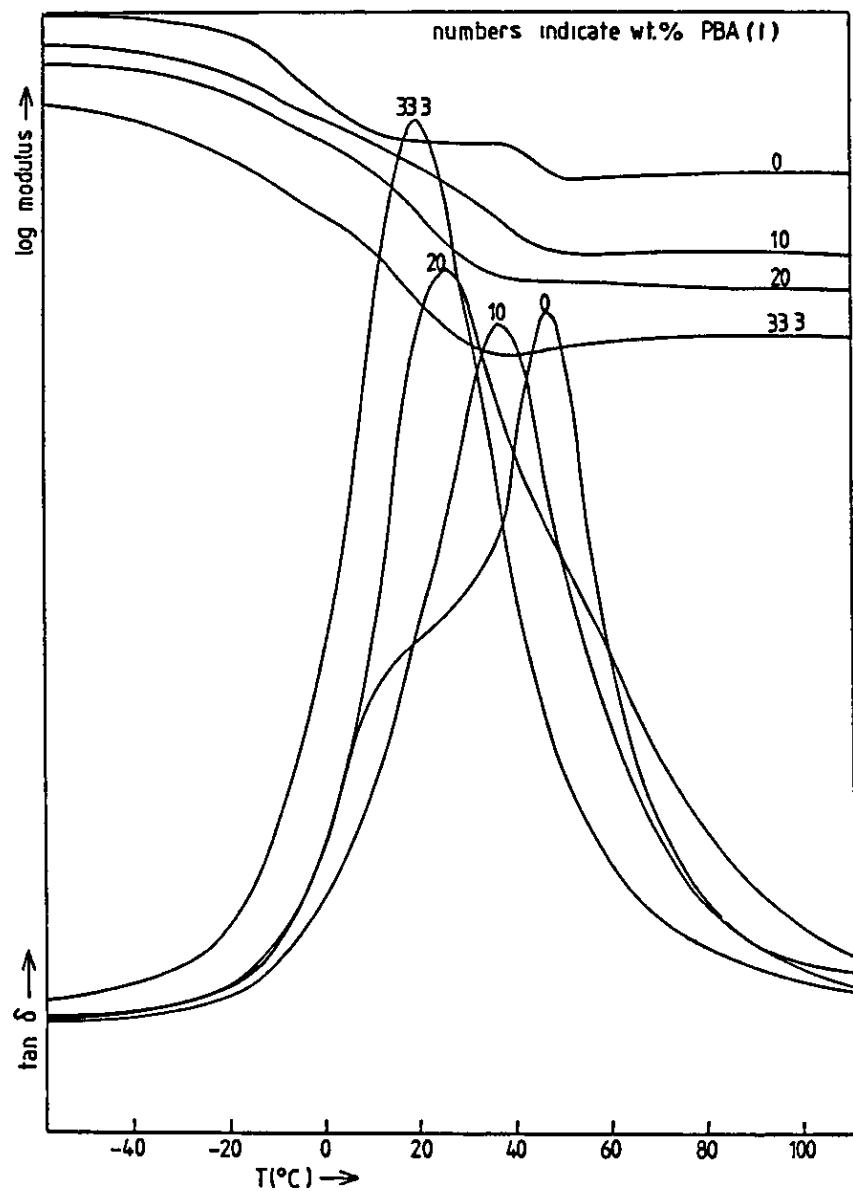
Figure 4.80   DMTA Results for PBA(1) Blends
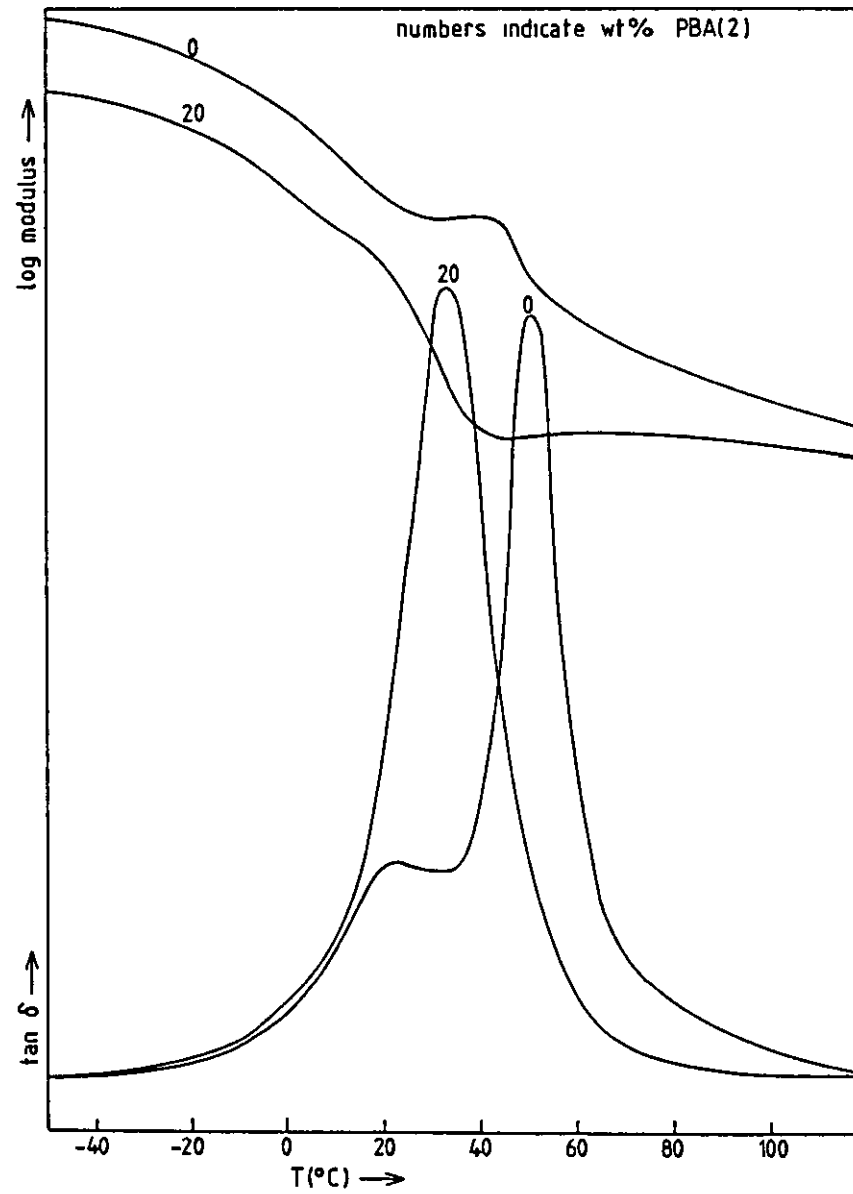3:1 Ratio of LF200 : 9A/303   (Table 4.13)
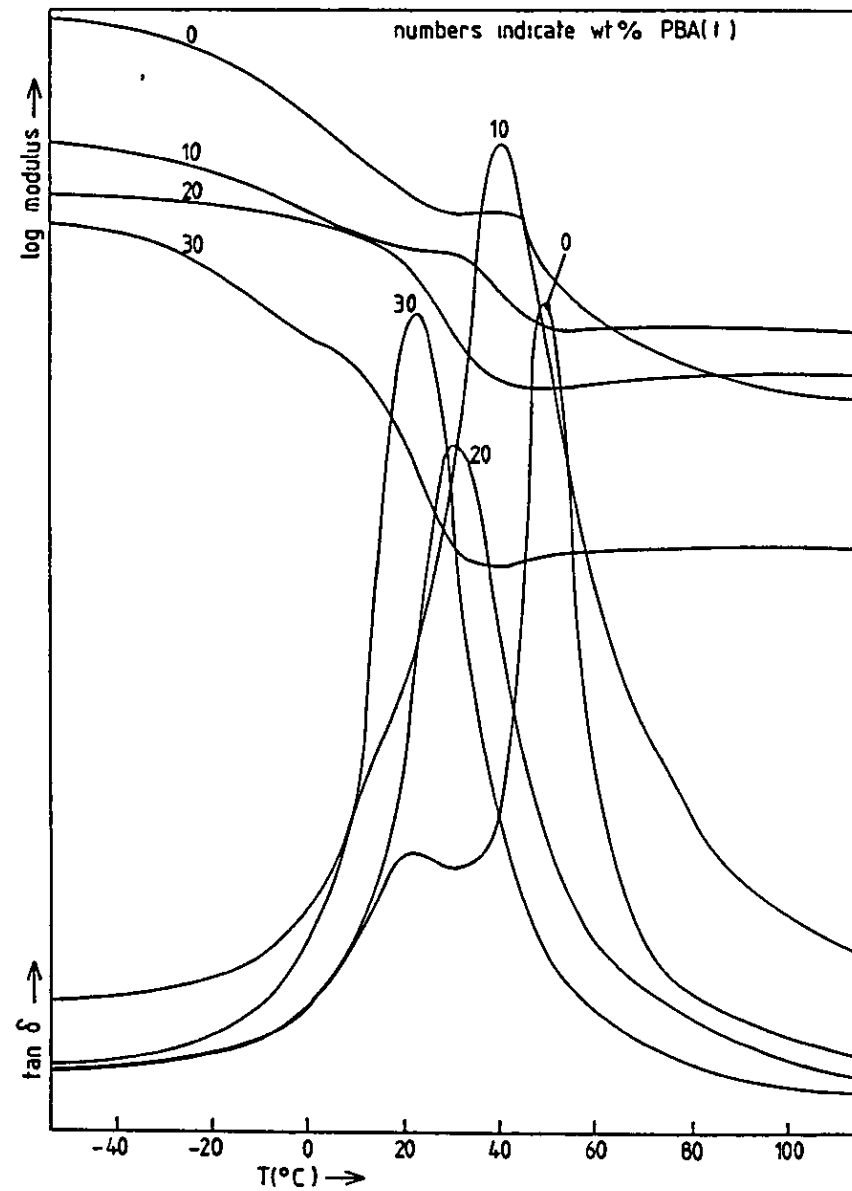
Figure 4.81

Effect of PBA(1) Content on the Tg of a Ternary Blend with LF200 and 9A303
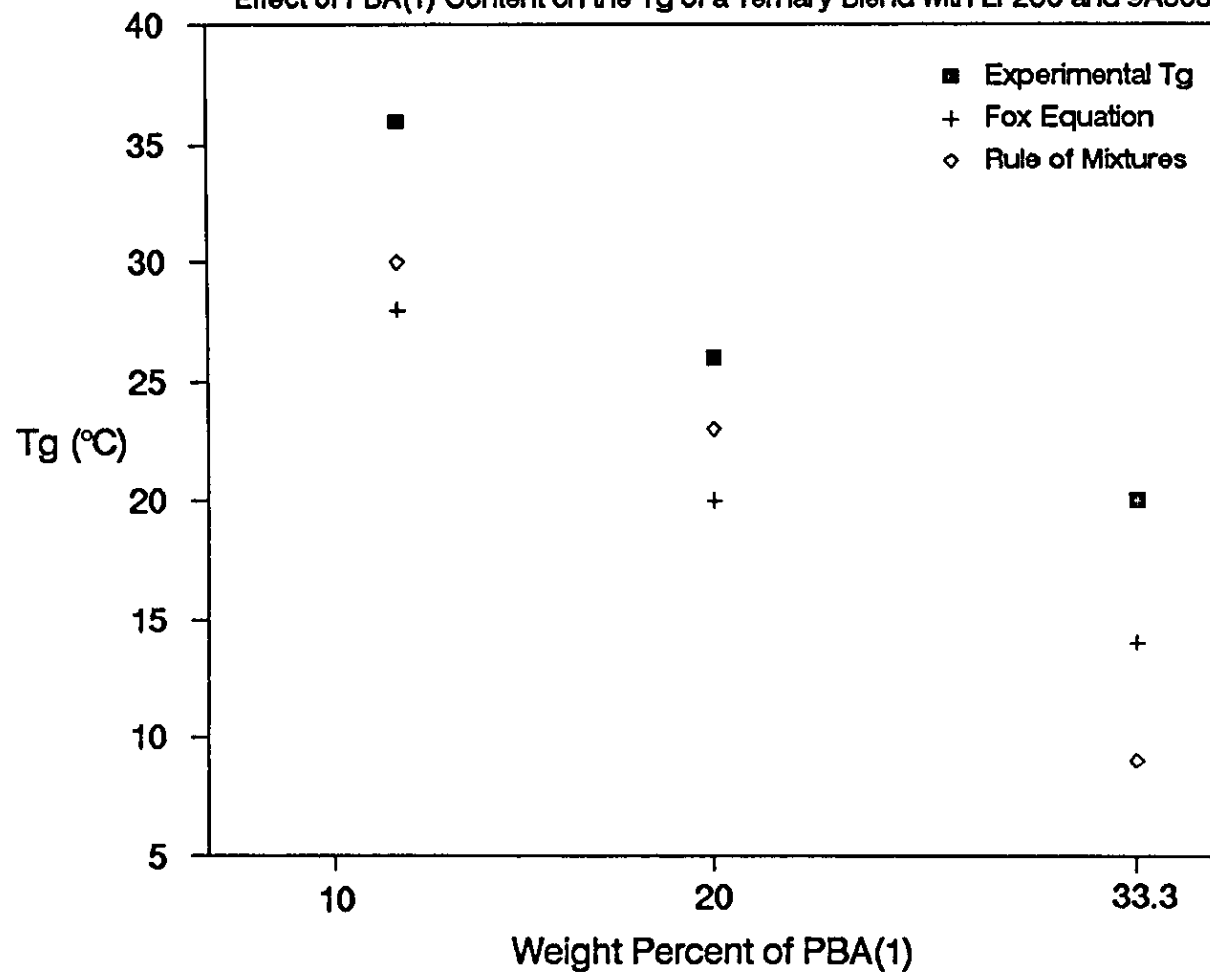
The infrared results are again inconclusive, as were the corresponding results for the ternary CM03 blends involving PBA(1), due to the large number of overlapping carbonyl bands present in the 1700 - 1735 cm^{-1} region of the spectrum.

9A/303 - PBA(2) - LF200 Blends

PBA(2) had the highest molecular weight of the poly(n-butyl acrylates) used ($\bar{M}n$ 6757), and so it is interesting to compare the results of these two blends involving PBA(1). Blend 187 having an equal proportion of the components does not yield a single tan δ

transition, but shows a shoulder on the main peak, at about 0°C, despite the position of the main peak being shifted to lower temperature. These observations can be best interpretated as being due to the existence of partially miscible phases within the blend. On the other hand, the 20:20:60 blend (187) shows a single narrow tan δ peak indicative of miscibility between the blend components. Blend 187 appears to be less miscible than the corresponding PBA(1) blend 139, whilst blend 188 gave very similar DMTA results to the corresponding blend 144. These observations are somewhat contradictory. See figures 4.82 and 4.83.

9A/303 - PBA(3) - LF200 Blends

PBA(3) has a number average molecular weight of 5200, intermediate between PBA(1) and PBA(2). Figures 4.84 and 4.85 show the DMTA results for the two blends prepared, 252 and 253. Each show single glass transitions for the ternary blends, with the 20:20:60 blend having the narrower tan δ peak width. Compared to the corresponding PBA(2) blends, 252 appears to be more miscible than 187, whilst 253 and 188 have quite similar DMTA results, based on the widths at half height of the tan δ peaks.

Figure 4.82   DMTA Results for PBA(2) Blends
1:1 Ratio of LF200 : 9A/303   (Table 4.13)

Figure 4.83   DMTA Results for PBA(2) Blends
3:1 Ratio of LF200 : 9A/303   (Table 4.13)

Figure 4.84   DMTA Results for PBA(3) Blends
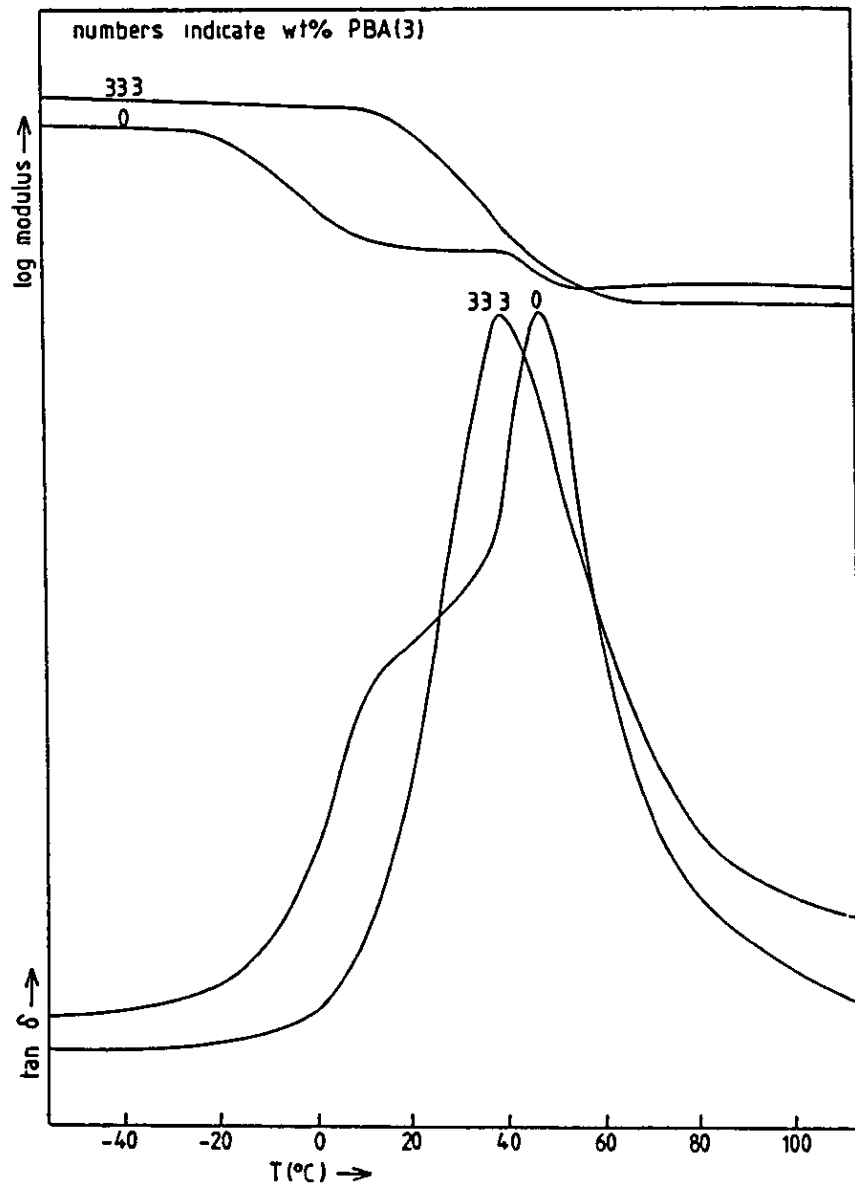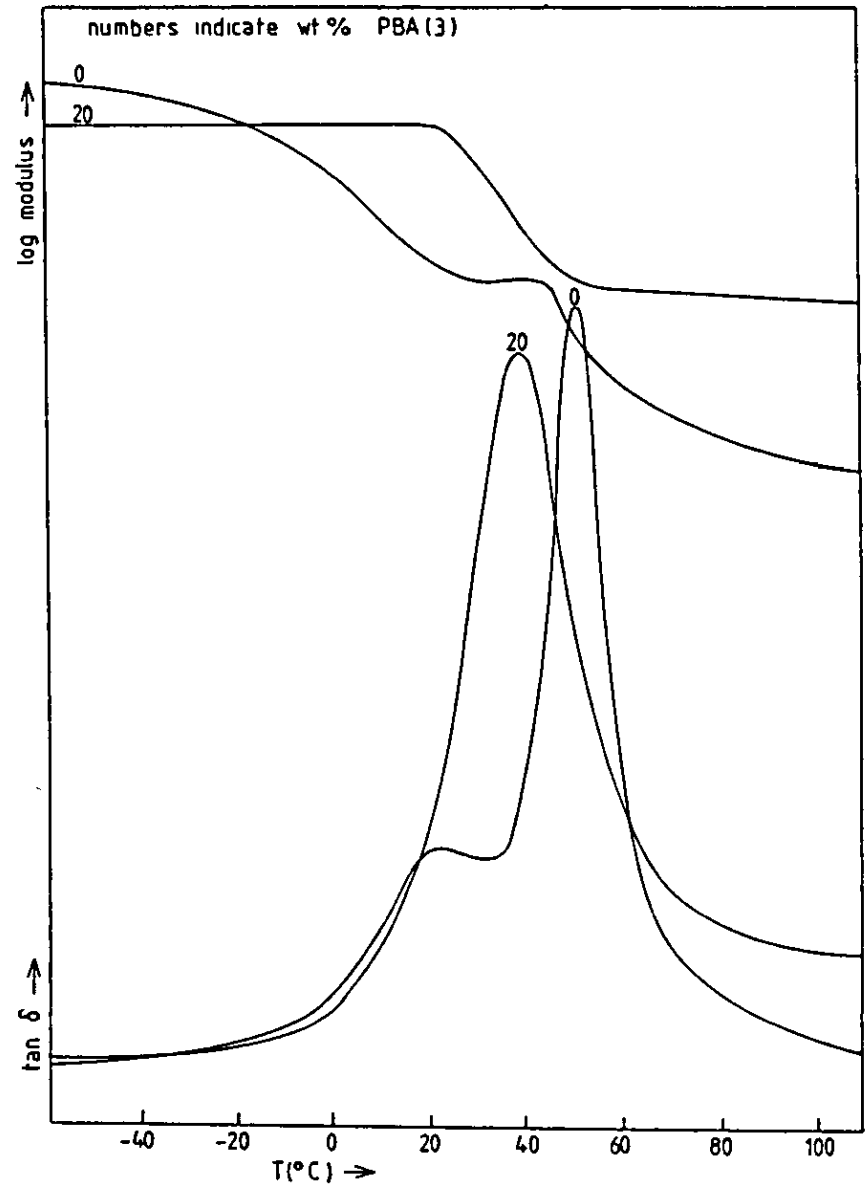1:1 Ratio of LF200 : 9A/303   (Table 4.13)

Figure 4.85   DMTA Results for PBA(3) Blends
3:1 Ratio of LF200 : 9A/303   (Table 4.13)

9A/303 - PPA - LF2000 Blends

No binary or ternary blends involving PPA with 9A/303, LF200 or CM03 have yet been found to be miscible, and it is true for these blends also. The DMTA results for both blends (figures 4.86 and 4.87) indicate three unmixed phases of PPA, 9A/303 and LF200 by virtue of the peaks at -20°C and 50°C and the shoulders at 20-25°C. PPA is clearly not a suitable compatibilising agent for either 9A/303 or CM03 with LF200.

Summary of CM03 and 9A/303 Blends

In general, it seems that the addition of either low molecular weight poly(n-butyl acrylate) or poly(propylene glycol) improves the miscibility of the polymers CM03 and 9A/303 with LF200, manifested in the appearance of single glass transition temperatures for the ternary blends. It is now appropriate to speculate on the reasons for the observed miscibility enhancement.

Poly(propylene glycol) is miscible with LF200 as well as CM03 and 9A/303. It is not too surprising, therefore, to find that the addition of PPG to blends of LF200 and either CM03 or 9A/303 leads to a miscible system. It is conceivable that the low molecular weight PPG is acting as an interface between the two otherwise immiscible components, thereby preventing their phase separation. FTIR showed there to be hydrogen bonding interactions between the methacrylic acid carbonyl groups of the acrylic component and the ether oxygen of the PPG. This probably accounts for the miscibility of PPG with 9A/303 and CM03, at least to some extent. The presence of ether groups in the structure of LF200 could be why PPG is miscible with the fluorpolymer. No specific interactions were detected in the LF200 - PPG blends, however, and it is difficult to

Figure 4.86   DMTA Results for PPA Blends
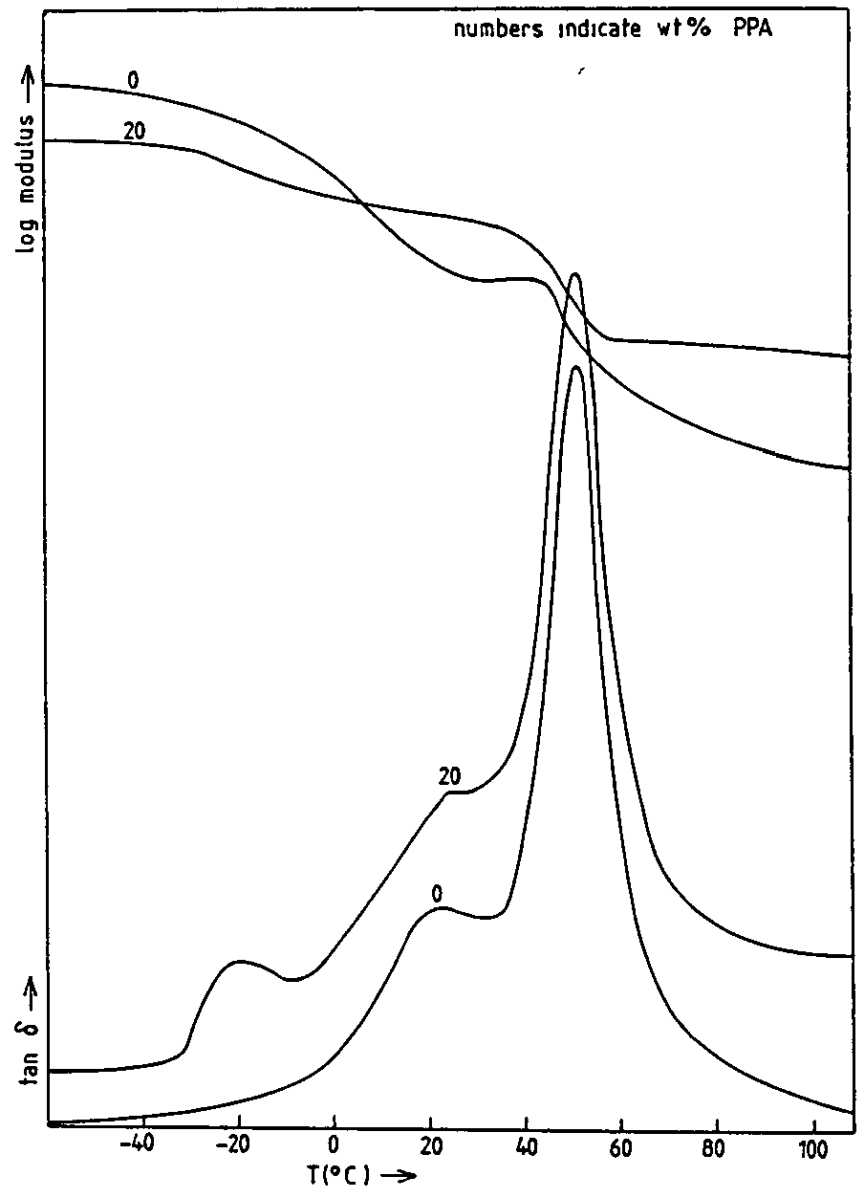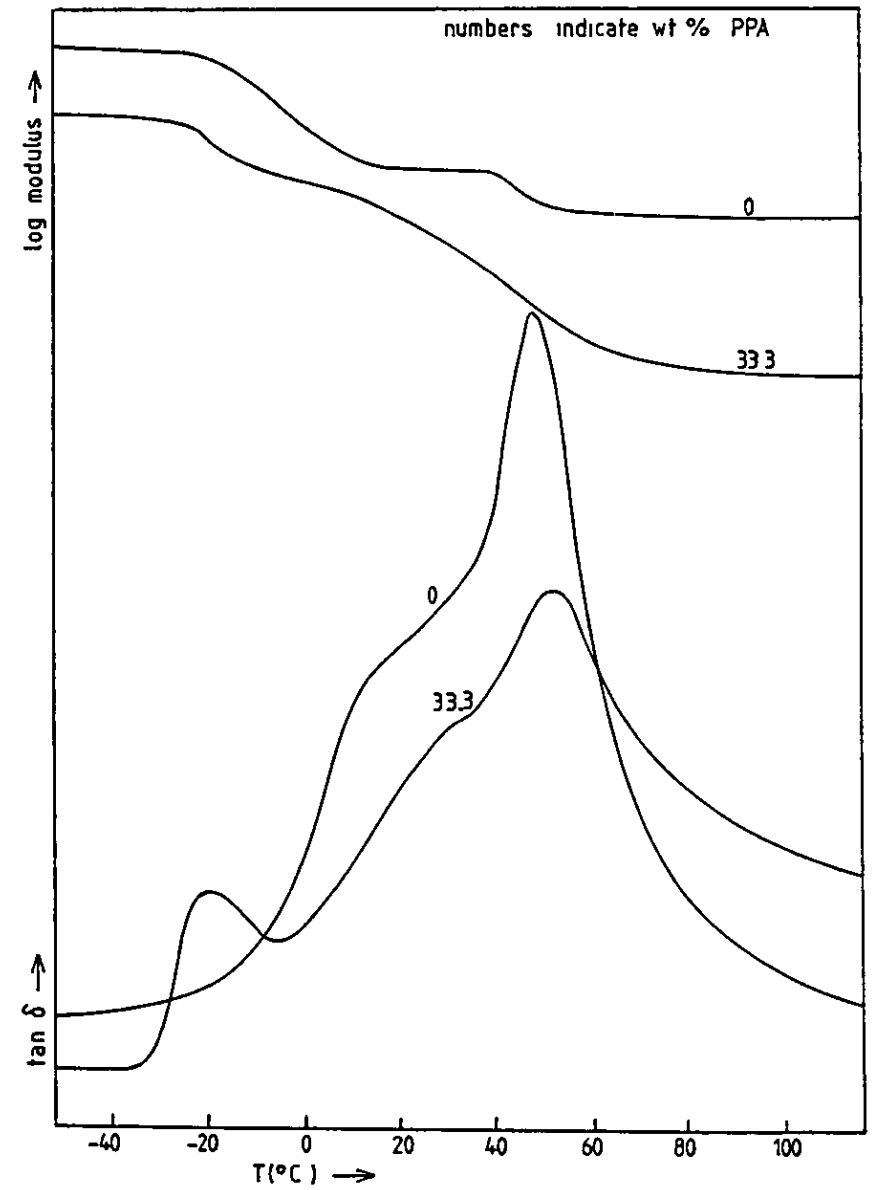1:1 Ratio of LF200 : 9A/303 (Table 4.13)

Figure 4.87   DMTA Results for PPA Blends
3:1 Ratio of LF200 : 9A/303 (Table 4.13)

say for sure why the two polymers mix.

Reasons for the apparent effectiveness of poly(n-butyl acrylate) are less obvious, although PBA was found to be miscible with LF200. Blends of PBA with 9A/303 and CM03 showed at best partial miscibility, despite each of these materials containing large proportions of butyl acrylate units. However, ternary blends of LF200, PBA and CM03 or 9A/303 were found to be miscible. No specific interactions were detected between LF200 and PBA, but it is uncertain whether such interactions exist between PBA and 9A/303 or CM03. None were found by FTIR, but because of the complexity of the overlapping carbonyl bands in the infrared spectrum, band shifts may have been obscured. If miscibility in the ternary blends is not due to specific interactions, which is likely, the reason for the miscibility enhancing effect of PBA is not clear, unless it is a factor of the polymers having low molecular weight. More work is required in the area of polymer blend miscibility in order to understand more fully the mixing behaviour of polymers and in particular, to understand the reasons why polymers form miscible blends, when a mechanism other than specific interactions is responsible for the miscibility.

4.10 Scanning Electron Microscopy Results

The conclusions regarding miscibility for all of the blends studied are based almost solely on the results of dynamic mechanical thermal analysis. However, as with other thermal methods of analysis, DMTA is only of limited use when the glass transition temperatures of the blend components are very similar. This is clearly a problem with a number of the blends in this study (see section 4.3, for example). In order to be able to reach more

-132-

definite conclusions about miscibility, scanning electron microscopy (SEM) was used to analyse several two and three component blends. Unfortunately a problem was encountered in practice, which prevented the analysis of many of the systems studied, because the blend films were too soft to be mounted successfully in the microscope (see section 3.4.3). Blends having a Tg of less than 30-35°C, produced films which were not rigid enough to be mounted edgewise onto the specimen holder. Because of this only a limited number of blends could be studied in this way. However, LF200, CM03 and the blends 156, 112 and 102 were suitable for study, see table 4.14. The scanning electron micrographs for these material are shown in appendix 4. As expected LF200 and CM03 appeared to be single phase materials, confirming the observation of a single Tg for each polymer as found by DMTA. Blend 102, comprising 75% LF200 and 25% 9A/303, showed two glass transitions and so it is not surprising to find that something resembling a two-phase structure is observed by SEM. The micrograph shows domains of approximate size 2-5μm in a more continuous phase. There also appears to be much smaller domains and some that are larger than this. Presumably the continuous phase would correspond to the major component LF200, with 9A/303 being the discrete phase having a range of domain sizes.

The 50:50 blend of the ST-MAA copolymer 163 and LF200, shown to be clearly two-phase by SEM. The micrograph has an unusual appearance, however with the continuous phase apparently comprising of much more than the expected 50%. The reason for this is not obvious, but it may be that the portion of the specimen photographed is not representative of the whole specimen.

The ternary blend of 9A/303, PPG(1) and LF200 (156) is particularly interesting. Two sample films were prepared, one by solution casting and the other by melt pressing. The first point to

-133-

Table 4.14   SEM Results

Blend No.	Composition	Method of Film Preparation	Observation
-	100% LF200	cast from chloroform	single phase
-	100% CM03	cast from chloroform	single phase
102	9A/303/LF200 25:75	melt pressed	two phase
156	9A/303/PPG(1)/LF200 22.5:10:67.5	melt pressed — — cast from chloroform —	single phase two phase
112	163/LF200 50:50	melt pressed	two phase

notice is that the melt pressed film had a greater optical clarity than the film cast from chloroform. The electron micrographs of specimens taken from each of the films also show a distinct difference, with the melt pressed specimen appearing single phase and the solution cast specimen appearing two-phase. The domain sizes in the two-phase specimen ranged from 1 to $4\mu m$, that is, larger than the size of phase necessary to cause the scattering of light. It is therefore, easy to see why this sample had a translucent appearance. Clearly, the method of sample preparation has an important effect on the phase separation behaviour of this blend. It seems to be the case, that melt pressing leads to a much greater homogeneity than casting from chloroform. It is perhaps for this reason that DMTA specimens indicated a single phase structure for this and similar blends, since they were also prepared by melt pressing. The solution cast sample has been referred to as two-phase, but of course there are three components present and it is possible, if not likely, that each forms a separate phase when the sample is prepared in this way.

It has been shown that SEM, used in conjunction with DMTA can more conclusively define the miscibility of a polymer blend, especially if the components have similar Tg values. However, since only a limited number of samples were studied by SEM, it would be a little unwise to draw definite conclusions about the remaining binary and ternary blends. More work would be required to confirm that the tentative conclusions, based on these few results, apply in general to the other blend systems studied.

5.0 Conclusions

The initial aim of this study was to investigate the potential for producing a miscible blend, comprising the high performance surface coating polymer, Lumiflon LF200 and lower cost, lower performance acrylic-based surface coating materials. The hope was to utilise the potential of these polymers for hydrogen bonding interactions, in order to promote miscibility in the blend system. Dynamic mechanical thermal analysis showed that the fluropolymer LF200 was neither miscible with the model copolymers of styrene and methacrylic acid, nor with the surface coating materials. FTIR analysis indicated a lack of any specific interactions between the components of these blends and this could be at least one reason why miscibility was not achieved.

Further observations were made on blends when LF200 was mixed with several different homopolymers and copolymers. A number of miscible blends were produced, as confirmed by single glass transitions and optical clarity. LF200 was found to be miscible with low molecular weight poly(n-butyl acrylate) (PBA), over a wide range of compositions in each case. Miscibility was also found in blends of LF200 with EVA and PEG, at low levels of these polymers. It is also possible that blends of LF200 with PBMA, PDMAEMA and PVAc show single phase behaviour, but this could not be confirmed by DMTA, because of the proximity of the glass transition temperatures of these polymers to that of LF200 (PVAc and PBMA blend with LF200 did however, form transparent films). These results showed clearly that there was good potential for producing miscible blends of LF200 with polymers having either carbonyl or ether functional groups (eg. PBA, PPG, EVA, etc).

From this information and the knowledge that miscible blends

-135-

have previously been produced between polyethers and copolymers containing MAA units, it seemed logical to attempt to mix PPG with the MAA - containing acrylic systems, CM03 and 9A/303. This was done and the results indicated considerable miscibility in each of these blends, with single Tg transitions being observed, coupled with the observation of hydrogen bonding interactions between the MAA carbonyl and PPG ether groups using FTIR spectroscopy. Since PPG is miscible with both LF200 and each of the acrylic polymers, CM03 and 9A/303, it might be expected that a ternary blend involving these polymers might produce at least some degree of miscibility. The DMTA results showed that this is indeed the case, with all such blends showing single Tg transitions over a range of compositions. PPG appears therefore, to act as a polymeric compatibilising agent. To date, no similar systems have been reported in the literature, most compatibilisers being block copolymers (usually containing monomer units common to the two immiscible polymers involved).

Poly(n-butyl acrylate) (PBA) also appeared to be a possible candidate to improve the miscibility of LF200 and the acrylic polymers CM03 and 9A/303, since PBA is miscible on it's own with LF200 and because the acrylic polymers produced, in nearly all cases, single phase (hence, single Tg) miscible blends. No specific interactions were detected in any of these blends by FTIR, although the presence of such interactions could not be completely ruled out, because of the complexity of interpreting the combined carbonyl band at 1700-1735 cm^{-1} in the IR spectra.

It seems therefore, that both PBA and PPG act as compatibilising agents for the systems mentioned, but it is not clear whether the two polymers improve the miscibility by the same mechanism, unless the miscibility enhancement is a function of their low molecular weight.

The work has shown that dynamic mechanical thermal analysis can be a valuable technique in the study of blend miscibility, provided the Tg transitions of the blend components occur at sufficiently different temperatures (ideally > 20°C apart). The problem of similar glass transition temperatures arose for a number of the blends studied, making it difficult to reach firm conclusions about the miscibility of the component polymers.

Scanning electron microscopy was chosen in order to help determine unambiguously the nature of any phase separation present, if any, in such blends, as a means of corroborating the DMTA results. Unfortunately, practical problems were encountered (section 4.10) which restricted the use of this technique. However, based on the few micrographs which were obtained successfully, it was apparent that SEM could be very useful for the study of multicomponent systems. Electron micrographs (appendix 4) confirmed the DMTA findings of both single and two-phase nature for blends studied by both techniques. The microscopic characterisation also revealed that the method of blend film preparation affected the phase separation behaviour of some blends; melt pressed films showed a single phase, whilst films cast from chloroform showed two or more phases. This phenomenon could also explain why blend films having a translucent appearance when cast from solution, give only a single glass transition, since the DMTA specimens were melt pressed.

In view of the results and developments in this thesis, the following proposals are recommended for further work:

1. Investigation into the effect of molecular weight on the miscibility enhancing nature of low molecular weight compatibilising agents such as PBA and PPG, for LF200/acrylic blends and more generally to other polymer blends.

2. Further work should be carried out using scanning electron microscopy, in order to investigate more thoroughly the morphology and phase behaviour of Lumiflon/acrylic blends.

3. Assessment of the potential of Lumiflon/ acrylic blends for surface coating applications, in terms of degree of miscibility and type of morphology for partially separated phases.

4. More work is required to understand more fully the reasons for miscibility in systems in which specific interactions are not present.

REFERENCES

1. Paul, D.R., Newman, S., "Polymer Blends", Volumes 1 and 2, Academic, N.Y. (1979).

2. Olabisi, O., Robeson, L.M., Shaw, M.T., "Polymer-Polymer Miscibility", Academic, N.Y. (1979).

3. Manson, J.M., Sperling, L.H., "Polymer Blends and Composites", Heydon (1976).

4. Solc, K., "Polymer Compatibility and Incompatibility", Harwood, N.Y. (1982).

5. Williams, P.W., PhD Thesis, Loughborough University of Technology (1985).

6. Nishi, T., Wang, T.T., Macromolecules, $\underline{8}$, 809 (1975).

7. Murff, S.R., Barlow, J.W., Paul, D.R., J. Appl. Poly. Sci., $\underline{29}$, 3231 (1984).

8. Kaplan, D.S., J. Appl. Poly. Sci., $\underline{20}$, 2615 (1976).

9. Rosen, S.L., Poly. Eng. Sci., $\underline{7}$, 115 (1967).

10. Coleman, M.M., Moskala, E.J., Polymer, $\underline{24}$, 251 (1983).

11. Hara, M., Eisenberg, A., Macromolecules, $\underline{17}$, 1335 (1984).

12. Fernandes, A.C., Barlow, J.W., Paul, D.R., J. Appl. Poly. Sci., $\underline{32}$, 5481 (1986).

13. Smith. P., Eisenberg, A., J. Poly. Sci., Poly. Lett. Edn., $\underline{21}$, 223 (1983).

14. Xanthos, M., Poly. Eng. Sci., $\underline{21}$, 985 (1988).

15. Barlow, J.W., Paul, D.R., Poly. Eng. Sci., $\underline{21}$, 985 (1981).

16. Fayt, R., Jerome, R., Teyssié, Ph., Poly. Eng. Sci., $\underline{24}$, 525 (1984).

17. Sperling, L.H., "Interpenetrating Polymer Networks and Related Materials", Plenum (1981).

18. Christiansen, W.H., Paul, D.R., Barlow, J.W., J. Appl. Poly. Sci., $\underline{34}$, 537 (1987).

19. Shah, V.S., Keitz, J.D., Paul, D.R., Barlow, J.W., J. Appl. Poly. Sci., $\underline{32}$ 3863 (1986).

20. Akijama, S., MacKnight, W.J., Karasz, F.E., Nambu, I., Polymer Communications, $\underline{28}$, 236 (1987).

21. Krause, S., Pure and Appl. Chemistry, $\underline{58}$, 1553 (1976).

22. Krause, S., chapter VI in reference 89.

23. Jasse, B., chapter 3, "Developments in Polymer Characterisation-4", Dawkins, J.V., ed., Applied Science (1983).

24. Coleman, M.M., Painter, P.C., Appl. Spectroscopy Reviews, 20, 255 (1984).

25. Fried, J.R., chapter 4 in "Developments in Polymer Characterisation-4", Dawkins, J.V., ed., Applied Science (1983).

26. Fowler, M.E., Barlow, J.W., Paul, D.R., Polymer, 28 1177 (1987).

27. Rostami, S., Walsh, D.J., Macromolecules, 10, 681 (1977).

28. Bernstein, R.E., Cruz, C.A., Paul, D.R., Macromolelcules, 10, 681 (1977).

29. Flory, P.J., "Principles of Polymer Chemistry", Cornell, N.Y. (1953).

30. Huggins, M.L., "Physical Chemistry of High Polymers", Wiley, (1953).

31. Schweizer, K.S., Curro, J.G., Polymer Preprints, 30, 50 (1989).

32. Richards, R.W., chapter 4 in "Developments in Polymer Characterisation -1", Dawkins, J.V., ed., Applied Science (1978).

33. Tomlins, P.E., Higgins, J.S., Macromolecules, 21, 425 (1988).

34. Ito, H., Russell, T.P., Wignall, G.D., Macromolecules, 20, 2213 (1987).

35. Tompa, H., Trans. Faraday Soc., 45, 1142 (1949).

36. Koningsveld, R., Brit. Poly. J., 7, 435 (1975).

37. Flory, P.J., Orwell, R.A., Vrij, A., J. Am. Chem. Soc., 86, 3515 (1964).

38. Flory, P.J., J. Am. Chem. Soc., 87, 1833 (1965).

39. Flory, P.J., Discuss. Faraday Soc., 49, 7 (1970).

40. Sanchez, I.C., Lacome, R.H., J. Physical Chem., 80, 2352 (1976).

41. Sanchez, I.C., Lacome, R.H., J. Physical Chem., 80, 2568C (1976).

42. Sanchez, I.C., J. Macromol. Sci., Macromolecules, 11, 1145 (1978).

43. Sanchez, I.C., J. Macromol. Sci. (Phys.), B17, 565 (1980).

44. Prigogine, I., "The Molecular Theory of Solutions", North Holland Publ., Amsterdam (1957).

45. McMaster, L.P., Macromolecules, 6, 760 (1973).

46. Kambour, R.P., Bendler, J.T., Bopp, R.C., Macromolecules, 16, 753 (1983).

47. Paul, D.R., Barlow, J.W., Polymer, 25, 487 (1984).

48. Roe, R.J., Rigby, D., Adv. Poly. Sci., 82, 103 (1987).

49. Hildebrand, J.H., Scott, R.C., "Solubility of Non-Electrolytes", Reinhold Publ. Corp., N.Y. (1950).

50. Olabisi, O., Simha, R., J. Appl. Poly. Sci., 21, 149 (1977).

51. Landry, C.J.T., Yang, H., Machell, J.S., Polymer, 32, 44 (1991).

52. Manjun He, Yangming Lui, Yi Feng, Ming Jiang, Han, C.C., Macromolecules, 24, 464 (1991).

53. ten Brinke, G., Karasz, F.E., MacKnight, W.J., Macromolecules, 16, 1827 (1983).

54. van Krevelen, D.W., "Properties of Polymers", Elsevier, Amsterdam, (1976).

55. Card, T.W., Al-Saigh, Z.Y., Munk, P., Macromolecules, 18, 1030 (1985).

56. Deshpande, D.D., Paterson, D., Schreiber, H., Su, C.S., Macromolecules, 7, 530 (1974).

57. Su, C.S., Paterson, D., Macromolecules, 10, 708, (1977).

58. Olabisi, O., Macromolecules, 8, 316 (1975).

59. Walsh, D.J., McKeown, J.G., Polymer, 21, 1335 (1980).

60. Doube, C.P., Walsh, D.J., Euro. Poly. J., 17, 63 (1981).

61. El-Hibri, M.J., Cheng, W., Macromolecules, 21, 3458 (1988).

62. Mandal, B.M., Bhattacharya, C., Bhattacharyya, S.N., J. Macromol. Sci., Chem., A26, 175 (1989).

63. Wignall, G.D., Crist, B., Russell, T.P., Thomas, E.L., eds., "Scattering, deformation and Fracture in Polymers", MRS Symposia Proceedings No. 79, Materials Research Society, Pittsburg (1987).

64. Higgins, J.S., Chapter 4 in "Developments in Polymer Characterisation -4", Dawkins, J.V., ed., Applied Science (1983).

65. Wignall, G.D., Macromolecules, 20, 2213, (1987).

66. Curro, J.S., Schweizer, K.S., Phys. Rev. Lett., 60, 809 (1985).

67. Lai, C.H., Paul, D.R., Barlow, J.W., Macromolecules, 21, 2492 (1988).

68. Lai, C.H., Paul, D.R., Barlow, J.W., Macromolecules, 22, 374 (1989).

69. Abrams, D.S., Prausnitz, J.M., Am. Chem. J., 21, 116 (1975).

70. Guggenheim, E.A., Proc. Royal Society, London, Ser. A, 183, 213 (1944).

71. Guggenheim, E.A., "Mixtures", Clarendon, Oxford (1952).

72. Kammer, H.-W., Inoue, T., Ougizawa, T., Polymer, 30, 888 (1989).

73. Pfennig, J.L.G., Keskkula, H., Barlow, J.W., Paul, D.R., Macromolecules, 18, 1937 (1985).

74. Painter, P.C., Yung Park, Coleman, M.M., Macromolecules, 22, 570 (1989).

75. Painter, P.C., Yung Park, Coleman, M.M., Macromolecules, 22, 580 (1989).

76. Kretschmer, C.B., Wiebe, R., J. Chem. Phys., 22, 1697 (1954).

77. Coleman, M.M., Lichkus, A.M., Painter, P.C., Macromolecules, 22, 586 (1989).

78. Kolařík, J., Adv. Poly. Sci., 46, 119 (1982).

79. Fox, T.G., Flory, P.J., J. Am. Chem. Soc., 70, 2384 (1948).

80. Fox, T.G., Flory, P.J., J Appl. Phys., 21, 581 (1950).

81. Doolittle, A.K., J. Appl. Phys., 22, 1471 (1951).

82. Doolittle, A.K., J. Appl. Phys., 23, 236 (1952).

83. Williams, M.L., Landel, R.F., Ferry, J.D., J. Am. Chem. Soc., 77, 3701 (1955).

84. Kauzmann, W., Chem. Rev., 43, 219 (1848).

85. Gibbs, J.H. Dimarzio, E.A., J. Chem. Phys., 28, 373 (1958).

86. Adams, G., Gibbs, J.H. J. Chem. Phys., 43, 139 (1965).

87. Cohen, M.H., Grest, G.S., Phys. Rev., B20, 1077 (1979).

88. Chow, T.S., Macromolecules, 22, 698 (1989).

89. Brandrup, J., Immergut, E.H., eds., "Polymer Handbook", 3rd Edn., Wiley, N.Y. (1989).

90. Kennedy, J.P., Tornquist, E.G.M., eds., chapter 1 in "High Polymers, volume XXIII, Polymer Chemistry of Synthetic Elastomers, part 1", Interscience (1968).

91. Wood, L.A., J. Poly. Sci., 28, 319 (1958).

92. Gordon, M., Taylor, J.S., J. Appl. Chem., 2, 493 (1952).

93. Fox, T.G., Bull. Am. Phys. Soc., 1, 123 (1956).

94. Kelley, F.N., Bueche, F., J. Poly. Sci., 50, 549 (1961).

95. Gibbs, J.H., Dimarzio, J., J. Poly. Sci., 40, 121 (1959).

96. Johnston, N.W., Polymer Preprints, Am. Chem. Soc., Div. Poly. Chem., 10, 609 (1969).

97. Couchman, P.R., Karasz, F.E., Macromolecules, 11, 117 (1978).

98. Couchman, P.R., Poly. Eng. Sci., 24, 135 (1984).

99. Goldstein, M., Macromolecules, 18, 277 (1985).

100. Brekner, M.J., Schneider, H.A., Cantow, H.J., Polymer, 29, 78 (1988).

101. Aubin, M., Prud'homme, R.E., Poly. Eng. Sci., 28, 1355 (1988).

102. Kovacs, A.J., Adv. Poly. Sci., 3, 394 (1963).

103. Brown, G., Kovacs, A.J., "Physics of Non-Crystalline Solids", Prins, J.A., ed., North Holland, Amsterdam (1965).

104. Xinya Lu, Bingzheng Jiang, Polymer, 32, 471 (1991).

105. Wetton, R.E., Croucher, T.G., Fursdon, J.W.M., chapter 5 in "Polymer Characterisation. Spectroscopic, Chromatographic and Physical Instrumental Methods", Crawer, C.D., ed., Adv. Chem. Ser., Am. Chem. Soc., Washington DC (1983).

106. Richardson, M.J., chapter 7 in "Developments in Polymer Characterisation -1", Dawkins, J.V., ed., Applied Science (1978).

107. Billmeyer, F.W., "Textbook of Polymer Science", 3rd Edn., Wiley (1984).

108. Finemann, M., Ross, S.D., J. Poly. Sci., 5, 259 (1950).

109. Kelen. T., Tudos, F., J. Macromol. Sci., A9, 1 (1975).

110. Kennedy, J., Kelen, T., Tudos, F., J. Poly. Sci., A1, 13, 2277 (1975).

111. Joon, Y. Lee, Painter, P.C., Coleman, M.M., Macromolecules, 21, 346 (1988).

112. Coleman, M.M., Joon, Y. Lee, Serman, C.J., Zhiqiang Wang, Painter, P.C., Polymer, 30, 1298 (1989)

113. Coleman, M.M., Painter, P.C., Appl. Spectro. Rev., 20, 255 (1984).

114. Sandler, S.R., Karo, W., "Polymer Synthesis -1", Academic Press (1974).

115. Boudevska, H., Toderova, O., Makromol. Chem., 186, 1711 (1985).

116. Gibson, B - Unpublished Results (Loughborough University).

117. Dawkins, J.V., Yeadon, G., "Development in Polymer Characterisation -1", Dawkins, J.V. ED., Applied Science (1978).

118. Moskala, E.J., Howe, S.E., Painter, P.C., Coleman, M.M., Macromolecules, 17, 1671 (1984).

119. Coleman, M.M., Skrovanek, D.J., Jiangbin Hu, Painter, P.C., Macromolecules, 21, 59 (1988).

120. Joon, Y. Lee, Painter, P.C., Coleman, M.M., Macromolecules, 21, 2636 (1988).

121. Lichkus, A.M., Painter, P.C., Coleman, M.M., Macromolecules, 21, 2636 (1988).

122. van Tam Bui, Baril D., Thanh Long Vu, Makromol. Chem., Macromol. Symp., 16, 267 (1988).

123. Sawyer, L.C., Grubb, D.T., "Polymer Microscopy", Chapman and Hall (1987).

124. Nishi, T., Wang, T.T., Macromolecules, 8, 909 (1975).

125. Plans, J., MacKnight, W.J., Karasz, F.E., Macromolecules, 17, 1100 (1984).

126. Fayt, R., Jerome, R., Teyssie, Ph., Poly. Eng. Sci., 27, 328 (1987).

127. Shah, V.S., Keitz, J.D., Paul, D.R., Barlow, J.W., J. Appl. Poly Sci., 32, 3863 (1986).

128. Saburo Akijama, MacKnight, W.J., Farasz, F.E., Junji Nambu, Poly. Comm., 28, 236 (1987).

129. Christiansen, W.H., Paul, D.R., Barlow, J.W., J. Appl. Poly. Sci., 34, 539 (1987).

130. Landry, C.J.T., Yang, H. Machell, J.S., Polymer, 32, 44 (1991).

131. Remiro, P.M., Nazabal, J., J. Appl. Poly. Sci., 42, 1475 (1991).

132. Clark, M.B., Jr., Burkhardt, C.A., Gardella, J.A., Jr., Macromolecules, 24, 799 (1991).

133. Schneider, H.A., Makromol. Chem., 189, 1941 (1988).

134. Schneider, H.A., Polymer, 30, 771 (1989).

APPENDIX 1:   NMR SPECTRA

NMR: ST/MAA Copolymer 7

TMS

← δ (ppm)

NMR: ST/MAA Copolymer 8

TMS

← δ (ppm)

NMR: ST/MAA Copolymer 9

TMS

$\longleftarrow \delta$ (ppm)

10 9 8 7 6 5 4 3 2 1 0
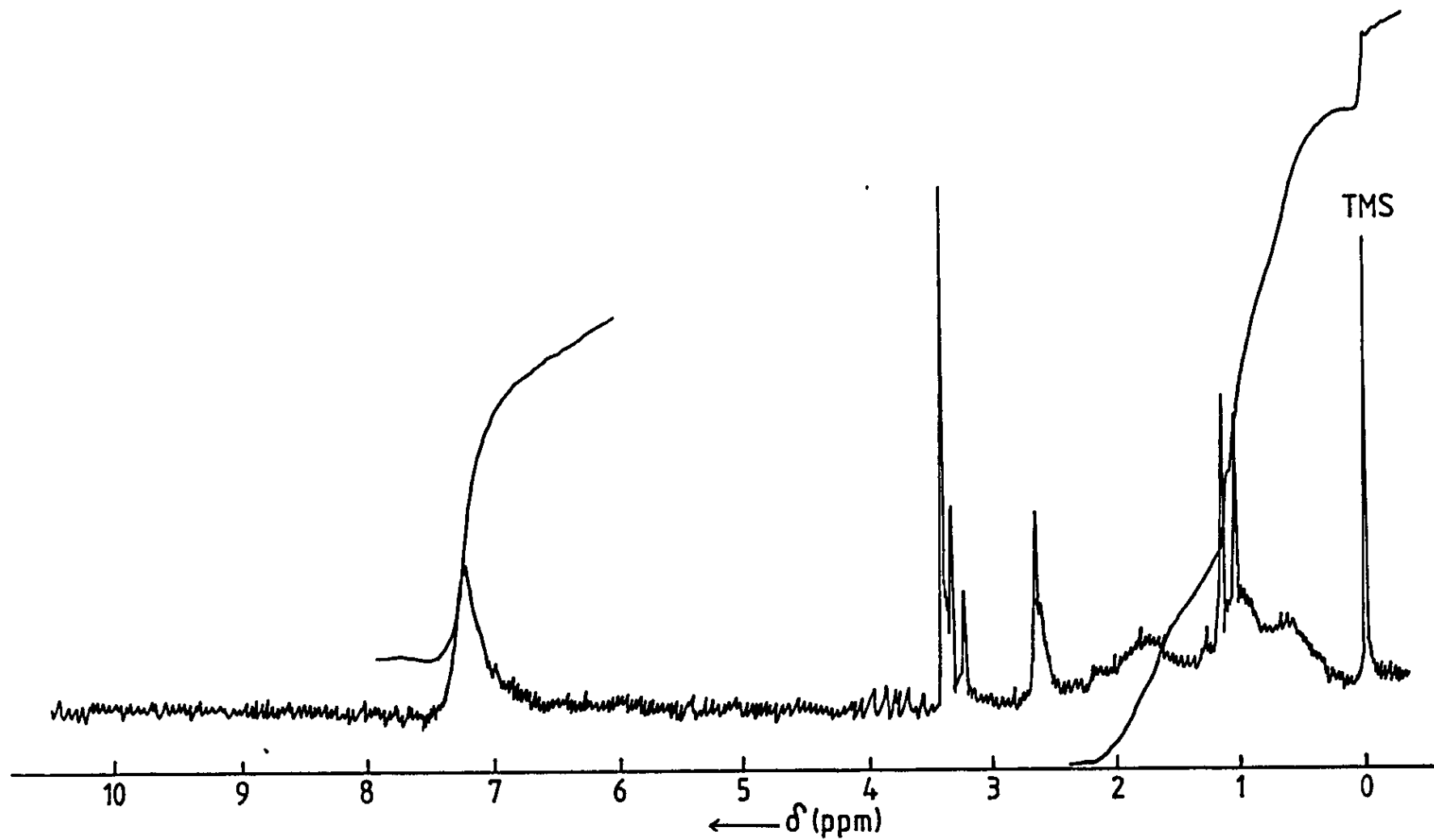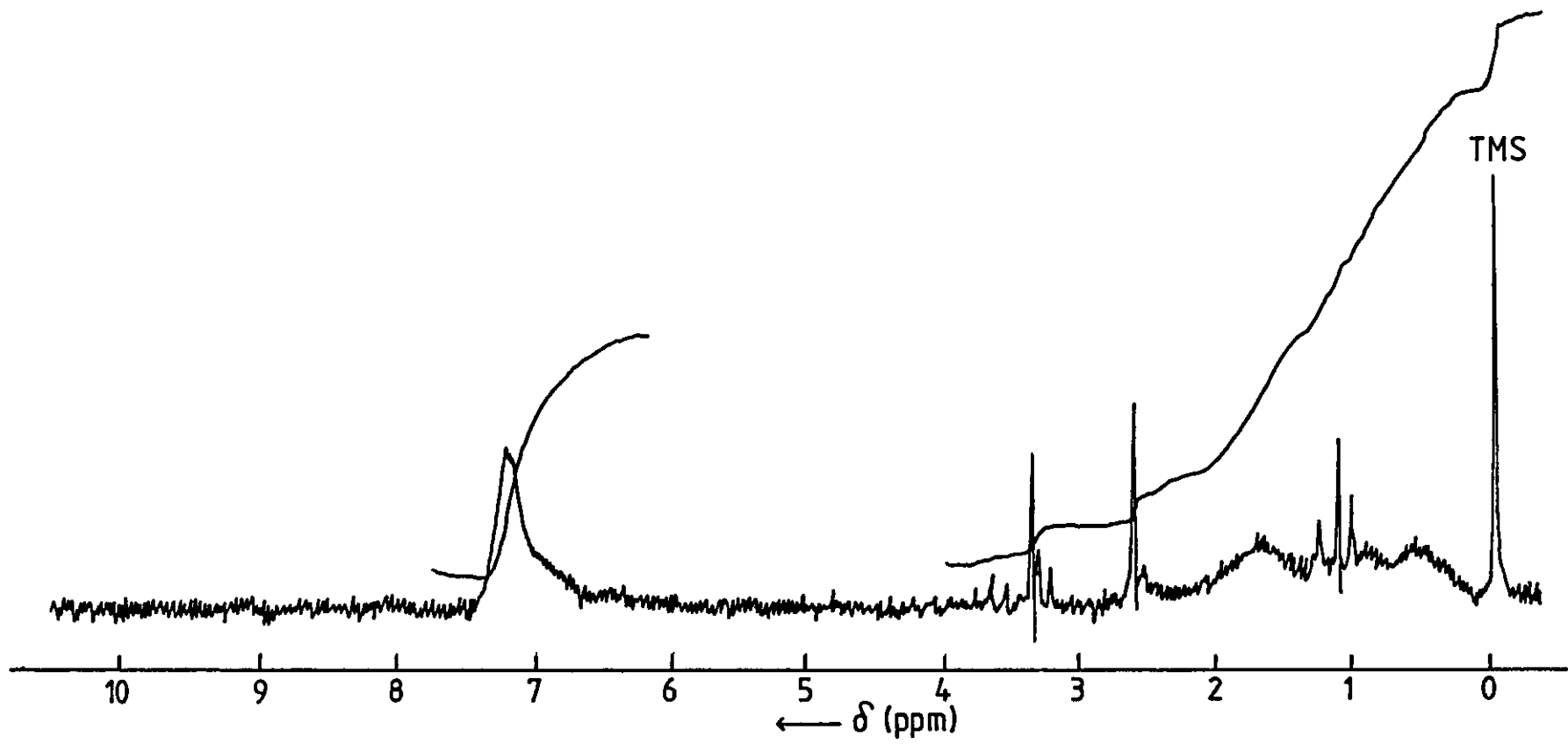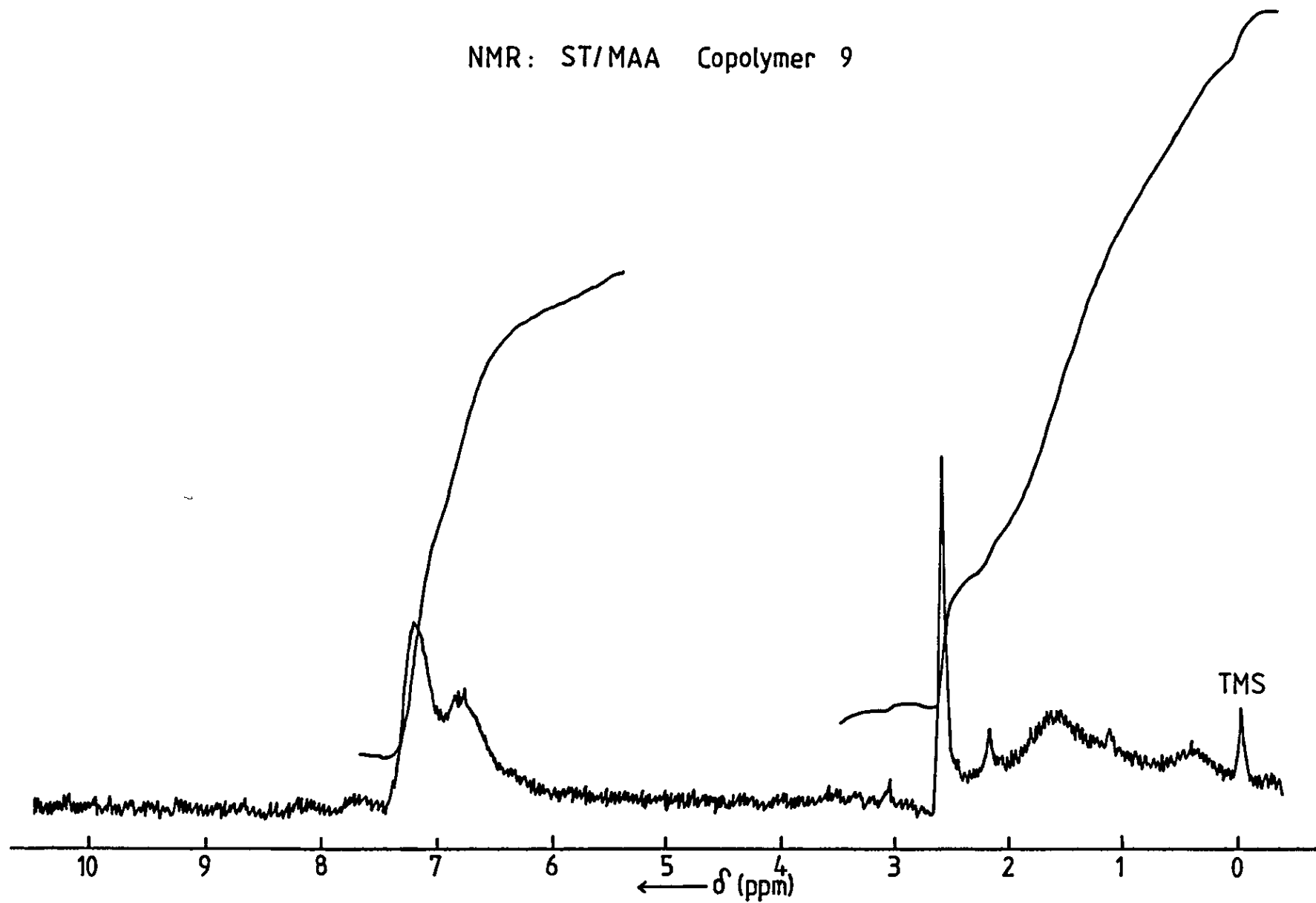
NMR: ST/MAA Copolymer 29

TMS

← δ (ppm)
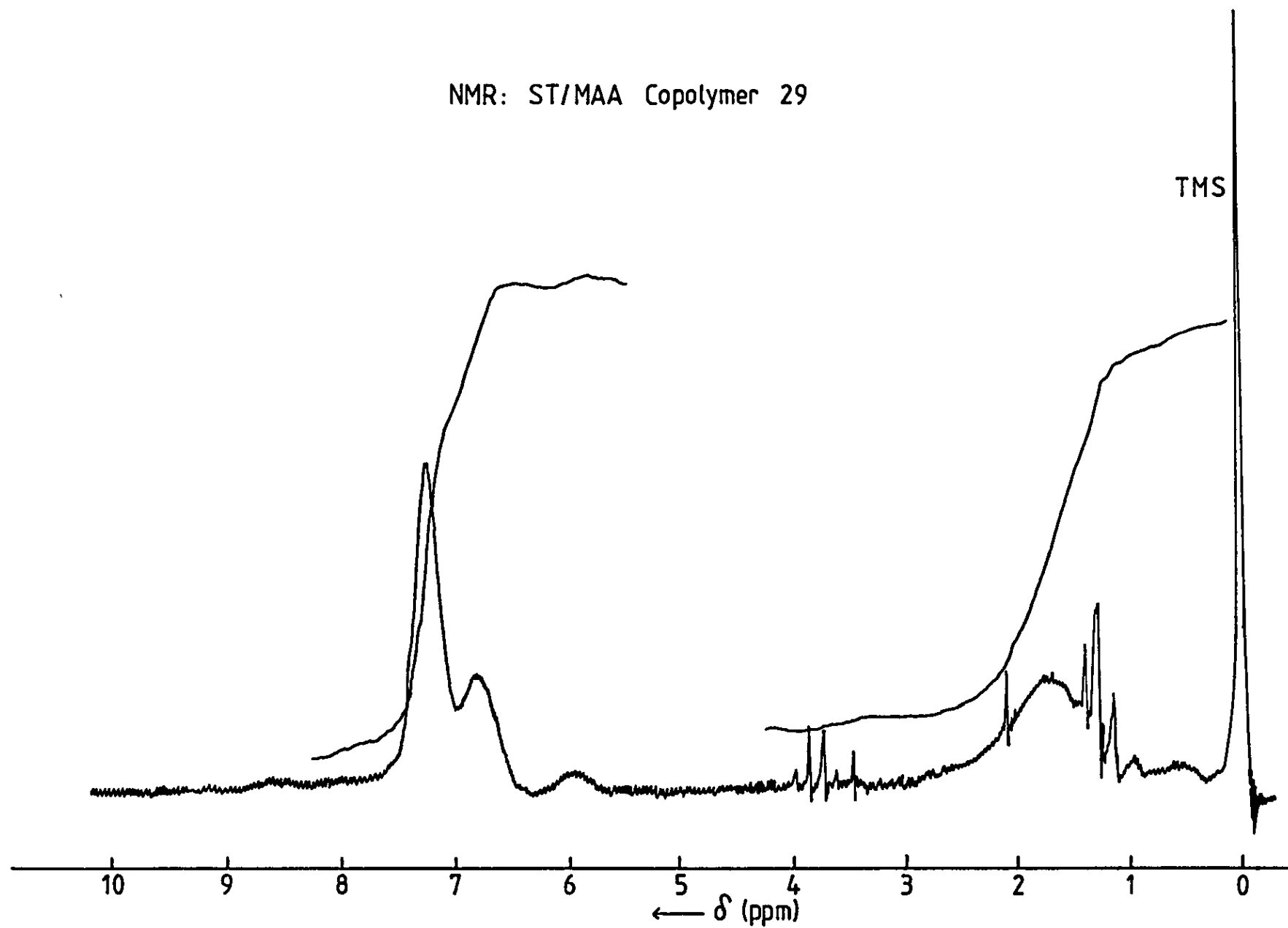
NMR: ST/MAA Copolymer 30

$\longleftarrow \delta$ (ppm)

TMS
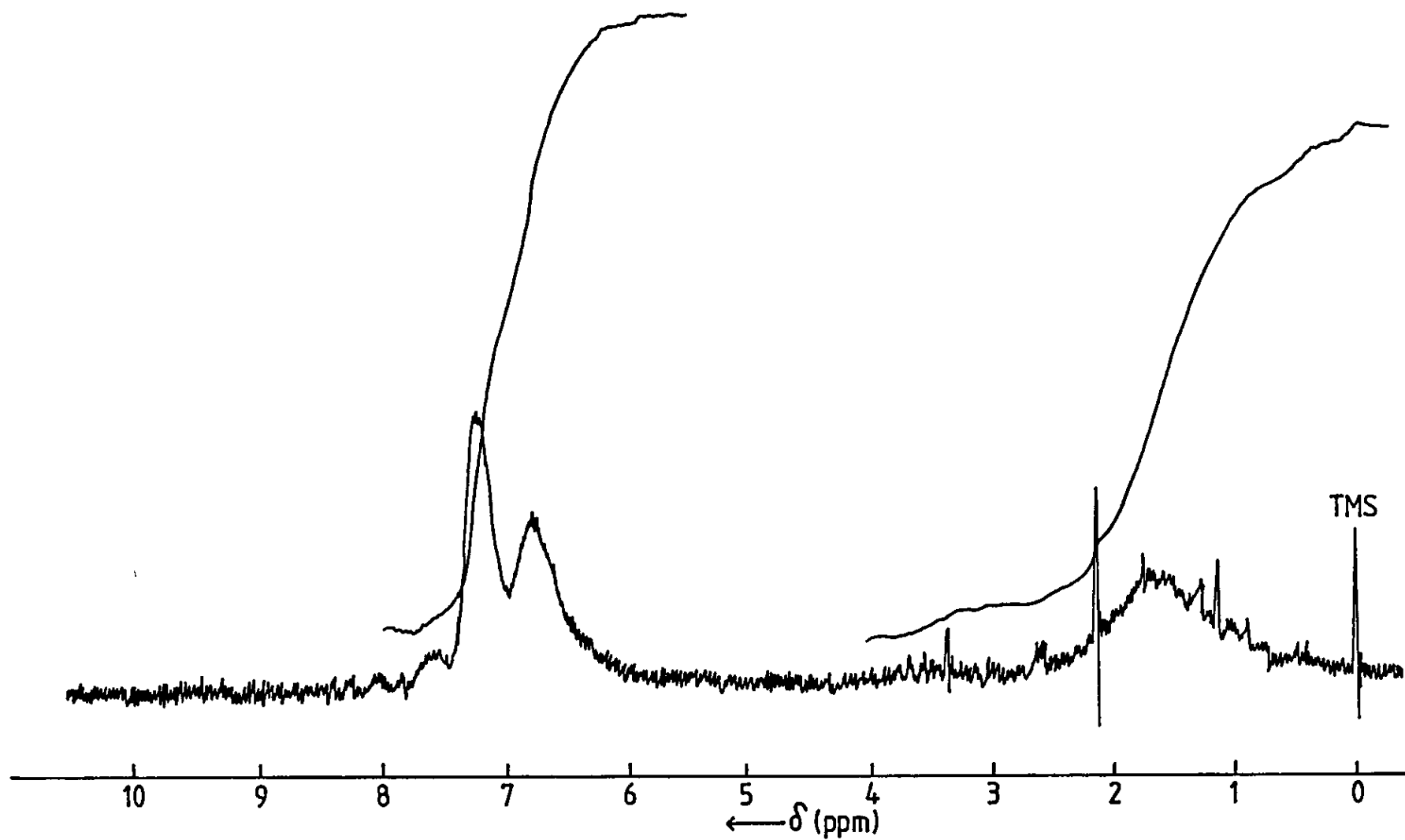
NMR : ST/MAA Copolymer 63

TMS

← δ (ppm)
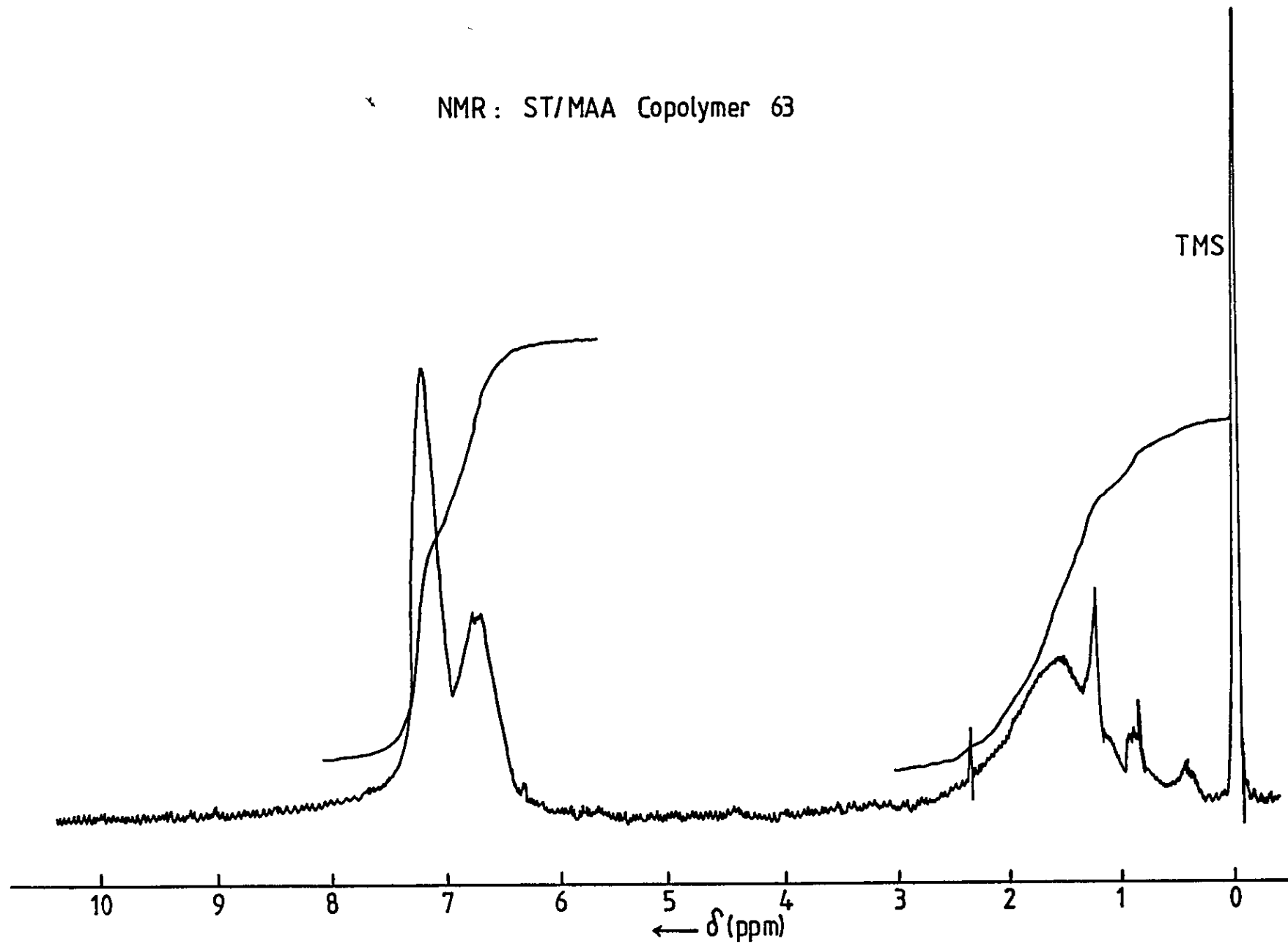
NMR: Lumiflon LF200

TMS

δ (ppm)
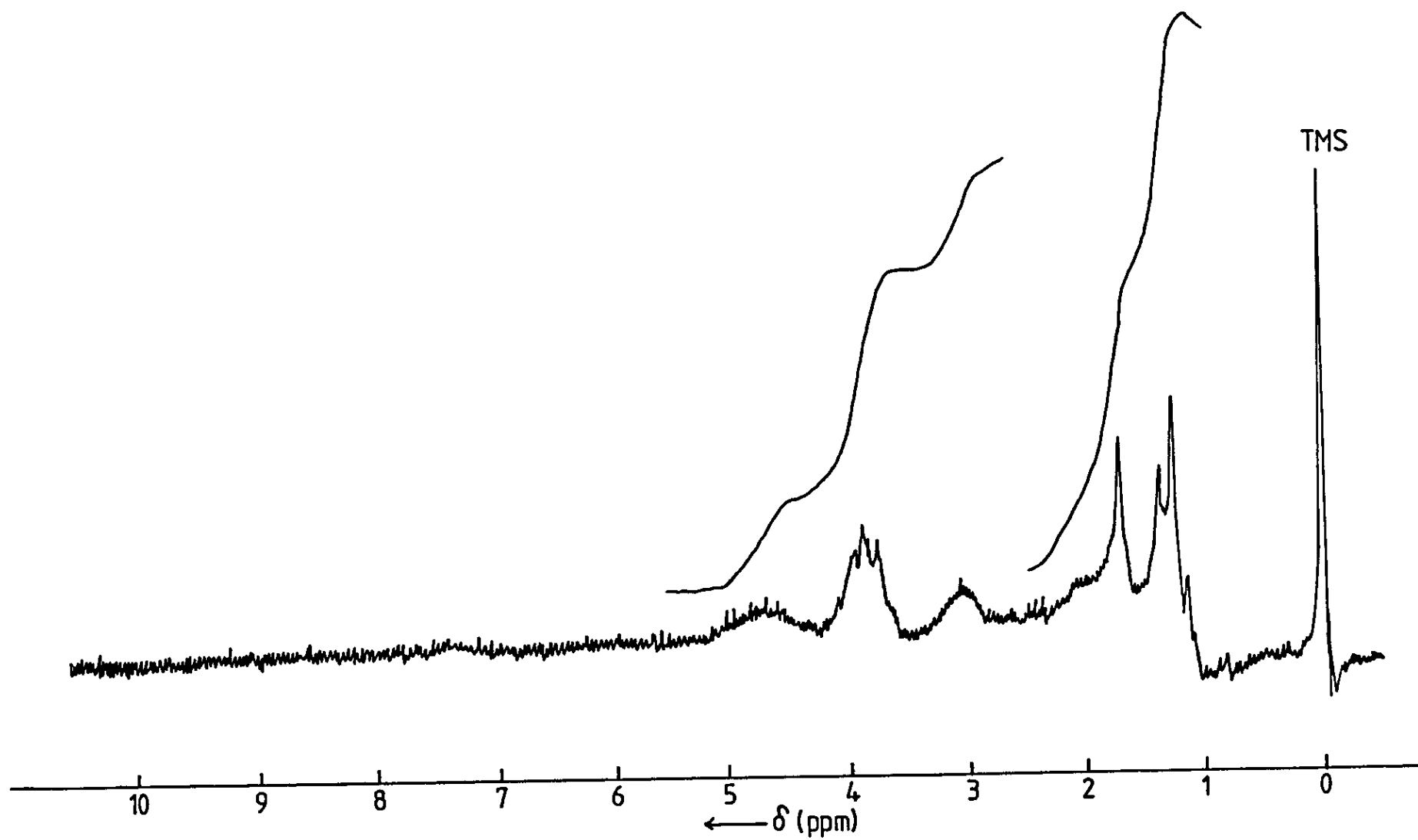
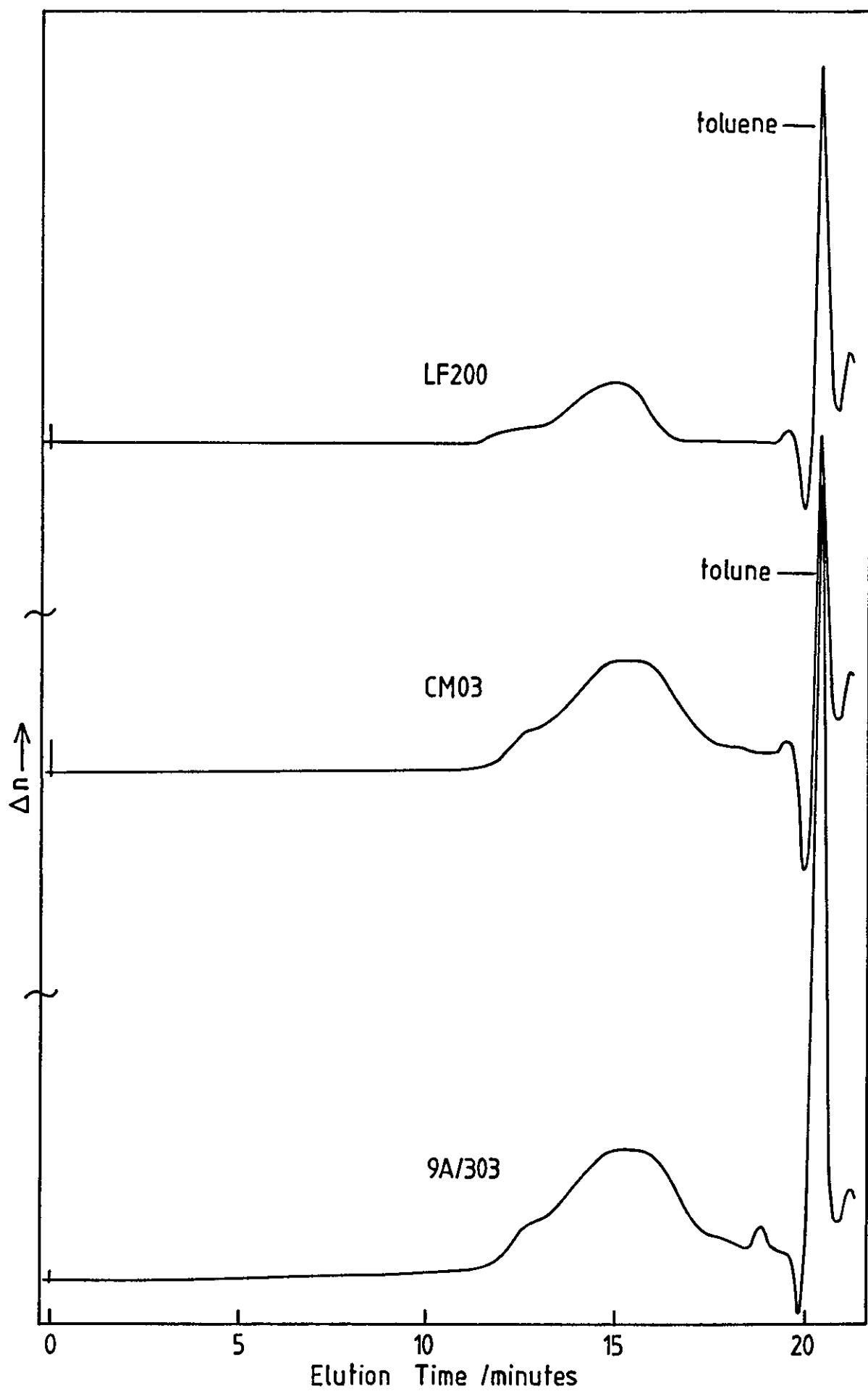NMR: CMO3
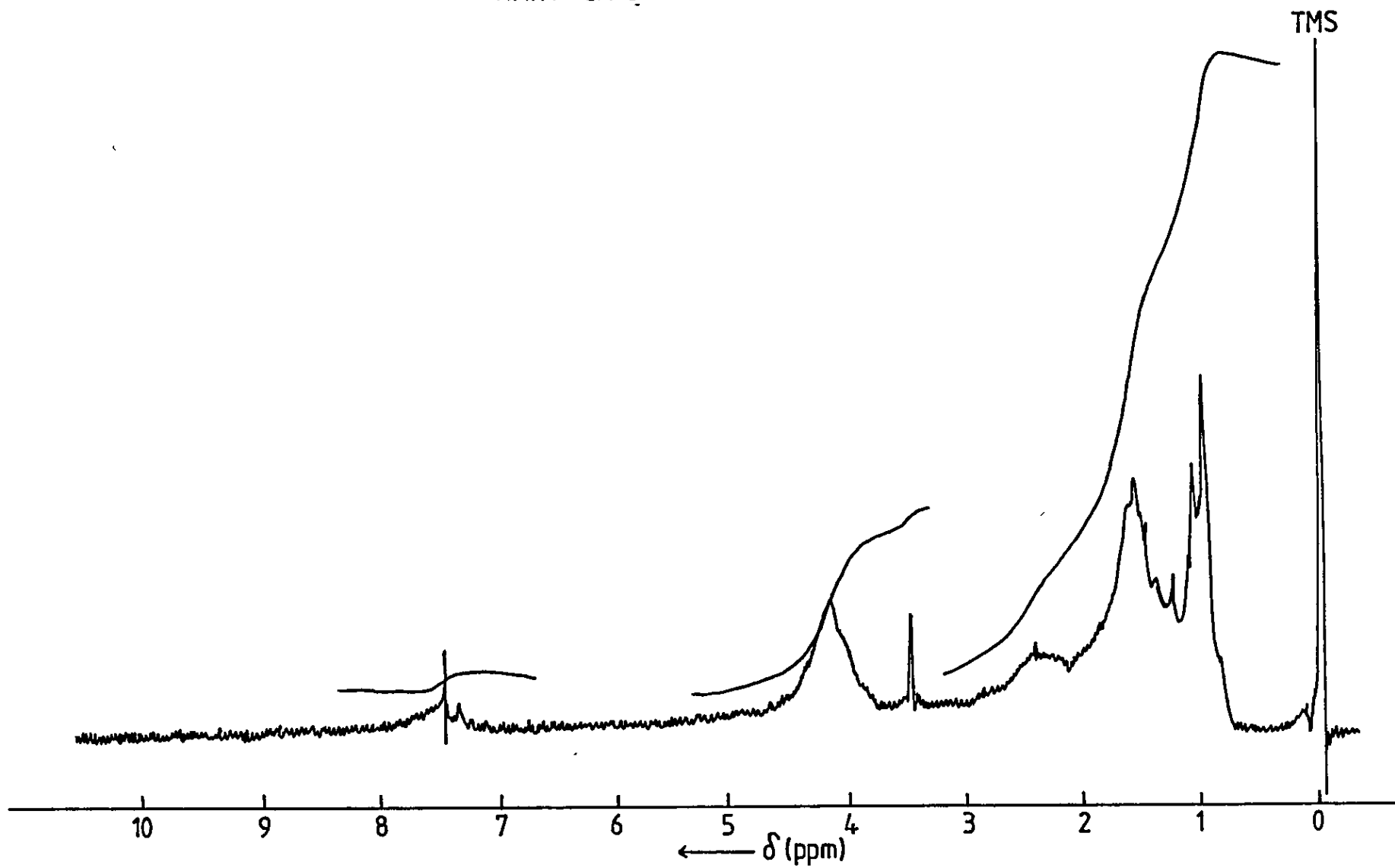
NMR: 9A/303
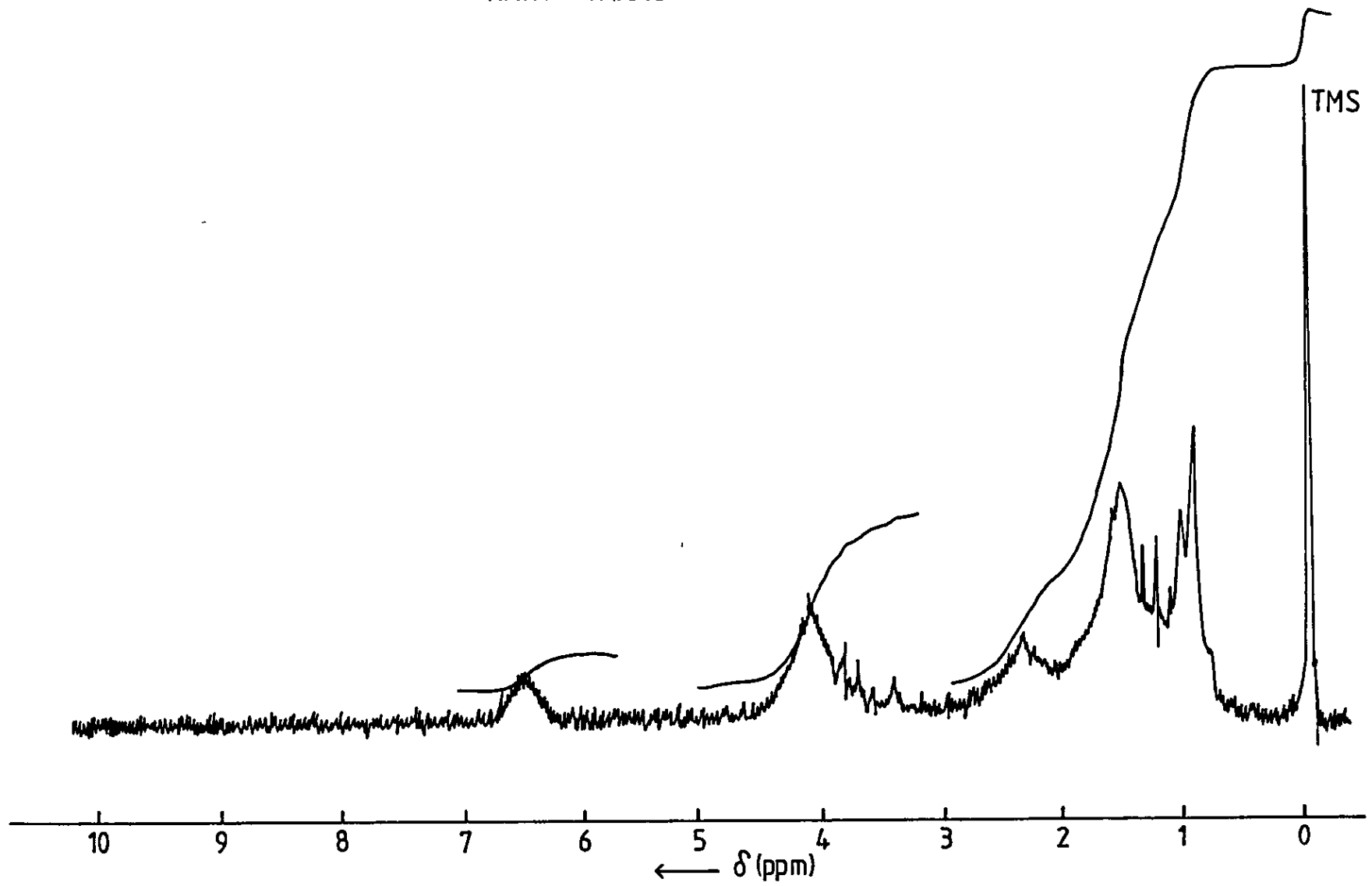
NMR: Styrene/Acrylonitrile Copolymer (SAN)

TMS

10   9   8   7   6   5   4   3   2   1   0

⟵ δ (ppm)
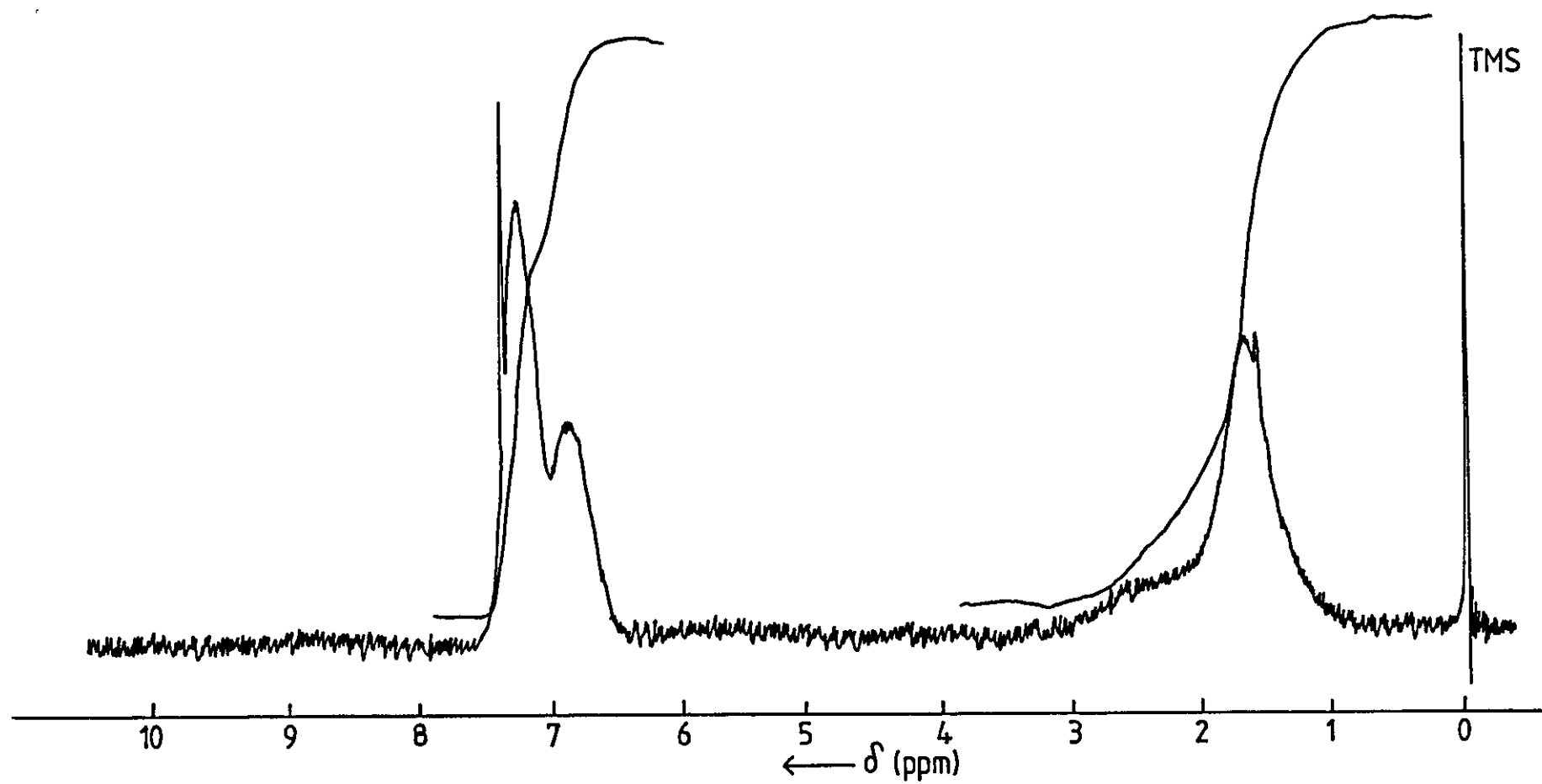
APPENDIX 2:   GPC CHROMATOGRAMS

GPC Chromatograms for ST/MAA Copolymers

ST/MAA Copolymer 29

ST/MAA Copolymer 163

toluene

Elution Time /minutes
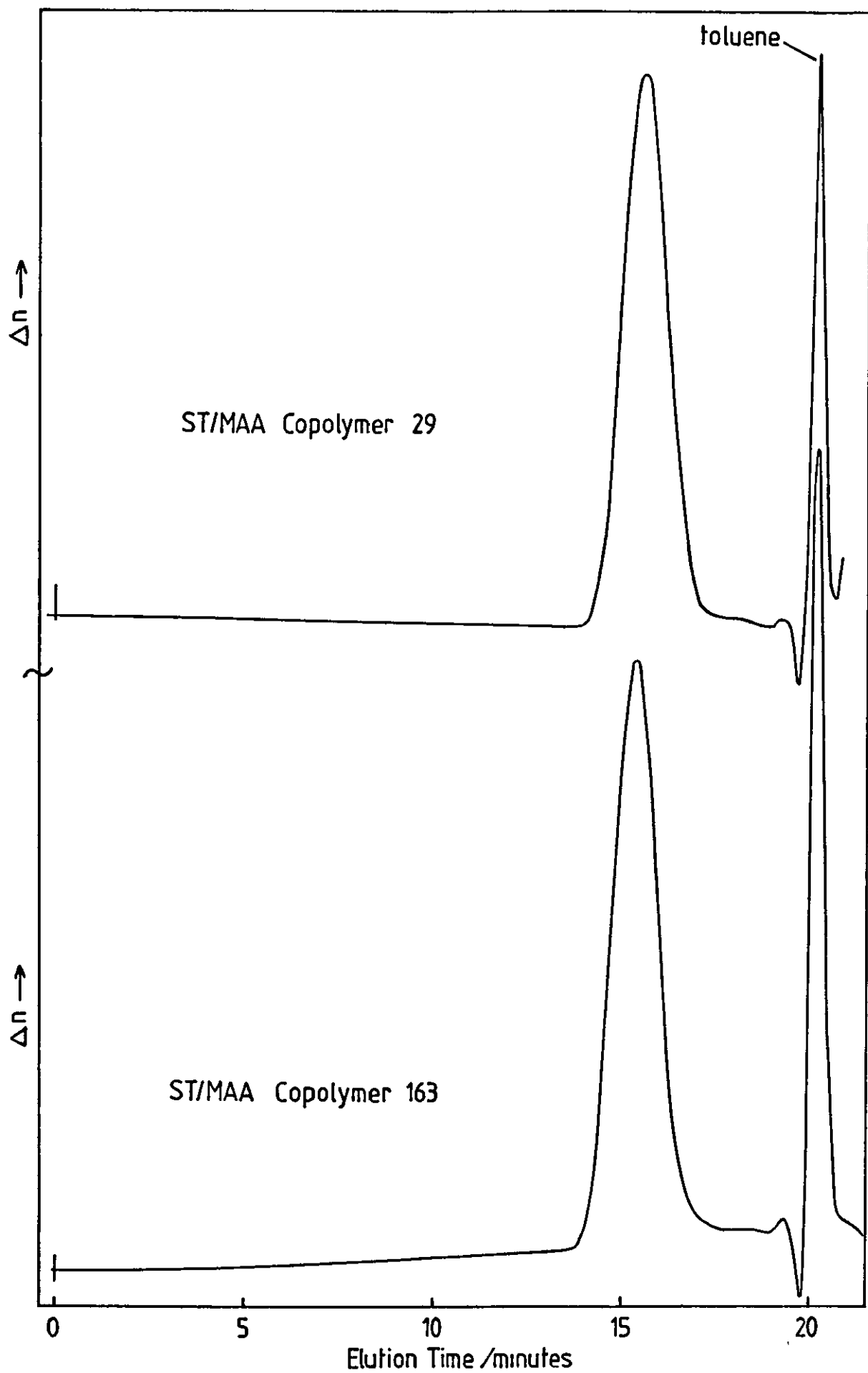
GPC Chromatograms for LF200, CM03 & 9A/303

LF200

toluene

tolune

CM03

9A/303

$\Delta n \rightarrow$

Elution Time /minutes

GPC Chromatograms for PBMA, PDMAEMA & PPA
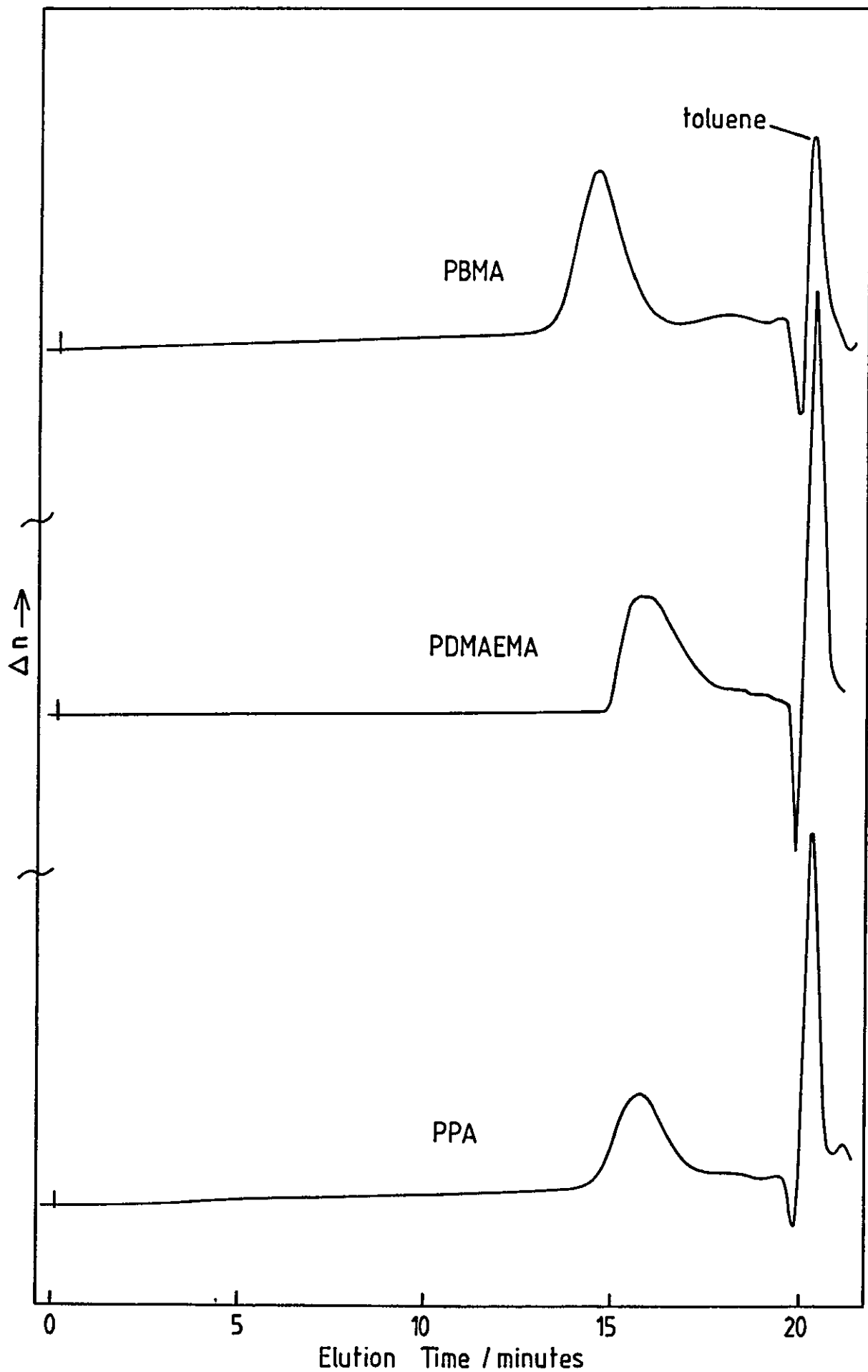
GPC Chromatograms for PPG(1) & PPG(2)

Δn →

PPG(1)

toluene

PPG(2)

toluene

Elution Time /minutes

GPC Chromatograms for PBA(1),(2) & (3)

500 Å Column·

PBA(1)

PBA(3)

toluene

Mixed gel column:

PBA(2)

toluene

Δn →

Elution Time / minutes

APPENDIX 3: FTIR SPECTRA

ST/MAA COPOLYMER   (29)

ABSORBANCE

1.6191
1.2868
0.9646
0.6224
0.2901

4000.0   3433.3   2866.7   2300.0   1733.3   1166.7   600.00

WAVENUMBER (CM-1)

ST/MAA COPOLYMER   (163)

ABSORBANCE

2.3843
2.8000
1.2158
0.6316
0.0473

4000.0   3433.3   2866.7   2300.0   1733.3   1166.7   600.00

WAVENUMBER (CM-1)

LUMIFLON LF200

CM03

ABSORBANCE

WAVENUMBER (CM-1)

XENACRYL 9A/303   28 Oct 89 11: 48: 17

ABSORBANCE

WAVENUMBER (CM-1)

POLY (PROPYLENE GLYCOL)   PPG (2)

POLY (BUTYL ACRYLATE)   PBA (3)

POLY(PROPYLENE ADIPATE)   PPA

ABSORBANCE

1.8484 1.3790 0.9098 0.4402 -0.0291

4000.0   3433.3   2866.7   2300.0   1733.3   1166.7   600.00

WAVENUMBER (CM-1)

SETAL 1711   26 Jan 89 10: 09: 32

ABSORBANCE

2.7639 2.0580 1.3521 0.6462 -0.0597

4000.0   3433.3   2866.7   2300.0   1733.3   1166.7   600.00

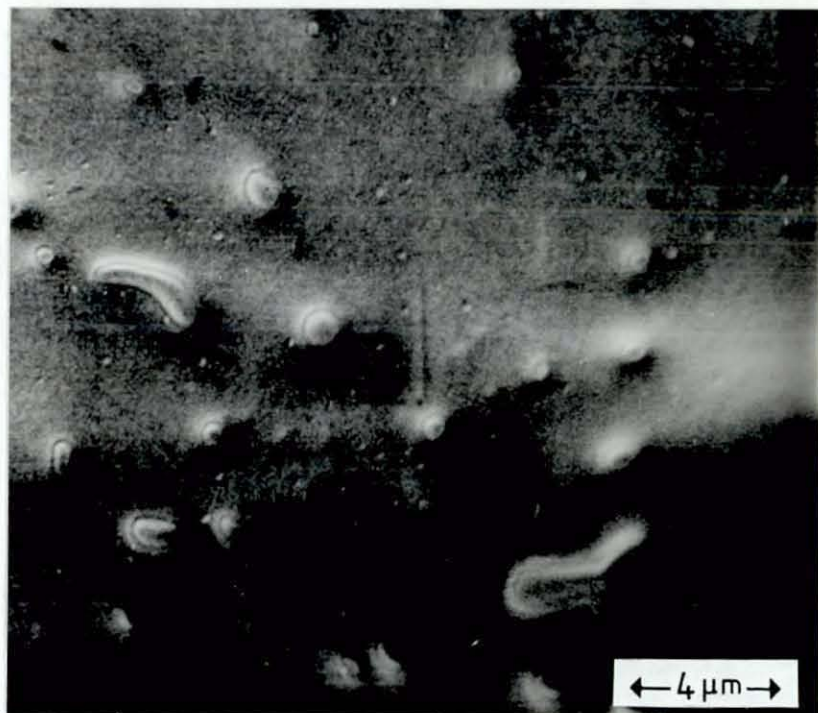WAVENUMBER (CM-1)

APPENDIX 4: SEM MICROGRAPHS

SEM Micrograph of LF200 (2000 ×)

←10 μm→
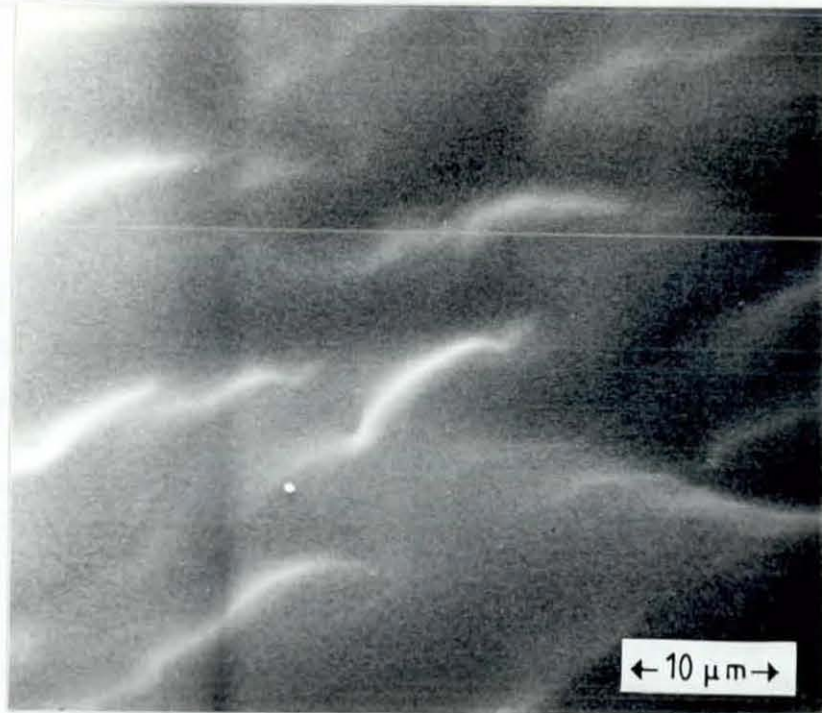
SEM Micrograph of CMO3 (2000 ×)

←10 μm→
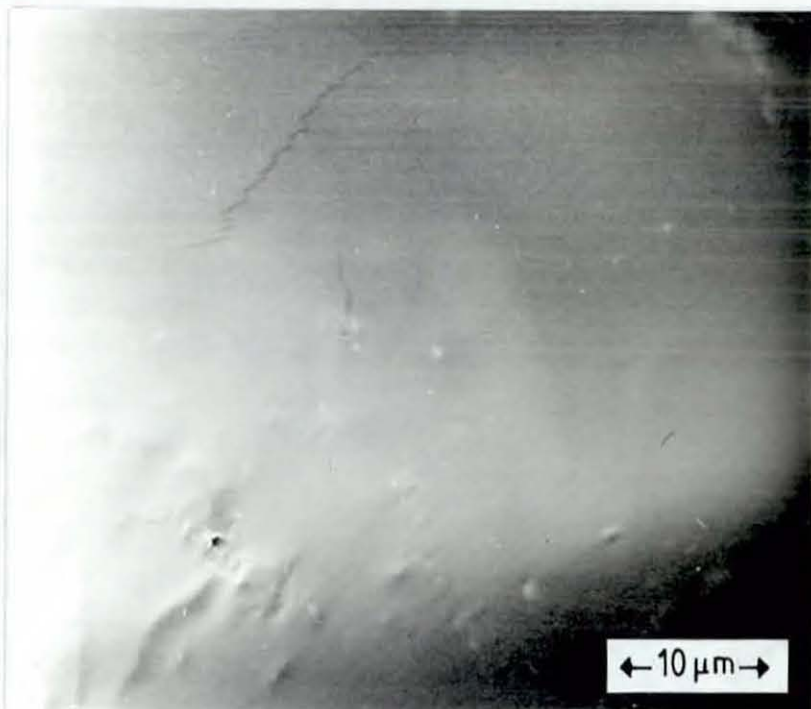
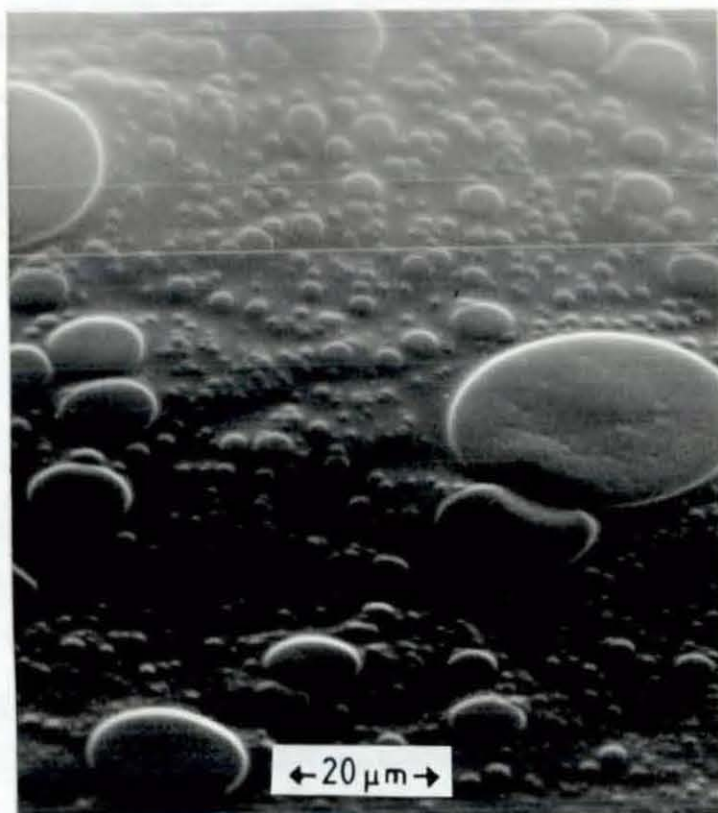SEM Micrograph of Blend 102 (5000 x)
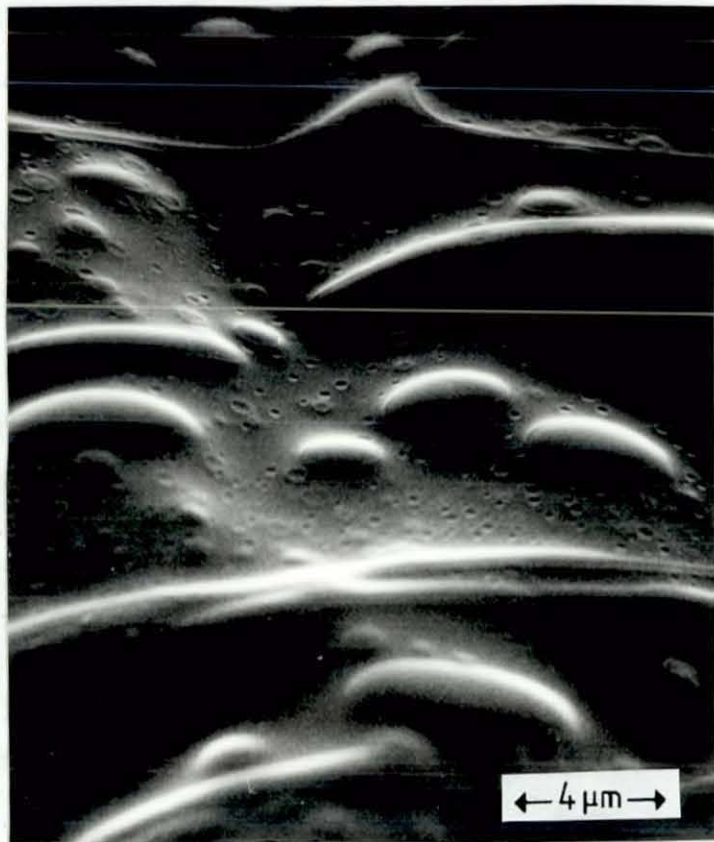
SEM Micrograph of Blend 112 (5000 x)

SEM Micrograph of Blend 156 (1000 ×)
[solution cast]

←20 μm→

SEM Micrograph of Blend 156 (2000 ×)
[melt pressed]

←10 μm→

APPENDIX 5

COMPARISON OF IMPREGNATED FILTER PAPER VS. BAR SAMPLES FOR DMTA

Comparison of DMTA Results Using a Bar vs Paper Sandwich Specimen for Poly(vinyl acetate)